Australian Government
Geoscience Australia

Compilation of SHRIMP U-Pb geochronological data

Olympic Domain, Gawler Craton, South Australia, 2001-2003

Elizabeth A. Jagodzinski

Record
2005/20

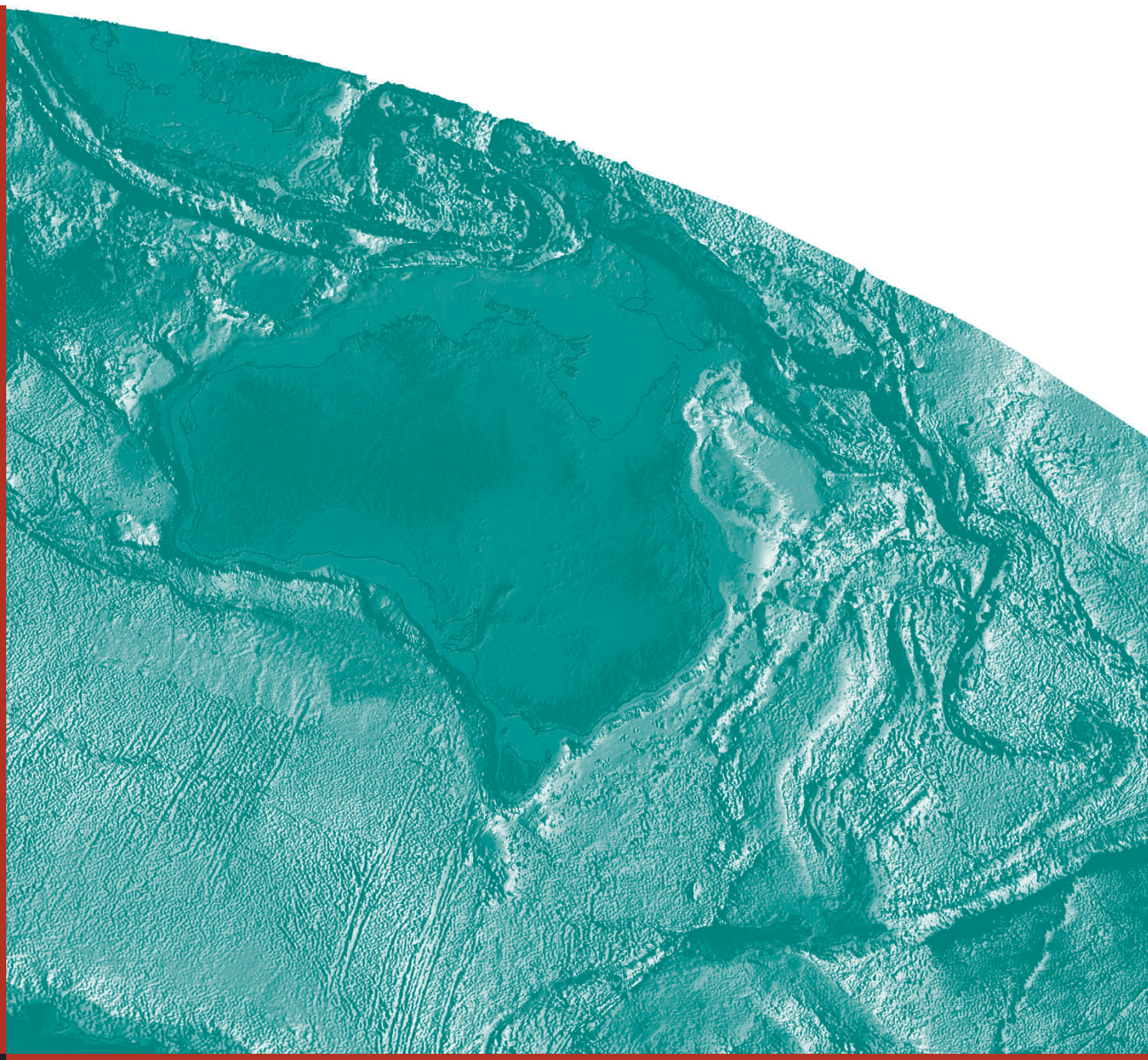

Australian Government

Geoscience Australia

Government of South Australia

MINERALS & ENERGY

Compilation of SHRIMP U-Pb geochronological data, Olympic Domain, Gawler Craton, South Australia, 2001-2003

Geoscience Australia

Record 2005/20

Elizabeth A. Jagodzinski[1,2]

[1] Geoscience Australia, GPO Box 378, Canberra ACT 2601

[2] Current address c/ Geological Survey, PIRSA, GPO Box 1671, Adelaide, 5001.
e-mail: Jagodzinski.Liz@saugov.sa.gov.au

Department of Industry, Tourism and Resources

Minister for Industry, Tourism and Resources: The Hon. Ian Macfarlane, MP
Parliamentary Secretary: The Hon. Warren Entsch, MP
Secretary: Mark Paterson

Geoscience Australia

Chief Executive Officer: Dr Neil Williams

ISSN: 1448-2177
ISBN: 1 920871 60 8

GeoCat No: 63530

Bibliographic reference: Jagodzinski, E.J. 2005. Compilation of SHRIMP U–Pb geochronological data, Olympic Domain, Gawler Craton, South Australia, 2001–2003. Geoscience Australia, Record 2005/20, 197 pp.

Contents

List of Figures

List of Tables

Introduction

This record contains zircon U-Pb geochronological data obtained between July 2001 and May 2003 on diamond drillcore from the Olympic Domain, Gawler Craton, South Australia. The data were collected as part of the Gawler Craton Project; a collaboration between Geoscience Australia (GA) and the Division of Mineral and Energy, Primary Industry and Resources, South Australia (PIRSA). The project aims to provide an improved geological and metallogenic framework for the Gawler Craton, with initial emphasis on the Olympic Domain.

The term Olympic Domain (formerly 'Olympic Subdomain'; Daly et al. 1998) refers to the eastern extension of the Gawler Craton, concealed beneath Mesoproterozoic, Neoproterozoic and Cambrian sedimentary rocks of the Stuart Shelf. It also encompasses outcrop and subcrop of the Gawler Craton further south in the Moonta-Wallaroo region of the Yorke Peninsula (Figure 1). The sedimentary cover sequence of the Stuart Shelf is between about 300 and 1000 m thick, and the only knowledge of the underlying crystalline basement comprising the Olympic Domain is derived from exploratory drillholes. The long distances between drillholes impede inter-hole correlations. Thus U-Pb isotope dating of rocks intersected by (diamond) drillcore plays a key role in regional stratigraphic studies, establishing an absolute basis for temporal correlations across the Olympic Domain.

This record describes the samples analysed and the analytical results obtained, and provides a brief discussion of their geochronological interpretation. The broader geological implications of the data will be published elsewhere.

For samples from the Olympic Dam deposit and surrounding prospects (Horn Ridge, Snake Gully, Wirrda Well, Acropolis, Burden Hill and Island Dam), and from the Mount Woods Inlier, drillhole collar locations were provided by collaborating company geologists. For drillcore stored at the PIRSA core library and under open file status, collar locations were obtained from the PIRSA database, SAGEODATA. Grid references in this record refer to the Geocentric Datum of Australia 1994 (GDA1994). Drillhole locations are shown in Figure 2.

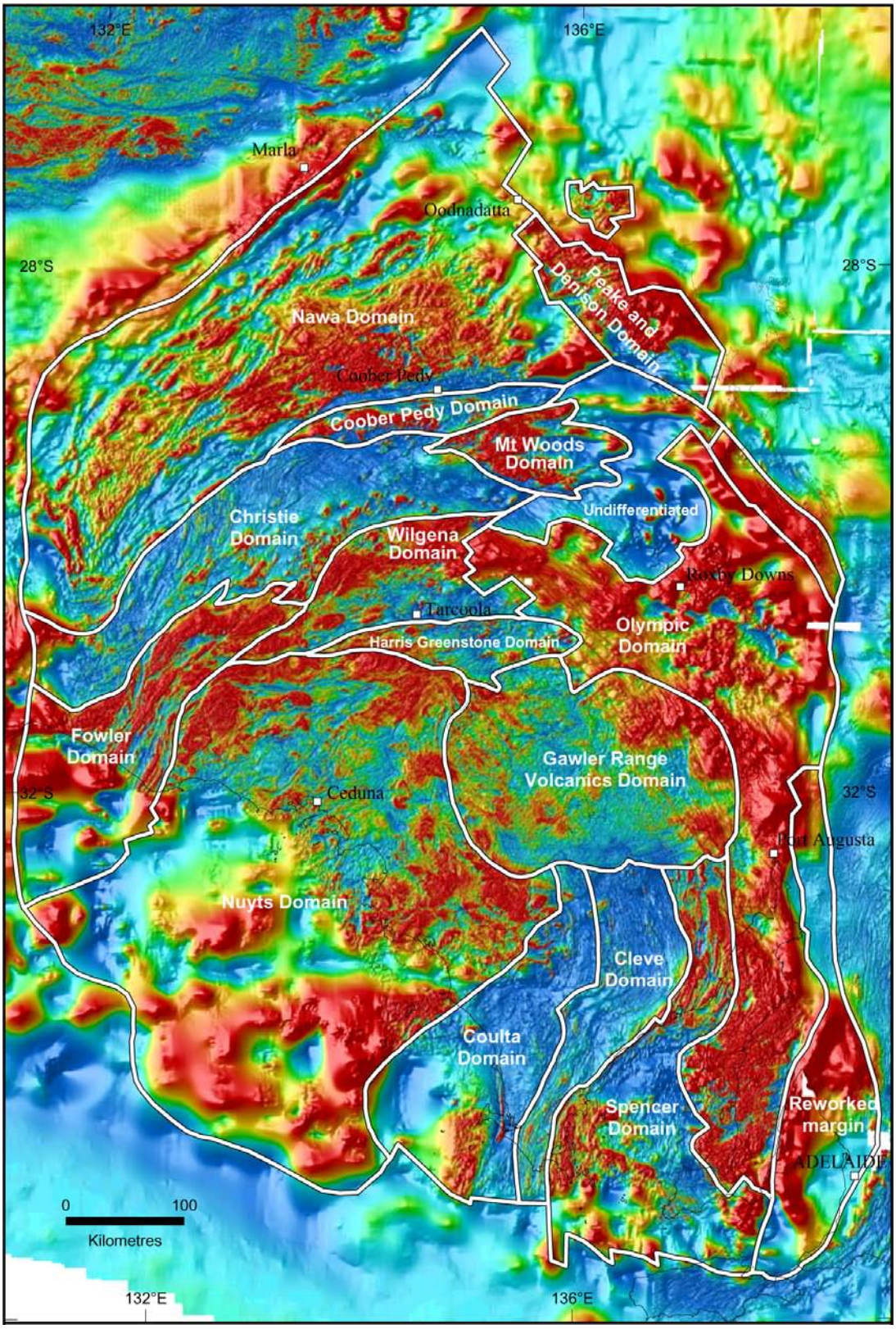

Figure 1. Tectonic Domains of the Gawler Craton (after Ferris et al. 2002).

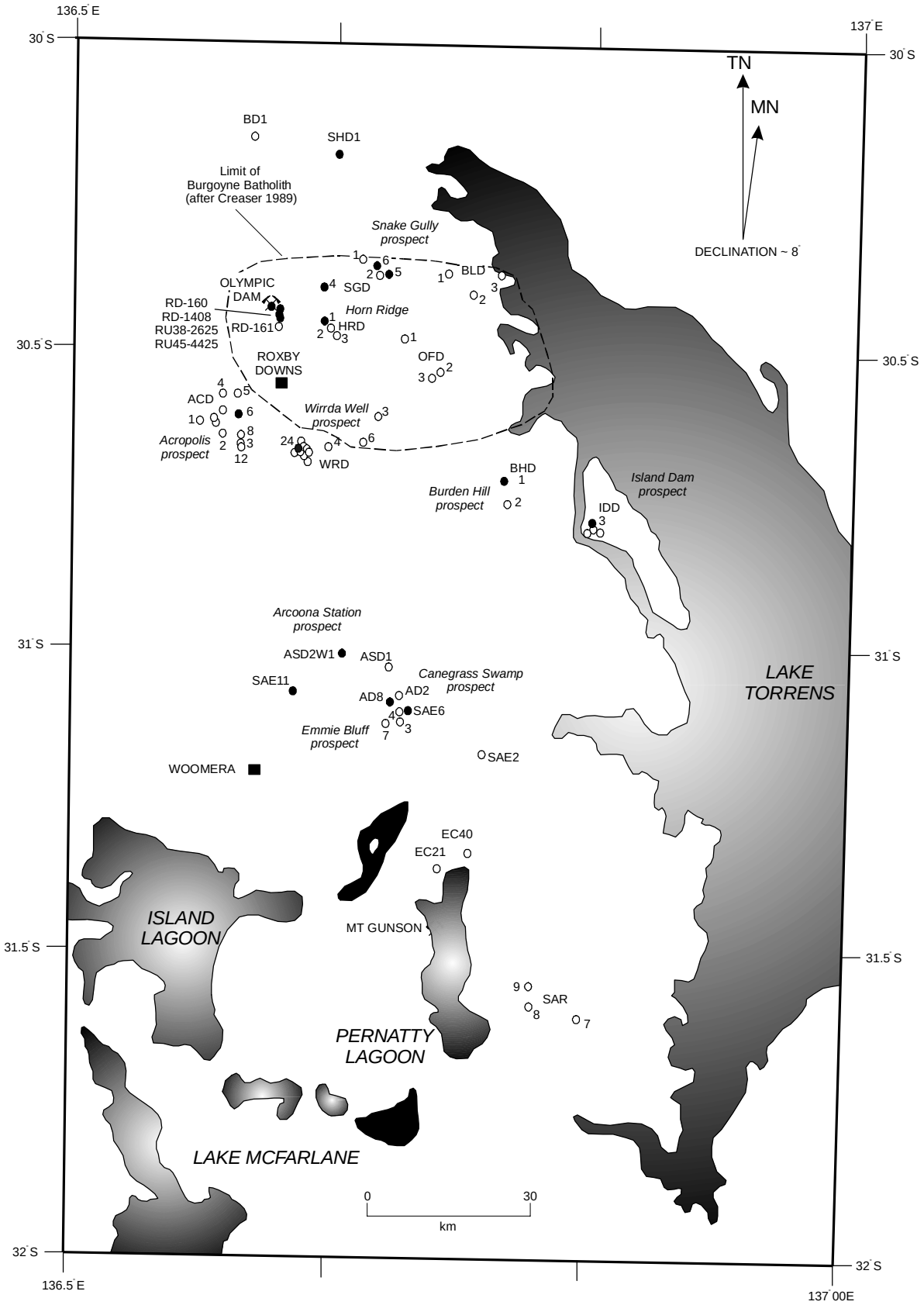

Figure 2a. Location of samples analysed. Filled circles are drillholes containing material analysed in this study. Some other prospects are also displayed. Drillholes SOC8 and LG-DDH2 lie to the south of this figure. SR9, DD86EN26 and PK1 lie to the northwest, within the Mt Woods Inlier (Figure 2b).

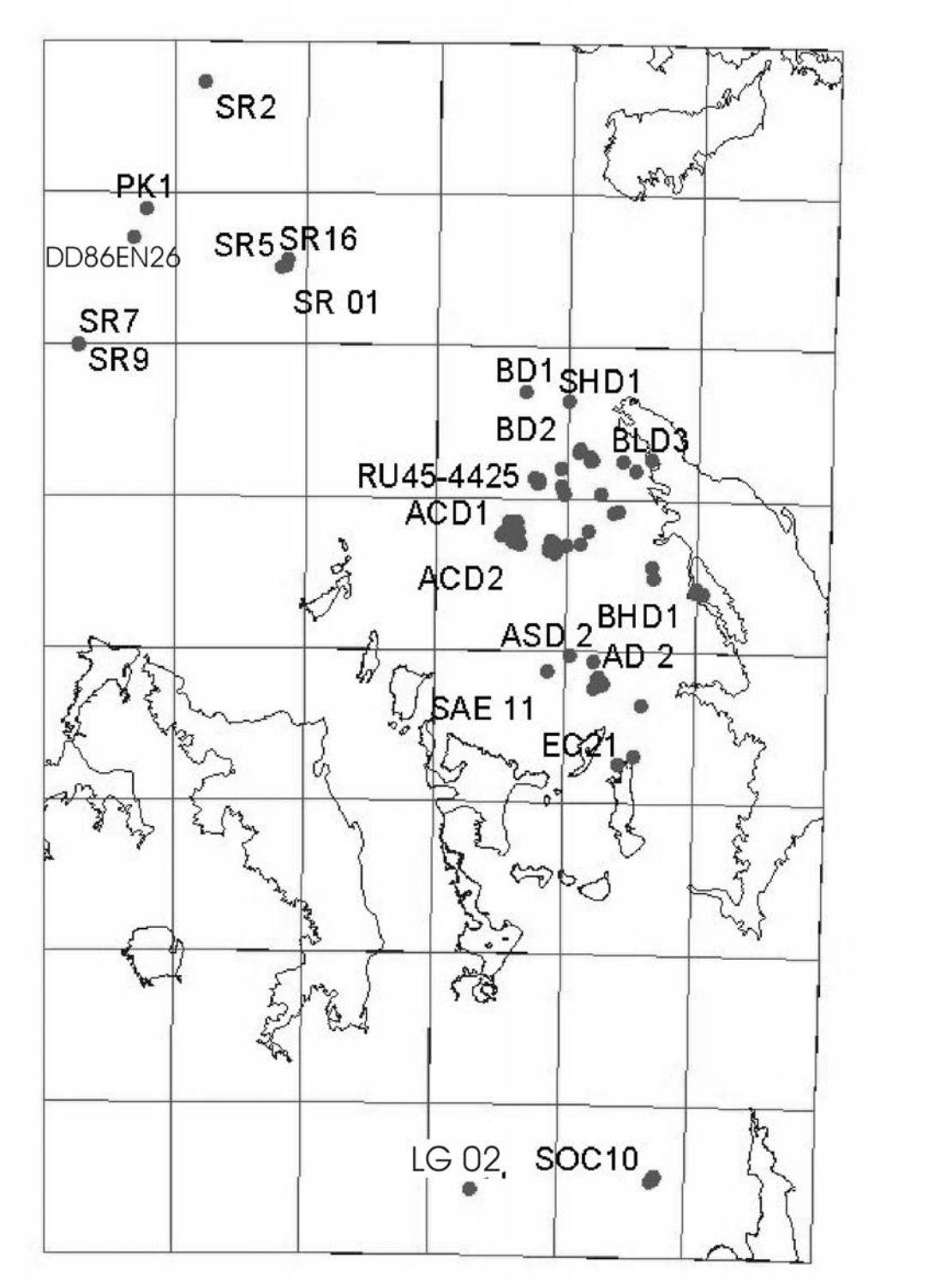

Figure 2b. Broader view of the Stuart Shelf showing drillhole locations for samples analysed in the Mt Woods Inlier and southern Stuart Shelf (Mt Gunson region).

Previous Geochronology

Geochronological data for the Olympic Domain (where it underlies the Stuart Shelf) have been presented by Mortimer et al. (1988a), Johnson and Cross (1991) and Creaser and Cooper (1993). A synthesis of existing geochronological data is presented in Table 1 (table does not include data from the Moonta-Wallaroo region, Yorke Peninsula, which are summarised in Cowley et al. 2003). These analyses provide a framework for the age of the succession hosting the Olympic Dam Cu-U-Au-Ag deposit. The deposit is hosted by the Olympic Dam Breccia Complex (ODBC; Reeve et al. 1990). The ODBC occurs wholly within the Roxby Downs Granite, an evolved pluton within the Burgoyne Batholith of the Hiltaba Suite. Granitoids from the Hiltaba Suite in the Olympic Dam region yield a range in ages from 1588 ± 4 Ma to 1613 ± 20 Ma. However, the older crystallisation ages from drillholes RD80 and RD87 are ID-TIMS ages derived from extremely altered samples of Roxby Downs Granite, and may be inaccurate and/or imprecise, giving a false representation of the duration of felsic magmatism. Most analyses fall within a narrower age range, between 1588 and 1598 Ma. The ages correlate with the precise U-Pb zircon ages that exist for the upper and lower units of the Gawler Range Volcanics (1592 ± 3 Ma and 1591 ± 3 Ma, respectively: Fanning et al. 1988).

The ODBC formed at *ca* 1590 Ma, contemporary with the Gawler Range Volcanics/Hiltaba Suite volcano-plutonic event. The age of the Roxby Downs Granite (1588 ± 4 Ma, Creaser and Cooper 1993; 1595 ± 11 Ma, 1598 ± 14 Ma, Johnson 1993) constrains the maximum age of brecciation and mineralisation. The minimum age of brecciation is constrained by SHRIMP U-Pb zircon dates on dykes and diapiric material that intruded the breccias during the waning stages of the hydrothermal system (1593 ± 7 Ma, 1584 ± 20 Ma, 1586 ± 7 Ma; Johnson and Cross 1991). Johnson and Cross (1991) establish an association between brecciation and mineralisation on the basis of lithological, textural and geochemical characteristics.

Although the *ca* 1590 Ma magmatic episode and associated hydrothermal activity are fairly well constrained, no definitive data exist for the older deformed granitoids and (meta)sedimentary sequences within the Olympic Domain. Mortimer et al. (1988a) established that the deformed granitoids are older than the Hiltaba Suite, having a possible age of about 1800 Ma, but the TIMS analyses (Thermal Ionisation Mass Spectrometry) provided very poor age estimates due to the isotopic complexity of the grains, believed to reflect high discordance and inheritance within the zircon population.

Table 1: Summary of available U-Pb geochronology for the Olympic Domain

Locality/DH	Suite/Group	Lithology	Age	MSWD	Method*	n	Reference
1590 Ma magmatic episode							
RD647	ODBC	felsic 'peperite' dyke	1584±20		5	13	Johnson & Cross 1991, Johnson 1993
DDH6	Roopena Volcs	tuffaceous rock	1587±15		5	31	Johnson 1993
RD 161	Hiltaba Suite	Roxby Downs Granite	1588±4	1.3	1	3 fractions	Creaser & Cooper, 1993
OFD 3	Hiltaba Suite	Quartz monzonite	1590±10	2.6	2	4 zirc/1titanite	Creaser & Cooper, 1993
PD 3	Hiltaba Suite	Quartz monzodiorite	1590±5	3	1	6 fractions	Mortimer et al. 1988a
ACD 5	GRV	Quartz latite	1591±10	7.9	1	6 fractions	Mortimer et al. 1988a, Creaser & Cooper 1993
BLD 2	Hiltaba Suite	Quartz monzonite	1592±5	0.7	1	5 fractions	Creaser & Cooper, 1993
RD32	ODBC	felsic peperite dyke	1592±8		5	19	Johnson 1993
WRD 3	Hiltaba Suite	Quartz monzodiorite	1593±3.4		3	1 titanite	Creaser & Cooper, 1993
29NB49S Dr	Hiltaba Suite	granite microbreccia	1595±11		5	9	Johnson 1993
33NB53W Dr	ODBC	diatreme lapilli tuff	1597±8		5	27	Johnson 1993
32LK58NW D	Hiltaba Suite	granite microbreccia	1598±14		5	11	Johnson 1993
WRD 6	Hiltaba Suite	Quartz monzonite	1598±2.3		3	1 titanite	Creaser & Cooper, 1993
ACD 2,3 PD2,3	Hiltaba Suite	Veins & granitoids	1602±7	0.65	4	7 fractions	Mortimer et al. 1988a
RD 80	Hiltaba Suite	quartz syenite	1606±7		1	2 fractions	Mortimer et al. 1988a
RD 87	Hiltaba Suite	quartz syenite	1613±20	3.6	1	6 fractions	Mortimer et al. 1988a
Older granitoids							
BLD1		anorthosite gabbro	1764±12		5	12	Johnson 1993
WRD 2	Donington Suite	deformed granitoid	1803		1	1 zircon	Mortimer et al. 1988a
PD 2	Donington Suite	deformed granitoid	1813±90	22.5	1	4 fractions	Mortimer et al. 1988a

* 1 = TIMS U-Pb zircon = 2: TIMS U-Pb zircon-titanite; 3 = TIMS U-Pb titanite; 4 = TIMS U-Pb apatite; 5 = SHRIMP U-Pb zircon

Project Aims

The main aim of this geochronological study is to identify the various crustal components that comprise the Olympic Domain, and host the mineral systems. This requires the synthesis of existing data, identification of outstanding stratigraphic issues and their resolution where possible. The data presented in this record should provide a basis for the construction of a unified, formal stratigraphy for the Olympic Domain, which will then allow temporal correlation of its components with rock units in other domains of the Gawler Craton.

Given the abundance of data already in existence for the Hiltaba Suite, the main focus of the project was to reliably date the older deformed granitoid and (meta)sedimentary successions intruded by the undeformed Hiltaba Suite (Parts 1 and 2 of this record). In Part 3, a new age determination is presented for the Hiltaba Suite and contemporary coarse-grained mafic rocks in the Olympic Dam region, for comparison with existing TIMS and SHRIMP U-Pb zircon ages of the Roxby Downs Granite, greater Burgoyne Batholith and ODBC, and for comparison with new data for the Hiltaba Suite in the Mount Woods Inlier. Part 4 presents data from a suite of magmatic to hydrothermal samples collected from the Olympic Dam deposit. A summary of the U-Pb ages zircon ages obtained in this study is presented in Table 2.

Table 2. Summary of U-Pb zircon ages obtained in this study.

DDH	Sampno	Lithology	Mount	Age (Ma)	MSWD	n^u/n^t
Donington Suite						
WRD24	200036 6034	megacrystic syenogranite	Z3678	1849.6±3.5	1.14	19/22
ACD6	200036 6029	tonalite-norite-adamellite	Z3678	1853.3±3.7	1.40	20/28
SGD4	200036 6004	megacrystic granodiorite	Z3677	1854.0±3.3	1.43	31/32
BHD1	200036 6020	megacrystic granodiorite	Z3678	1857.7±3.9	1.40	19/19
IDD3	200036 6032	megacrystic syenogranite	Z3678	1860.4±4.1	1.48	23/24
(meta)sedimentary units						
SHD1	200036 6103	paragneiss	Z3931	1750 ± 6	2.0	35/51
SGD6	200036 6008	meta-siltstone	Z3677	1854.5±5.4	1.6	15/34
				ca 1770		3/34
SAE6	200036 6110	meta-arkose	Z3931	1853.4±5.0	1.16	30/30
SAE11	200036 6127	fine-grained sandstone	Z3931	1854 ± 6	1.9	30/32
ASD2W1	200036 6102	schist	Z3931	1863.3 ± 3.3		
			Older grains	1901 ± 7		
AD8	200036 6133	meta-arkose	Z3966	1852 ± 7	1.5	27/30
BUTE5	200036 6131	Wandearah Metasiltstone	Z3966	1762 ± 7	1.9	47/75
				1862 ± 8	0.87	14/75
LG DDH2	200036 6130	high grade calc silicate	Z3966	2009 ± 10	1.6	20/93
				2481 ± 6	1.16	10/93
				2514 ± 6	1.7	17/93
SOC8	200036 6115	volcaniclastic sandstone	Z3966	1756 ± 8	1.3	27/30
SR9	200036 6137	meta-greywacke	Z3966	2543 ± 6	1.5	31/34
Hiltaba Suite (felsic)						
HRD1	200036 6000	quartz monzonite	Z3677	1594.4±3.4	1.26	24/25
DD88EN26	200136 8015f	leucogranite	Z3962	1586.3±2.8	1.17	37/39
Hiltaba Suite (mafic)						
SGD4	2000366005	microdiorite dyke	Z3677	1595.6±3.8	1.24	24/25
PK1	200236 8028b	leucogabbro	Z3962	1586.8±4.1	1.71	43/44
			rims	1576.2±7.0	1.23	20/23
Dykes and volcaniclastic rocks, Olympic Dam						
RU38 2625	200036 6164	volcaniclastic sandstone	Z4125	1594.5±3.3	1.6	20/22
RD 1408	200036 6165	chloritised dyke	Z4125	1597.5±3.7	1.6	22/22
RU45 4425	200036 6166	sericitised feldspathic dyke	Z4125	1596.0±4.4	2.0	24/29

Age (Ma) is the weighted mean $^{207}Pb/^{206}Pb$ age.
n^u is the number of analyses in the calibration data subset averaged to give $^{207}Pb/^{206}Pb$ age.
n^t is the total number of analyses for the sample.

Analytical Procedures

Sample processing

The samples were obtained from drill core in collaboration with company geologists. Each sample was inspected and cleaned in the mineral separation lab at Geoscience Australia. Drill core was broken down to 2–5 cm pieces using a pre-cleaned hydraulic splitter. The pieces were ultrasonically washed in water, and dried under heat lamps. The first crush used a jaw crusher, or Rocklabs Boyd crusher. Milling used a rotary disc mill or a Rocklabs Continuous Ring Mill.

The initial density separation was undertaken using a Wilfley table. This washed away the fine dust and reduced the sample to about 5% of its original weight. Any highly magnetic grains were then removed using a hand magnet. A second density separation stage used Tetrabromoethane (2.96 g/ml), followed by magnetic separation using a Frantz isodynamic separator. The non-magnetic fraction then underwent a third density separation in Methylene Iodide (3.3 g/ml) and additional Frantz separation.

Zircon selection was biased towards the least magnetic, clearest grains, without discrimination between grain morphologies. Where available, several hundred zircon grains per sample were selected for mounting by handpicking using a binocular microscope. The zircon grains were encapsulated in epoxy, together with the multi-grain zircon standard QGNG (Daly et al. 1998) and a small quantity of the standard SL13. The mounts were polished to expose grains in section. All grains were photographed in transmitted and reflected light, and imaged by cathodoluminescence (CL) on a Hitachi S2250 NSEM located in the Electron Microscopy Unit at the Australian National University.

All SHRIMP mounts were ultrasonically cleaned in petroleum spirit, rinsed in quartz-distilled water and gold-coated with high purity gold.

Data acquisition

The analyses were made on the SHRIMP I (mounts Z3931 and Z3966) and SHRIMP II (mounts Z3677, Z3678, Z3962 and Z4215) ion microprobes at the Research School of Earth Sciences, Australian National University and the SHRIMP IIA ion microprobe at Curtin University (re-analysis of mount Z3931). A raster (surface-cleaning) time of 3 minutes was used, and data were acquired over 7 scans through the mass sequence (5-7 scans for the metasedimentary units reported in Part 2). The primary O_2^- beam was typically ~ 11 nA, but down to ~ 5 nA for zircon overgrowths in sample 200236-8028B, producing positive secondary ions from elliptical spots approximately 20–30 µm and 20–30 µm in size, respectively. Significant spectral interferences were removed by operating at a mass resolution in excess of 5000 at 1% peak height (Compston et al. 1984).

The whole-rock geochemical analyses in Appendix 2 were analysed in the Geoscience Australia Minerals Division Geochemical Laboratory. FeO was analysed by titrimetry, and all other major elements by fused disc X-Ray Fluorescence. All trace elements were analysed by Inductively Coupled Plasma Mass Spectrometry (ICP-MS).

Data reduction

Differential fractionation between U and Pb was monitored by reference to a $^{206}Pb/^{238}U$ ratio of 0.3341 for interspersed analyses of the 1850 Ma QGNG zircon standard, based on the power law relationship $^{206}Pb^{+}/U^{+} = a(UO^{+}/U^{+})^{2}$. Th/U ratios were derived from the linear relationship $^{232}ThO/^{238}U = (0.03446.UO^{+}/U^{+} + 0.868).ThO^{+}/UO^{+}$. Radiogenic Pb compositions were initially determined by subtracting contemporaneous common Pb (after Stacey and Kramer 1975). All data were processed using SQUID 1.11 (Ludwig, 2001), and plotted using ISOPLOT/EX 2.4 (Ludwig 1999). This version of SQUID permits operator-specified variations in the exponent used in the Pb/U calibration (equivalent to varying the slope of the conventional ln[Pb/U]:ln[UO/U] calibration line). For all analytical sessions reported here, however, these parameters were within error of the default value of 2.0.

Data presentation

All weighted mean $^{207}Pb/^{206}Pb$ ages determined from grouped data are derived from ^{204}Pb-corrected $^{207}Pb/^{206}Pb$ ratios. Ages are calculated from the U and Th decay constants of Jaffey et al. 1971, as recommended by Steiger and Jäger (1977). Their uncertainties are quoted in at the 95% ($t\sigma$) confidence level. Where age errors are > 5 Ma, the ages are rounded off to integers and the corresponding uncertainties are rounded up to cover the range that is required by additional decimal places (e.g. 1850.2 ± 5.2 rounds to 1850 ± 6 Ma). All data from individual analyses are tabulated with 1σ uncertainty, and the tabulated data are all common-Pb corrected and corrected for overcounts on the ^{204}Pb mass peak (after Black in press). Data are plotted on concordia diagrams with 2σ precision. Unless otherwise stated in the text, analyses that are more than 10% discordant are excluded from the weighted mean age calculations.

Data compilation for the QGNG standard

Introduction

The QGNG standard zircon was used for Pb/U calibration and as a monitor of $^{207}Pb/^{206}Pb$ reproducibility and accuracy. In each session, standard analyses were interspersed with sample analyses, and were collected under the same standardised conditions. Data were processed using SQUID 1.11 (Ludwig, 2001), in conjunction with sample data for each session. Radiogenic Pb compositions were initially determined by subtracting contemporaneous common Pb (Stacey and Kramer 1975).

Data

The QGNG data were assessed session-by-session. The first consideration is the $^{206}Pb/^{238}U$ calibration, and at this stage it is not uncommon to reject some data. The $^{207}Pb/^{206}Pb$ data are then assessed, and treated much as those for a sample. The notes on QGNG data that accompany each of the sample reports follow this sequence.

After this initial assessment and culling, the QGNG data sets yield weighted mean $^{207}Pb/^{206}Pb$ ages with MSWD values ranging between 0.96–2.5 (Table 3). When the data are compiled (Figure 3) the session-to-session scatter gives an MSWD of 2.0 (probability of fit = 0.07), and the average $^{207}Pb/^{206}Pb$ age of 1849.5 ± 1.9 Ma is slightly below, but just within error of the TIMS reference value of 1851.6 ± 0.6 Ma (2σ; Black et al. 2003).

There is no significant between-session variation in $^{207}Pb/^{206}Pb$ data for QGNG. However, both SHRIMP I sessions yield younger $^{207}Pb/^{206}Pb$ ages (average 1845.3 ± 3.2 Ma; n=2) than the sessions analysed on SHRIMP II (average 1849.9 ± 1.1 Ma; n=4), and significantly younger than the TIMS reference value. Z4125, analysed on SHRIMP II, also yields a younger $^{207}Pb/^{206}Pb$ age than the TIMS reference value. To compensate for this offset, data for all sessions (except mount Z3962) have been corrected for overcounts at the mass ^{204}Pb peak (after Black in prep). This forces the average $^{207}Pb/^{206}Pb$ age for QGNG during a session to the TIMS reference value.

Table 3. Data for QGNG for each session.

Session	Date	Instrument	t[207/206]	+/- 95%	MSWD	POF	n^u	n^t
Uncorrected								
Z3931	26/04/02	SHRIMP I	1846.3	3.9	1.5	0.02	37	37
Z3966	11/06/02	SHRIMP I	1843	6	2.5	0.0	50	51
Z3677	08/04/01	SHRIMP II	1850.7	1.9	1.09	0.33	35	35
Z3678	05/06/01	SHRIMP II	1850.0	2.5	0.96	0.53	24	24
Z4125	30/04/03	SHRIMP II	1848.4	2.5	1.8	0.01	26	26
Z3962	22/04/03	SHRIMP II	1850.0	2.1	1.14	0.28	27	30

t[207/206] is the weighted mean $^{207}Pb/^{206}Pb$ age.
POF is the probability of fit of the analyses in the calibration data subset averaged to give t[207/206].
n^u is the number of analyses in the calibration data subset averaged to give t[207/206].
n^t is the number of analyses recorded for the session.

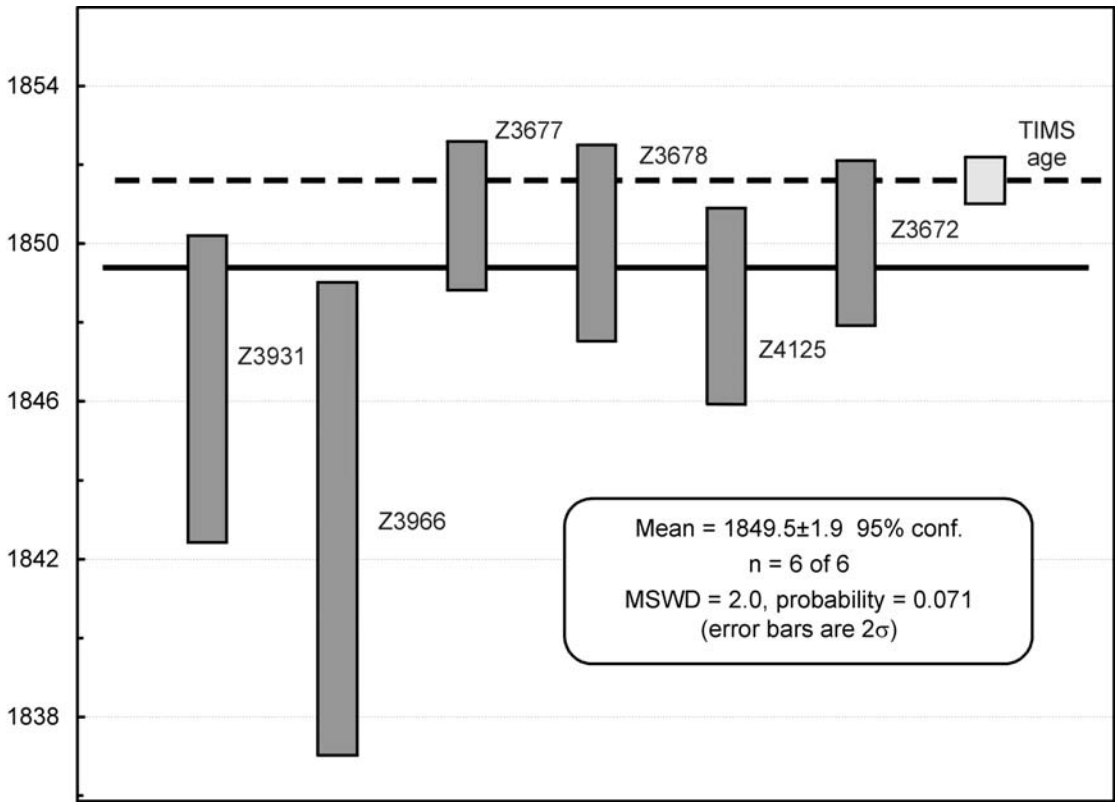

Figure 3a. Uncorrected data for QGNG. Data are in sequence, from Table 3. The solid line represents the mean age for the 6 sessions. The dashed line represents the TIMS reference age for the standard.

Part 1: Donington Suite

Previous work

Creaser (1989) constructed an informal stratigraphic framework for the Olympic Dam region of the Olympic Domain (Figure 4), subdividing older deformed granitoids, intruded by the Hiltaba Suite, into two suites based on petrographic and geochemical studies. All granitoids exhibiting evidence for deformation, and with a distinctive mineralogical feature: large, pink alkali feldspar megacrysts, were assigned to Suite #1. Creaser (1989) assigned an age of 1810-1845 Ma to Suite #1 based on the approximate U-Pb zircon ages of Mortimer et al. (1988a), and speculated their correlation with the 'Lincoln Complex' (now renamed the Donington Suite) on the southern Eyre Peninsula. In a later publication, Creaser (1995) refers to the suite as 'the 1843 Ma Donington Suite', assigning the age based on data for the Donington Suite from the southern and central Eyre Peninsula (Mortimer et al. 1988b).

For the Suite #2 granitoids, the situation is more complex. Suite #2 is a loose grouping of lithologically diverse mafic and felsic granitoids that 'appear to occupy a similar structural position'. Where intrusive relationships are unknown, granitoids are included in Suite #2 if they are deformed (unlike the Hiltaba Suite), but petrographically unlike Suite #1. Creaser (1989) acknowledged that the coherence of the suite may require revision after further detailed petrographic and isotopic work. The only age constraints on the Suite #2 granitoids were Rb-Sr minimum age estimates of 1748 Ma (muscovite), 1738 Ma (biotite) and 1686 Ma (biotite). Creaser (1989) assigned an age of 1685-1750 Ma to the suite and suggested the Moody Granite Suite of the southern Eyre Peninsula as a possible correlative.

Sampling rationale

To test Creaser's stratigraphic model, granitoids representing both Suite #1 and Suite #2 were collected for U-Pb dating.

Three Suite #1 megacrystic granites (*sensu lato*) were collected, from the Snake Gully (SGD4), Wirrda Well (WRD24) and Island Dam (IDD3) prospects. The megacrystic granites at Snake Gully and Wirrda Well are heterogeneously deformed, with intense deformation partitioned into thin zones of shear in a mylonitic fabric is developed. In contrast, the megacrystic granite at Island Dam exhibits a pervasive protomylonitic, steeply-dipping (45-60°) foliation.

Representatives of Suite #2 were collected from the Burden Hill (BHD1) and Acropolis (ACD6) prospects. The two representatives of Suite #2 are very different in character. The Burden Hill granodiorite is moderately to intensely foliated, exhibiting a pervasive, steeply dipping fabric (60-90°) very similar to the Suite #1 megacrystic granite from IDD3. ACD6 intersects a heterogeneous granitoid body, ranging from biotite tonalite and biotite norite to adamellite. It is heterogeneously deformed, with intense strain partitioned into thin intervals of low-angle shear (10-20°). Other units assigned to Suite #2 that have been analysed are; (1) schist within diamond drillhole ASD2W1 (Arcoona Station prospect); and (2) gneiss within drillhole SHD1 (Saddle Hill prospect). The results of these analyses are presented in Part 2 of this report.

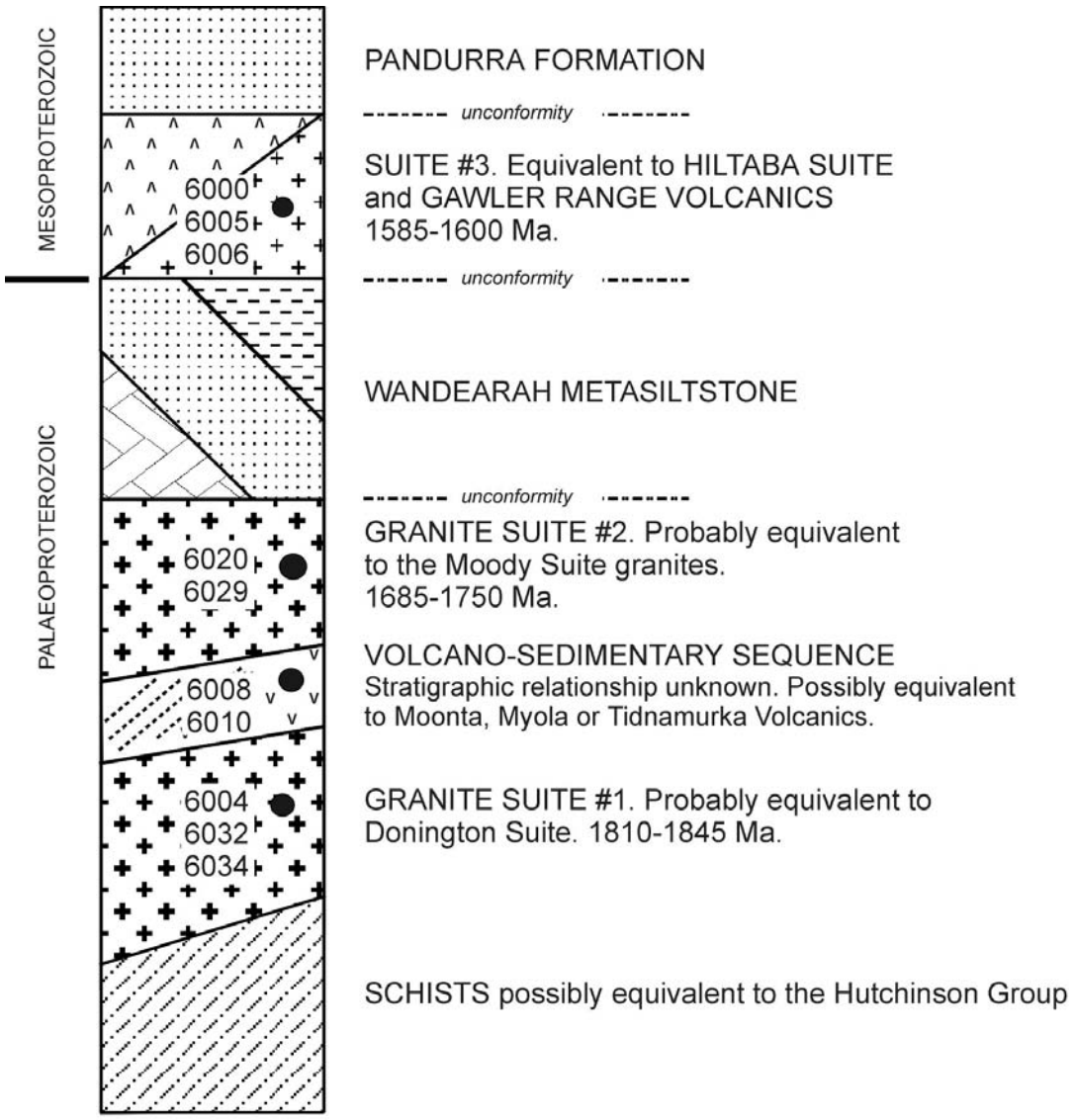

Figure 4. Stratigraphic column for the Olympic Domain constructed by Creaser (1989), illustrating the context of some samples analysed in this study (those from the Olympic Dam region).

200036 6004: megacrystic granodiorite, Snake Gully

1:250,000 sheet: Andamooka (SH5312)

1:100,000 sheet: Mattawearah (6237)

AMG: 689940 E 6634800 N

Location: The sample was taken from diamond drillhole SGD4, depth interval 341-347, 369.3-370.8, 379-382, 387.5-393, 476-480 m. The diamond drillhole is located within the Snake Gully prospect northeast of Olympic Dam.

Description: At Snake Gully, megacrystic granodiorite outcrops in drillholes SGD2 and SGD4 (Figure 5). The granodiorite is characterised by the presence of large, pink microcline megacrysts (~30%) exhibiting simple twinning, up to 7 cm in length. The granodiorite is heterogeneously deformed, ranging from weakly foliated, with chlorite and biotite defining a crude fabric, to moderately foliated, with aligned feldspars and flattened aggregates of quartz. Intense deformation is partitioned into thin zones of shear in which a schistose or mylonitic fabric is developed. These zones of intense shear are only a few metres thick, and grade sharply into less deformed rock.

In thin section, the groundmass (to the K-feldspar megacrysts) comprises 50% plagioclase, 30% quartz, 15-20% biotite, 1% oxide and accessory zircon. Plagioclase occurs partly as weakly sericitised and partly albitised grains to 8mm long and partly in large lenses of fine-grained micromosaic with minor quartz and biotite. Some of the fine-grained plagioclase and quartz also occurs within the larger plagioclase grains, partly disseminated and partly in veins and fractures, suggesting recrystallisation of the coarser plagioclase. There are also large lenses of unusually equigranular quartz, with most grains 1-2 mm in diameter, as well as fine-grained recrystallised quartz and rare feldspar. Lenses of fine-grained schistose biotite are mostly about 10mm long and enclose lenses of opaque oxide, including magnetite and hematite. Zircon is unusually abundant in the biotite-rich lenses, as crystals to 0.3 mm long, rarely with fractured, possibly inherite, cores. K-feldspar is confined to the megacrystic phase and does not appear in the groundmass.

(Purvis 2003)

Mount: Z3677

Description of zircons

The zircons from sample 200036 6004 are euhedral, with blunt and normal pyramids about equally common (Figure 6). Aspect ratios are mostly about 2:1, but range up to 4:1. Average length is about 100 μm. Most grains have continuous prismatic zoning. In rare instances, small subhedral to anhedral cores occur within the zoned zircon. Some grains contain fluid, rod-like silicate and round dark inclusions, and some are cracked and/or hematite stained. Grains containing dark inclusions, cracks and/or red hematite staining were avoided during analysis, in an effort to minimise common Pb contribution to the analyses.

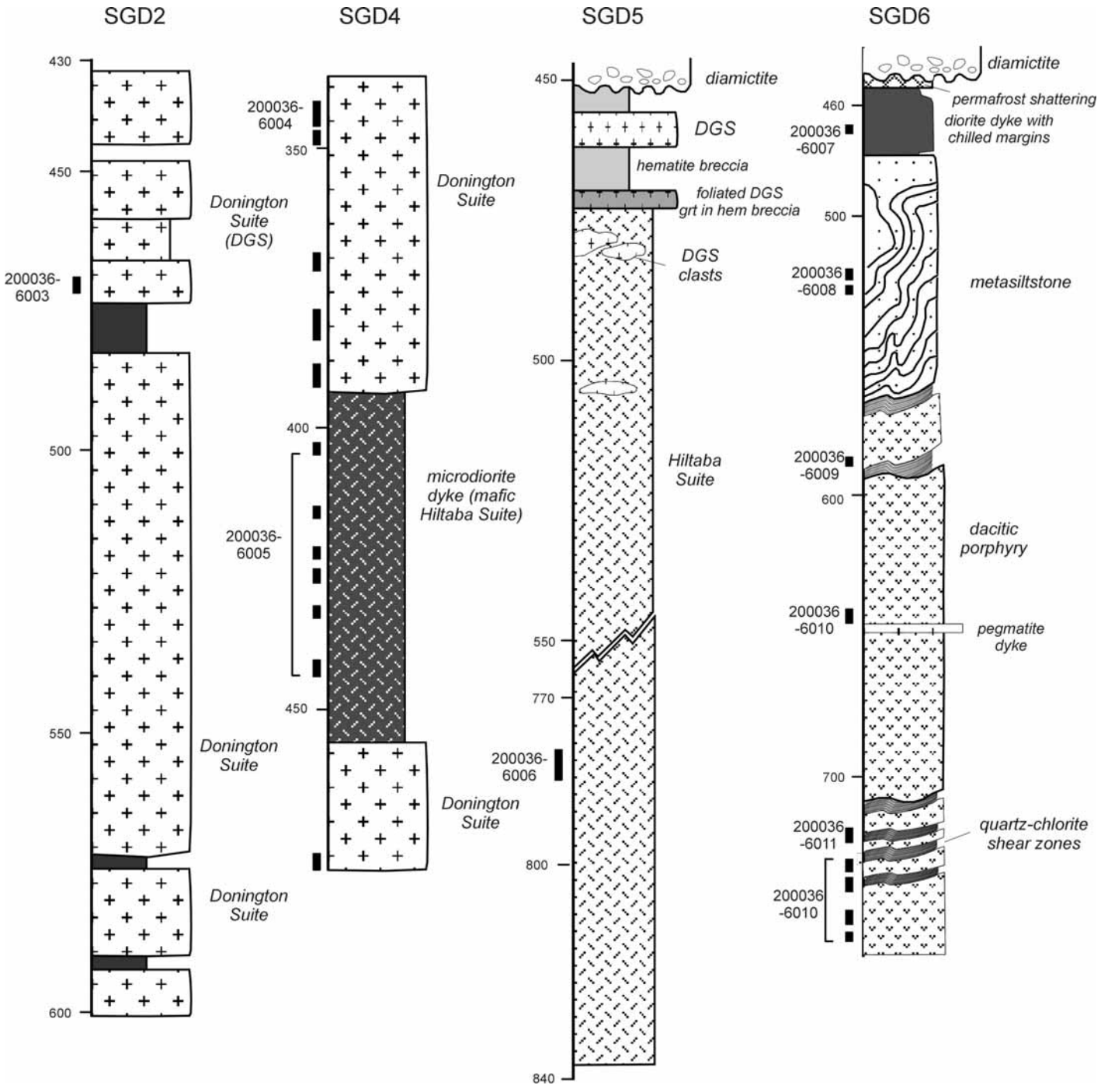

Figure 5. Stratigraphic logs for Snake Gully drill holes SGD 2,4,5 and 6 showing the location of samples collected for SHRIMP U-Pb dating.

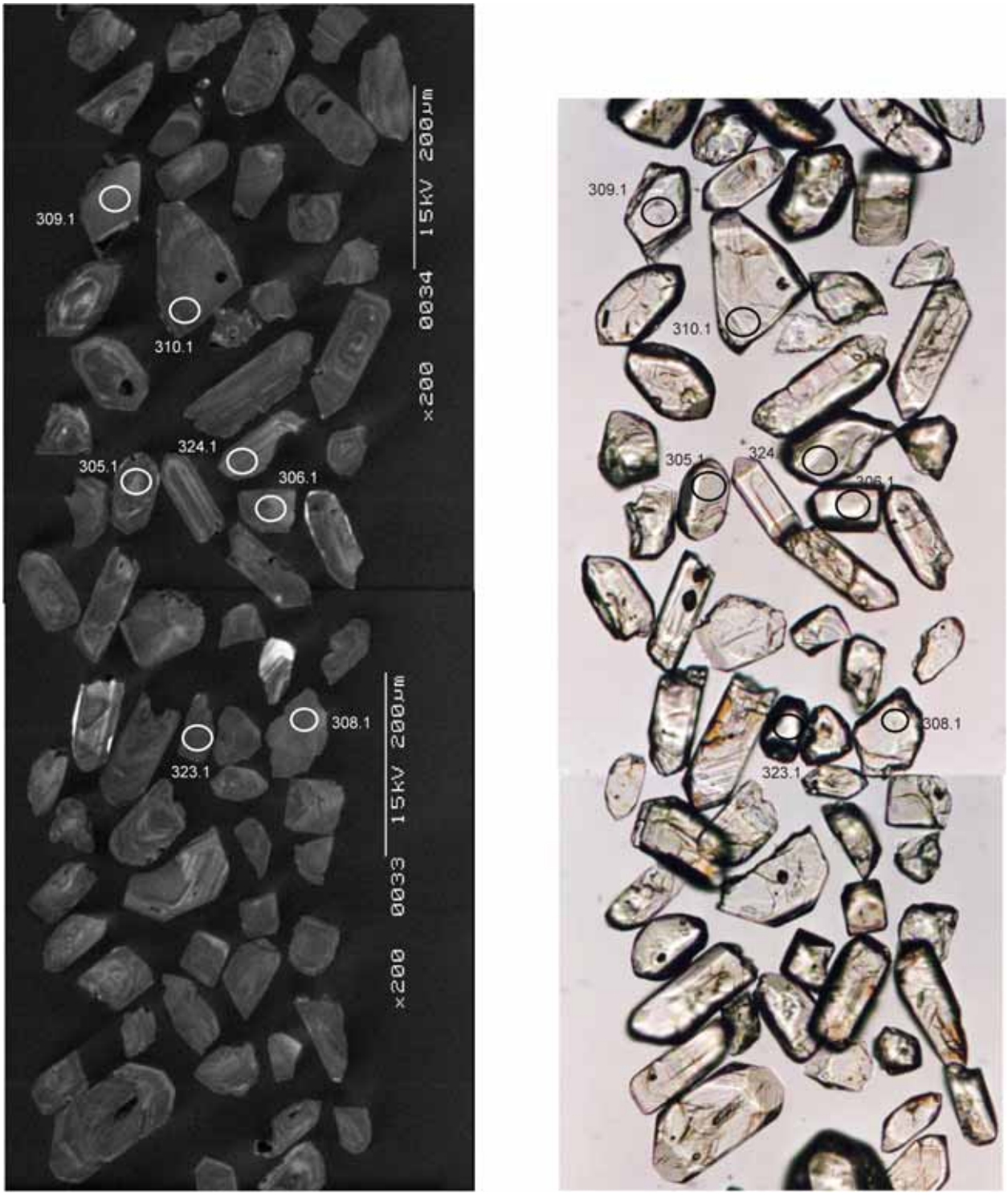

Figure 6. Representative CL (left) and transmitted light (right) images for sample 200036 6004: megacrystic granodiorite, Snake Gully prospect. SHRIMP analysis spots are labelled. Scale bar is 200 µm.

Concurrent standard data

Z3677 and sample 200036 6029 on mount Z3678 were analysed over the 4 day session. Data for the standard are presented in Appendix 3. Twenty six QGNG analyses for Z3677 give a calibration exponent of 2.08, with an upper limit of 2.26 and lower limit of 1.85 (at 95% confidence level). The weighted mean $^{207}Pb/^{206}Pb$ age for all 26 analyses is 1851.7 ± 2.4 Ma (MSWD = 1.12; probability of fit =0.31). Nine QGNG analyses for Z3678 give a calibration exponent of 2.29 with an upper limit of 2.98 and lower limit of 1.61. The weighted mean $^{207}Pb/^{206}Pb$ age for all 9 analyses is 1848.9 ± 3.5 Ma (MSWD = 1.05; probability of fit = 0.39). Because no significant calibration shift is observed between the two data batches, both have been combined for data processing. This yields a calibration exponent of 2.08, with an upper limit of 2.22 and lower limit of 1.86. Thus the nominal value of 2.0 has been used in data reduction. The $^{206}Pb/^{238}U$ reproducibility for QGNG is 1.34% (1σ; n = 35 of 35). The weighted mean $^{207}Pb/^{206}Pb$ age for all 35 analyses is 1850.7 ± 1.9 (MSWD = 1.09; probability of fit = 0.33).

The analyses are corrected for overcounts at mass ^{204}Pb (after Black in press, calculated assuming $^{206}Pb/^{238}U$-^{207}Pb-^{235}U age concordance), which forces the weighted mean $^{207}Pb/^{206}Pb$ age for QGNG to the TIMS reference value. The recalculated age for QGNG becomes 1851.6 ± 2.2 Ma (MSWD = 1.13; probability of fit = .27; n = 35 of 35). The sample data below are also corrected for overcounts.

Element abundance calibration was based on SL13 (n = 1).

Sample data

Thirty one of the 32 analyses yield a weighted mean age of 1853.0 ± 3.3 Ma. When corrected for overcounts at mass ^{204}Pb, the age becomes 1854.0 ± 3.3 Ma (MSWD = 1.43; probability of fit = 0.06; Figure 7,8). Grain (305.1) has a distinctively high Th/U ratio (Table 4), and is clearly older than the other analyses. Cathodoluminescence shows that the ion beam inadvertently overlapped a small, anhedral, luminescent core within the zircon grain.

Geochronological interpretation

The $^{207}Pb/^{206}Pb$ age of 1854.0 ± 3.3 Ma is considered to be the crystallisation age of the megacrystic granite.

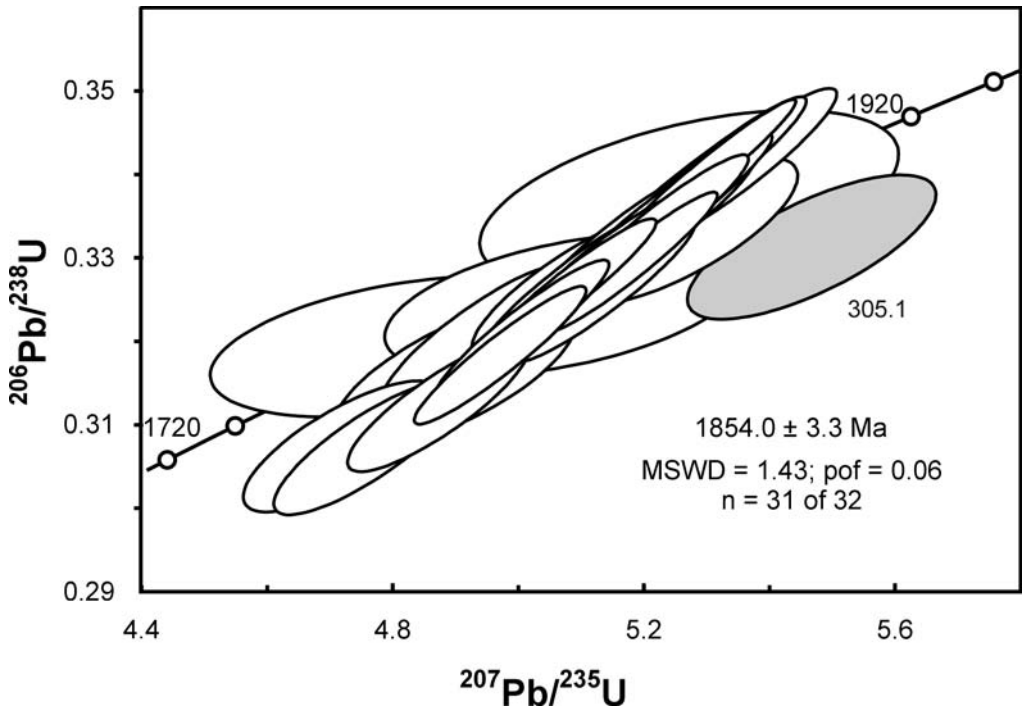

Figure 7. Concordia diagram for zircons in sample 200036 6004 showing radiogenic Pb compositions White-filled symbols represent analyses used in the weighted mean age calculation. Light grey ellipse represents xenocrystic grain.

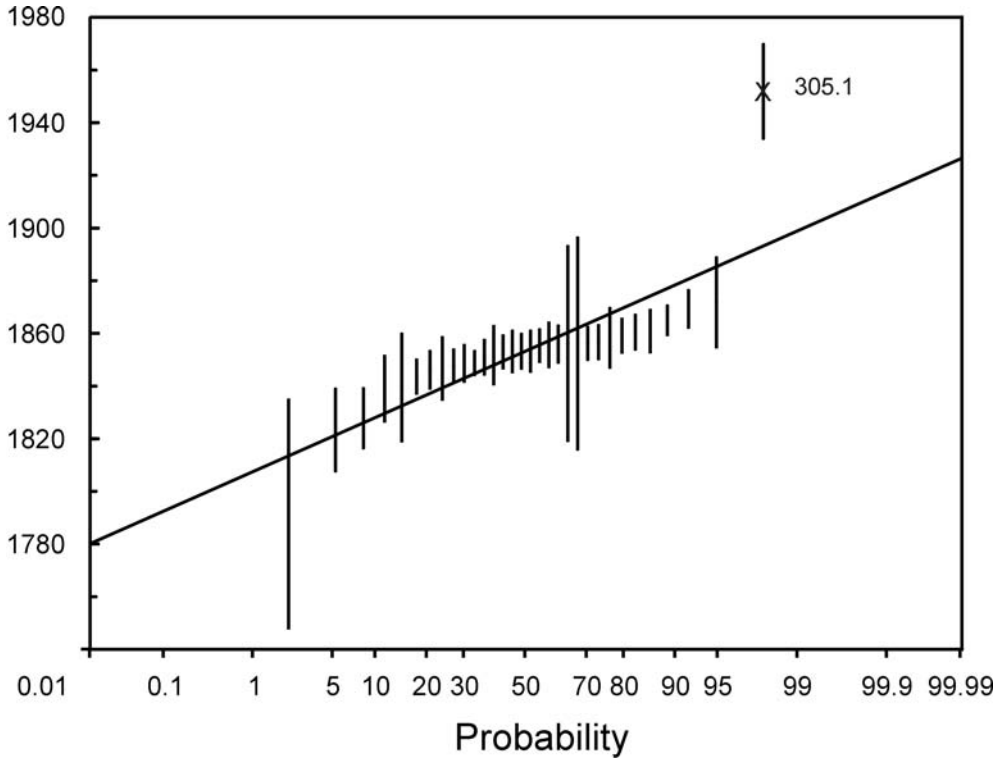

Figure 8. Probability diagram for individual zircon ages for sample 200036 6004. Error bars are 1σ. 305.1.is clearly older than the other analyses.

Table 4. SHRIMP analytical results for zircon from sample 200036 6004.

Spot	U (ppm)	Th (ppm)	$^{206}Pb_c$ (%)	$^{206}Pb^*$ (ppm)	$^{206}Pb^*/^{238}U$	±	$^{207}Pb^*/^{235}U$	±	$^{207}Pb^*/^{206}Pb^*$	±	conc (%)	207Pb/206Pb Age(Ma)	±
301.1	198	96	0.13	57	0.332	0.005	5.16	0.08	0.11295	0.00047	100	1848	8
302.1	444	227	0.47	119	0.312	0.004	4.87	0.07	0.11326	0.00052	94	1852	8
303.1	371	193	0.68	98	0.307	0.004	4.72	0.07	0.11150	0.00069	95	1824	11
304.1	270	142	0.11	75	0.321	0.004	5.00	0.07	0.11308	0.00043	97	1850	7
305.1	240	171	0.73	69	0.331	0.005	5.46	0.09	0.11979	0.00097	94	1953	14
306.1	275	102	0.09	75	0.318	0.004	4.97	0.07	0.11337	0.00043	96	1854	7
307.1	233	83	0.06	66	0.332	0.005	5.19	0.07	0.11351	0.00039	100	1856	6
308.1	241	100	0.06	70	0.336	0.005	5.25	0.07	0.11356	0.00039	100	1857	6
309.1	209	82	0.04	58	0.325	0.005	5.13	0.08	0.11440	0.00046	97	1871	7
310.1	419	149	0.21	120	0.333	0.005	5.22	0.07	0.11357	0.00035	100	1857	6
311.1	442	88	0.26	124	0.325	0.005	5.09	0.08	0.11367	0.00067	98	1859	11
312.1	355	151	0.51	100	0.326	0.005	5.07	0.08	0.11295	0.00054	98	1847	9
313.1	312	169	0.10	91	0.340	0.005	5.30	0.07	0.11322	0.00041	102	1852	7
314.1	251	128	2.02	70	0.319	0.004	4.82	0.10	0.10960	0.00164	100	1792	27
315.1	314	156	0.10	89	0.329	0.005	5.17	0.07	0.11410	0.00034	98	1866	6
316.1	198	98	0.07	55	0.326	0.005	5.07	0.07	0.11278	0.00041	99	1845	6
318.1	323	137	0.08	90	0.326	0.005	5.08	0.07	0.11303	0.00037	98	1849	6
319.1	251	124	1.49	74	0.336	0.005	5.27	0.13	0.11360	0.00204	101	1857	32
320.1	248	96	0.36	68	0.319	0.004	4.92	0.07	0.11181	0.00060	98	1829	10
321.1	200	108	0.66	58	0.333	0.005	5.25	0.08	0.11457	0.00087	99	1873	14
322.1	389	145	0.01	113	0.340	0.005	5.29	0.07	0.11308	0.00029	102	1849	5
323.1	335	169	1.79	95	0.324	0.005	5.07	0.10	0.11360	0.00148	97	1857	23
324.1	206	90	0.08	60	0.337	0.005	5.27	0.08	0.11340	0.00048	101	1855	8
325.1	417	213	0.54	114	0.315	0.004	4.89	0.09	0.11250	0.00113	96	1840	19
326.1	401	142	0.19	115	0.334	0.005	5.23	0.07	0.11351	0.00051	100	1856	8
327.1	216	78	0.09	61	0.327	0.005	5.13	0.08	0.11385	0.00043	98	1862	7
328.1	282	115	0.05	80	0.329	0.005	5.14	0.07	0.11336	0.00040	99	1854	6
329.1	203	97	0.00	58	0.331	0.005	5.20	0.08	0.11377	0.00041	99	1861	7
330.1	217	111	0.13	64	0.340	0.005	5.34	0.08	0.11387	0.00049	101	1862	8
331.1	246	122	0.08	70	0.330	0.005	5.17	0.08	0.11356	0.00043	99	1857	7
332.1	559	234	0.20	159	0.329	0.005	5.15	0.07	0.11334	0.00046	99	1854	7
333.1	277	142	0.38	73	0.307	0.004	4.76	0.07	0.11250	0.00069	94	1840	11

Data are 1σ precision. All Pb data are common Pb corrected based on measured ^{204}Pb (after Stacey and Kramer 1975).
Analysis date 8/4/2001; SHRIMP II

200036 6034: megacrystic syenogranite, Wirrda Well

1:250,000 sheet: Andamooka (SH5312)

1:100,000 sheet: Koolymilka (6236)

AMG: 685248 E 6605018 N

Location: The sample was taken from diamond drillhole WRD24, depth interval 578.7-579.5, 618.5-619.5, 854-855 m (Figure 9). The diamond drillhole is located within the Wirrda Well prospect near Olympic Dam.

Description: At Wirrda Well, the megacrystic granite is heterogeneously deformed, ranging from weakly foliated, with chlorite defining a crude fabric, to moderately foliated, with aligned feldspars and flattened aggregates of quartz. Intense deformation is partitioned into thin zones of shear in which a schistose or mylonitic fabric is developed (Figure 9). At Wirrda Well, subeconomic mineralisation and intense hydrothermal alteration (sericitisation, chloritisation and hematisation) and brecciation occurs. The low Ca and Na content of the granite (Table 29) reflects the intense sericitisation observed. No relict biotite is preserved, and the mafic component is green, reflecting chlorite replacement. The megacrystic granite intersected by WRD24 is less brecciated than in other WRD drill holes, and a sample was obtained from the least altered intervals within this drill hole.

In thin section the sample contains megacrysts of microcline 40-45 mm long and 20-25 mm wide. Abundant sericitised plagioclase occurs as anhedral to euhedral grains 2-6 mm long, both in and adjacent to the microcline, and patches and veins of fluorite and sericite occur in the microcline, locally with minor hematite. The groundmass (to the microcline megacrysts) is very quartz-rich, with perhaps 35% plagioclase altered completely to sericite and chlorite, as well as altered biotite (10-15%), euhedral crystals of zircon about 0.1 mm in diameter, and minor hematite and chalcopyrite. Aggregates of chlorite, sericite, quartz and carbonate in various proportions have replaced biotite flakes to 4 mm long. Grains and lenses of opaque oxide occur in the altered biotite.

(Purvis 2003)

Mount: Z3678

Description of zircons

The zircons from sample 200036 6034 are predominantly broken, possibly due to the pervasive fracturing within the megacrystic syenogranite, or perhaps larger grains were broken during crushing in the lab. The broken fragments are about 80–100 μm in size (Figure 10). Complete grains exhibit blunt to low angle pyramidal terminations. Most grains reveal internal zoning under cathodoluminescence, with the zones commonly truncated by broken grain boundaries. Small round to rod-shaped silicate inclusions are present in some grains. The few grains that are cracked and/or hematite-stained were avoided during analysis.

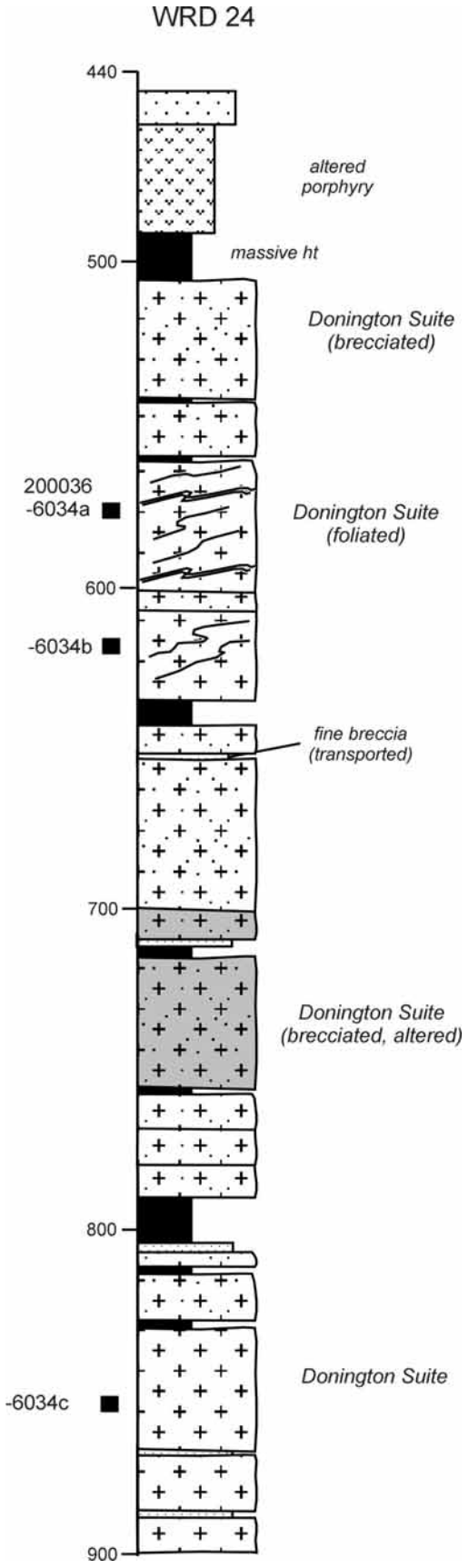

Figure 9. Stratigraphic logs for Wirrda Well drill hole WRD24 showing the location of samples collected for SHRIMP U-Pb dating.

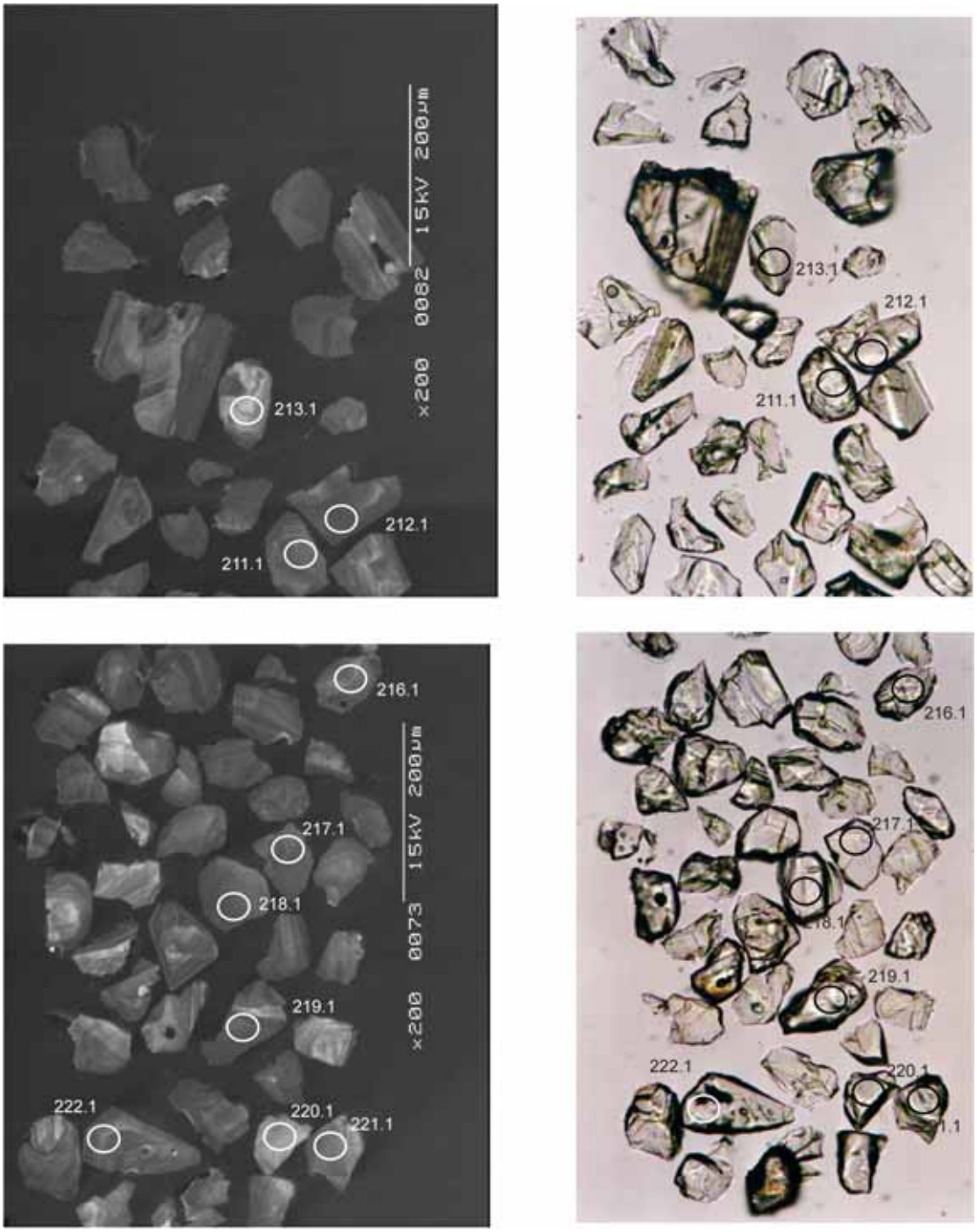

Figure 10. Representative CL (left) and transmitted light (right) images for sample 200036 6034: megacrystic syenogranite, Wirrda Well prospect. SHRIMP analysis spots are labelled. Scale bar is 200 µm.

Concurrent standard data

Data for the standard are presented in Appendix 3. No data were excluded from the Pb/U calibration, to give a calibration exponent of 2.22, with an upper limit of 2.43 and a lower limit of 2.01 (at the 95% confidence level). Thus the nominal value of 2.0 has been used in data reduction. The $^{206}Pb/^{238}U$ reproducibility for QGNG is 1.16% (1σ; n=24 of 24). The weighted mean $^{207}Pb/^{206}Pb$ age for all 24 analyses is 1850.0 ± 2.5 Ma (MSWD = 0.95; probability of fit = .53).

The analyses are corrected for overcounts at mass ^{204}Pb (after Black in press, calculated assuming $^{206}Pb/^{238}U$-^{207}Pb-^{235}U age concordance), which forces the weighted mean $^{207}Pb/^{206}Pb$ age for QGNG to the TIMS reference value. The recalculated age for QGNG becomes 1851.3 ± 2.4 Ma (MSWD = 0.96; probability of fit = .51; n=24 of 24). The sample data below are also corrected for overcounts.

Element abundance calibration was based on SL13 (n = 1).

Sample data

The 22 analyses do not conform to a single population, yielding an unacceptable MSWD of 3.9. Five of the analyses are variably discordant (Figure 11). A probability diagram suggests that three of these discordant analyses have distinctly low $^{207}Pb/^{206}Pb$ ages; the most discordant, high U grain (215.1), and two grains with high common Pb (216.1 and 206.1; Figure 12). The remaining 19 analyses yield a weighted mean $^{207}Pb/^{206}Pb$ age of 1847.6 ± 3.6 Ma. When corrected for overcounts at mass ^{204}Pb, the age becomes 1849.6 ± 3.5 Ma, with an acceptable MSWD of 1.14 (probability of fit = 0.3).

Geochronological interpretation

The $^{207}Pb/^{206}Pb$ age of 1849.6 ± 3.5 Ma is considered to be the crystallisation age of the megacrystic granite.

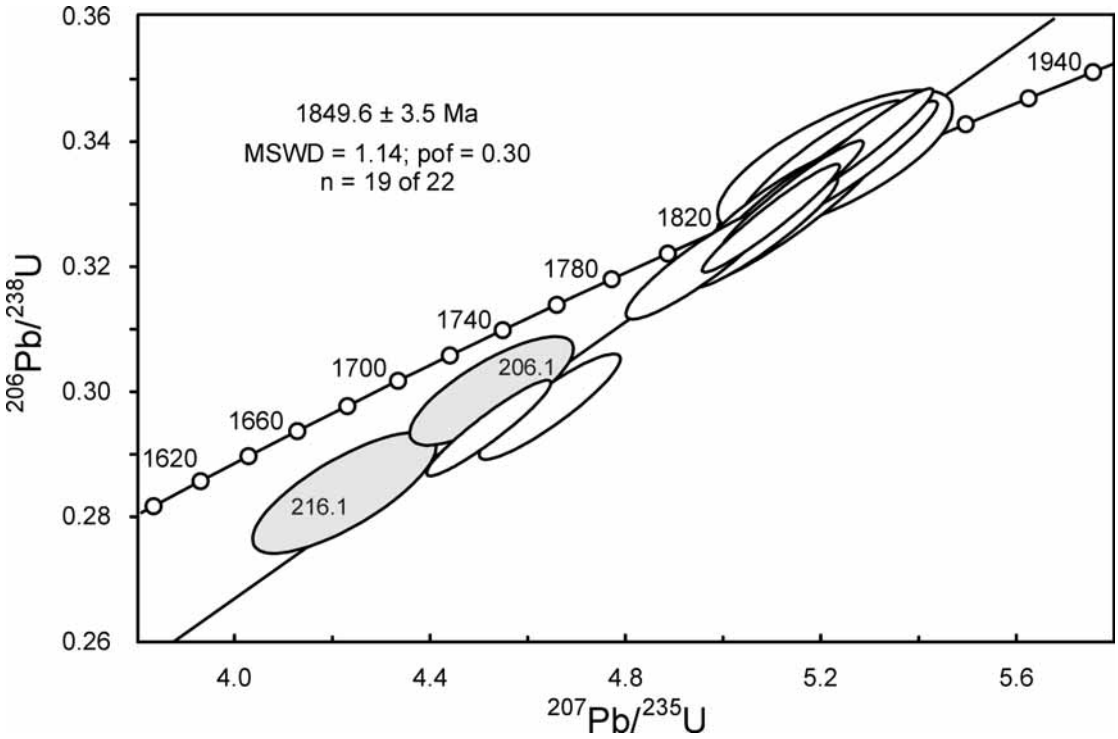

Figure 11. Concordia diagram for zircons in sample 200036 6034. White-filled symbols represent analyses used in the weighted mean age calculation. Discordant, high common Pb analyses are light grey. One discordant analysis (215.1) plots below the range of the figure.

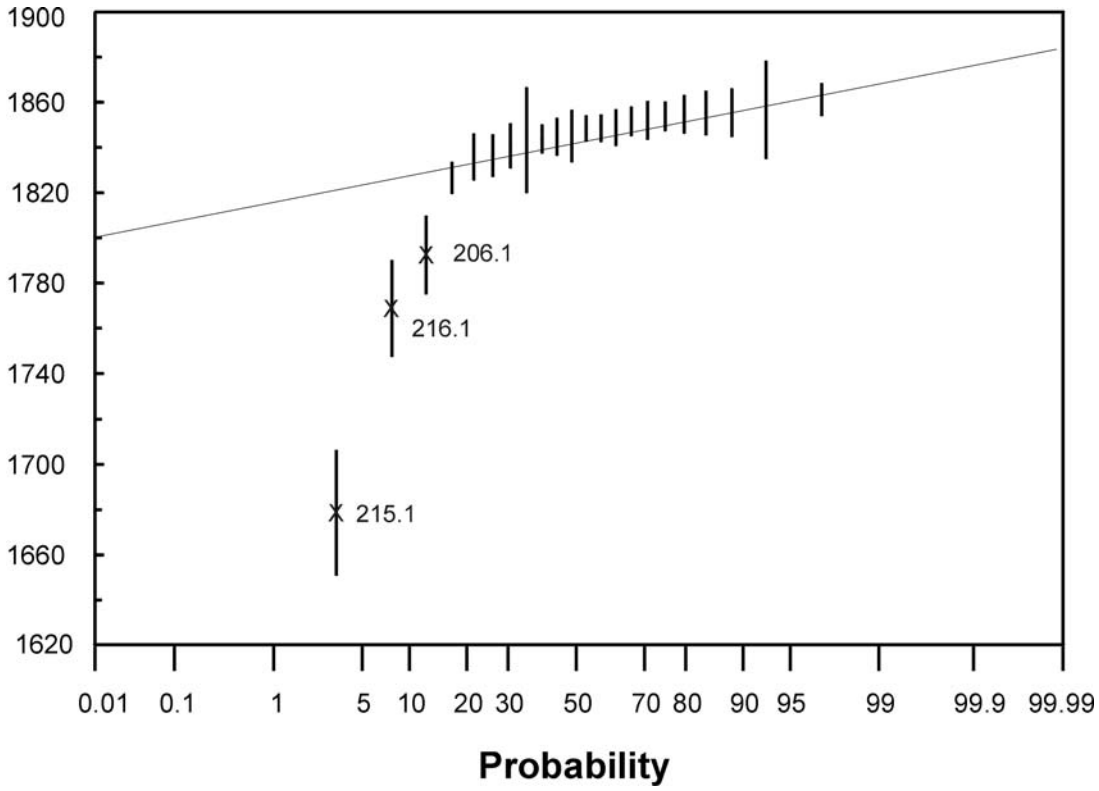

Figure 12. Probability diagram for sample 200036 6034. The three youngest analyses are clearly younger than the main population.

Table 5. SHRIMP analytical results for zircon from sample 200036 6034.

Spot	U (ppm)	Th (ppm)	$^{206}Pb_c$ (%)	$^{206}Pb^*$ (ppm)	$^{206}Pb^*/^{238}U$	±	$^{207}Pb^*/^{235}U$	±	$^{207}Pb^*/^{206}Pb^*$	±	conc (%)	207Pb/206Pb Age(Ma)	±
201.1	99	96	0.01	28	0.332	0.004	5.18	0.07	0.11309	0.00062	100	1850	10
202.1	149	145	-0.02	43	0.333	0.004	5.20	0.07	0.11322	0.00051	100	1852	8
203.1	150	88	0.01	42	0.329	0.004	5.13	0.07	0.11297	0.00050	99	1848	8
204.1	236	122	0.02	66	0.324	0.004	5.08	0.07	0.11346	0.00040	98	1856	6
205.1	158	80	0.06	44	0.324	0.004	5.07	0.07	0.11355	0.00050	97	1857	8
206.1	92	42	0.39	24	0.298	0.004	4.52	0.07	0.10986	0.00099	94	1797	16
207.1	163	95	0.02	45	0.319	0.004	4.94	0.06	0.11244	0.00054	97	1839	9
208.1	398	155	0.84	110	0.318	0.004	4.97	0.08	0.11360	0.00136	96	1858	21
209.1	118	59	0.05	33	0.327	0.004	5.09	0.07	0.11276	0.00058	99	1844	9
210.1	271	173	0.49	69	0.295	0.004	4.62	0.06	0.11351	0.00060	90	1856	10
211.1	178	106	0.07	51	0.333	0.004	5.21	0.07	0.11339	0.00050	100	1854	8
212.1	359	133	0.15	90	0.292	0.004	4.51	0.06	0.11173	0.00042	90	1828	7
213.1	50	35	0.04	14	0.335	0.005	5.24	0.10	0.11330	0.00125	101	1852	21
214.1	101	56	-0.03	28	0.327	0.005	5.13	0.13	0.11370	0.00216	98	1860	35
215.1	858	413	1.41	124	0.166	0.003	2.36	0.05	0.10310	0.00155	59	1681	27
216.1	232	135	0.57	56	0.282	0.004	4.22	0.08	0.10840	0.00119	90	1772	21
217.1	258	144	0.04	73	0.330	0.004	5.13	0.07	0.11283	0.00038	99	1845	6
218.1	303	141	0.02	88	0.338	0.004	5.27	0.07	0.11311	0.00036	101	1850	6
219.1	308	126	0.03	86	0.326	0.004	5.08	0.07	0.11310	0.00035	98	1850	6
220.1	96	47	0.11	28	0.335	0.004	5.20	0.07	0.11249	0.00066	101	1840	11
221.1	178	79	-0.02	51	0.336	0.004	5.27	0.07	0.11396	0.00046	100	1864	7
222.1	249	123	0.04	70	0.328	0.004	5.13	0.07	0.11332	0.00040	99	1853	6

Data are 1σ precision. All Pb data are common Pb corrected based on measured ^{204}Pb (after Stacey and Kramer 1975).
Analysis date 4/6/2001; SHRIMP II

200036 6032: intensely foliated megacrystic syenogranite, Island Dam

1:250,000 sheet: Andamooka (SH5312)

1:100,000 sheet: Scott (6436)

AMG: 739355 E 6590276 N

Location: The sample was taken from diamond drillhole IDD3, depth interval 447.7-448.4, 453.6-454.2, 470.6-470.8, 501.2-501.6 m (Figure 13). The diamond drillhole is located within the Island Dam prospect of the Olympic Domain.

Description: This is a foliated syenogranite with a protomylonitic texture. It has about 35% microcline as augen 2-10 mm or more in length, partly pulled apart or fragmented, locally with fragments in an imbricate pattern. Lenses of recrystallised feldspar are also abundant and largely composed of microcline. Partly recrystallised ribbons of quartz, to 20 mm long, are abundant (30-35%), with highly strained old grains and lenses composed of small, recrystallised new grains. Plagioclase (~10-15%) is partly replaced by sericite and occurs partly as scattered, rounded grains to 3mm long and partly in aggregates of recrystallised feldspar that seem to be dominated by microcline. Lenses of schistose sericite are also abundant (15-20%), as well as biotite lamellae and lenses rich in coarser-grained muscovite, to 1 mm in grainsize (7-8%). Some of the schistose biotite (7-8%) has been altered to chlorite and muscovite. Rare lenses of decussate fine-grained biotite have been totally altered to chlorite, muscovite and carbonate. Disseminated zircon, to 0.2mm in grainsize, occurs mostly in micaceous lamellae, and there is minor opaque oxide.

(Purvis 2003)

Mount: Z3678

Description of zircons

Zircons extracted from sample 200036 6032 are euhedral to subhedral, with blunt to normal pyramids or slightly rounded terminations (Figure 14). Aspect ratios are mostly between 1:1 and 2:1. Grains range between 70 and 270 μm in length. Cathodoluminescence shows that nearly all grains consist of uninterrupted prismatic zones that would have formed during a single igneous event. A few grains also contain small, poorly luminescent cores. Small round to rod-shaped silicate inclusions are present in some grains. Many grains contain cracks, and or are hematite stained. These grains were avoided during analysis.

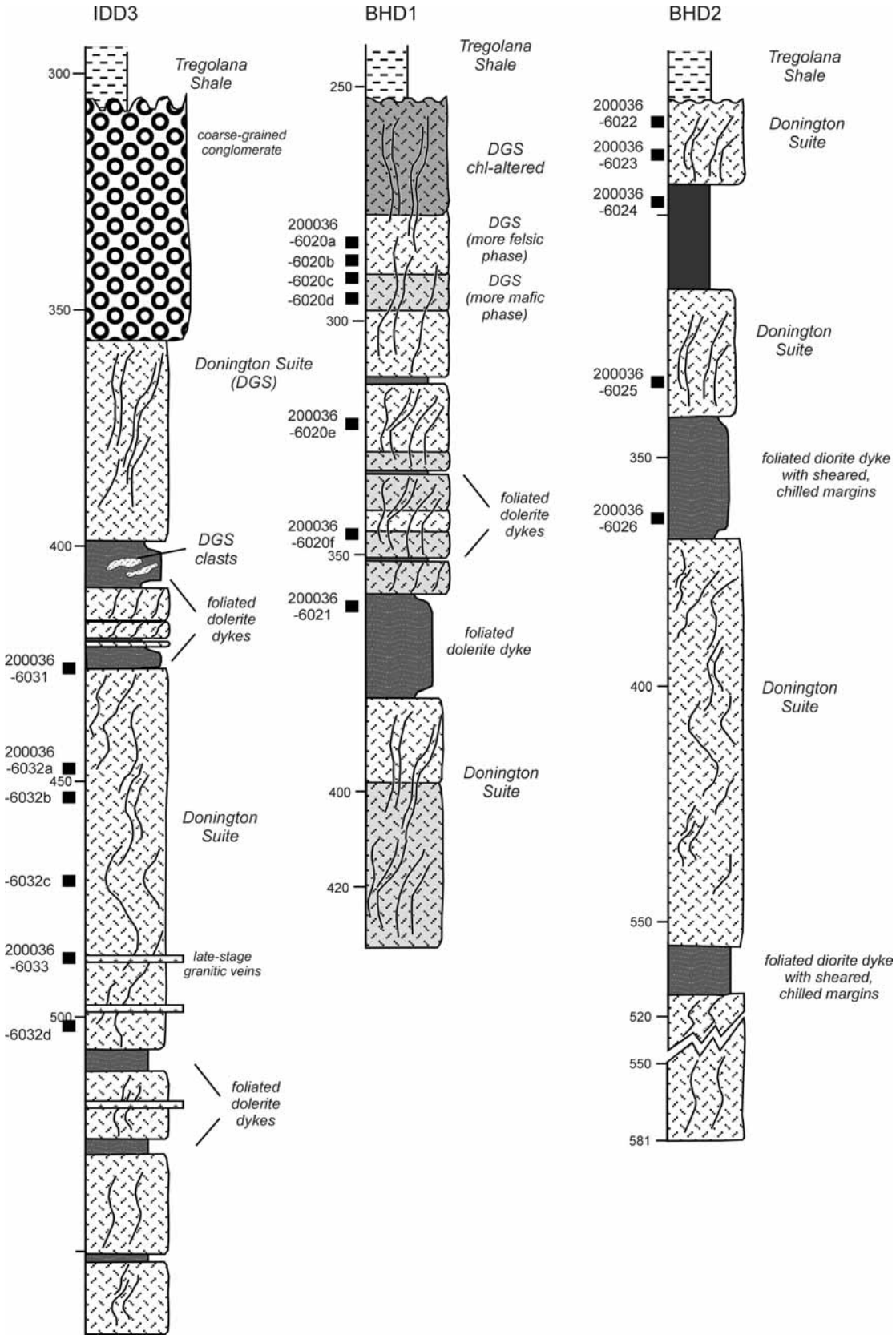

Figure 13. Stratigraphic logs for drill holes from Island Dam and Burden Hill showing the location of samples collected for SHRIMP U-Pb dating and geochemical analysis.

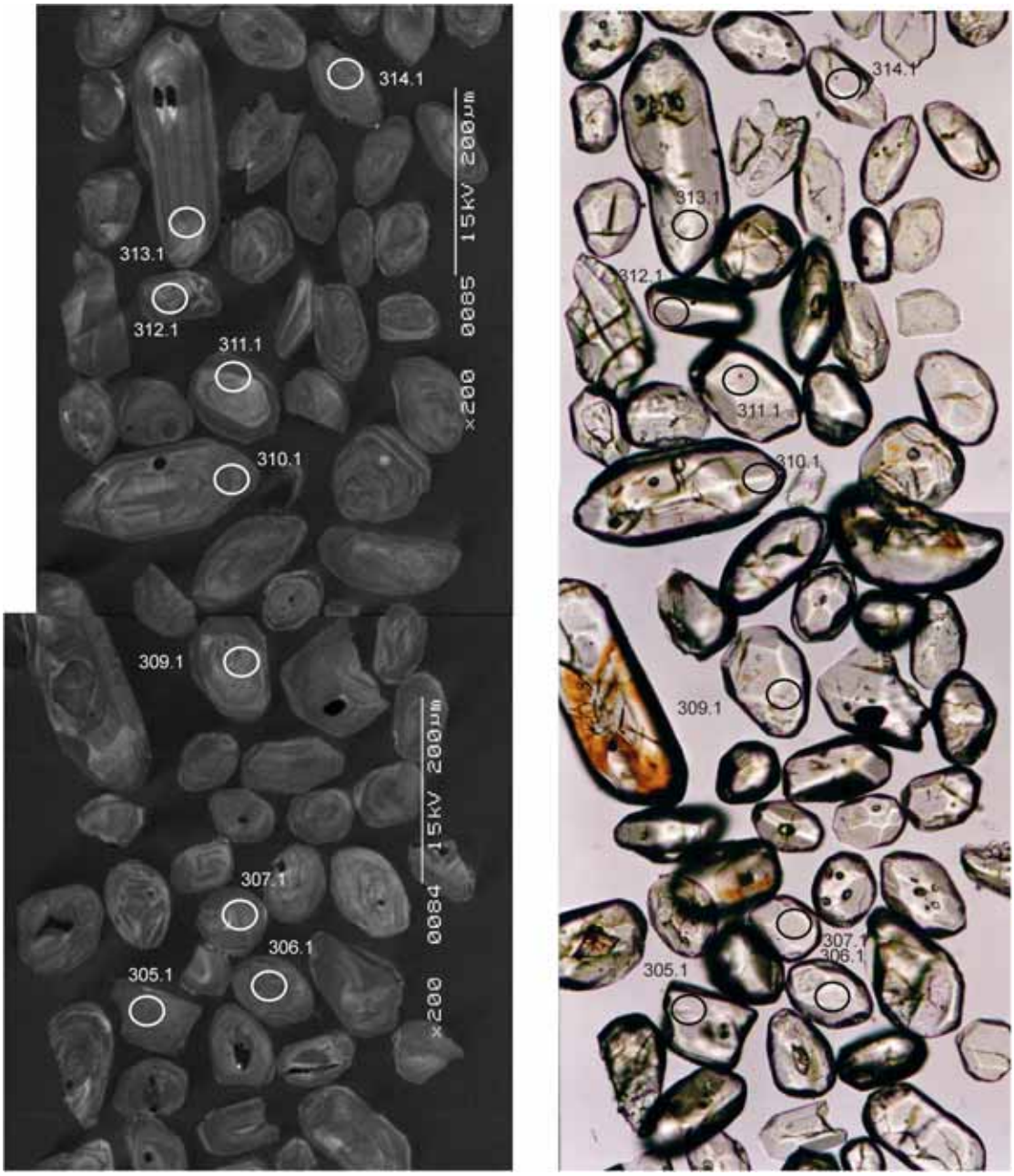

Figure 14. Representative CL (left) and transmitted light (right) images for sample 200036 6032: intensely deformed megacrystic syenogranite, Island Dam prospect. SHRIMP analysis spots are labelled. Scale bar is 200 µm.

Concurrent standard data

Data for the standard are presented in Appendix 3. No data were excluded from the Pb/U calibration, to give a calibration exponent of 2.22, with an upper limit of 2.43 and a lower limit of 2.01 (at the 95% confidence level). Thus the nominal value of 2.0 has been used in data reduction. The $^{206}Pb/^{238}U$ reproducibility for QGNG is 1.16% (1σ; n=24 of 24). The weighted mean $^{207}Pb/^{206}Pb$ age for all 24 analyses is 1850.0 ± 2.5 Ma (MSWD = 0.95; probability of fit = .53).

The analyses are corrected for overcounts at mass ^{204}Pb (after Black in press, calculated assuming $^{206}Pb/^{238}U$-^{207}Pb-^{235}U age concordance), which forces the weighted mean $^{207}Pb/^{206}Pb$ age for QGNG to the TIMS reference value. The recalculated age for QGNG becomes 1851.3 ± 2.4 Ma (MSWD = 0.96; probability of fit = .51; n=24 of 24). The sample data below are also corrected for overcounts.

Element abundance calibration was based on SL13 (n = 1).

Sample data

Twenty three of the twenty four analyses yield a weighted mean age of 1858.5 ± 4.1 Ma. When corrected for overcounts at mass ^{204}Pb, the age becomes 1860.4 ± 4.1 Ma (MSWD = 1.48; probability of fit = .07; Figure 15). The probability diagram suggests that the youngest analysis (323.1) is an outlier (Figure 16), and its inclusion would yield an unacceptably high MSWD of 1.68. Grain 323.1 has higher common ^{206}Pb and is more discordant than the other grains, suggesting Pb loss has occurred.

Geochronological interpretation

The $^{207}Pb/^{206}Pb$ age of 1860.4 ± 4.1 Ma is considered to be the crystallisation age of the megacrystic granite.

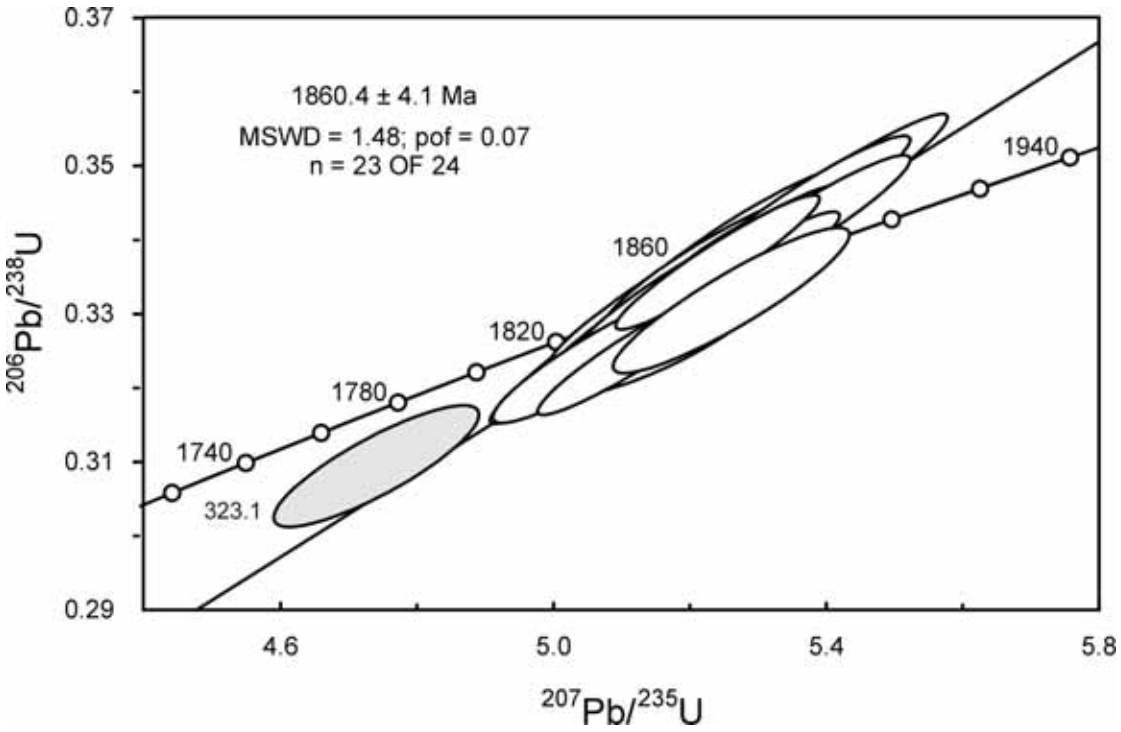

Figure 15. Concordia diagram for zircons in sample 200036 6032 showing radiogenic Pb compositions. White-filled symbols represent analyses used in the weighted mean age calculation. Light grey ellipse represents Pb loss.

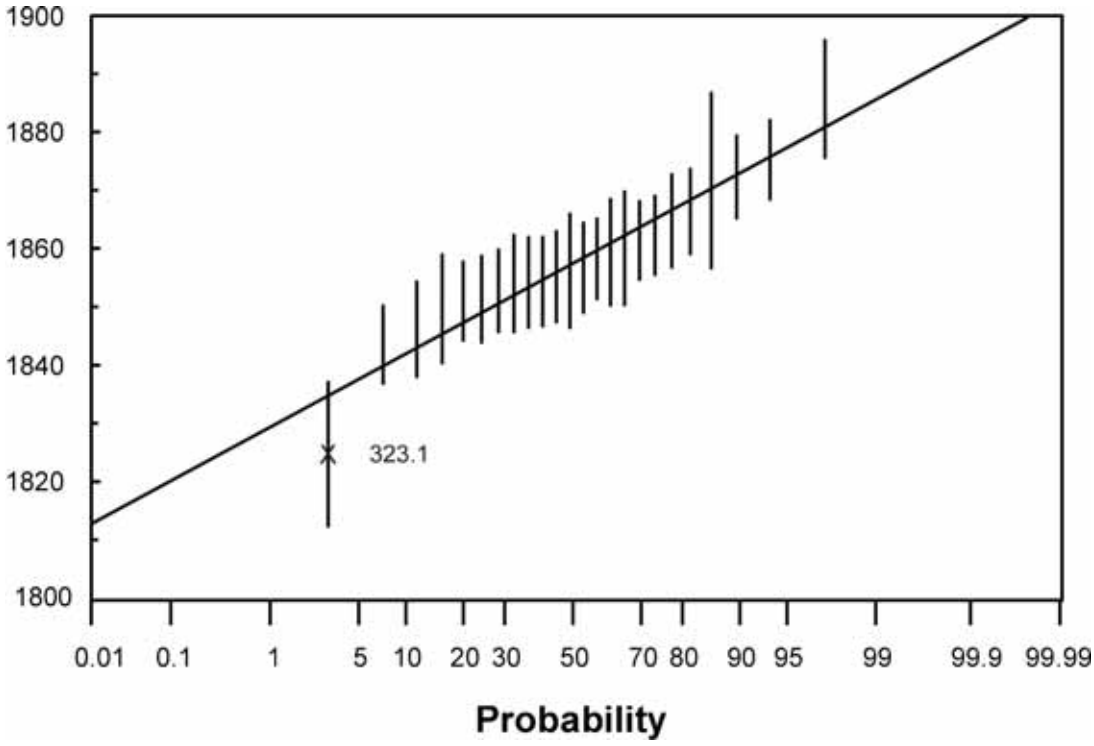

Figure 16. Probability diagram of individual zircon ages for sample 200036 6032.

Table 6. SHRIMP analytical results for zircon from sample 200036 6032.

Spot	U (ppm)	Th (ppm)	$^{206}Pb_c$ (%)	$^{206}Pb^*$ (ppm)	$\frac{^{206}Pb^*}{^{238}U}$	±	$\frac{^{207}Pb^*}{^{235}U}$	±	$\frac{^{207}Pb^*}{^{206}Pb^*}$	±	conc (%)	207Pb/206Pb Age(Ma)	±
301.1	229	89	0.10	65	0.331	0.004	5.18	0.07	0.11331	0.00045	100	1853	7
302.1	166	76	0.03	48	0.335	0.004	5.23	0.07	0.11326	0.00055	100	1852	9
303.1	232	163	0.05	66	0.329	0.004	5.16	0.07	0.11365	0.00045	99	1859	7
304.1	202	85	0.15	56	0.322	0.004	5.05	0.07	0.11383	0.00056	97	1862	9
305.1	219	88	0.01	61	0.326	0.004	5.11	0.07	0.11376	0.00042	98	1860	7
306.1	228	119	0.03	66	0.335	0.004	5.23	0.07	0.11329	0.00041	101	1853	7
307.1	201	78	-0.01	57	0.331	0.004	5.20	0.07	0.11401	0.00048	99	1864	8
308.1	195	64	0.06	56	0.334	0.009	5.23	0.14	0.11363	0.00057	100	1858	9
309.1	151	69	0.05	44	0.338	0.004	5.27	0.07	0.11304	0.00050	101	1849	8
310.1	198	99	0.03	58	0.340	0.004	5.36	0.07	0.11427	0.00043	101	1868	7
311.1	206	52	0.04	58	0.328	0.004	5.13	0.07	0.11351	0.00047	99	1856	7
312.1	190	92	-0.03	54	0.330	0.004	5.18	0.07	0.11389	0.00063	99	1862	10
313.1	187	114	-0.02	53	0.329	0.004	5.16	0.07	0.11396	0.00043	98	1864	7
314.1	180	82	0.29	51	0.330	0.004	5.25	0.08	0.11551	0.00064	97	1888	10
315.1	185	76	0.00	54	0.343	0.004	5.36	0.07	0.11343	0.00044	102	1855	7
316.1	166	95	0.05	48	0.337	0.004	5.27	0.07	0.11353	0.00050	101	1857	8
317.1	182	74	-0.03	52	0.333	0.004	5.26	0.07	0.11467	0.00047	99	1875	7
318.1	149	69	-0.01	43	0.336	0.004	5.29	0.07	0.11423	0.00051	100	1868	8
319.1	200	122	-0.02	56	0.323	0.004	5.12	0.07	0.11484	0.00046	96	1877	7
320.1	228	90	0.20	64	0.326	0.004	5.14	0.08	0.11461	0.00095	97	1874	15
321.1	170	114	-0.05	48	0.329	0.004	5.15	0.07	0.11354	0.00052	99	1857	8
322.1	229	107	0.03	65	0.331	0.004	5.15	0.07	0.11282	0.00041	100	1845	7
323.1	276	70	0.42	73	0.307	0.004	4.73	0.07	0.11165	0.00075	95	1826	12
324.1	152	67	0.00	44	0.336	0.004	5.27	0.07	0.11361	0.00048	101	1858	8

Data are 1σ precision. All Pb data are common Pb corrected based on measured ^{204}Pb (after Stacey and Kramer 1975).
Analysis date 4/6/2001; SHRIMP II

200036 6020: megacrystic granodiorite, Burden Hill (intensely foliated granodiorite)

1:250,000 sheet: Andamooka (SH5312)

1:100,000 sheet: Andamooka (6336)

AMG: 723430 E 6594500 N

Location: The sample was taken from diamond drillhole BHD1, depth interval 283.6-284, 285.5-285.7, 286.5-286.9, 290.5-291, 296.7-298.2, 321.8-322.2 m (Figure 13). The diamond drillhole is located within the Burden Hill prospect of the Olympic Domain.

Description: This sample has abundant augen of largely sericitised plagioclase and less abundant microcline to 4 mm long, with aggregates of epidote in some augen of plagioclase and microcline. The groundmass is laminated with quartz-rich lamellae, feldspathic or quartzofeldspathic lamellae and micaceous lamellae mostly less than 3 mm wide. The quartz is all recrystallised but has some lenses with low-angle grain-boundaries suggesting old-grain control. The feldspar within the groundmass includes sericitised plagioclase as well as less abundant microcline. Abundant schistose biotite has been totally altered to chlorite and leucoxene, but schistose sericite is also common. Rare opaque grains occur, mostly in epidote, and there is accessory apatite as well as zircon to 0.1 mm in grainsize. The mineralogy indicates a gneissic granodiorite.

(Purvis 2003)

Mount: Z3678

Description of zircons

Zircons extracted from sample 200036 6020 are euhedral and have squat to rounded shapes, with blunt or low angle pyramids or slightly rounded terminations, and aspect ratios mostly between 1:1 and 1.5:1 (Figure 17). The grains are fairly uniform in size, averaging about 80 μm in length. Cathodoluminescence identifies ubiquitous prismatic zoning, consistent with an igneous origin. Some grains also contain round, poorly luminescent cores. Small round to rod-shaped silicate inclusions are present in some grains. Hematite and cracks affect a fair proportion of grains, and these were avoided during analysis.

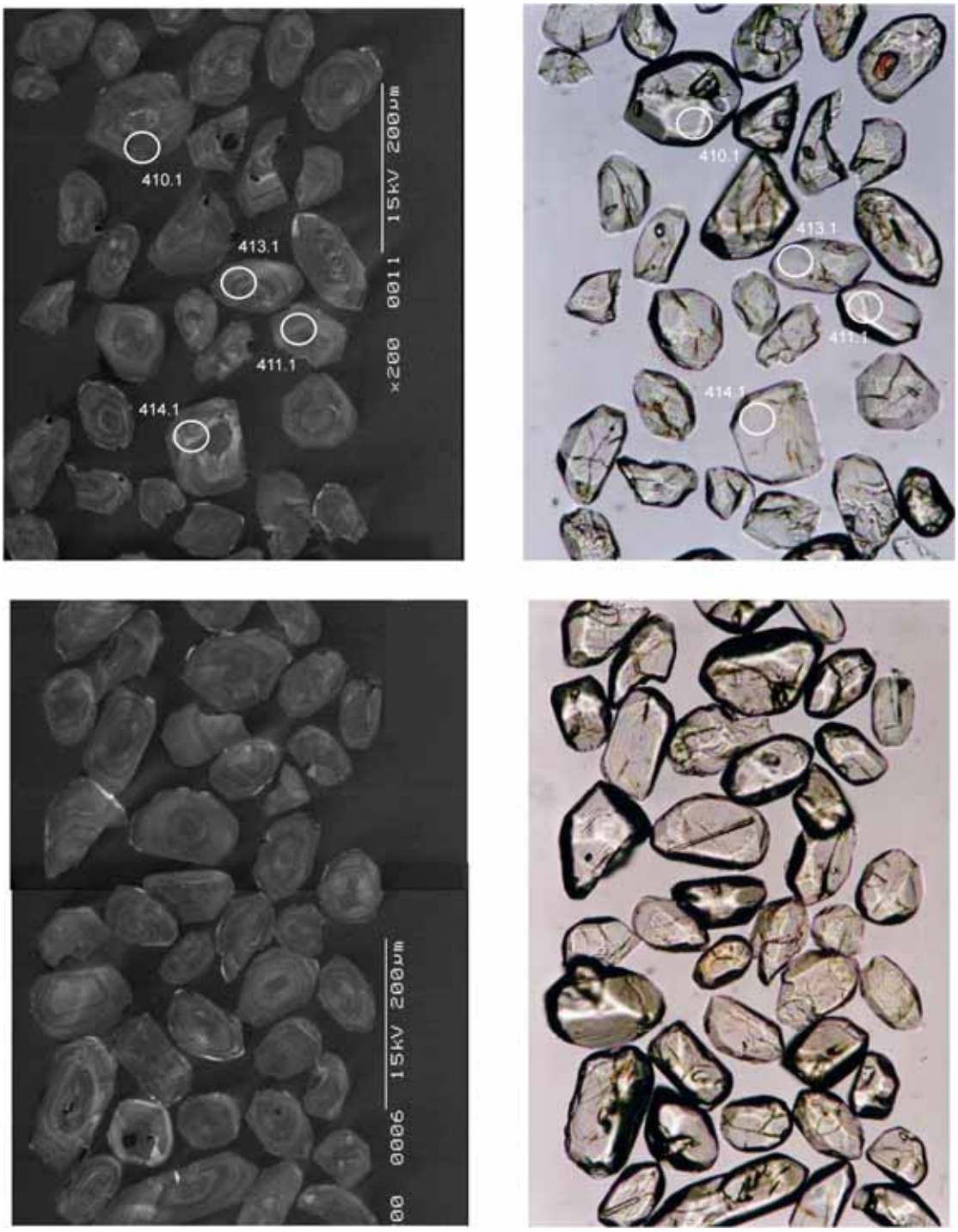

Figure 17. Representative CL (left) and transmitted light (right) images for sample 200036 6020: intensely foliated megacrystic granodiorite, Burden Hill prospect. SHRIMP analysis spots are labelled. Scale bar is 200 µm.

Concurrent standard data

Data for the standard are presented in Appendix 3. No data were excluded from the Pb/U calibration, to give a calibration exponent of 2.22, with an upper limit of 2.43 and a lower limit of 2.01 (at the 95% confidence level). Thus the nominal value of 2.0 has been used in data reduction. The $^{206}Pb/^{238}U$ reproducibility for QGNG is 1.16% (1σ; n=24 of 24). The weighted mean $^{207}Pb/^{206}Pb$ age for all 24 analyses is 1850.0 ± 2.5 Ma (MSWD = 0.95; probability of fit = .53).

The analyses are corrected for overcounts at mass ^{204}Pb (after Black in press, calculated assuming $^{206}Pb/^{238}U$-^{207}Pb-^{235}U age concordance), which forces the weighted mean $^{207}Pb/^{206}Pb$ age for QGNG to the TIMS reference value. The recalculated age for QGNG becomes 1851.3 ± 2.4 Ma (MSWD = 0.96; probability of fit = .51; n=24 of 24). The sample data below are also corrected for overcounts.

Element abundance calibration was based on SL13 (n = 1).

Sample data

All 19 analyses from this sample have indistinguishable $^{207}Pb/^{206}Pb$ ages (MSWD = 1.4; probability of fit = 0.12), which combine to yield a mean crystallisation age of 1855.9 ± 3.8 Ma. When corrected for overcounts at mass ^{204}Pb, the age becomes 1857.7 ± 3.9 Ma (Figures 18 and 19).

Geochronological interpretation

The $^{207}Pb/^{206}Pb$ age of 1857.7 ± 3.9 Ma is considered to be the crystallisation age of the megacrystic granite.

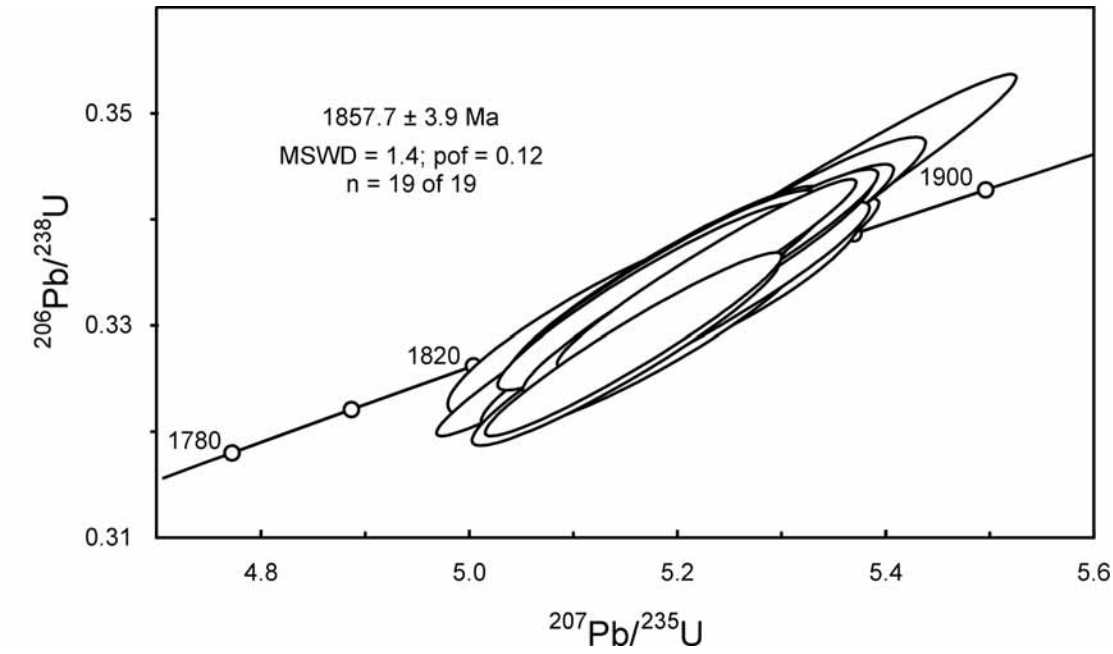

Figure 18. Concordia diagram for zircons in sample 200036 6020 showing radiogenic Pb compositions.

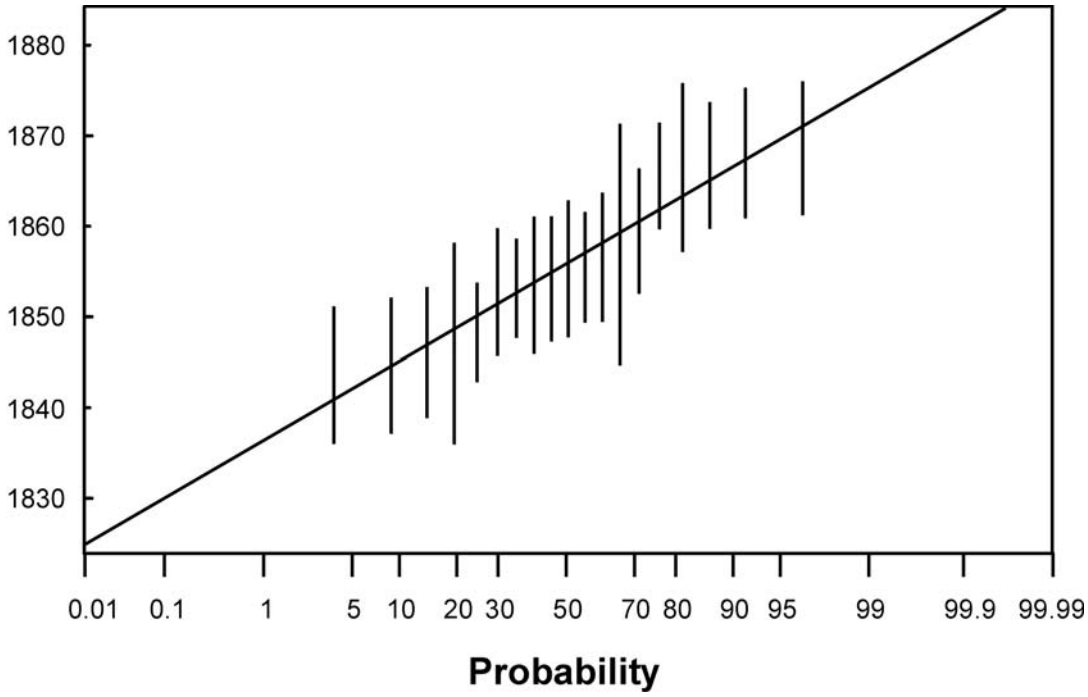

Figure 19. Probability diagram for individual zircon ages for sample 200036 6020. All ages are within error of each other.

Table 7. SHRIMP analytical results for zircon from sample 200036 6020.

Spot	U (ppm)	Th (ppm)	$^{206}Pb_c$ (%)	$^{206}Pb^*$ (ppm)	$^{206}Pb^*/^{238}U$	±	$^{207}Pb^*/^{235}U$	±	$^{207}Pb^*/^{206}Pb^*$	±	conc (%)	207Pb/206Pb Age(Ma)	±
401.1	229	142	0.06	65	0.332	0.004	5.17	0.07	0.11283	0.00045	100	1845	7
402.1	231	108	-0.04	65	0.326	0.004	5.14	0.07	0.11430	0.00047	97	1869	7
403.1	216	106	0.00	61	0.330	0.004	5.21	0.07	0.11441	0.00041	98	1871	7
404.1	380	177	0.03	107	0.327	0.004	5.14	0.07	0.11417	0.00035	98	1867	6
405.1	224	141	0.29	63	0.327	0.004	5.16	0.07	0.11427	0.00057	98	1868	9
406.1	331	191	0.00	95	0.333	0.004	5.21	0.07	0.11339	0.00033	100	1854	5
407.1	194	93	-0.01	56	0.337	0.007	5.26	0.11	0.11342	0.00061	101	1855	10
408.1	326	167	0.18	93	0.331	0.004	5.16	0.07	0.11295	0.00044	100	1847	7
409.1	243	103	0.05	70	0.334	0.004	5.22	0.07	0.11355	0.00045	100	1857	7
410.1	299	190	0.02	85	0.331	0.004	5.18	0.07	0.11354	0.00036	99	1857	6
411.1	219	93	0.53	63	0.331	0.004	5.19	0.07	0.11374	0.00082	99	1860	13
412.1	176	81	0.30	50	0.329	0.004	5.13	0.07	0.11308	0.00067	99	1850	11
413.1	229	94	0.02	66	0.334	0.004	5.23	0.07	0.11349	0.00041	100	1856	7
414.1	178	78	0.00	51	0.334	0.004	5.24	0.07	0.11367	0.00044	100	1859	7
415.1	213	108	0.02	61	0.331	0.004	5.22	0.07	0.11438	0.00043	99	1870	7
416.1	274	151	0.05	78	0.332	0.004	5.17	0.07	0.11288	0.00045	100	1846	7
417.1	362	175	0.03	102	0.327	0.004	5.10	0.07	0.11308	0.00033	99	1850	5
418.1	215	75	0.00	61	0.328	0.004	5.14	0.07	0.11383	0.00042	98	1862	7
419.1	187	79	0.04	54	0.337	0.004	5.27	0.07	0.11347	0.00045	101	1856	7

Data are 1σ precision. All Pb data are common Pb corrected based on measured ^{204}Pb (after Stacey and Kramer 1975).
Analysis date 4/6/2001; SHRIMP II

200036 6029: heterogeneous granitoid, Acropolis (biotite tonalite, biotite norite, adamellite)

1:250,000 sheet: Andamooka (SH5312)

1:100,000 sheet: Koolymilka (6236)

AMG: 674150 E 6611800 N

Location: The sample was taken from diamond drillhole ACD6, depth interval 694.5-695, 728-729, 735.8-736, 767-767.7, 773-773.7, 785.6-786 m (Figure 20). The diamond drillhole is located within the Acropolis prospect near Olympic Dam.

Description: A range of rocks from biotite tonalite and norite to adamellite are present in drillhole ACD6 (Figure 20). Creaser (1989) considered the variation to be a primary magmatic feature as contacts between the types appear gradational, and not sharply intrusive. Material for mineral separation was collected from five intervals within the drillhole, and the location of the samples described below are illustrated in Figure 20. The granitoid body is heterogeneously deformed, with intense strain partitioned into thin intervals of low-angle shear (10-20°). Elsewhere the granitoid appears largely undeformed, with only local development of a moderate to strong low-angle foliation.

1. *Biotite tonalite (200036 6029a):* This sample is a quartz-rich tonalite with 45% quartz, 40% plagioclase and 15% biotite. The plagioclase occurs as subhedral grains to 4 mm in diameter with weak sericite clouding, in a sea of quartz as ragged interlocking grains to 5 mm long, or separated by weakly deformed flakes of biotite. The biotite occurs as flakes to 3 mm long that are fresh apart from having expelled titanium as probable ilmenite during cooling. Zircon is disseminated, to 0.2 mm in grainsize, partly rounded and partly euhedral, with concentric zoning in the euhedral crystals. There are clay-filled fractures, adjacent to which the plagioclase has been altered to chlorite, sericite and carbonate in various proportions. The quartz and biotite seem to reflect minor deformation.

2. *Adamellite (200036 6029b):* This sample is a megacrystic monzogranite (adamellite) with subequal amounts of normative orthoclase and plagioclase indicated by the analysis. The visually estimated mineralogy indicates 35% quartz, 30% K-spar, 30% plagioclase, 4% biotite and accessories. Megacrysts of K-spar are disseminated, partly with incipient microcline twinning, to 12 mm long, rarely enclosing plagioclase. Separate plagioclase laths are also abundant, but are less than 4 mm long. Some of the plagioclase is deformed, with bent twin planes, and myrmekite is abundant between plagioclase and K-spar. The quartz occurs as ragged interlocking grains to 5 mm long, but is not highly deformed. The biotite is partly poikilitic and may be optically continuous over areas 10 x 3 mm. Areas to 5 mm in diameter have biotite altered variously to clay, chlorite and carbonate, and some of the biotite has been altered to clay with secondary K-spar and leucoxene. Weak sericite alteration is seen in the plagioclase. Accessory opaque oxide has been partly altered to leucoxene, and small zircon crystals occur, to 0.1 mm in grainsize.

3. *Plagioclase-rich biotite norite (200036 6029c):* The geochemical analyses for this interval indicates a nepheline-normative mafic lithology, with 46-48% SiO_2 (Table 29). The visually estimated primary mineralogy includes 70% plagioclase, 20% orthopyroxene, 7-8% biotite and 2-3% opaque oxide + apatite. Partly sericitised plagioclase is the most abundant mineral, with grains from 0.4 mm to 5 mm long, contributing possibly

15% sericite to the mineral assemblage. Orthopyroxene is also common, with anhedral, prismatic and poikilitic grains to 6 mm long, rarely altered to colourless amphibole. There is also possibly minor poikilitic clinopyroxene, but this is not certain. Biotite occurs within orthopyroxene and disseminated, as flakes to 4mm long. Accessories include fine-grained opaque oxide and apatite, and there may be interstitial quartz. The normative nepheline is a reflection of the abundance of biotite. The original lithology is a plagioclase-rich biotite norite.

(Purvis 2003)

Mount: Z3678

Description of zircons

The zircons extracted from sample 200036 6029 have aspect ratios range between 1:1 and 2.5:1 with rare elongate grains up to 4.5:1 (Figure 21). Most have low angle pyramids or rounded terminations and a slightly rounded morphology. Cathodoluminescence reveals that zoning is ubiquitous. Some grains contain anhedral, poorly luminescent cores. Small round to rod-shaped silicate inclusions are present in some grains. Cracked and hematite-stained grains are common, but were avoided during analysis.

Concurrent standard data

Z3677 and sample 200036 6029 on mount Z3678 were analysed over the 4 day session. Data for the standard are presented in Appendix 3. Twenty six QGNG analyses for Z3677 give a calibration exponent of 2.08, with an upper limit of 2.26 and lower limit of 1.85 (at 95% confidence level). The weighted mean $^{207}Pb/^{206}Pb$ age for all 26 analyses is 1851.7 ± 2.4 Ma (MSWD = 1.12; probability of fit =0.31). Nine QGNG analyses for Z3678 give a calibration exponent of 2.29 with an upper limit of 2.98 and lower limit of 1.61. The weighted mean $^{207}Pb/^{206}Pb$ age for all 9 analyses is 1848.9 ± 3.5 Ma (MSWD = 1.05; probability of fit = 0.39). Because no significant calibration shift is observed between the two data batches, both have been combined for data processing. This yields a calibration exponent of 2.08, with an upper limit of 2.22 and lower limit of 1.86. Thus the nominal value of 2.0 has been used in data reduction. The $^{206}Pb/^{238}U$ reproducibility for QGNG is 1.34% (1σ; n = 35 of 35). The weighted mean $^{207}Pb/^{206}Pb$ age for all 35 analyses is 1850.7 ± 1.9 (MSWD = 1.09; probability of fit = 0.33).

The analyses are corrected for overcounts at mass ^{204}Pb (after Black in press, calculated assuming $^{206}Pb/^{238}U$-^{207}Pb-^{235}U age concordance), which forces the weighted mean $^{207}Pb/^{206}Pb$ age for QGNG to the TIMS reference value. The recalculated age for QGNG becomes 1851.6 ± 2.2 Ma (MSWD = 1.13; probability of fit = .27; n = 35 of 35). The sample data below are also corrected for overcounts.

Element abundance calibration was based on SL13 (n = 1).

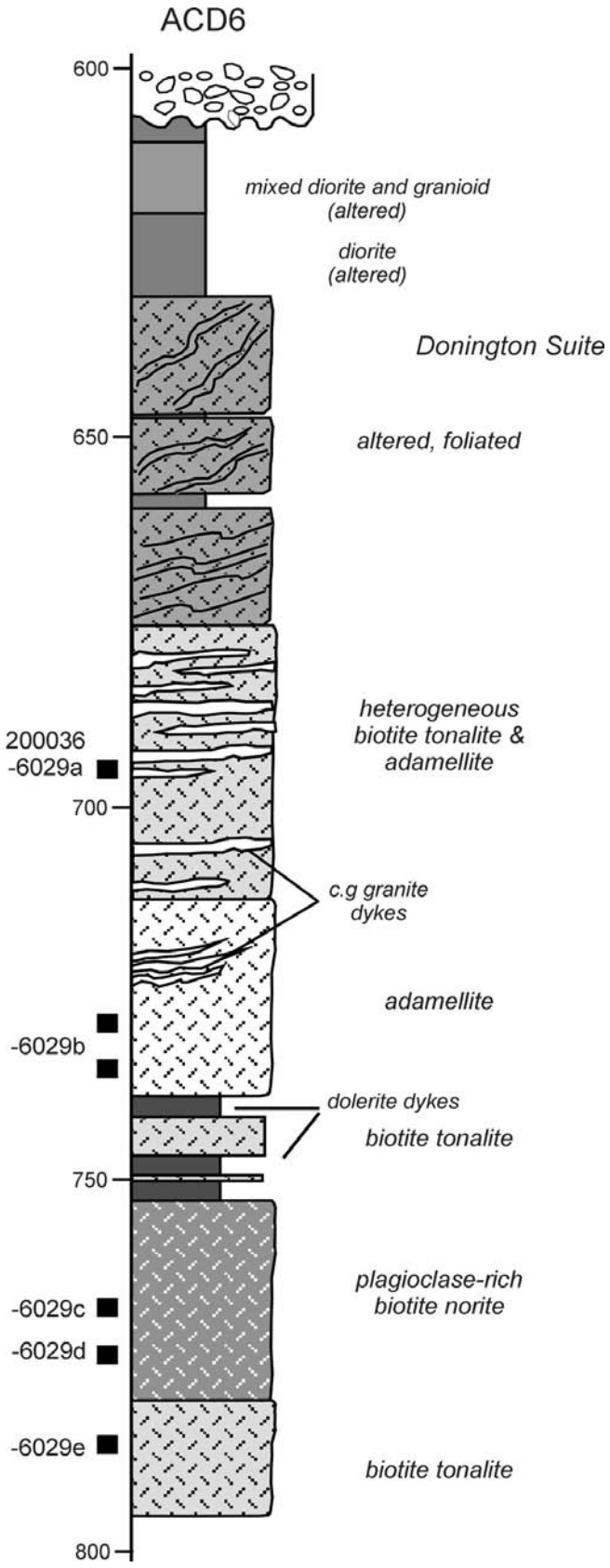

Figure 20. Stratigraphic log for Acropolis drill hole ACD6 showing the location of samples collected for SHRIMP U-Pb dating and geochemical analysis.

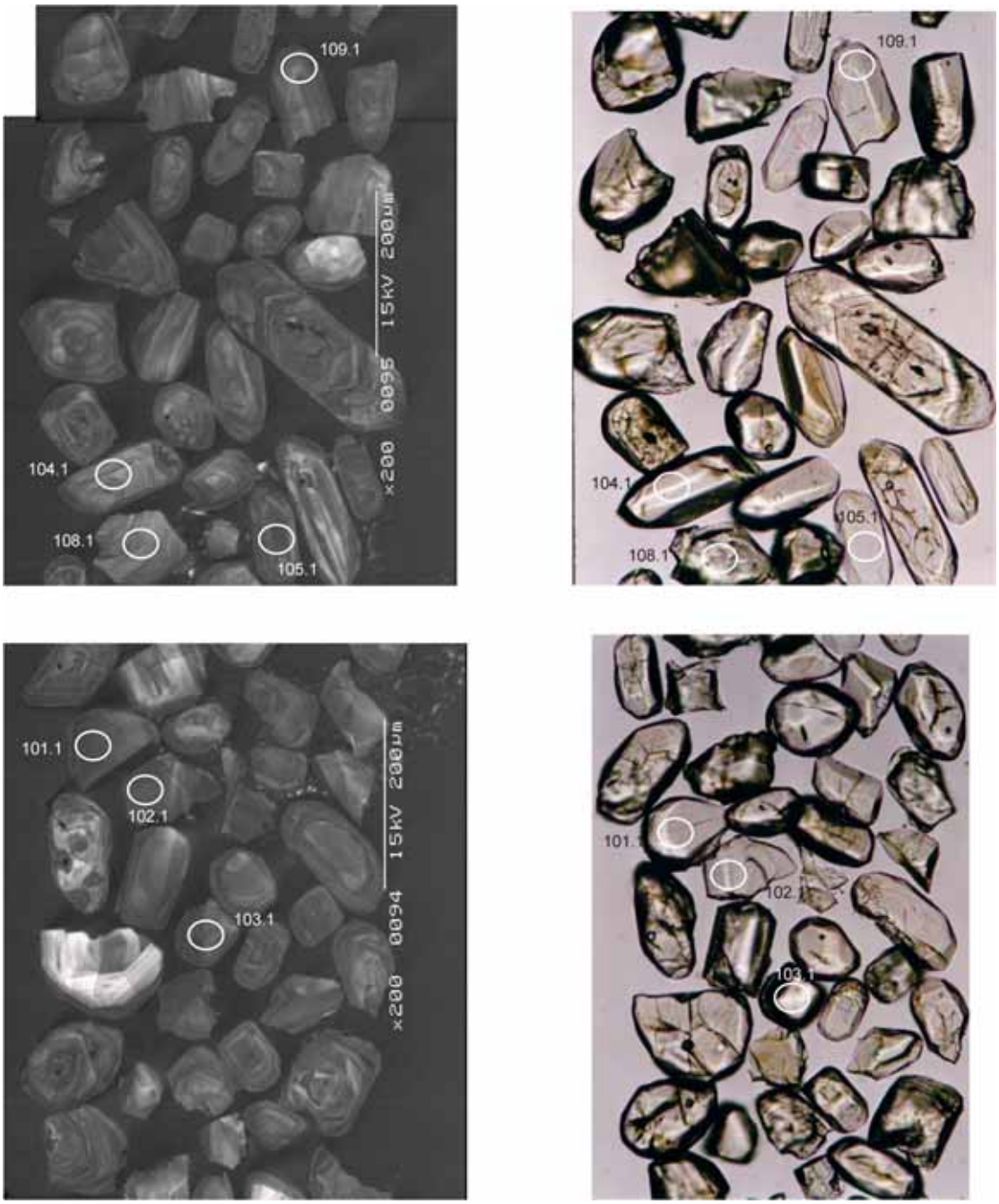

Figure 21. Representative CL (left) and transmitted light (right) images for sample 200036 6029: heterogeneous granitoid, Acropolis prospect. SHRIMP analysis spots are labelled. Scale bar is 200 µm.

Sample data

A total of 28 grains were analysed. The five oldest grains are clearly xenocrystic. Two of these have near concordant ages of *ca* 2450 Ma, and the other three spread between *ca* 1950 and 1990 Ma (Figure 22a). The remaining 23 analyses form an alignment that intersects concordia at about 1850 Ma, with a tail of up to 23% discordance (Figure 23). Three of the discordant analyses have high common Pb (Table 8), and the probability diagram suggests they are outliers (Figure 22b). The remaining 20 analyses yield a weighted mean age of 1852.2 ± 3.6 Ma. When corrected for overcounts at mass ^{204}Pb, the age becomes 1853.3 ± 3.7 Ma (MSWD = 1.4; probability of fit = 0.12).

Geochronological interpretation

The ^{207}Pb/^{206}Pb age of 1853.3 ± 3.7 Ma is considered to be the crystallisation age of the megacrystic granite.

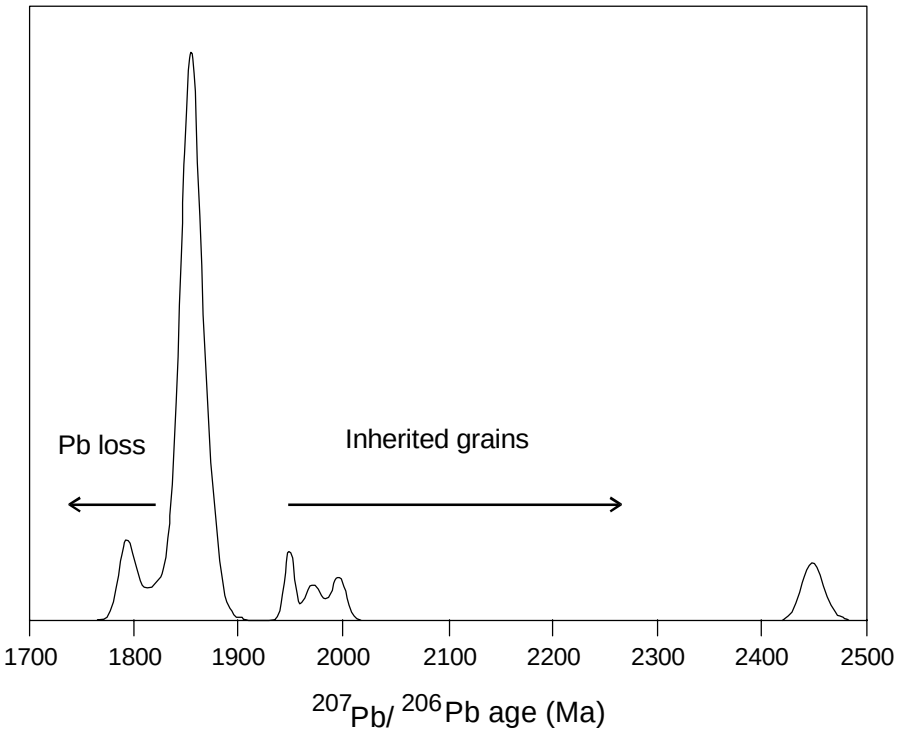

Figure 22a. Probability density distribution of ^{207}Pb/^{206}Pb ages for the zircons in sample 200036 6029 illustrating the full range of inherited zircon ages.

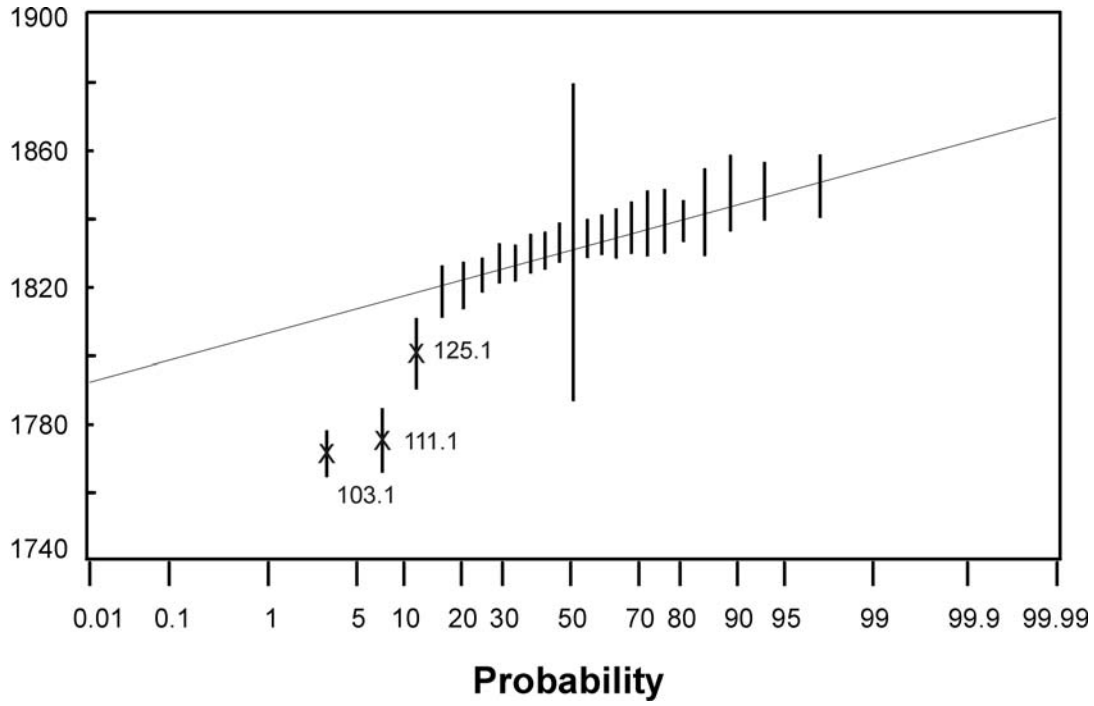

Figure 22b. Probability diagram for individual zircon ages. Error bars are 1σ. Five xenocrystic grains plot above the range of this diagram. Three analyses clearly represent outliers from the main population that have lost radiogenic Pb.

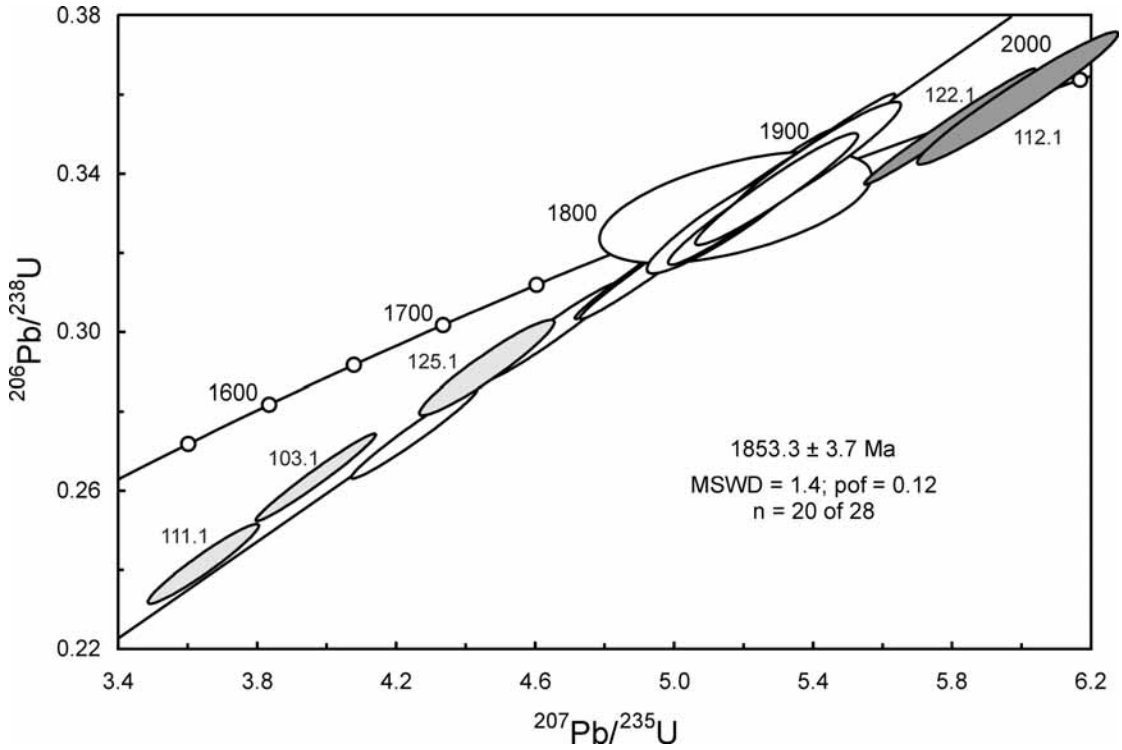

Figure 23. Concordia diagram for zircons in sample 200036 6029. Three xenocrystic grain plot above the range of this diagram. Other xenocrysts are shaded in dark grey. White-filled symbols represent analyses used in the weighted mean age calculation. Discordant, high common Pb analyses are light grey.

Table 8. SHRIMP analytical results for zircon from sample 200036 6029.

Spot	U (ppm)	Th (ppm)	$^{206}Pb_c$ (%)	$^{206}Pb^*$ (ppm)	$^{206}Pb^*/^{238}U$	±	$^{207}Pb^*/^{235}U$	±	$^{207}Pb^*/^{206}Pb^*$	±	conc (%)	207Pb/206Pb Age(Ma)	±
101.1	437	199	0.24	102	0.271	0.004	4.20	0.06	0.11256	0.00042	84	1841	7
102.1	387	21	0.01	111	0.333	0.005	5.18	0.07	0.11275	0.00032	100	1844	5
103.1	457	106	0.27	102	0.260	0.004	3.92	0.06	0.10956	0.00041	83	1792	7
104.1	189	109	0.04	54	0.332	0.005	5.23	0.08	0.11443	0.00058	99	1871	9
105.1	318	214	0.03	87	0.318	0.004	4.97	0.07	0.11321	0.00033	96	1852	5
106.1	250	117	0.04	71	0.331	0.005	5.16	0.07	0.11316	0.00035	100	1851	6
107.1	292	162	0.03	78	0.312	0.004	4.87	0.07	0.11298	0.00033	95	1848	5
108.1	137	84	0.05	43	0.364	0.005	6.17	0.10	0.12278	0.00048	100	1997	7
109.1	246	91	0.02	66	0.312	0.004	4.88	0.07	0.11337	0.00035	94	1854	6
110.1	224	67	0.13	57	0.296	0.004	4.59	0.07	0.11249	0.00046	91	1840	7
111.1	272	117	0.30	56	0.238	0.003	3.60	0.05	0.10983	0.00055	77	1797	9
112.1	46	61	0.14	19	0.468	0.007	10.28	0.17	0.15939	0.00092	101	2449	10
113.1	98	37	0.08	28	0.333	0.005	5.22	0.09	0.11386	0.00060	99	1862	10
114.1	184	141	1.08	52	0.327	0.005	5.12	0.15	0.11340	0.00284	98	1855	46
115.1	229	43	0.02	65	0.328	0.005	5.14	0.07	0.11354	0.00045	99	1857	7
116.1	213	126	0.03	60	0.329	0.005	5.16	0.07	0.11378	0.00038	99	1861	6
117.1	116	52	0.07	33	0.330	0.005	5.18	0.08	0.11380	0.00057	99	1861	9
118.1	305	124	0.18	85	0.324	0.005	5.09	0.08	0.11392	0.00080	97	1863	13
119.1	283	66	0.01	80	0.329	0.005	5.14	0.07	0.11344	0.00034	99	1855	6
120.1	166	65	0.02	47	0.330	0.005	5.17	0.08	0.11368	0.00044	99	1859	7
121.1	201	108	0.04	56	0.327	0.005	5.15	0.08	0.11434	0.00054	98	1869	9
122.1	62	26	-0.02	24	0.455	0.008	10.04	0.19	0.16000	0.00109	99	2456	12
123.1	366	182	0.03	109	0.348	0.005	5.73	0.08	0.11950	0.00031	102	1949	5
124.1	231	97	0.02	68	0.341	0.005	5.34	0.07	0.11352	0.00036	89	1857	6
125.1	756	54	0.84	188	0.287	0.004	4.41	0.07	0.11132	0.00062	97	1821	10
126.1	316	164	0.02	87	0.319	0.004	4.97	0.07	0.11299	0.00035	99	1848	6
127.1	97	36	0.03	30	0.355	0.006	5.92	0.10	0.12113	0.00057	101	1973	8
128.1	106	53	0.07	31	0.339	0.005	5.34	0.09	0.11436	0.00069	97	1870	11

Data are 1σ precision. All Pb data are common Pb corrected based on measured ^{204}Pb (after Stacey and Kramer 1975).
Analysis date 26/4/2001; SHRIMP II

Discussion of results

The new data confirm the presumed correlation of the Suite #1 foliated megacrystic granites with the voluminous Donington Suite of the eastern Eyre Peninsula (Mortimer et al. 1988a; Creaser and Cooper 1993; Creaser 1995). An unexpected outcome is that the Suite #2 mafic granitoids are also contemporary with the Donington Suite, as they were considered to be about 80 m.y. younger (Creaser 1989).

The Donington Suite forms a distinctive batholith-scale body on the aeromagnetic image of the southern Gawler Craton, and is exposed on the southern Eyre Peninsula and western Yorke Peninsula. The following descriptions of the Donington Suite on the eastern Eyre Peninsula are taken from Schwarz (2003). The suite comprises a broad spectrum of co-magmatic lithologies, all intruded in a relatively short time frame while each previous unit was at least partially molten. The Wanna Megacrystic Granite Gneiss is the most voluminous component of the Donington Suite, and an obvious correlative of the distinctive megacrystic granites of the Olympic Domain. It is variably deformed, displaying a weak to ultramylonitic foliation, and locally a gneissic character, with zoned, ovoid-shaped augen of microcline and plagioclase up to 4 cm in size. It varies from granite to granodiorite in composition, with each containing enclaves of the other, suggesting the variation is a primary magmatic feature. A similar compositional heterogeneity is observed within the intensely foliated megacrystic granites at Burden Hill and Island Dam, but not the predominantly weakly-deformed granites at Wirrda Well and Snake Gully, suggesting primary inhomogeneities may be enhanced during deformation.

Earlier intrusive phases of the Donington Suite are more primitive in composition, and were believed to be emplaced under high PT, granulite facies conditions (> 8 Kb, ~ 845ºC; Mortimer et al. 1988b). The oldest phase, comprising less than 5% of the Donington Suite, is the pyroxene-bearing Quartz Gabbronorite at Cape Donington, which contains zoned orthopyroxene, clinopyroxene and plagioclase phenocrysts and interstitial biotite, alkali feldspar and quartz. This unit supplies the SHRIMP zircon standard QGNG. The Memory Cove Charnockite (~30% of the Donington Suite) is a hypersthene-bearing granodiorite/charnockite that largely retains anhydrous granulite metamorphic assemblages, with hydration resulting in conversion of hypersthene to hornblende locally.

In addition to these earlier more mafic units, a minor granodiorite unit appears to be contemporary with the Wanna Megacrystic Granite Gneiss. They both exhibit gradational contacts, and appear very similar in character in areas of high strain, where the phenocrysts have been flattened and recrystallised to produce an even texture (Schwarz in prep.). The granodiorite comprises orbicular, medium-grained grey granodiorite with large pink K-feldspar aggregates, and even grained, grey granite gneiss.

Finally, the Colbert Suite intrudes and contains foliated megacrystic xenoliths of the older Donington Suite units. It comprises narrow dyke-like bodies (up to 15 m wide) of hornblende granite and alkali-feldspar granite, and large amorphous bodies (up to 30 m wide) of medium- to coarse-grained leucogranodiorite. Where there is a lack of mafic minerals to define a foliation, the unit appears undeformed in hand specimen.

Age comparisons

Table 9 lists the available U-Pb ages for the Donington Suite on the Eyre Peninsula, for comparison with the ages obtained in this study. The new ages from the Olympic Domain accord well with those available for the Donington Suite on the Eyre Peninsula, suggesting the magmatic event was short lived, even though magmatism was of batholithic proportions. The eight ages combine to give a weighted mean age of 1851.9 ± 1.4 Ma (MSWD = 4.5; probability of fit = 0). The high MSWD is due to the significantly older ages of the IDD3 and BHD1 granitoids (Figure 24). It is not possible to statistically discriminate between the other ages (i.e. granitoids from ACD6, WRD24, SGD4, Memory Cove Charnockite and Colbeck Suite) and all are within error of the QGNG TIMS reference age.

The difference between the ages for BHD1 and WRD24 (obtained during the same session on SHRIMP) generates a Student's *t* value of 2.97, which is significant for 36 degrees of freedom (n-2) at the 95% confidence level (for which *t* is 2.03). This suggests that the apparent age difference between BHD1 and IDD3, and the other granitoids is real, and that the emplacement age of the intensely foliated granites from IDD3 and BHD1 is older than that of the heterogeneously deformed, predominantly weakly foliated granitoids of ACD6, WRD24 and SGD4.

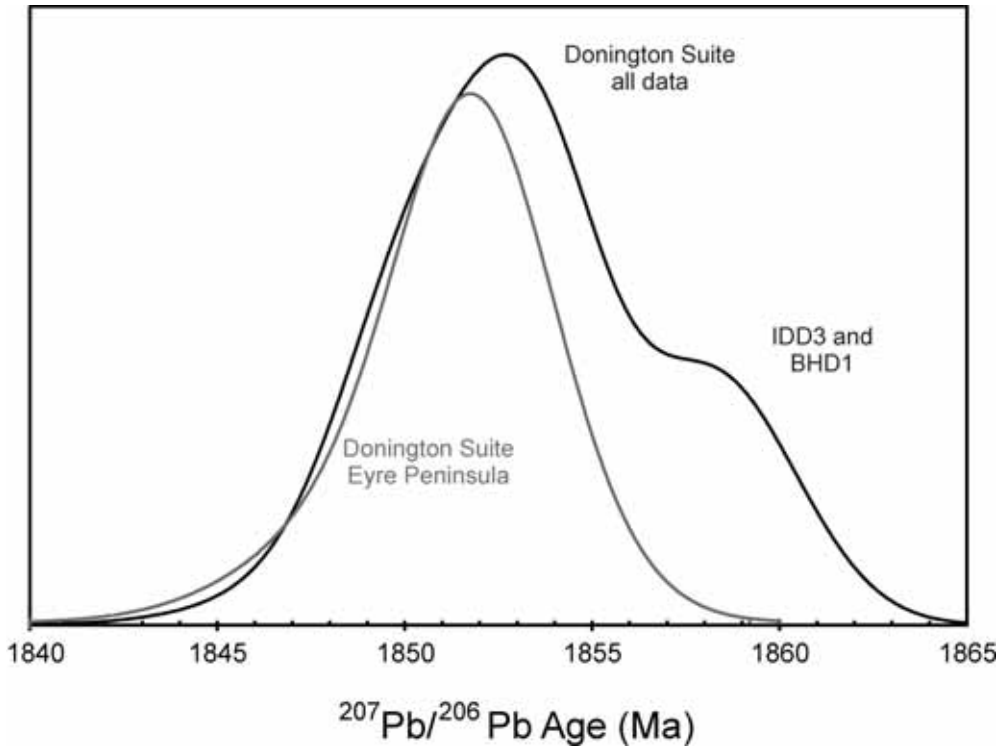

Figure 24. Probability density distribution of available U-Pb ages for the Donington Suite. Data are from Table 9. Errors are 2σ. NB: for plotting purposes only, the 2σ error for QGNG was increased from 0.6 to 3.7 Ma (average error of the 7 SHRIMP ages) to avoid biasing the histogram due to the higher precision of the TIMS age.

Table 9: Summary of available U-Pb zircon ages for the Donington Suite.

Unit	Location	Age	Method	Reference
mx granite (WRD24)	Olympic Domain	1849.6±3.5	SHRIMP	this study
granodiorite (ACD6)	Olympic Domain	1853.3±3.7	SHRIMP	this study
mx granite (SGD4)	Olympic Domain	1854.0±3.3	SHRIMP	this study
mx granite (BHD1)	Olympic Domain	1857.7±3.9	SHRIMP	this study
mx granite (IDD3)	Olympic Domain	1860.4±4.1	SHRIMP	this study
Quartz Gabbronorite (QGNG)	Eyre Peninsula	1851.6±0.6	IDTIMS	Black et al. 2003
Memory Cove Charnockite	Eyre Peninsula	1850.0±6.5	SHRIMP	Fanning 1997
Colbert Suite	Eyre Peninsula	1852.5±4.4	SHRIMP	Fanning 1997

Suite #2

Creaser (1989) had difficulty correlating the Suite #2 granites regionally due to their wide variety and scattered occurrence, but settled on a correlation with the Moody Suite based on geochemical similarities. The correlation assumed the mafic and felsic components of Suite #2 form a composite I-S suite, similar to the Moody Tank granites (Mortimer et al. 1988b). However, a revision of Suite #2 in light of the *ca* 1850 Ma ages obtained for the representatives analysed in this study, suggests most components can be assigned to the Donington Suite.

The Burden Hill granitoids can be reassigned to the Suite #1 megacrystic granites of Creaser (1989). The absence of obvious K-feldspar megacrysts gives the Burden Hill granites a more mafic appearance, which may be the reason why they were excluded from Suite #1, and placed in Suite #2. However, large K-feldspar phenocrysts up to 5 cm long occur in BHD1, stretched out parallel to the foliation (Figure 25). This suggests this granite was megacrystic, but extreme attenuation has produced a more uniform layering due to increased segregation of felsic (pink feldspar, quartz) and mafic minerals (biotite, chlorite). They are granitic in composition, not tonalitic, as surmised by Creaser (1989), with similar geochemistry to the megacrystic granite at IDD3 (Table 29). The granitoids in all three drill holes (BHD1, BHD2 and IDD3) are similar in character, exhibiting a pervasive, steeply-dipping fabric, and intruded by foliated mafic dykes with fine-grained chilled margins. This is also a distinctive feature of the Donington Suite, which is intruded by the mafic Tournefort Dyke Swarm on the Eyre Peninsula.

Figure 25: Intensely foliated granitoids from Burden Hill (BHD1) and Island Dam.

Given the range of mafic lithologies within the Donington Suite, the Suite #2 mafic granitoids can also be reassigned to the Donington Suite, based on the 1853.3 ± 3.7 Ma age obtained for ACD6. Creaser (1989) describes mafic granulite xenocrysts within the diorite/tonalites at TWN3, which may represent early phase material similar to the Memory Cove Charnockite on the Eyre Peninsula.

Most felsic granitoids of Suite #2 occur as dykes cross cutting Suite #1 megacrystic granites and Suite #2 mafic granitoids. Creaser (1989) raised the alternative possibility that these rocks are aplites associated with Suite #1. They occupy a similar position to the late-stage dykes of the Colbert Suite, which also intrude earlier mafic and megacrystic granite phases of the Donington Suite.

Given the reassignment of most of Suite #2 to an older magmatic event, there is now little evidence of 1685-1750 Ma magmatism in the Olympic Domain. Only the anorthositic gabbro in BLD1 has yielded a comparable, slightly older age of 1764 ± 12 Ma (Johnson 1993).

Where the Olympic Domain forms a basement to the Stuart Shelf, the period between 1730-1770 Ma appears to be largely represented by (meta)sedimentary sequences similar to the Wandearah Metasiltstone, which may have a local volcanic or volcaniclastic component. This period of crustal evolution is characterised throughout the Gawler Craton by deposition of volcanic and sedimentary sequences. These packages include the Moonta Porphyry (1737 ± 5 Ma; Fanning et al. 1988), Wardang Volcanics and Doora Schist (1730-1750 Ma) and Wandearah Metasiltstone (1740-1770 Ma; unpublished data) of the Moona-Wallaroo region, the Price Metasediments of the western Eyre Peninsula (1764 ± 17 Ma; Oliver and Fanning 1997) and the McGregor Volcanics, Moonabie Formation (~1740 Ma; Fanning et al. 1988) and Myola Volcanics (1791 ± 4 Ma; Fanning et al. 1988) of the northeastern Eyre Peninsula.

Part 2: (meta)sedimentary units

200036 6008: meta-siltstone, Snake Gully

1:250,000 sheet: Andamooka (SH5312)

1:100,000 sheet: Yarrawurta (6337)

AMG: 700600 E 6638600 N

Location: The sample was taken from diamond drillhole SGD6, depth interval 520-521.5, 526.7-527.6 m (Figure 5). The diamond drillhole is located within the Snake Gully prospect to the northeast of Olympic Dam.

Description: The hand specimen represents a fine-grained thinly laminated meta-sedimentary rock composed mainly of drab greenish layers with lesser paler drab brownish cream layers. The sample responds weakly to the hand magnet, suggesting minor magnetite is present.

In thin section, the sample displays a uniformly fine-grained clastic sedimentary texture, modified by weak metamorphic grain suturing, fracturing, and pervasive alteration. The meta-siltstone formed as a fine-grained silty clastic sediment composed of abundant small crystal fragments (quartz, plagioclase, zircon) accompanied by fine argillaceous materials. Quartz (52%) occurs as small equant anhedral quartz grains distributed uniformly throughout the rock, with suturing of quartz-quartz grain contacts. Plagioclase (15%) occurs as small anhedral grains and microgranular aggregates distributed throughout the rock, but more abundant in indistinct horizons inferred to represent primary layering. Trace zircon occurs as small subrounded grains ~0.1-0.2 mm in size.

Subsequent recrystallisation in response to a low-grade regional metamorphic event generated the new foliated assemblage of sericite (25%) + chlorite (5%) + minor opaques (?magnetite replaced by ?hematite). The preferred orientation of sericite and chlorite flakes defines a moderate foliation subparallel to the primary layering. Quartz and plagioclase remained stable from the primary clastic assemblage, and underwent grain suturing and incipient recrystallisation. At this time, or toward the end of this event, thin fractures were filled by dolomite + chlorite (the chlorite identical to that disseminated through the rock as foliated flakes), and fine sericite formed as selvedges marginal to the fractures. Hematite formed as tiny grains in the fracture-filling dolomite, and as replacements of ?magnetite.

See Appendix 1 for full petrographic report (Mason 2003).

Mount: Z3677

Description of zircons

The sample contains abundant equant to moderately elongate (< 3:1) zircons, between 50-100 μm long (Figure 26). Most are detrital grains, moderately to well rounded, with finely pitted surfaces indicative of sedimentary transport. Cathodoluminescence shows that prismatic zoning is ubiquitous (although this is rarely visible optically), suggesting an initially igneous origin for the detrital grains. A few grains preserve simple euhedral pyramidal and prismatic facets, and these were preferentially targeted for analysis. The grains are clear and optically homogeneous, with no visible cores and few fluid and rod-like silicate inclusions.

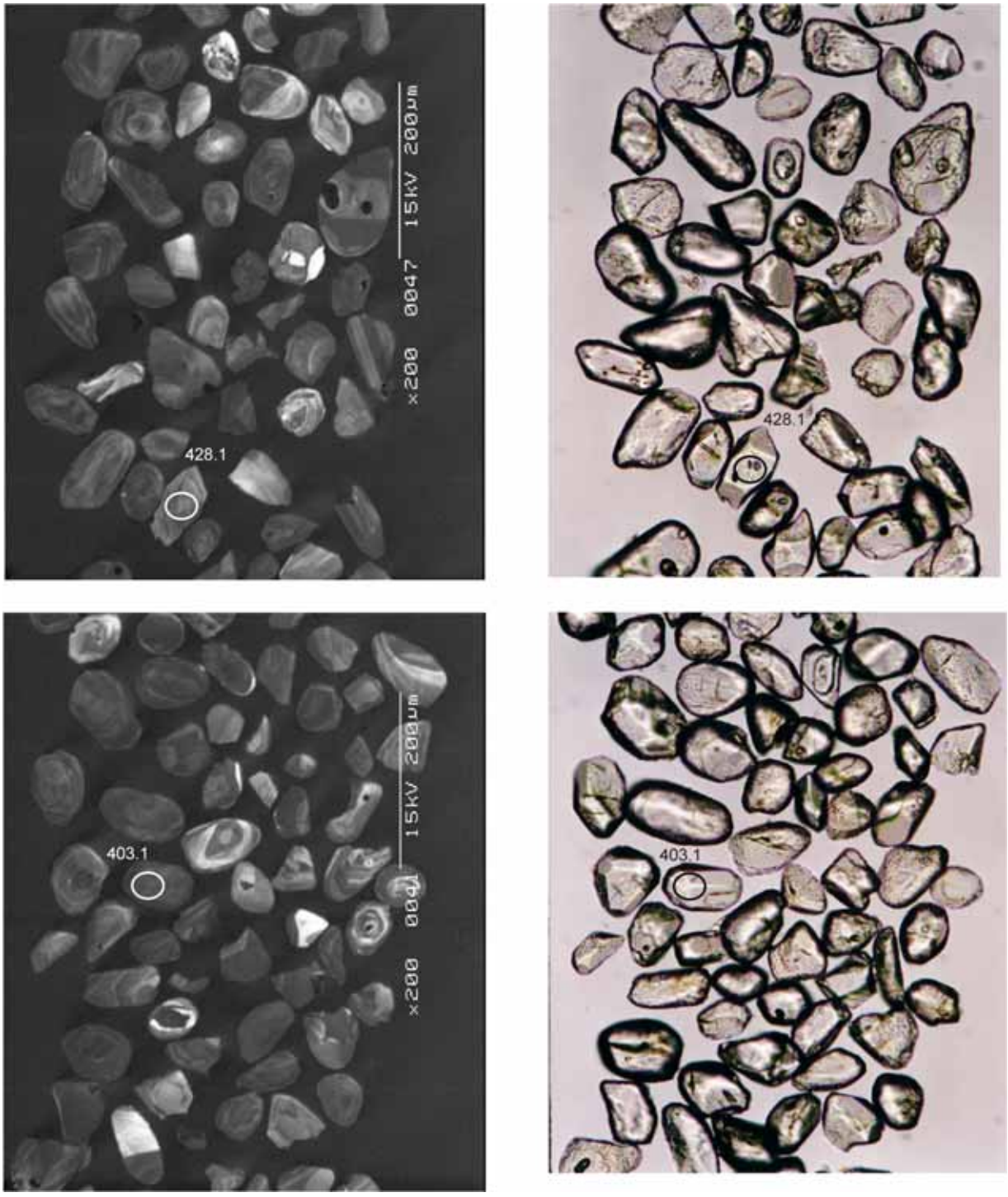

Figure 26. Representative CL (left) and transmitted light (right) images for sample 200036 6008: meta-siltstone, Snake Gully prospect. SHRIMP analysis spots are labelled. Scale bar is 200 µm.

Concurrent standard data

Z3677 and sample 200036 6029 on mount Z3678 were analysed over the 4 day session. Data for the standard are presented in Appendix 3. Twenty six QGNG analyses for Z3677 give a calibration exponent of 2.08, with an upper limit of 2.26 and lower limit of 1.85 (at 95% confidence level). The weighted mean $^{207}Pb/^{206}Pb$ age for all 26 analyses is 1851.7 ± 2.4 Ma (MSWD = 1.12; probability of fit =0.31). Nine QGNG analyses for Z3678 give a calibration exponent of 2.29 with an upper limit of 2.98 and lower limit of 1.61. The weighted mean $^{207}Pb/^{206}Pb$ age for all 9 analyses is 1848.9 ± 3.5 Ma (MSWD = 1.05; probability of fit = 0.39). Because no significant calibration shift is observed between the two data batches, both have been combined for data processing. This yields a calibration exponent of 2.08, with an upper limit of 2.22 and lower limit of 1.86. Thus the nominal value of 2.0 has been used in data reduction. The $^{206}Pb/^{238}U$ reproducibility for QGNG is 1.34% (1σ; n = 35 of 35). The weighted mean $^{207}Pb/^{206}Pb$ age for all 35 analyses is 1850.7 ± 1.9 (MSWD = 1.09; probability of fit = 0.33).

The analyses are corrected for overcounts at mass ^{204}Pb (after Black in press, calculated assuming $^{206}Pb/^{238}U$-^{207}Pb-^{235}U age concordance), which forces the weighted mean $^{207}Pb/^{206}Pb$ age for QGNG to the TIMS reference value. The recalculated age for QGNG becomes 1851.6 ± 2.2 Ma (MSWD = 1.13; probability of fit = .27; n = 35 of 35). The sample data below are also corrected for overcounts.

Element abundance calibration was based on SL13 (n = 1).

Sample data

A total of 34 grains were analysed, producing a spread of ages between 1760 Ma and 2740 Ma, with the greatest concentration of data occurring at about 1850 Ma (Figure 27a, Table 10). The 15 oldest zircon ages represent single-phase grains (as opposed to cores). As all but two of the analyses are at least 90% concordant, their $^{207}Pb/^{206}Pb$ compositions should provide reliable age estimates. The exceptions are analyses 425.1 and 430.1. There are too few analyses of these older grains to delineate data concentrations, although they may be postulated to occur at about 1920 and 2000 Ma, and there appears to be a hiatus between about 2200 and 2480 Ma. Fourteen of the analyses cluster close to concordia at about 1850 Ma (Figure 28). These analyses yield a weighted mean age of 1852.4 ± 5.5 Ma. When corrected for overcounts at mass ^{204}Pb, the age becomes 1854.4 ± 5.3 Ma, with an acceptable MSWD of 1.56 (probability of fit = 0.09).

Three analyses appear to be younger than 1850 Ma, plotting close to concordia at about 1765 Ma. With so few analyses, it is difficult to attribute geological significance to this younger age with confidence. The near concordance of the analyses suggests they should approximate the age of crystallisation of the grains, but it is also possible that the younger ages reflect isotopic resetting of 1850 Ma grains. However, alteration of the sample is very minor and the young grains are clear, with no evidence of lattice damage (cracks, metamict areas). The analyses are well off the vector generated by the recent Pb loss for the 1850 Ma grains, and they do not contain high U or common Pb, which might be indicative of radiogenic Pb loss. Instead, their U and Th contents are lower than the discordant 1850 Ma grains (Figure 28). These factors favour ca 1765 Ma as the crystallisation age of the grains, making this a probable older limit for the sedimentary deposition of this rock.

Geochronological interpretation

Creaser (1989) described the meta-siltstone and underlying porphyry in SGD6 as a 'deformed volcano-sedimentary unit' and was uncertain of its stratigraphic position, assigning it to lie between his Suite #1 (Donington Suite, *ca* 1850 Ma) and Suite #2 (?1685-1750 Ma) granitoids.

The maximum age for the metasediment is considered to be *ca* 1765 Ma. The provenance for detrital zircons is dominantly *ca* 1850 Ma, but includes components at least as old as 2470 Ma.

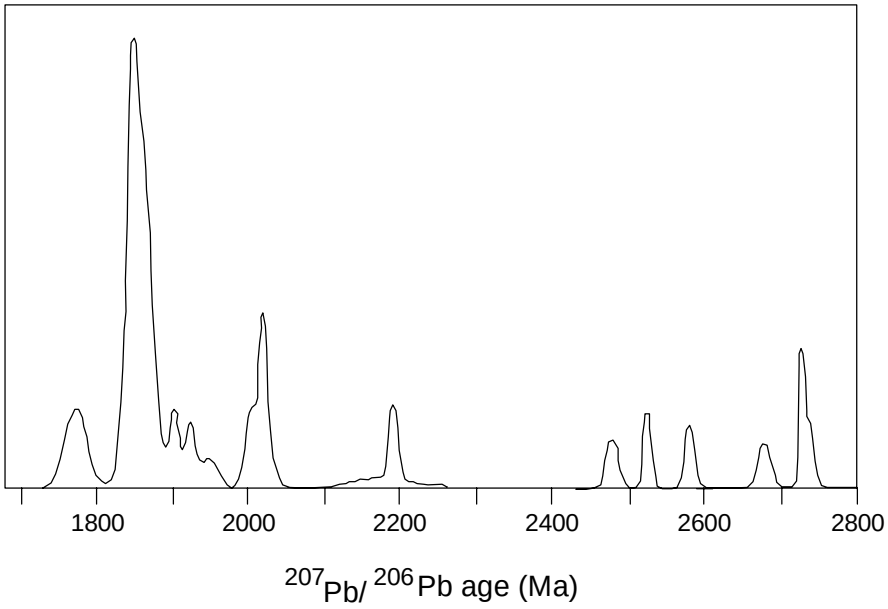

Figure 27a. Probability density distribution of $^{207}Pb/^{206}Pb$ ages for the zircons in sample 200036 6008, illustrating the wide range of ages for the detrital zircons.

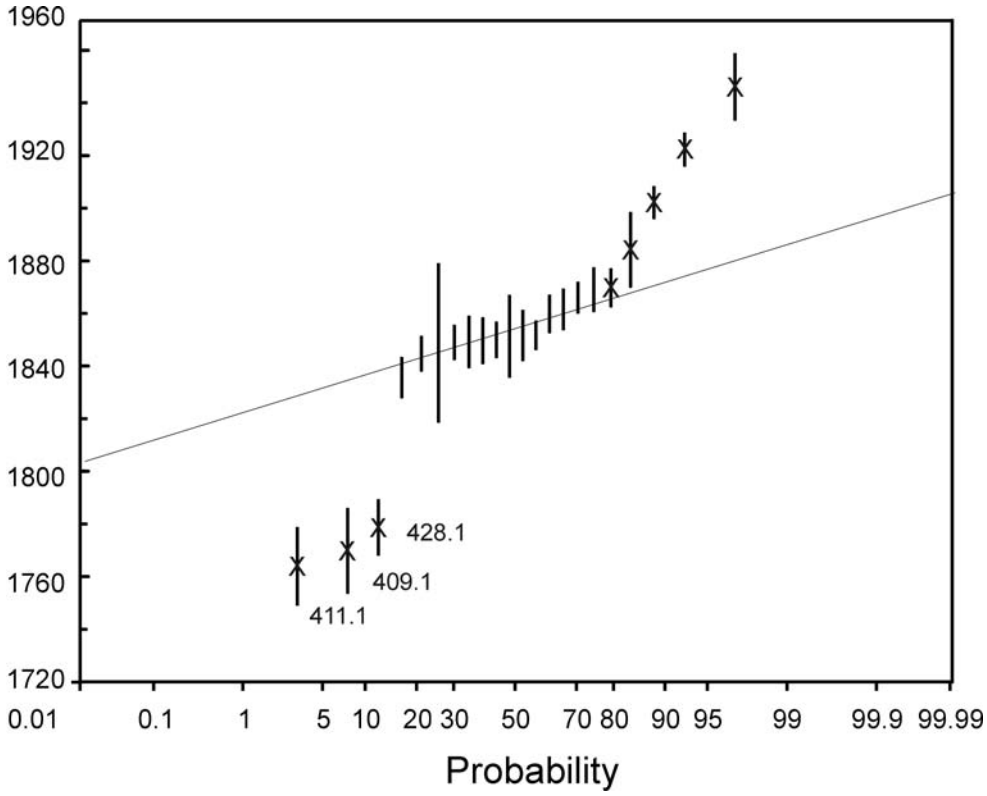

Figure 27b. Probability diagram for individual zircon ages. The oldest grains plot above the range of this diagram. The three youngest values plot well below the main population and are likely to be derived from a ca 1770 Ma source.

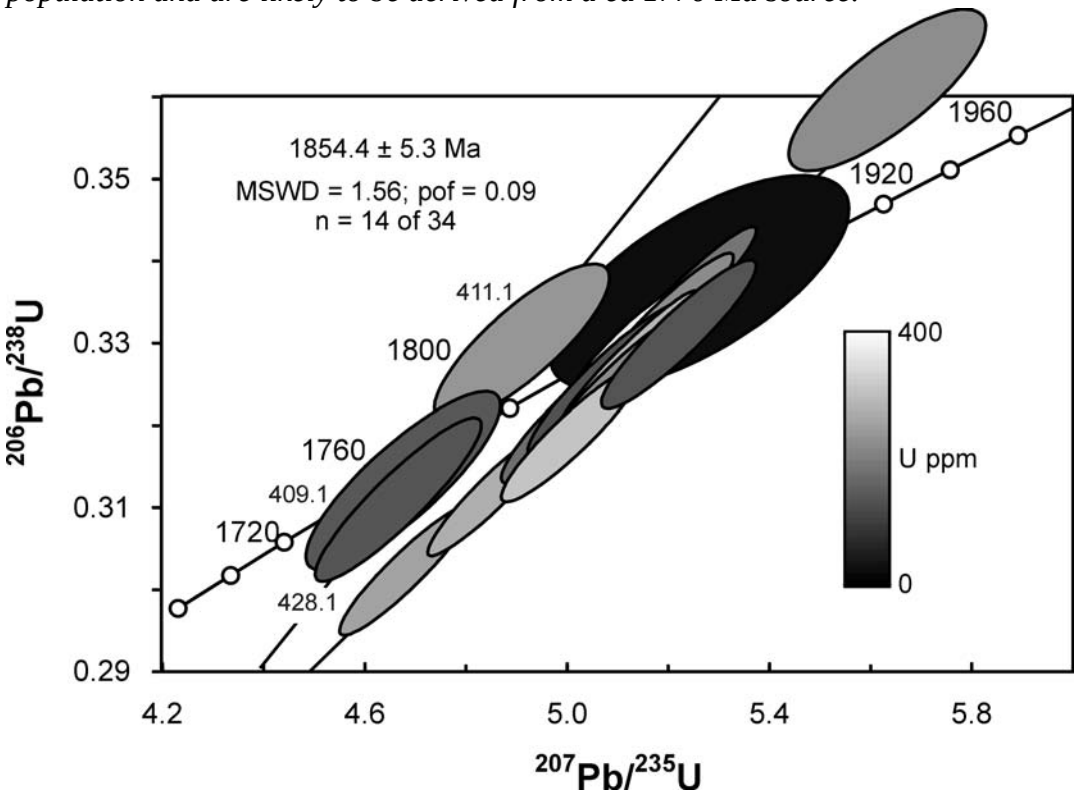

Figure 28. Concordia diagram for the youngest grains in sample 200036 6008 showing radiogenic Pb compositions. Error ellipses are shaded according to the U content of the analyses.

Table 10. SHRIMP analytical results for zircon from sample 200036 6008.

Spot	U (ppm)	Th (ppm)	$^{206}Pb_c$ (%)	$^{206}Pb^*$ (ppm)	$^{206}Pb^*/^{238}U$	±	$^{207}Pb^*/^{235}U$	±	$^{207}Pb^*/^{206}Pb^*$	±	conc (%)	207Pb/206Pb Age(Ma)	±
401.1	256	153	0.12	66	0.302	0.004	4.67	0.07	0.11228	0.00045	93	1837	7
402.1	275	131	0.10	74	0.312	0.004	4.85	0.07	0.11283	0.00039	95	1846	6
403.1	255	95	0.06	72	0.330	0.005	5.20	0.07	0.11442	0.00043	98	1871	7
404.1	307	157	0.22	84	0.318	0.004	5.00	0.07	0.11389	0.00042	96	1862	7
405.1	90	53	0.01	37	0.483	0.007	11.49	0.17	0.17268	0.00062	98	2584	6
406.1	173	113	0.00	52	0.349	0.005	5.67	0.08	0.11783	0.00040	100	1924	6
407.1	286	122	0.01	80	0.327	0.005	5.11	0.07	0.11327	0.00033	99	1853	5
408.1	114	128	0.03	36	0.363	0.005	6.16	0.09	0.12315	0.00053	100	2002	8
409.1	139	94	0.34	37	0.313	0.005	4.67	0.08	0.10836	0.00087	99	1772	15
410.1	129	50	0.11	36	0.325	0.005	5.08	0.08	0.11333	0.00057	98	1854	9
411.1	236	117	0.42	67	0.330	0.005	4.90	0.08	0.10795	0.00074	104	1765	13
412.1	219	164	0.05	62	0.332	0.005	5.18	0.07	0.11318	0.00044	100	1851	7
413.1	20	4	0.53	6	0.337	0.006	5.29	0.13	0.11380	0.00182	101	1861	29
414.1	132	116	0.05	37	0.331	0.005	5.22	0.08	0.11443	0.00050	98	1871	8
415.1	517	94	0.04	158	0.355	0.005	6.08	0.09	0.12440	0.00025	97	2020	4
416.1	254	134	0.04	86	0.393	0.005	7.42	0.10	0.13716	0.00040	97	2192	5
417.1	86	53	0.05	34	0.464	0.007	10.39	0.16	0.16239	0.00075	99	2481	8
418.1	188	68	0.04	56	0.344	0.006	5.67	0.10	0.11941	0.00080	98	1947	12
419.1	113	98	0.01	33	0.336	0.006	5.34	0.11	0.11541	0.00089	99	1886	14
420.1	132	37	0.07	59	0.520	0.007	13.14	0.20	0.18316	0.00097	101	2682	9
421.1	259	85	0.04	83	0.371	0.006	6.33	0.10	0.12390	0.00062	101	2013	9
422.1	185	78	0.00	53	0.335	0.005	5.22	0.07	0.11313	0.00040	101	1850	6
423.1	219	88	-0.02	64	0.338	0.005	5.32	0.07	0.11419	0.00038	100	1867	6
424.1	220	131	0.43	69	0.360	0.005	5.63	0.09	0.11328	0.00086	107	1853	14
425.1	295	119	0.28	97	0.381	0.005	8.77	0.12	0.16693	0.00052	82	2527	5
426.1	103	96	0.09	35	0.399	0.006	6.86	0.11	0.12480	0.00070	107	2026	10
427.1	219	107	0.05	61	0.324	0.005	5.09	0.08	0.11381	0.00043	97	1861	7
428.1	134	80	0.07	36	0.311	0.005	4.66	0.08	0.10890	0.00059	98	1781	10
429.1	173	118	0.14	48	0.321	0.004	5.01	0.08	0.11318	0.00051	97	1851	8
430.1	150	97	0.31	55	0.428	0.007	11.18	0.19	0.18963	0.00068	84	2739	6
431.1	373	172	0.11	106	0.329	0.005	5.14	0.08	0.11310	0.00060	99	1850	10
432.1	304	200	0.04	132	0.506	0.007	13.17	0.18	0.18854	0.00038	97	2730	3
433.1	267	147	0.09	80	0.348	0.005	5.58	0.08	0.11649	0.00040	101	1903	6
434.1	17	7	0.31	6	0.421	0.010	7.92	0.24	0.13660	0.00273	104	2185	34

Data are 1σ precision. All Pb data are common Pb corrected based on measured ^{204}Pb (after Stacey and Kramer 1975).
Analysis date 8/4/2001; SHRIMP II

200036 6110: meta-arkose, Emmie Bluff

1:250,000 sheet: Torrens (SH5316)

1:100,000 sheet: Arcoona (6335)

AMG: 704979 E 6556172 N

Location: The sample was taken from diamond drillhole SAE6, depth interval 1110.3-1112.4 m (Figure 29). The diamond drillhole is located within the Emmie Bluff prospect of the Olympic Domain.

Description: In hand specimen the sample represents a pinkish arenaceous clastic sedimentary rock, in which indistinct lamination is defined by weak preferred orientation of slightly more elongate particles and weak particle size-layering. Rare small lustrous pyrite aggregates are observed under the hand lens. Uncommon thin dark reddish (hematite-filled) fractures cut the rock.

In thin section the sample displays a well-preserved framework-supported arenaceous clastic sedimentary texture, modified by grain boundary suturing and selective pervasive alteration effects. It is a poorly-sorted arkosic sandstone composed of subrounded to rounded grains of quartz (53%) and K-feldspar (35%), with minor to trace muscovite (<1%), Fe-Mg grains (?opaques, ?biotite), tourmaline, apatite and zircon. Zircon occurs in trace amount as small equant subrounded grains ~0.05-0.1 mm in size, very sparsely scattered through the rock. All clastic detritus is considered to have been derived from a felsic crystalline source.

The arkosic sandstone underwent low-grade metamorphism up to lower greenschist facies, with generation of new sericite (3%) + hematite (5%) + trace dolomite. Uncommon thin fractures were filled by quartz + hematite + trace chlorite. The development of pervasive hematitic staining of the K-feldspar grains during this event is responsible for the pink colour of the hand specimen.

See Appendix 1 for full petrographic report (Mason 2003).

Mount: Z3931

Description of zircons

The sample contains zircons with a large variation in size from about 40 µm to 300 µm (Figure 30). Grain shape is also variable but most grains are stubby, with low aspect ratios, < 2:1. Grains preserve blunt to rounded prismatic terminations or are equant and sub-rounded in shape. Many grains are clearly detrital, with finely pitted surfaces indicative of sedimentary transport. The zircons are pink to light brown in colour with fairly good clarity, and with few small, clear to brown blebby inclusions and hematite-stained cracks. Cathodoluminescence shows there are few obvious cores present, and that prismatic zoning is ubiquitous, suggesting an initially igneous origin for the detrital grains. In a few grains, the zoning is also visible optically.

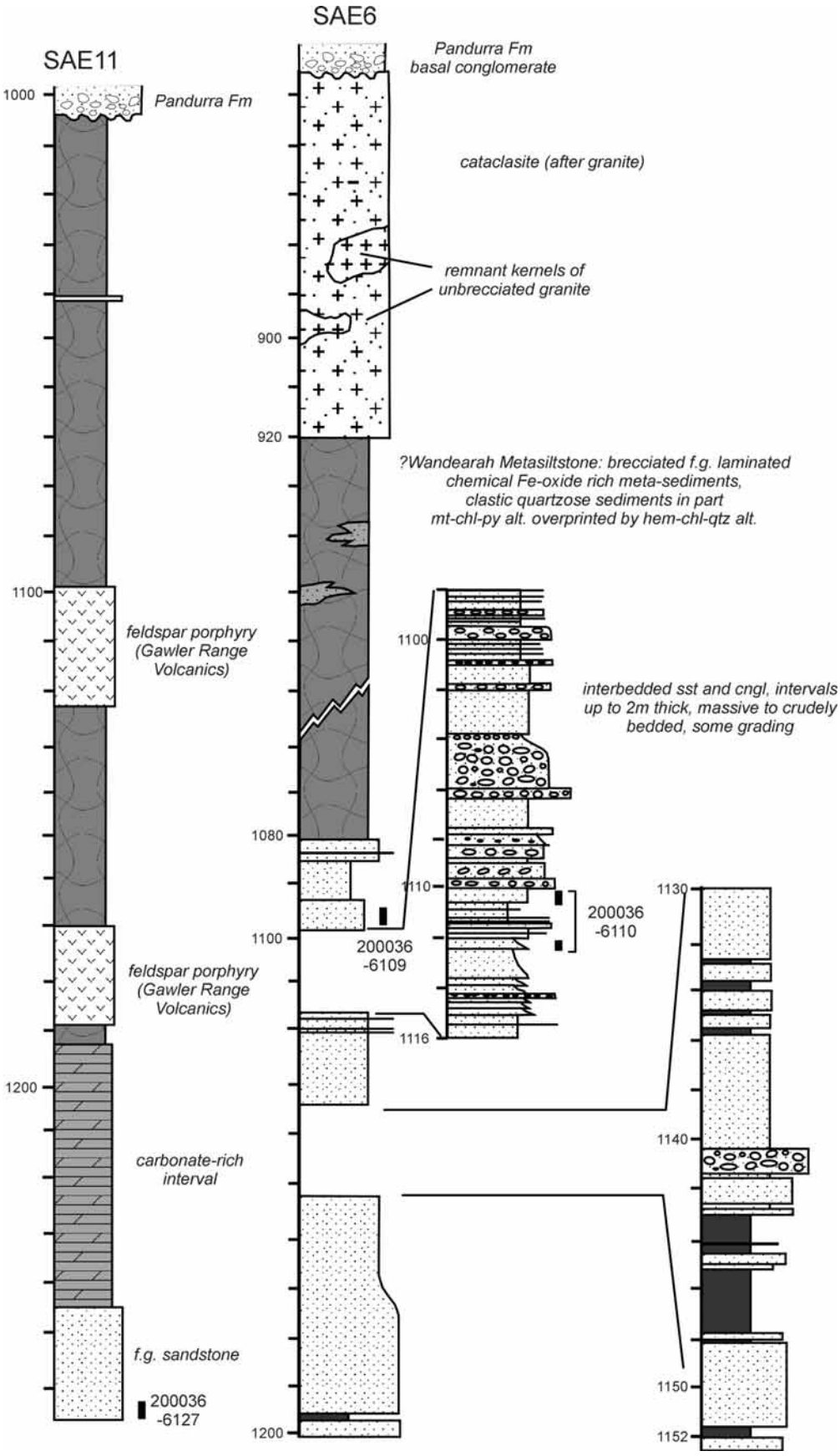

Figure 29. Stratigraphic logs for Emmie Bluff drill holes SAE6 and SAE11 showing the location of samples collected for SHRIMP U-Pb dating.

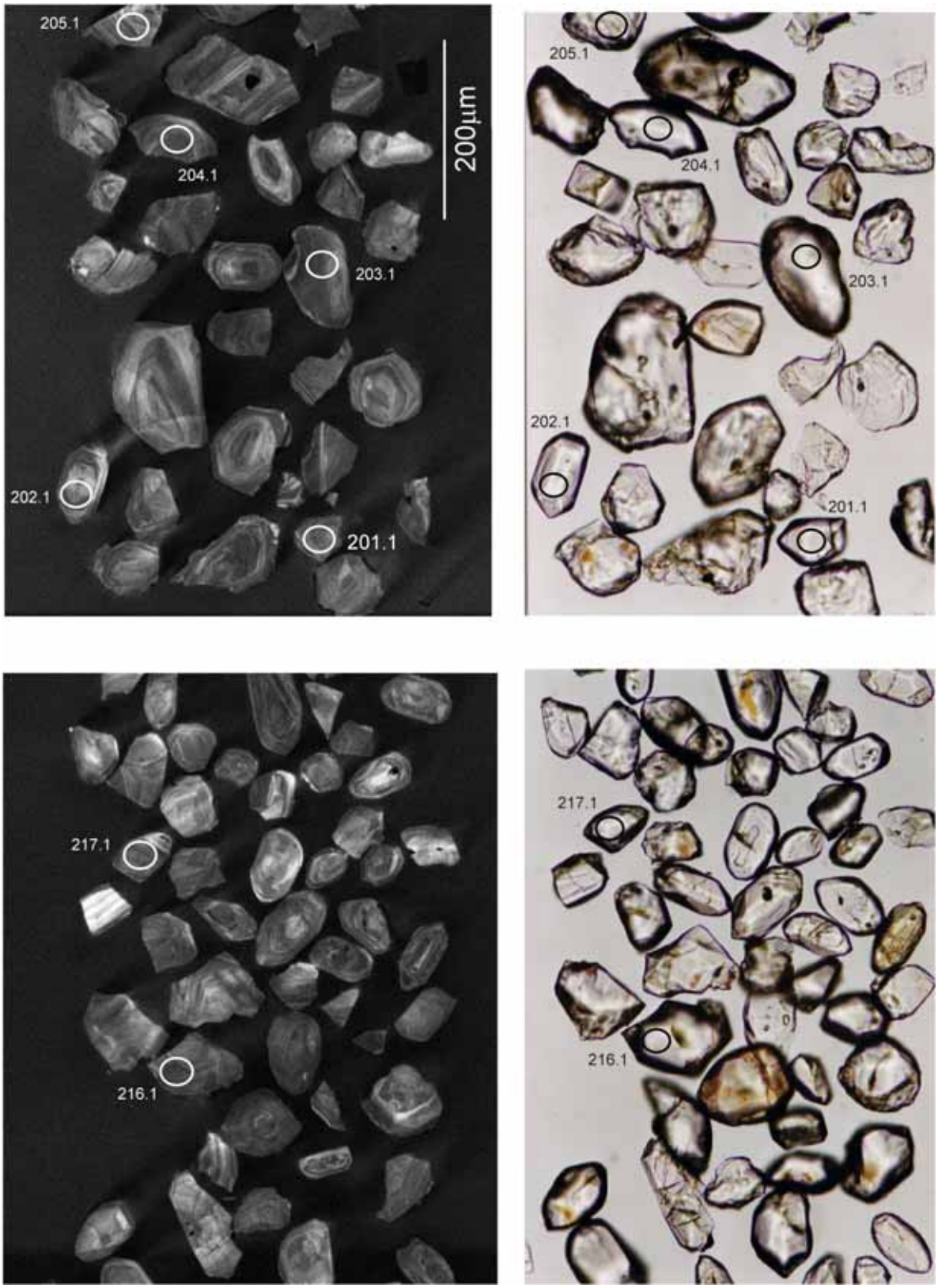

Figure 30. Representative CL (left) and transmitted light (right) images for sample 200036 6110: meta-arkose, Emmie Bluff prospect. SHRIMP analysis spots are labelled. Scale bar is 200 µm.

Concurrent standard data

Data for the standard are presented in Appendix 3. All $^{206}Pb/^{238}U$ QGNG analyses were included in the calibration, to give a calibration exponent of 1.73, with an upper limit of 2.0 and lower limit of 1.5 (at 95% confidence level). Thus the nominal value of 2.0 has been used in data reduction. The 37 $^{206}Pb/^{238}U$ analyses have a 1σ scatter of 2.64%. Element abundance calibration was based on SL13 (n = 1).

The weighted mean $^{207}Pb/^{206}Pb$ age for all 37 analyses is 1846.3 ± 3.9 Ma (MSWD is 1.5; probability of fit = .024). The analyses are corrected for overcounts at mass ^{204}Pb (after Black in press, calculated assuming $^{\mathbf{206}}Pb/^{238}U$-$^{207}Pb$-$^{235}U$ age concordance), which forces the weighted mean $^{207}Pb/^{206}Pb$ age for QGNG to the TIMS reference value. The recalculated age for QGNG becomes 1851.8 ± 3.5 Ma (MSWD = 1.3; probability of fit = .09; n = 37 of 37). The sample data below are also corrected for overcounts.

Sample data

All 30 analyses from this sample have indistinguishable $^{207}Pb/^{206}Pb$ ages that combine to yield a mean crystallisation age of 1846.7 ± 5.0 Ma. When corrected for overcounts at mass ^{204}Pb, the age becomes 1853.4 ± 5.0 Ma (MSWD = 1.16; probability of fit = 0.26; Figures 31, 32).

Geochronological interpretation

The maximum age for the meta-arkose is considered to be 1853.4 ± 5.0 Ma. The provenance for detrital zircons appears to be a local igneous source, solely comprising material of this age.

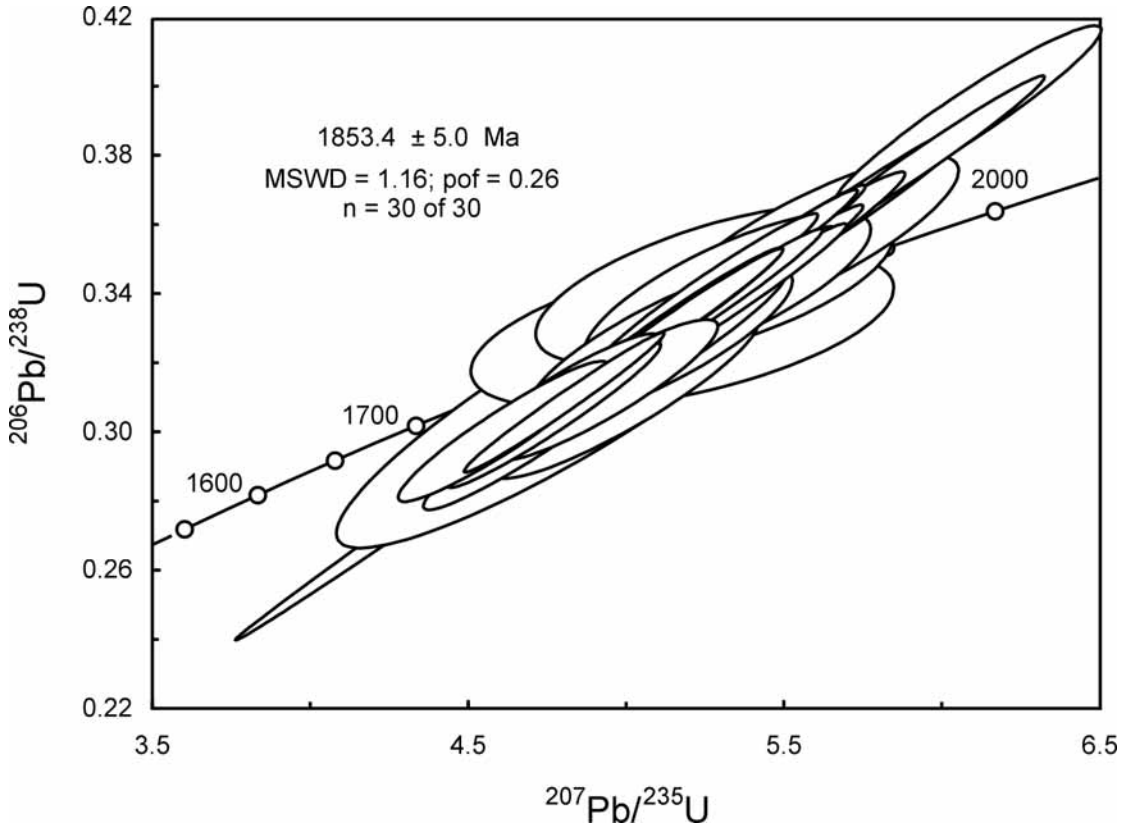

Figure 31. Concordia diagram for zircons in sample 200036 6110 showing radiogenic Pb compositions.

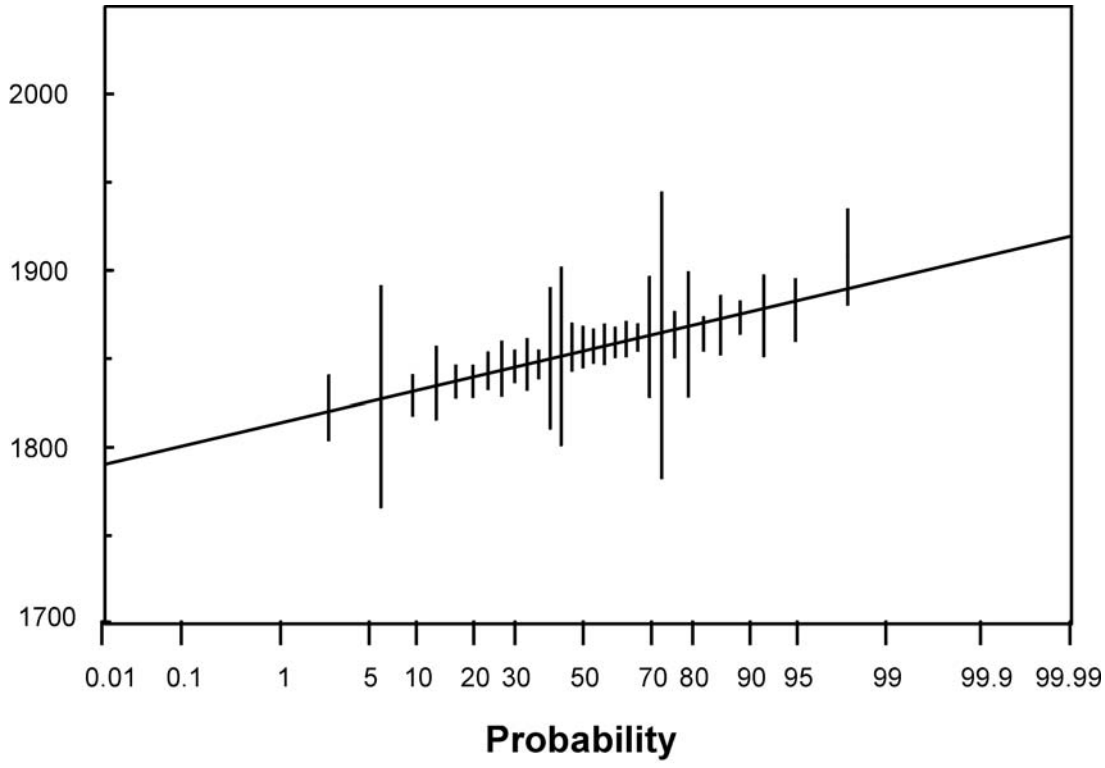

Figure 32. Probability diagram for individual zircon ages for sample 200036 6110. Error bars are 1σ. All analyses conform to a single population.

Table 11. SHRIMP analytical results for zircon from sample 200036 6110.

Spot	U (ppm)	Th (ppm)	$^{206}Pb_c$ (%)	$^{206}Pb^*$ (ppm)	$^{206}Pb^*/^{238}U$	±	$^{207}Pb^*/^{235}U$	±	$^{207}Pb^*/^{206}Pb^*$	±	conc (%)	207Pb/206Pb Age(Ma)	±
201.1	204	108	--	58	0.329	0.009	5.18	0.27	0.1140	0.0051	98	1863	81
202.1	182	111	0.13	53	0.340	0.010	5.29	0.15	0.1129	0.0009	102	1847	15
203.1	327	52	0.07	93	0.331	0.009	5.15	0.14	0.1128	0.0006	100	1846	9
204.1	210	100	--	59	0.325	0.009	5.10	0.17	0.1139	0.0022	97	1862	34
205.1	195	91	--	54	0.323	0.010	5.11	0.16	0.1149	0.0011	96	1878	18
206.1	235	106	0.01	61	0.299	0.009	4.72	0.15	0.1143	0.0011	89	1869	17
207.1	139	68	--	37	0.310	0.010	4.99	0.17	0.1168	0.0018	90	1908	27
208.1	443	124	0.03	116	0.305	0.009	4.77	0.14	0.1135	0.0009	92	1856	14
209.1	136	88	--	41	0.355	0.010	5.59	0.19	0.1140	0.0023	105	1864	35
210.1	211	63	--	62	0.340	0.009	5.24	0.15	0.1118	0.0007	103	1829	12
211.1	261	105	--	75	0.336	0.009	5.26	0.15	0.1136	0.0006	101	1857	10
212.1	158	151	--	41	0.300	0.008	4.60	0.14	0.1114	0.0011	92	1822	19
213.1	167	53	0.02	48	0.331	0.009	5.15	0.14	0.1127	0.0007	100	1843	11
214.1	155	88	--	47	0.352	0.009	5.51	0.15	0.1135	0.0007	104	1857	12
215.1	166	97	--	49	0.341	0.009	5.32	0.19	0.1131	0.0025	102	1850	40
216.1	236	112	--	68	0.338	0.009	5.34	0.14	0.1146	0.0006	100	1873	10
217.1	233	62	--	62	0.310	0.018	4.85	0.32	0.1132	0.0032	94	1851	51
218.1	250	100	0.07	66	0.308	0.008	4.80	0.13	0.1129	0.0005	93	1847	8
219.1	226	70	0.08	74	0.378	0.010	5.93	0.16	0.1137	0.0005	110	1859	9
220.1	137	64	0.75	41	0.343	0.009	5.28	0.23	0.1118	0.0039	104	1829	63
221.1	129	68	--	37	0.337	0.012	5.33	0.96	0.1150	0.0207	100	1873	320
222.1	335	90	--	90	0.312	0.008	4.93	0.15	0.1146	0.0015	93	1874	23
223.1	126	71	0.04	37	0.343	0.009	5.39	0.15	0.1140	0.0006	102	1864	10
224.1	169	86	0.10	51	0.348	0.009	5.39	0.15	0.1123	0.0006	105	1837	9
225.1	138	74	--	41	0.347	0.009	5.37	0.15	0.1123	0.0006	104	1837	9
226.1	202	101	0.80	54	0.308	0.009	4.76	0.14	0.1122	0.0012	94	1836	21
228.1	133	80	0.40	45	0.391	0.011	6.09	0.18	0.1128	0.0010	113	1845	16
229.1	250	299	--	69	0.322	0.032	5.05	0.51	0.1139	0.0005	96	1862	8
230.1	225	109	0.12	65	0.338	0.009	5.31	0.15	0.1138	0.0006	101	1861	10
231.1	233	158	0.29	73	0.364	0.010	5.71	0.17	0.1136	0.0007	107	1858	11

Data are 1σ precision. All Pb data are common Pb corrected based on measured ^{204}Pb (after Stacey and Kramer 1975).
Analysis date 26/4/2002; SHRIMP I

200036 6127: fine-grained sandstone, Emmie Bluff

1:250,000 sheet: Torrens (SH5316)

1:100,000 sheet: Woomera (6235)

AMG: 684879 E 6560672 N

Location: The sample was taken from diamond drillhole SAE11, depth interval 1264.4-1266.8 m (Figure 29). The diamond drillhole is located within the Emmie Bluff prospect of the Olympic Domain.

Description: The sample is a fine-grained sandstone with angular grains of quartz and microcline to 0.2 mm in grainsize, as well as apparently secondary reddish alkali feldspar, probably adularia. The quartz (40%) and microcline (30%) are present in subequal amounts, but the adularia is less abundant (~20%). Opaque oxide (5%) is also disseminated, with chlorite (~5%) and aggregates of possible anatase. Patches of carbonate are sparsely scattered and there are narrow veins with quartz and/or chlorite.

(Purvis 1999).

Mount: Z3931

Description of zircons

The sample contains small zircons ranging from about 30 µm to 200 µm in size (Figure 33). The grains are variable in shape, with many obviously detrital grains present, that are rounded to sub-rounded with finely pitted surfaces indicative of sedimentary transport. Prismatic terminations and crystal facets are preserved in many other grains. Aspect ratios are variable, but mostly < 3:1. The zircons are colourless to faint brown and clear, with few small, clear to brown blebby inclusions. Brown, hematite-stained cracks are common, and they contain no obvious cores. Cathodoluminescence shows that prismatic zoning is ubiquitous, suggesting an initially igneous origin for the detrital grains. In some grains, the zoning is also visible optically.

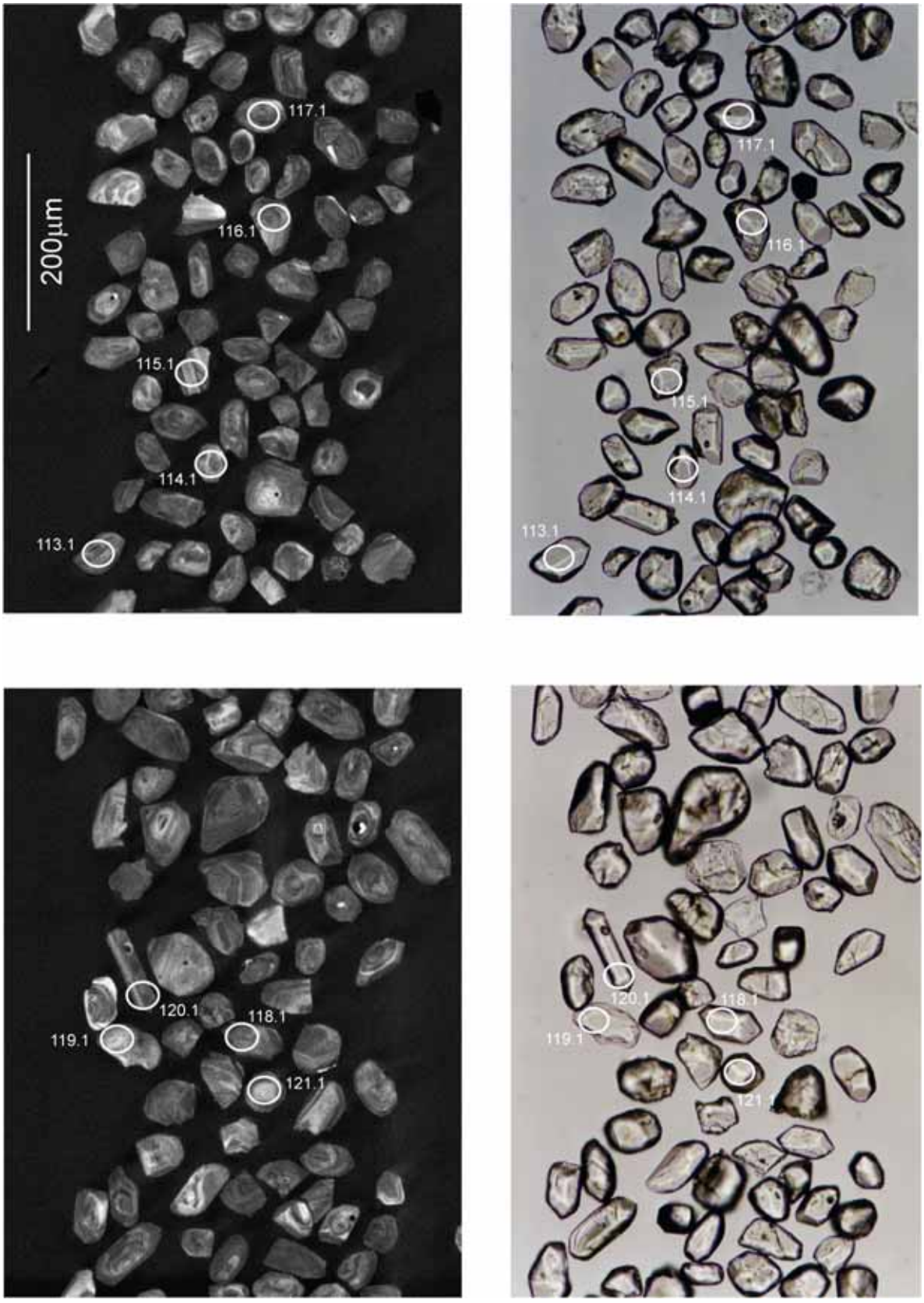

Figure 33. Representative CL (left) and transmitted light (right) images for sample 200036 6127: fine-grained sandstone, Emmie Bluff prospect. SHRIMP analysis spots are labelled. Scale bar is 200 µm.

Concurrent standard data

Data for the standard are presented in Appendix 3. All $^{206}Pb/^{238}U$ QGNG analyses were included in the calibration, to give a calibration exponent of 1.73, with an upper limit of 2.0 and lower limit of 1.5 (at 95% confidence level). Thus the nominal value of 2.0 has been used in data reduction. The 37 $^{206}Pb/^{238}U$ analyses have a 1σ scatter of 2.64%. Element abundance calibration was based on SL13 (n = 1).

The weighted mean $^{207}Pb/^{206}Pb$ age for all 37 analyses is 1846.3 ± 3.9 Ma (MSWD is 1.5; probability of fit = .024). The analyses are corrected for overcounts at mass ^{204}Pb (after Black in press, calculated assuming $^{\mathbf{206}}Pb/^{238}U$-$^{207}Pb$-$^{235}U$ age concordance), which forces the weighted mean $^{207}Pb/^{206}Pb$ age for QGNG to the TIMS reference value. The recalculated age for QGNG becomes 1851.8 ± 3.5 Ma (MSWD = 1.3; probability of fit = .09; n = 37 of 37). The sample data below are also corrected for overcounts.

Sample data

The 32 analyses do not conform to a single population. The two youngest analyses (115.1 and 132.1) are clearly younger that the others (Figure 34), plotting close to concordia at about 1780 Ma (Figure 35). The grains have slightly higher common radiogenic Pb, suggesting their younger age may reflect non-recent radiogenic Pb loss in *ca* 1850 Ma grains, but it is possible that *ca* 1780 Ma represents their crystallisation age.

The remaining 30 analyses yielded a weighted mean $^{207}Pb/^{206}Pb$ age of 1845.7 ± 4.9 Ma. When corrected for overcounts at mass ^{204}Pb, the age becomes 1854 ± 6 Ma (MSWD = 1.87; probability of fit = .003). Although the MSWD indicates there is still an unacceptable statistical scatter in the ages, there are no other obvious statistical outliers, and no geological reason to discard any other analyses.

Geochronological interpretation

The maximum age for the sandstone is considered to be ~ 1780 Ma. The provenance for detrital zircons appears to be a local igneous source, mainly, or possibly solely comprising material of ~1854 Ma in age.

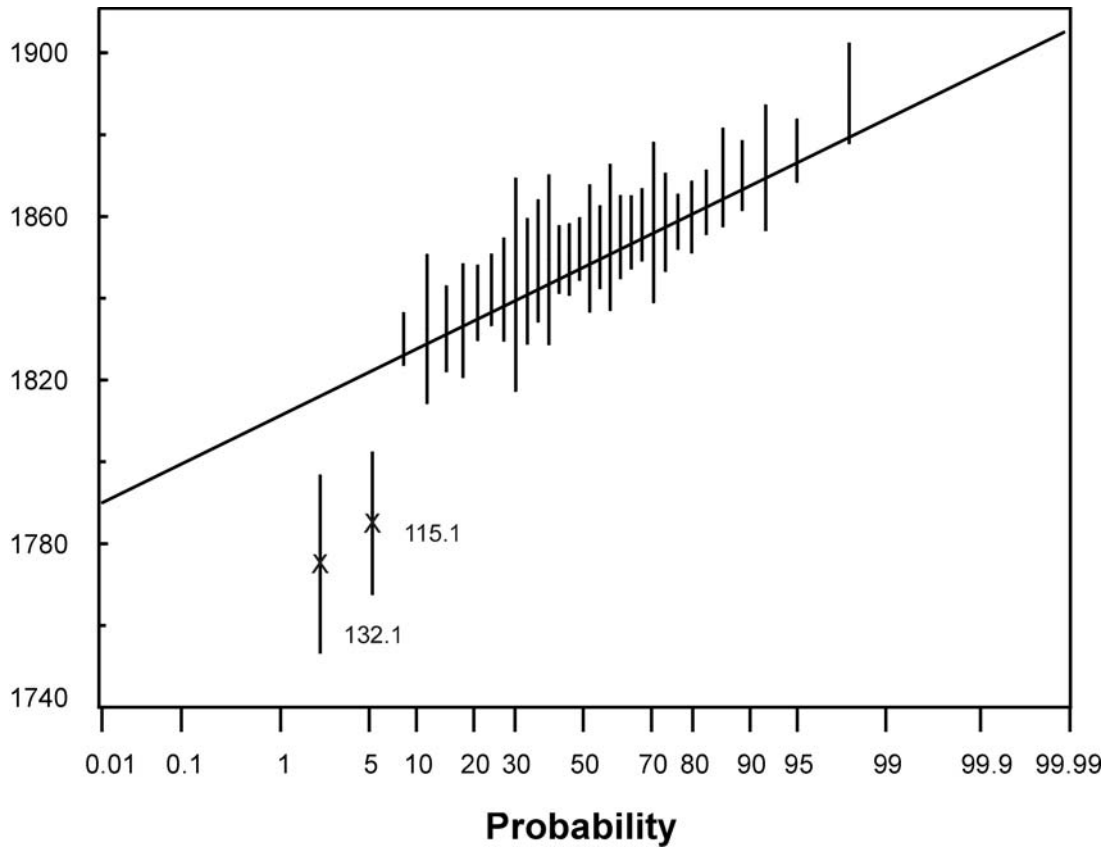

Figure 34. Probability diagram for individual zircon ages for sample 200036 6127. The two youngest analyses are clearly outliers from the main population.

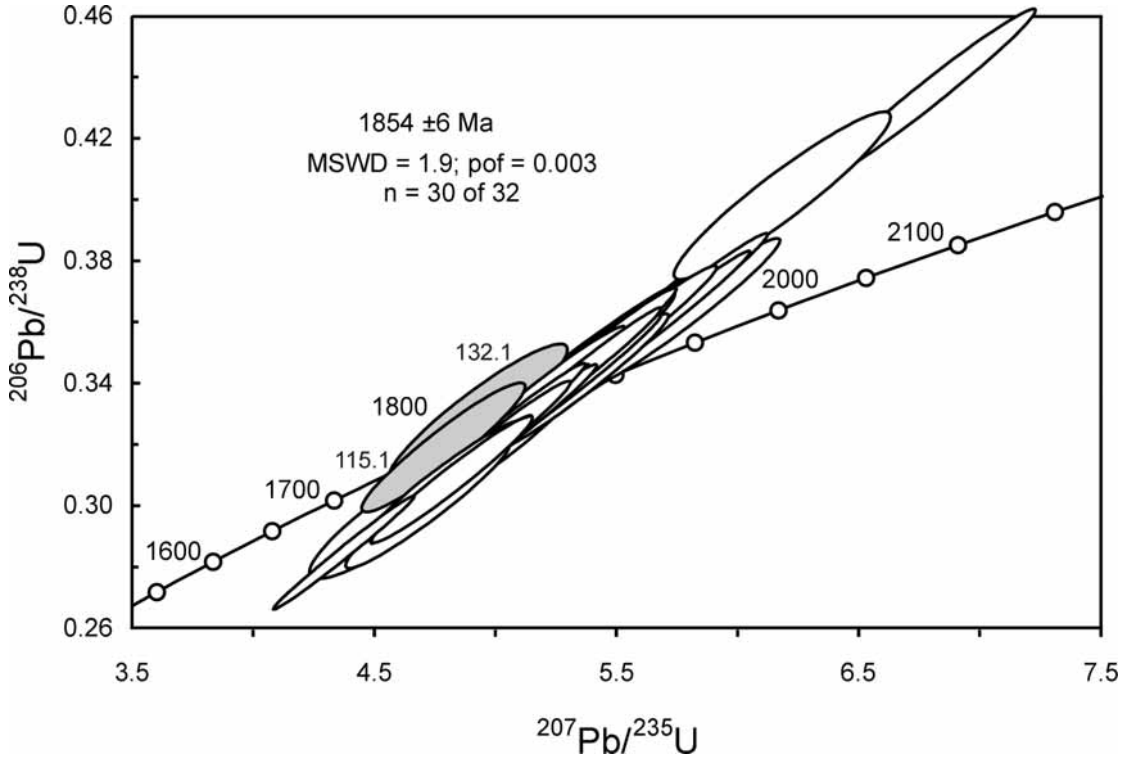

Figure 35. Concordia diagram for zircons in sample 200036 6127 showing radiogenic Pb compositions. White-filled symbols represent analyses used in the weighted mean age calculation. Younger grains are light grey.

Table 12. SHRIMP analytical results for zircon from sample 200036 6127.

Spot	U (ppm)	Th (ppm)	$^{206}Pb_c$ (%)	$^{206}Pb^*$ (ppm)	$^{206}Pb^*/^{238}U$	±	$^{207}Pb^*/^{235}U$	±	$^{207}Pb^*/^{206}Pb^*$	±	conc (%)	207Pb/206Pb Age(Ma)	±
101.1	136	81	0.06	39	0.336	0.009	5.23	0.15	0.1128	0.0010	101	1844	15
102.1	244	79	0.03	70	0.336	0.009	5.18	0.15	0.1120	0.0006	102	1833	10
103.1	274	100	0.06	75	0.319	0.009	4.97	0.14	0.1133	0.0006	96	1852	10
104.1	248	113	--	77	0.362	0.010	5.78	0.17	0.1157	0.0008	105	1890	12
105.1	228	205	0.09	69	0.351	0.010	5.50	0.17	0.1136	0.0012	104	1859	20
106.1	298	196	0.09	77	0.299	0.008	4.72	0.14	0.1145	0.0010	89	1872	15
107.1	236	134	0.25	60	0.296	0.009	4.60	0.15	0.1127	0.0016	90	1843	26
108.1	204	57	0.26	56	0.319	0.009	4.97	0.16	0.1131	0.0012	96	1849	21
109.1	291	179	0.07	87	0.346	0.009	5.37	0.15	0.1126	0.0008	104	1842	13
110.1	167	137	--	49	0.339	0.009	5.34	0.15	0.1143	0.0008	101	1870	12
111.1	331	86	0.00	92	0.324	0.009	5.04	0.14	0.1126	0.0005	98	1842	9
112.1	163	106	0.05	47	0.338	0.009	5.28	0.15	0.1134	0.0011	101	1855	18
113.1	228	129	--	67	0.339	0.009	5.33	0.14	0.1140	0.0005	101	1864	8
114.1	176	99	0.04	53	0.347	0.009	5.38	0.15	0.1124	0.0006	104	1839	9
115.1	194	229	0.56	53	0.318	0.009	4.79	0.14	0.1091	0.0010	100	1785	17
116.1	232	176	0.32	65	0.324	0.010	5.05	0.17	0.1131	0.0009	98	1849	15
117.1	291	514	0.71	101	0.401	0.011	6.19	0.19	0.1121	0.0011	116	1833	18
118.1	200	150	0.01	62	0.358	0.010	5.67	0.16	0.1148	0.0005	105	1876	8
119.1	106	40	0.00	32	0.354	0.010	5.54	0.16	0.1134	0.0006	105	1855	10
120.1	283	258	0.08	105	0.433	0.012	6.78	0.18	0.1135	0.0006	120	1856	9
121.1	155	95	--	41	0.308	0.008	4.82	0.13	0.1137	0.0008	93	1859	12
122.1	193	141	--	61	0.364	0.010	5.74	0.15	0.1144	0.0005	107	1870	9
123.1	234	114	0.09	69	0.342	0.009	5.33	0.14	0.1132	0.0005	102	1852	8
124.1	186	88	--	52	0.324	0.009	5.08	0.14	0.1137	0.0006	97	1860	9
125.1	199	184	--	52	0.306	0.009	4.78	0.14	0.1133	0.0010	92	1852	16
126.1	258	229	0.10	87	0.394	0.022	6.14	0.35	0.1131	0.0005	114	1850	8
127.1	433	249	0.09	105	0.284	0.008	4.37	0.12	0.1119	0.0004	86	1830	7
128.1	259	91	0.01	75	0.334	0.010	5.24	0.15	0.1137	0.0004	100	1859	7
129.1	230	105	0.04	64	0.323	0.009	5.04	0.14	0.1131	0.0005	98	1850	9
130.1	253	146	0.23	73	0.335	0.013	5.18	0.20	0.1122	0.0009	101	1835	14
131.1	243	205	0.03	64	0.308	0.009	4.82	0.13	0.1136	0.0006	93	1858	9
132.1	90	69	0.38	26	0.330	0.009	4.93	0.15	0.1085	0.0013	103	1775	22

Data are 1σ precision. All Pb data are common Pb corrected based on measured ^{204}Pb (after Stacey and Kramer 1975).
Analysis date 26/4/2002; SHRIMP I

200036 6133: meta-arkose, Arcoona Station

1:250,000 sheet: Torrens (SH5316)

1:100,000 sheet: Arcoona (6335)

AMG: 702536 E 6557922 N

Location: The sample was taken from diamond drillhole AD8, depth interval 901.1-.3, 901.8-902 m (Figure 36). The diamond drillhole is located within the Arcoona Station prospect of the Olympic Domain.

Description: In thin section the sample displays a fine-grained framework-supported arenaceous clastic sedimentary texture with mica-defined primary bedding plane orientation, modified by strong cataclastic deformation and selective pervasive alteration.

The clastic material is partly sorted but compositionally immature, comprising subrounded K-feldspar (44%), subrounded to angular quartz (20%), large muscovite flakes (10%), ?plagioclase, pseudomorphed by dense monominerallic mats of sericite, ?biotite replaced by hematite, and traces of subrounded tourmaline and zircon. Zircon grains are concentrated locally with hematite, in thin (~0.1-0.2 mm wide) laminae of inferred heavy mineral sedimentary origin. Primary bedding is pervasively defined by aligned muscovite and ?biotite flakes, and by the thin heavy-mineral-rich laminae. The clastic materials are inferred to have been derived from a felsic crystalline source.

The arkosic sandstone underwent burial and low-grade diagenetic processes, including grain suturing, but little or no metamorphic modification. The rock body later underwent severe brittle (cataclastic) deformation, with development of subparallel to anastomosing granulated bands. Partial rotation of primary lamination occurred between closely-spaced cataclastic bands. Pervasive low-grade alteration affected the rock, probably at this time, generating moderately abundant sericite + hematite. The sericite formed pervasively through the rock, both as matrix within the cataclastic bands and pervasively elsewhere, possibly by preferential replacement of ?plagioclase grains. The hematite formed as matrix in the cataclastic bands, as replacements of precursor Fe-rich materials in the heavy-mineral-rich laminae, and as replacements of primary ?biotite flakes.

See Appendix 1 for full petrographic report (Mason 2003).

Mount: Z3966

Description of zircons

The sample contains mostly well-rounded detrital zircons grains ranging between 30 µm to 200 µm in size, with variable aspect ratios < 3:1. Some grains also display finely pitted surfaces indicative of sedimentary transport. The zircons are clear and colourless to faint brown internally, with some external orange staining. Brown- and orange-stained cracks are common. Some grains contain small, clear inclusions or larger brown inclusions. The grains contain no obvious cores. Well-defined concentric zoning is present in most grains, as seen in the CL images (Figure 37), suggesting an igneous origin for the zircons.

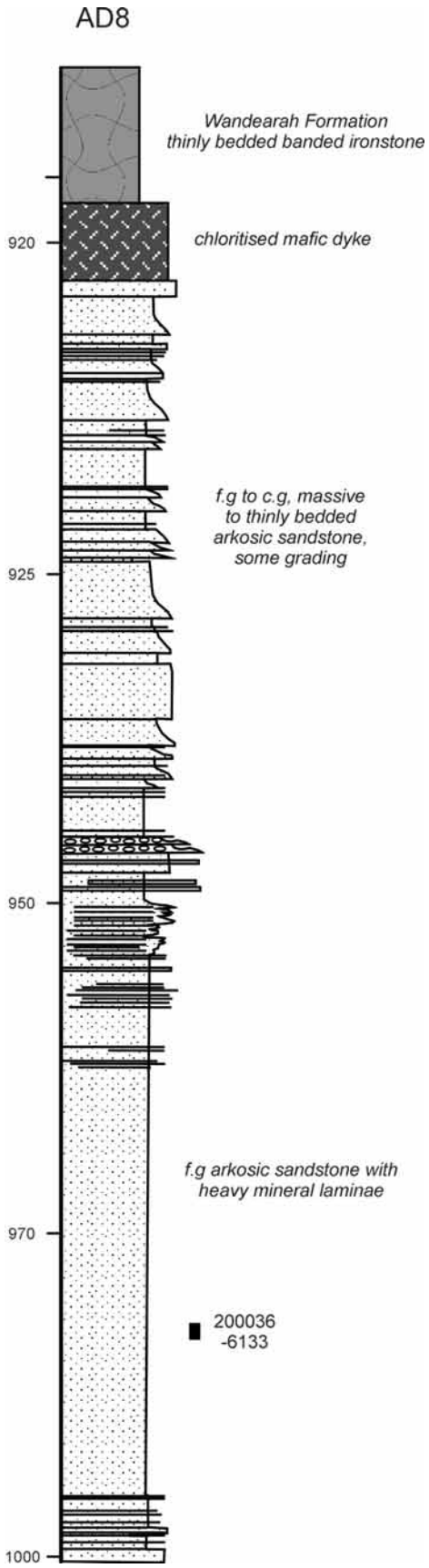

Figure 36. Stratigraphic log for diamond drill hole AD 8*, showing the location of sample collected for SHRIMP dating.*

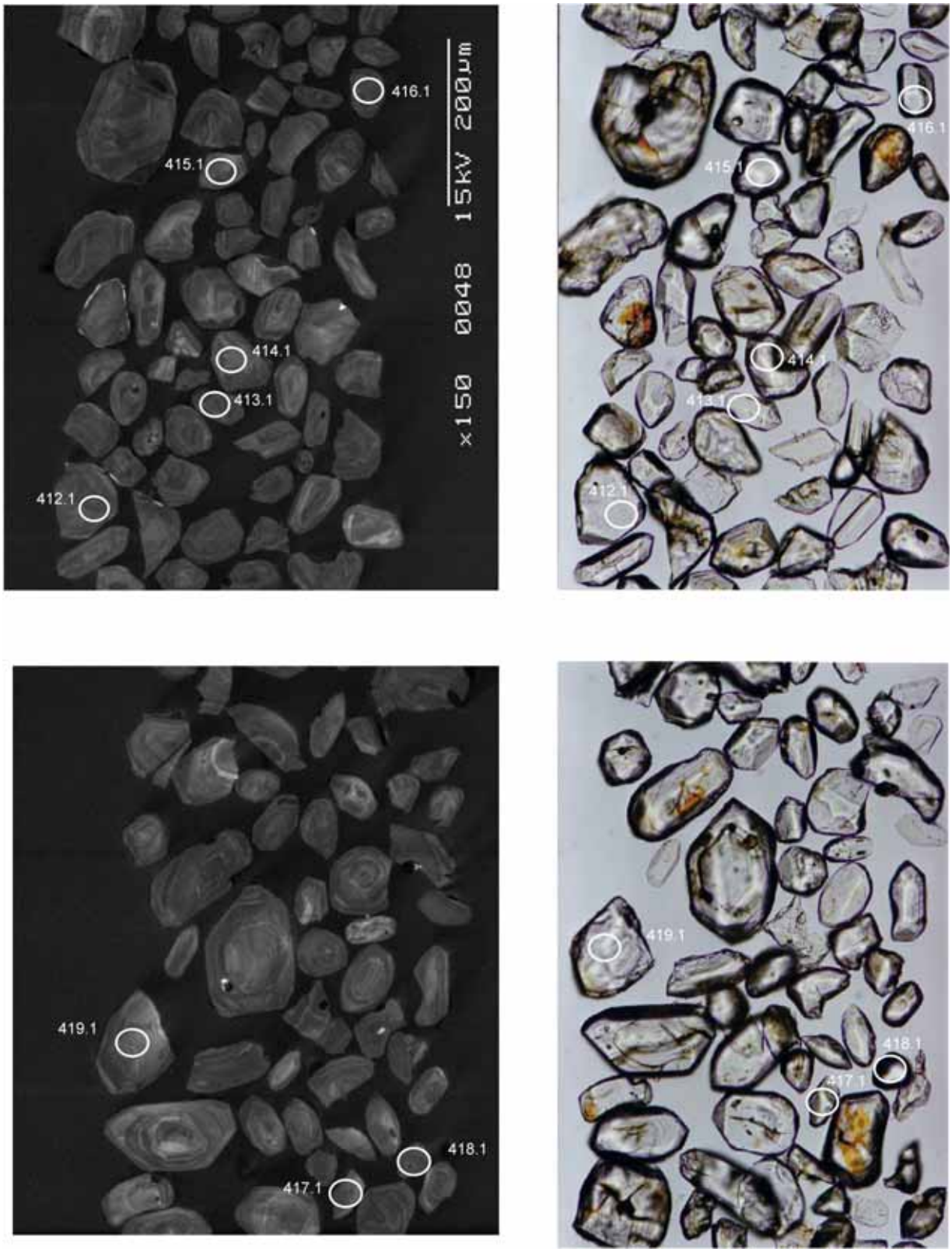

Figure 37. Representative CL (left) and transmitted light (right) images for sample 200036 6133: meta-arkose, Arcoona Station prospect. SHRIMP analysis spots are labelled. Scale bar is 200 μm.

Concurrent standard data

Data for the standard are presented in Appendix 3. The calibration exponent for this QGNG data set is 1.96, with an upper limit of 2.26 and a lower limit of 1.61 (at the 95% confidence level). Thus the nominal value of 2.0 has been used in data reduction. All analyses are used in the calibration. There are two outliers in $^{206}Pb/^{238}U$ (915.1 and 932.1) and these have been omitted, leaving 49 analyses with a 1σ scatter in $^{206}Pb/^{238}U$ of 3.58%. Element abundance calibration was based on SL13 (n = 1).

There is only one obvious outlier amongst the $^{207}Pb/^{206}Pb$ ages, (915.1) but the remaining 50 analyses do not conform to a normal distribution, yielding a weighted mean $^{207}Pb/^{206}Pb$ age of 1843 ± 6 Ma (MSWD = 2.5; probability of fit = 0). The analyses are corrected for overcounts at mass ^{204}Pb (after Black in press; calculated assuming $^{\mathbf{206}}Pb/^{238}U$-$^{207}Pb$-$^{235}U$ age concordance), which forces the weighted mean $^{207}Pb/^{206}Pb$ age for QGNG to the TIMS reference value. The sample data below are also corrected for overcounts at the ^{204}Pb mass peak.

The recalculated age for QGNG becomes 1851.9 ± 4.6 Ma (MSWD is 1.3; probability of fit is .09; n = 46 of 51). In this case, *SQUID* identifies 5 statistical outliers. Excluding the youngest analysis (915.1; age 1727 ± 15 Ma (1σ error)) from the age calculation is warranted, as the grain contains high common ^{206}Pb and is discordant, suggesting Pb loss may have occurred. However, there are no other obvious statistical outliers, and no geological reason for further culling of analyses. The remaining 50 analyses yield a weighted mean $^{207}Pb/^{206}Pb$ age of 1849 ± 6 Ma (MSWD = 2.2; probability of fit = 0). The high MSWD indicates the scatter in the analyses is greater than that predicted by counting statistics alone. The wide spread of ages is therefore attributed to a component of instrument uncertainty, and high MSWDs for the corresponding samples are also acceptable.

Sample data

Thirty grains were analysed. The analyses cluster close to concordia at about 1850 Ma (Figure 38). However, with a high MSWD of 1.9, they do not fulfil the requirements of a simple population. A probability density curve reveals a tail below the mean age (Figure 39), suggesting a component of non-recent radiogenic Pb loss in the grains. The youngest two analyses in the data set have high common ^{206}Pb and U contents. Eliminating the 4 youngest grains from the uncorrected dataset yields a weighted mean $^{207}Pb/^{206}Pb$ age of 1845 ± 7 Ma (MSWD = 1.3; probability = 0,13; n = 26). Eliminating the three youngest analyses from the overcount-corrected dataset (428.1, 413.1 and 418.1) results in a weighted mean $^{207}Pb/^{206}Pb$ age of 1852 ± 7 Ma (MSWD = 1.5, probability of fit = 0.047).

Geochronological interpretation

The maximum age for the sandstone is considered to be 1852 ± 7 Ma. The provenance for detrital zircons appears to be a local igneous source, solely comprising material of this age.

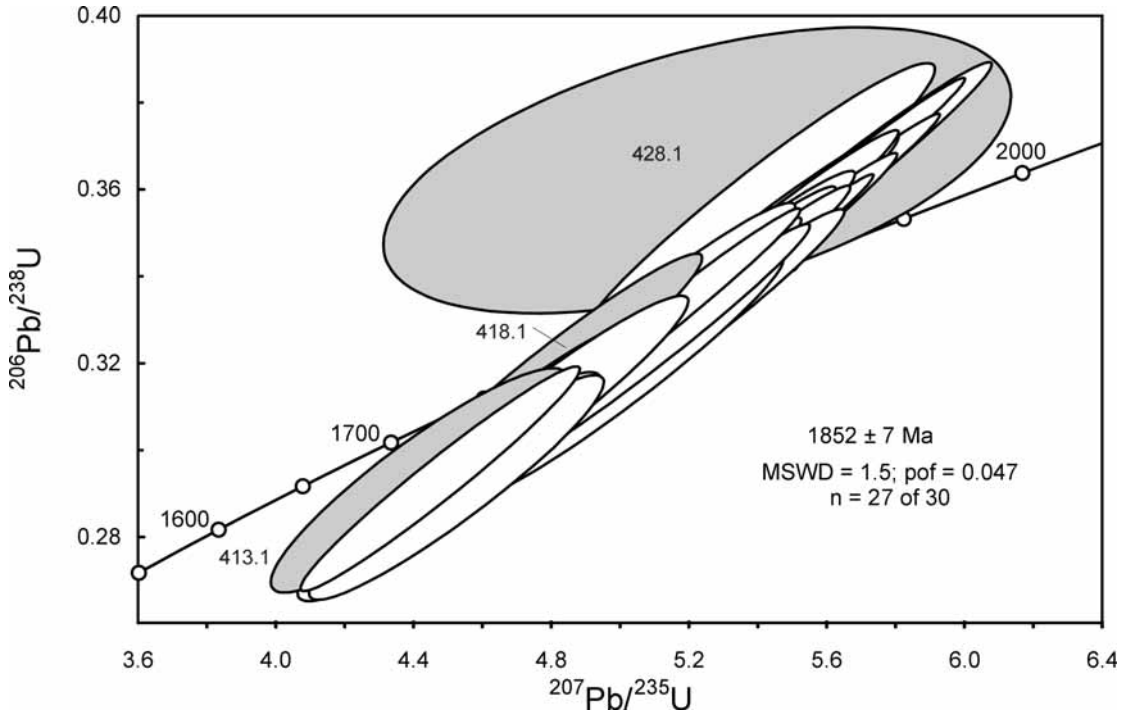

Figure 38. Concordia diagram for zircons in sample 200036 6133 showing radiogenic Pb compositions. White-filled symbols represent analyses used in the weighted mean age calculation. Light grey analyses signify likely Pb-loss.

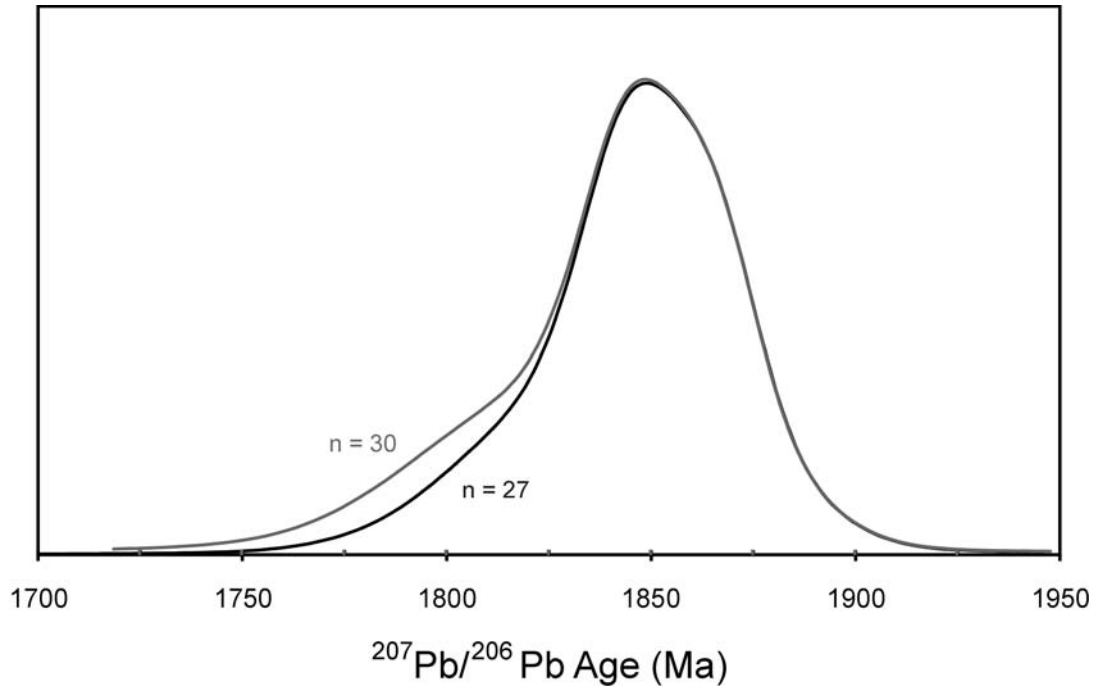

Figure 39. Probability density distribution of $^{207}Pb/^{206}Pb$ ages shows that a tail of Pb loss is produced by the youngest analyses. When the three youngest analyses are eliminated, the remaining 27 produce a distribution that is more normal.

Table 13. SHRIMP analytical results for zircon from sample 200036 6133.

Spot	U (ppm)	Th (ppm)	$^{206}Pb_c$ (%)	$^{206}Pb^*$ (ppm)	$^{206}Pb^*/^{238}U$	±	$^{207}Pb^*/^{235}U$	±	$^{207}Pb^*/^{206}Pb^*$	±	conc (%)	207Pb/206Pb Age(Ma)	±
401.1	338	159	0.15	94	0.323	0.012	5.09	0.19	0.11416	0.00082	97	1867	13
402.1	220	82	0.04	65	0.343	0.013	5.33	0.20	0.11263	0.00073	103	1842	12
403.1	158	118	-0.06	47	0.344	0.013	5.35	0.20	0.11290	0.00102	103	1846	16
404.1	174	64	-0.04	50	0.334	0.012	5.20	0.20	0.11291	0.00094	101	1847	15
405.1	319	76	0.15	87	0.315	0.012	4.90	0.19	0.11270	0.00135	96	1843	21
406.1	144	102	0.05	41	0.330	0.012	5.16	0.20	0.11356	0.00100	99	1857	16
407.1	175	71	0.01	49	0.324	0.012	5.06	0.19	0.11321	0.00084	98	1852	13
408.1	181	109	0.02	52	0.331	0.012	5.15	0.20	0.11296	0.00086	100	1848	14
409.1	124	63	0.23	38	0.357	0.013	5.40	0.21	0.10990	0.00121	109	1797	21
410.1	183	134	0.00	50	0.316	0.012	5.01	0.19	0.11470	0.00115	95	1876	19
411.1	382	185	0.27	107	0.327	0.012	5.07	0.19	0.11252	0.00064	99	1840	10
412.1	291	78	0.02	89	0.354	0.013	5.51	0.20	0.11277	0.00054	106	1845	9
413.1	400	108	2.05	103	0.293	0.011	4.42	0.18	0.10930	0.00186	93	1788	30
414.1	142	106	-0.11	40	0.328	0.012	5.15	0.31	0.11400	0.00536	100	1864	84
415.1	157	105	-0.20	45	0.331	0.012	5.20	0.19	0.11381	0.00074	99	1861	12
416.1	336	182	1.32	85	0.291	0.010	4.52	0.18	0.11260	0.00146	89	1842	24
417.1	333	139	0.52	89	0.308	0.011	4.76	0.18	0.11190	0.00123	95	1831	21
418.1	300	64	0.67	82	0.317	0.011	4.80	0.18	0.10970	0.00110	99	1794	18
419.1	196	73	-0.02	57	0.338	0.013	5.33	0.20	0.11419	0.00067	101	1867	11
420.1	201	68	1.12	51	0.291	0.011	4.51	0.18	0.11210	0.00168	90	1834	27
421.1	224	132	0.02	67	0.346	0.013	5.44	0.20	0.11388	0.00056	103	1862	9
422.1	384	108	0.68	98	0.293	0.011	4.48	0.17	0.11072	0.00094	92	1811	15
423.1	175	134	0.29	49	0.328	0.012	5.05	0.19	0.11160	0.00107	100	1826	17
424.1	474	387	0.96	124	0.303	0.011	4.64	0.18	0.11130	0.00134	94	1821	22
425.1	283	94	-0.05	81	0.334	0.012	5.27	0.19	0.11440	0.00055	99	1870	9
426.1	158	117	0.02	46	0.342	0.013	5.32	0.20	0.11281	0.00087	103	1845	14
427.1	171	46	0.09	53	0.357	0.013	5.58	0.21	0.11315	0.00076	106	1851	12
428.1	418	214	2.19	134	0.364	0.013	5.22	0.37	0.10400	0.00634	118	1696	110
429.1	201	160	-0.06	59	0.342	0.013	5.33	0.20	0.11295	0.00098	103	1847	16
430.1	190	65	-0.13	53	0.326	0.012	5.18	0.19	0.11512	0.00092	97	1882	14

Data are 1σ precision. All Pb data are common Pb corrected based on measured ^{204}Pb (after Stacey and Kramer 1975).
Analysis date 11/6/2002; SHRIMP I

200036 6102: schist, Arcoona Station

1:250,000 sheet: Torrens (SH5316)

1:100,000 sheet: Arcoona (6335)

AMG: 693035 E 6566428 N

Location: The sample was taken from diamond drillhole ASD2W1, depth interval 1069.2-.8, 1070.5-1071.5 m (Figure 40). The diamond drillhole is located within the Arcoona Station prospect of the Olympic Domain.

Description: The sample is a folded micaceous schist with millimetre- to centimetre-scale layers variously rich in muscovite, plagioclase and alkali feldspar. The alkali feldspar may be secondary, as layers rich in plagioclase pass into alkali feldspar-rich layers. Plagioclase comprises a micro-mosaic 0.2 to 1 mm in grainsize, with sericitised plagioclase passing into areas containing slightly reddish alkali feldspar ± plagioclase (50%). Quartz is irregularly distributed as the micromosaic passes from feldspathic to quartzofeldspathic to quartz-rich layers (average quartz is 15%). The schistosity is defined by muscovite flakes up to 0.4 mm long (30%). Minor green tourmaline is disseminated, elongate parallel to schistosity (3%). Minor chlorite occurs after schistose biotite (1-2%). Limonite, possibly after pyrite, is also disseminated, to 0.3 mm in grainsize (< 1%). Chlorite-rich shears occur at a low angle to the layering, passing into veins with clays, chlorite, quartz, carbonate and, in some areas, granular alkali feldspar, possibly adularia.

The original lithology may have been a quartzofeldspathic sandstone.

Purvis 1999.

Mount: Z3931

Description of zircons

The sample contains euhedral zircons and zircon fragments ranging between 100 to 200 µm in size. Whole grains are tabular to prismatic in shape with predominantly fairly blunt terminations and aspect ratios of about 2:1. Many grain fragments are equant and some grains, both equant and elongate, exhibit rounding and finely pitted surfaces characteristic of detrital grains. The zircons have good clarity and are colourless to pink, with few inclusions and cracks. No obvious cores are visible. Well-defined zoning is present in most grains, as seen in the CL images (Figure 41) and in the transmitted and reflected light photos. The grains display concentric euhedral zoning patterns typical of igneous crystallisation.

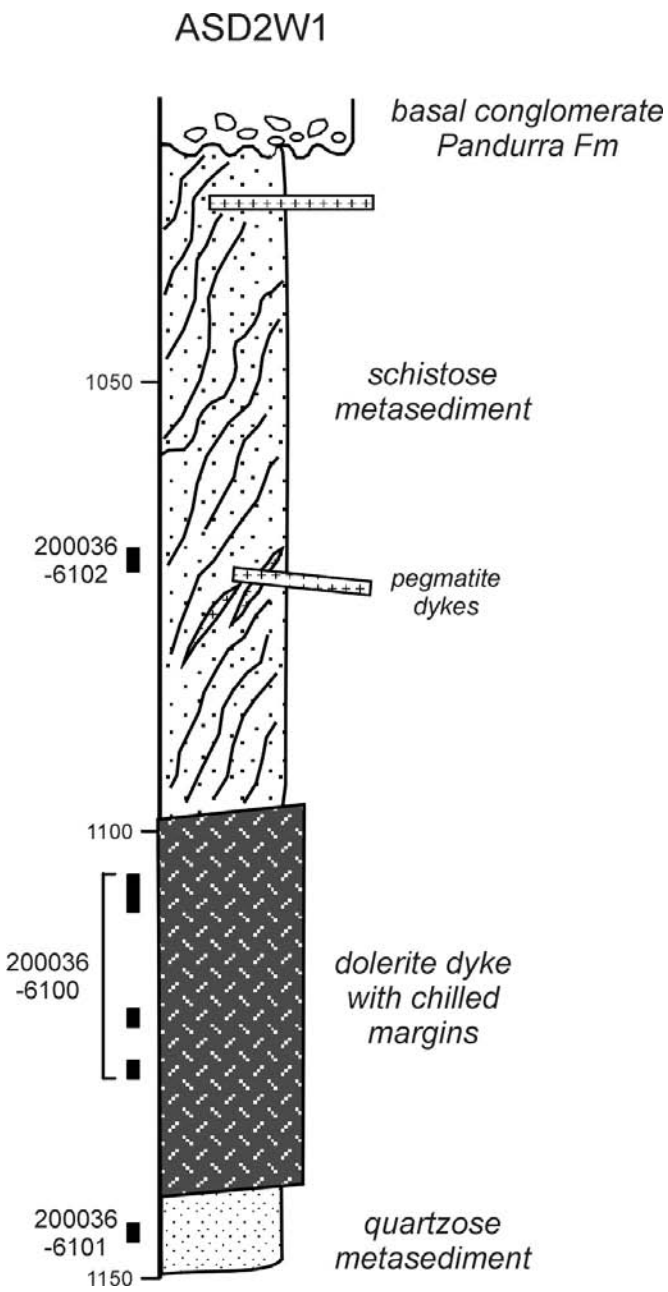

Figure 40. Stratigraphic log for diamond drill hole ASD2W1, showing the location of samples collected for SHRIMP U-Pb dating.

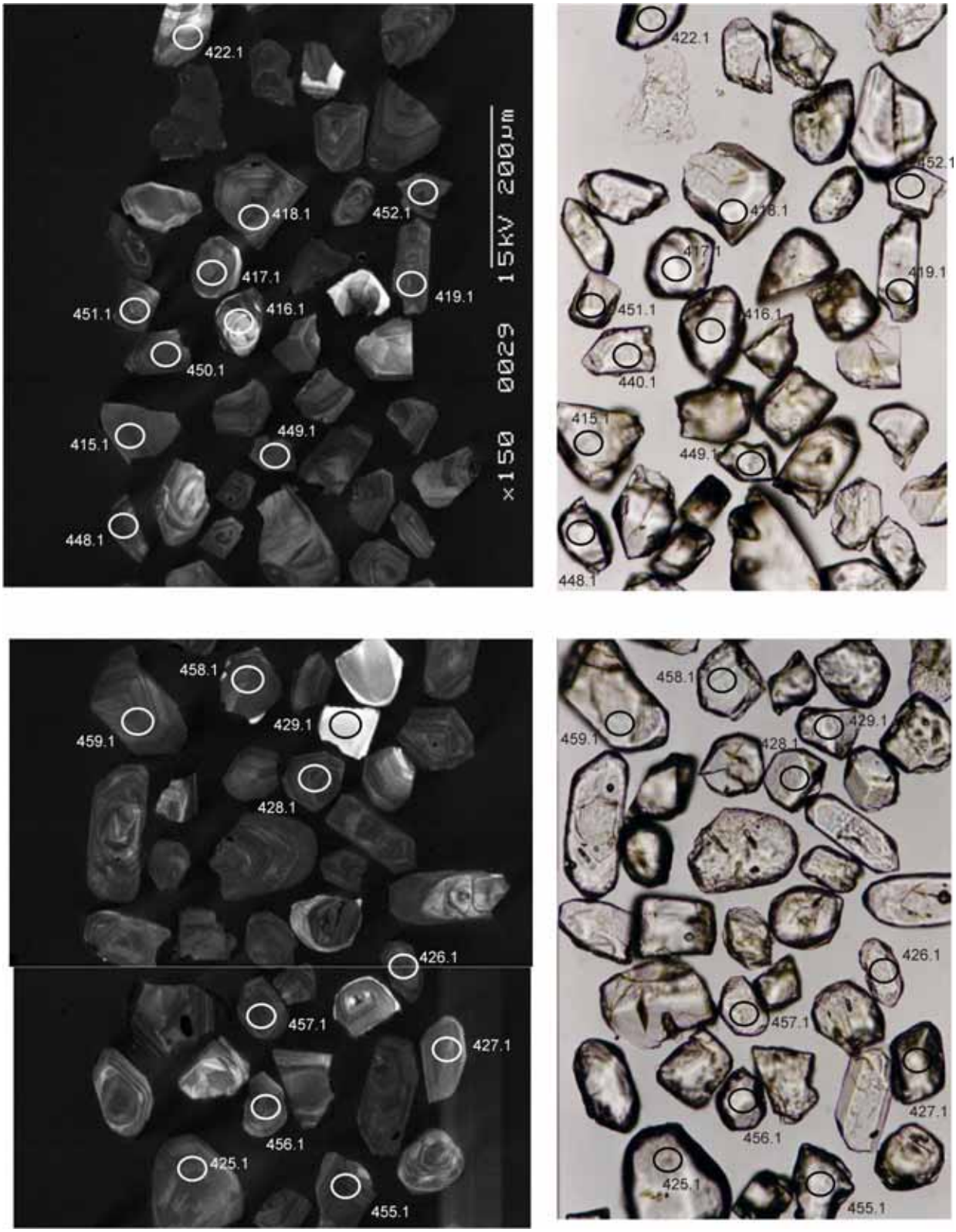

Figure 41. Representative CL (left) and transmitted light (right) images for sample 200036 6102: schist, Arcoona Station prospect. SHRIMP analysis spots are labelled. Scale bar is 200 μm.

Concurrent standard data

Session 1: SHRIMP I

Data for the standard are presented in Appendix 3. All $^{206}Pb/^{238}U$ QGNG analyses were included in the calibration, to give a calibration exponent of 1.73, with an upper limit of 2.0 and lower limit of 1.5 (at 95% confidence level). Thus the nominal value of 2.0 has been used in data reduction. The 37 $^{206}Pb/^{238}U$ analyses have a 1σ scatter of 2.64%. Element abundance calibration was based on SL13 (n = 1).

The weighted mean $^{207}Pb/^{206}Pb$ age for all 37 analyses is 1846.3 ± 3.9 Ma (MSWD is 1.5; probability of fit = .024). The analyses are corrected for overcounts at mass ^{204}Pb (after Black in press, calculated assuming $^{\mathbf{206}}Pb/^{238}U$-$^{207}Pb$-$^{235}U$ age concordance), which forces the weighted mean $^{207}Pb/^{206}Pb$ age for QGNG to the TIMS reference value. The recalculated age for QGNG becomes 1851.8 ± 3.5 Ma (MSWD = 1.3; probability of fit = .09; n = 37 of 37). The sample data below are also corrected for overcounts.

Session 2: SHRIMP IIA

No data were excluded from the Pb/U calibration, to give a calibration exponent of 2.00, with a lower limit of 1.85 and an upper limit of 2.09 (at the 95% confidence level). Thus the nominal value of 2.0 has been used in data reduction. There are three outliers in $^{206}Pb/^{238}U$ (Q.1, Q7.1 and Q52.1) and these have been omitted, leaving 49 analyses with a 1σ scatter in $^{206}Pb/^{238}U$ of 1.28%. The 52 analyses yield a weighted mean $^{207}Pb/^{206}Pb$ age of 1850.9 ± 2.5 Ma (MSWD = 1.4; probability of fit = 0.026). The slightly high MSWD indicates a slight scatter beyond that predicted by counting statistics alone. One grain (Q34) is younger than the others and has higher common ^{206}Pb, suggesting Pb loss may have occurred. When analysis Q34.1 is eliminated from the data set, the remaining 51 analyses yield an age of 1851.2 ± 2.4 Ma (MSWD = 1.2; probability of fit = 0.14).

The analyses are corrected for overcounts at mass ^{204}Pb (after Black in press, calculated assuming $^{206}Pb/^{238}U$-^{207}Pb-^{235}U age concordance), which forces the weighted mean $^{207}Pb/^{206}Pb$ age for QGNG to the TIMS reference value. The sample data for session 2 are also corrected for overcounts.

Element abundance calibration was based on SL13 (n = 2).

Sample data

Sample 200036 6102 was analysed over 2 sessions. The data from both sessions are combined in Figure 42, to show the full range of ages obtained for the sample. The zircons range between 1600 and 2720 Ma in age. The 7 youngest grains exhibit elevated common radiogenic Pb ± elevated U contents, and three of these analyses are notably discordant or reverse discordant (Table 14). The younger ages are therefore attributed to Pb loss. Figure 43 displays the main cluster of near-concordant analyses between 1800 and 1920 Ma. These analyses form a distinctive double peak on the probability density diagram (Figure 42) that indicates the presence of at least two age populations. The 14 oldest zircon ages represent single-phase grains (as opposed to cores). As all but one analysis is at least 90% concordant, their $^{207}Pb/^{206}Pb$ compositions should provide reliable age estimates. The exception is analysis 445.1. There are too few analyses of these older grains to delineate data concentrations,

although they may be postulated to occur at about 2000 and 2450 Ma, and there appears to be a hiatus between about 2250 and 2450 Ma.

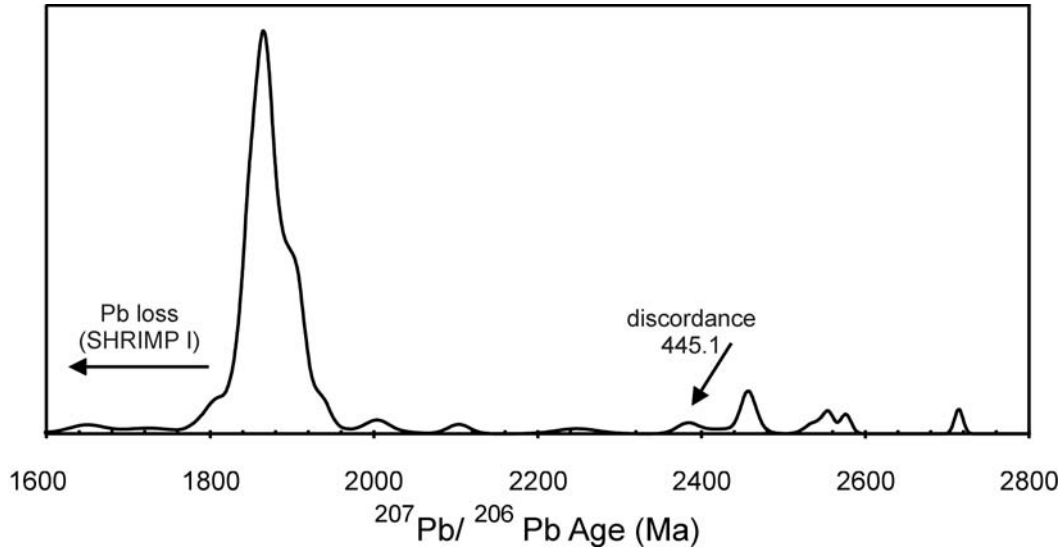

Figure 42. Probability density distribution of $^{207}Pb/^{206}Pb$ ages illustrating the full range for sample 200036 6102 (both sessions).

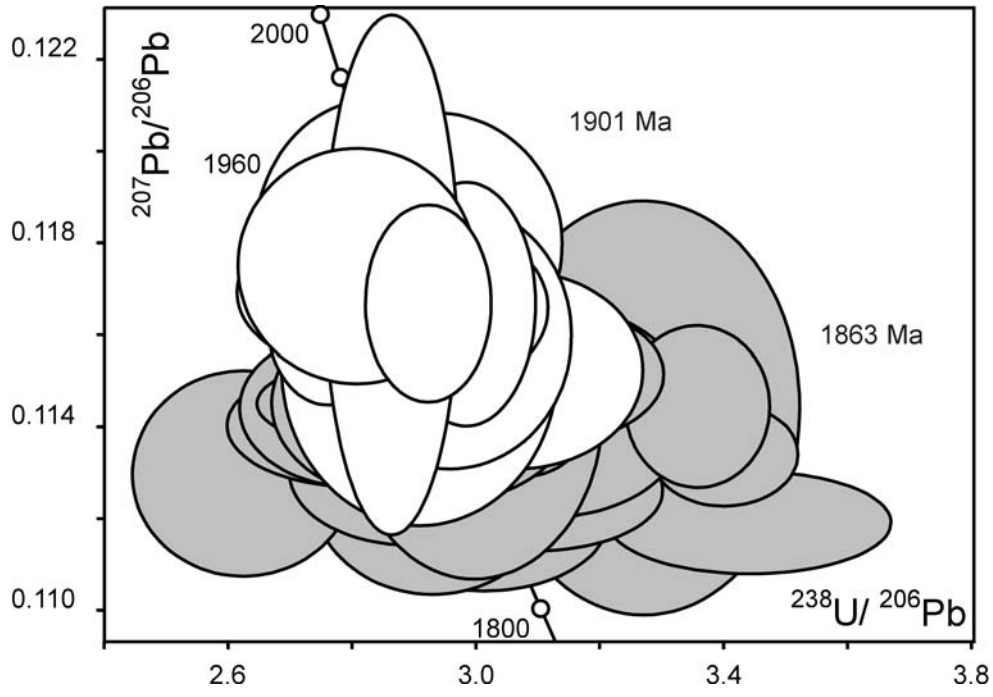

Figure 43. Concordia plot for the main near-concordant group of zircons in sample 200036 6102 (both sessions). The analyses have been divided into two populations represented by grey (1863 Ma) and white (1901 Ma) error ellipses (see discussion below). There is clearly considerable overlap between the two populations.

Session 1: SHRIMP I

The results from the first session (April 2002, SHRIMP I at RSES, ANU) are ambiguous. A total of 59 grains were analysed. The main near-concordant cluster of analyses at 1800-1920 Ma shows considerable scatter, and it is impossible to resolve the spread of analyses into its separate age components (Figure 44). A Probability density curve suggests at least two, possibly three age populations are present at *ca* 1860 and *ca* 1900 Ma, with some younger analyses possibly attributable to Pb loss.

The sample was therefore re-analysed in January 2005 on SHRIMP II (A) at Curtin University in Perth, attempting to better delineate the populations in the main age grouping, with the better precision generally afforded by SHRIMP II machines.

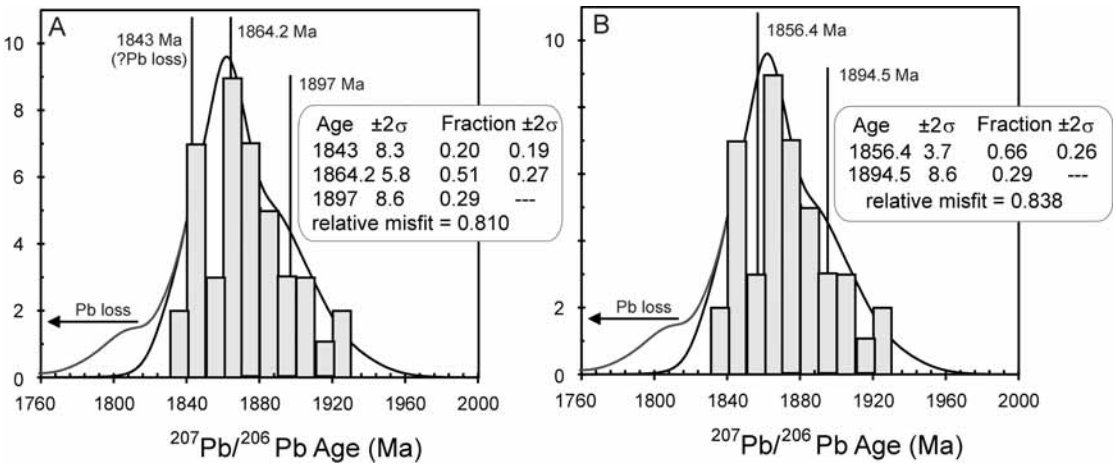

Figure 44. Probability density distribution showing $^{207}Pb/^{206}Pb$ ages for the main cluster of analyses obtained for 200036 6102 in session 1 (SHRIMP I). The data subset contains at least two age populations that cannot be separated with confidence. The mixture modelling algorithm of Sambridge and Compston (1994) calculates the two component ages to be ca 1860 and 1895 Ma, with a possible third component at ca 1843 Ma. Figures A and B illustrate two possible interpretations assuming (A) 3 populations and (B) 2 populations within the data set. The tail of Pb loss below 1800 Ma illustrated in the figures is not included in the modelling calculations.

Session 2: SHRIMP IIA

Thirty four new analyses were obtained in session 2 (January 2005, SHRIMP IIA, Curtin University), resulting in a total of 93 analyses over the two sessions. As with session 1, the main group of near-concordant analyses shows significant scatter in excess of the error predicted by counting statistics, forming a distinctive double peak on the probability density curve (Figure 45a). In this session it is possible to delineate the two age populations with more confidence, as there appears to be an inflection point between the 8 oldest and 21 youngest analyses (Figure 45b). Using the uncorrected dataset, the mixture modelling algorithm of Sambridge and Compston (1994) calculates the two component ages to be 1861.8 ± 4.0 Ma and 1900 ± 8 Ma. Using the data correct for overcounts at mass ^{204}Pb, a near-identical result is obtained; the algorithm calculates the two component ages to be 1863.3 ± 3.9 Ma and 1901 ± 7 Ma.

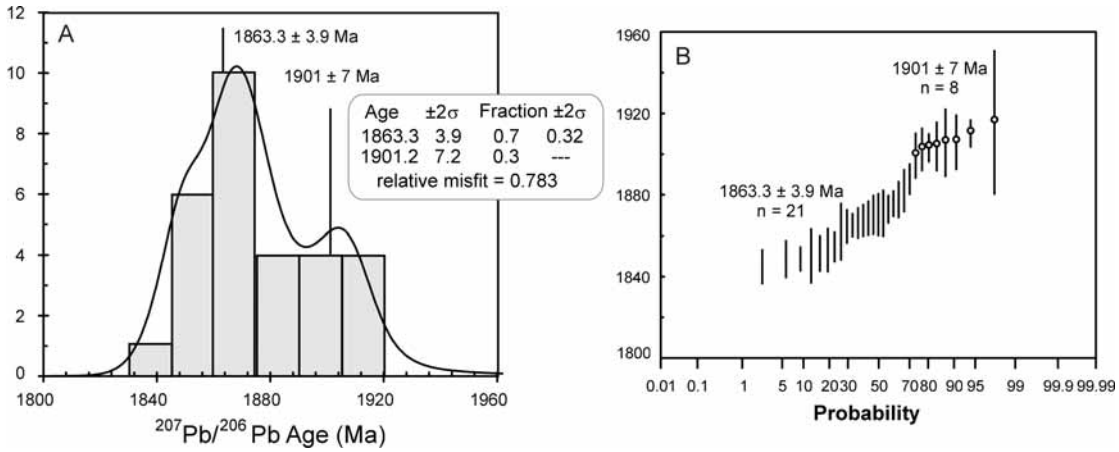

Figure 45 (A) Probability density distribution showing a distinctive double peak indicative of two age populations in the data subset. The mixture modelling algorithm of Sambridge and Compston (1994) calculates the two component ages to be 1863.3 and 1901 Ma. (B) Probability diagram for the main group of analyses (Session 2), showing an inflection point between the 8 oldest and 21 youngest analyses.

Geochronological interpretation

The ages obtained in both sessions agree well. As the two main age populations were delineated most clearly in session 2, 1863.3 ± 3.9 Ma is taken as the crystallisation age of the youngest population of grains, and 1901 ± 7 Ma the age of the older population.

The maximum age for the schist is 1863.3 ± 3.9 Ma. This age is significantly older than most ages obtained for the Donington Suite in this study, but close in age to the intensely foliated megacrystic granites at the Burden Hill and Island Dam prospects The spread of ages suggests a multiple source region with components at least as old as 2700 Ma, and includes a source ~1900 Ma old. To date, there are no known stratigraphic units of this age within the Gawler Craton, which may have sourced the detrital zircons of this age.

Table 14. SHRIMP analytical results for zircon from sample 200036 6102.

Spot	U (ppm)	Th (ppm)	$^{206}Pb_c$ (%)	$^{206}Pb^*$ (ppm)	$^{206}Pb^*/^{238}U$	±	$^{207}Pb^*/^{235}U$	±	$^{207}Pb^*/^{206}Pb^*$	±	conc (%)	207Pb/206Pb Age(Ma)	±
Session 1: analysis date 26/4/2002; SHRIMP I													
401.1	79	177	-0.03	23	0.344	0.011	5.47	0.19	0.1153	0.0014	101	1885	22
402.1	183	77	0.23	54	0.341	0.010	5.55	0.17	0.1180	0.0012	98	1926	18
403.1	48	38	-1.01	13	0.327	0.011	5.55	0.21	0.1232	0.0021	90	2003	29
404.1	240	135	0.11	66	0.320	0.009	5.04	0.15	0.1143	0.0009	96	1869	15
405.1	258	135	-0.22	68	0.306	0.009	4.83	0.17	0.1144	0.0018	91	1870	29
409.1	230	139	0.04	66	0.332	0.009	5.13	0.14	0.1120	0.0006	101	1832	10
410.1	165	109	-0.03	49	0.350	0.010	5.52	0.16	0.1145	0.0008	103	1872	13
411.1	45	44	-0.27	14	0.365	0.031	5.89	0.20	0.1172	0.0016	103	1914	25
412.1	139	87	-0.11	43	0.356	0.010	5.77	0.17	0.1175	0.0010	102	1918	16
413.1	162	77	0.07	47	0.338	0.009	5.30	0.15	0.1137	0.0008	101	1860	13
414.1	164	70	0.14	54	0.381	0.011	5.94	0.17	0.1130	0.0009	111	1848	15
415.1	173	101	0.00	75	0.504	0.014	11.16	0.31	0.1604	0.0007	107	2460	8
416.1	53	64	-0.03	23	0.498	0.014	11.02	0.32	0.1605	0.0011	105	2461	12
417.1	164	76	-0.06	50	0.353	0.010	5.59	0.19	0.1149	0.0023	104	1878	36
418.1	206	97	0.03	60	0.341	0.009	5.35	0.14	0.1137	0.0005	102	1859	8
419.1	171	106	0.02	53	0.357	0.011	5.61	0.17	0.1140	0.0005	105	1865	9
420.1	226	106	0.02	67	0.343	0.009	5.39	0.15	0.1139	0.0005	102	1862	8
421.1	90	65	-0.07	26	0.338	0.009	5.34	0.15	0.1146	0.0009	100	1873	14
422.1	118	93	-0.07	37	0.369	0.010	5.89	0.17	0.1158	0.0008	106	1893	12
423.1	158	53	-0.09	46	0.338	0.009	5.41	0.16	0.1160	0.0012	99	1895	18
424.1	161	98	-0.05	46	0.334	0.009	5.26	0.16	0.1144	0.0015	99	1870	24
425.1	160	73	-0.01	47	0.344	0.009	5.48	0.15	0.1157	0.0006	101	1891	9
426.1	282	126	0.25	79	0.323	0.009	4.93	0.14	0.1108	0.0007	100	1813	12
427.1	146	75	0.10	43	0.342	0.009	5.30	0.15	0.1126	0.0009	103	1842	15
428.1	253	148	0.02	71	0.329	0.009	5.12	0.14	0.1130	0.0005	99	1848	8
429.1	131	115	1.19	28	0.243	0.007	3.42	0.13	0.1022	0.0027	81	1664	49
430.1	117	113	0.02	33	0.325	0.010	5.16	0.15	0.1151	0.0007	96	1882	10
431.1	243	65	0.09	73	0.351	0.009	5.50	0.15	0.1138	0.0005	104	1861	8
432.1	224	156	0.00	66	0.343	0.009	5.37	0.14	0.1138	0.0004	102	1861	7
433.1	305	151	0.07	88	0.334	0.009	5.22	0.15	0.1133	0.0004	100	1854	7
434.1	171	73	-0.02	49	0.331	0.009	5.26	0.14	0.1152	0.0006	98	1883	9
435.1	171	82	-0.04	51	0.345	0.010	5.48	0.16	0.1152	0.0007	101	1883	12
436.1	205	131	-0.18	58	0.327	0.009	5.19	0.15	0.1152	0.0009	97	1883	14
437.1	250	139	-0.10	72	0.335	0.009	5.30	0.14	0.1145	0.0006	100	1872	10
438.1	104	143	0.17	42	0.472	0.013	10.94	0.31	0.1681	0.0011	98	2538	11
439.1	631	194	1.02	92	0.167	0.005	2.34	0.07	0.1013	0.0011	35	1649	20
440.1	313	158	0.02	78	0.291	0.008	4.49	0.12	0.1119	0.0005	89	1831	7
441.1	202	121	0.61	54	0.308	0.010	4.70	0.16	0.1105	0.0012	96	1808	20
442.1	79	31	0.89	25	0.364	0.010	5.33	0.17	0.1060	0.0016	114	1731	28
443.1	26	14	0.52	10	0.440	0.013	9.56	0.33	0.1574	0.0025	97	2427	27
444.1	166	104	-0.04	51	0.354	0.010	5.75	0.17	0.1178	0.0014	102	1923	21
445.1	165	143	0.38	52	0.362	0.010	7.64	0.21	0.1533	0.0012	80	2383	13
446.1	192	126	0.03	55	0.331	0.009	5.19	0.14	0.1138	0.0005	99	1860	7
447.1	84	46	0.90	29	0.389	0.011	7.60	0.24	0.1416	0.0021	94	2247	25
448.1	293	151	0.06	84	0.334	0.009	5.19	0.14	0.1126	0.0004	101	1843	7
449.1	162	213	0.18	50	0.357	0.010	5.63	0.16	0.1144	0.0007	105	1870	11

450.1	353	205	0.49	99	0.324	0.009	4.93	0.14	0.1105	0.0007	100	1807	11
451.1	156	158	0.00	48	0.357	0.010	5.76	0.16	0.1169	0.0007	103	1909	10
452.1	189	113	0.02	56	0.343	0.009	5.39	0.15	0.1138	0.0005	102	1861	8
453.1	116	58	0.06	48	0.482	0.013	11.28	0.30	0.1698	0.0007	99	2555	7
454.1	177	137	0.39	45	0.292	0.008	4.41	0.12	0.1095	0.0008	92	1791	14
455.1	263	214	-0.02	78	0.345	0.009	5.51	0.15	0.1160	0.0005	101	1895	8
456.1	184	92	0.15	55	0.346	0.010	5.38	0.15	0.1130	0.0006	103	1848	10
457.1	275	144	0.05	82	0.347	0.009	5.39	0.15	0.1129	0.0004	104	1846	7
458.1	220	124	0.02	98	0.517	0.014	13.32	0.36	0.1868	0.0006	99	2714	5
459.1	176	93	-0.01	51	0.337	0.009	5.30	0.14	0.1141	0.0005	100	1865	8
460.1	262	103	0.00	80	0.353	0.010	5.58	0.15	0.1145	0.0004	104	1872	6
461.1	124	52	0.02	37	0.342	0.009	5.50	0.15	0.1166	0.0008	100	1904	12
462.1	145	114	0.01	40	0.323	0.009	5.01	0.14	0.1126	0.0005	98	1842	9
Session 2: analysis date 20/1/2005; SHRIMP IIA													
402.2	135	61	0.00	39	0.339	0.014	5.56	0.08	0.11883	0.00057	97	1939	9
463.1	280	110	0.09	71	0.294	0.014	4.60	0.07	0.11340	0.00046	88	1855	7
464.1	171	113	0.07	48	0.325	0.015	5.13	0.08	0.11439	0.00061	97	1870	10
465.1	219	147	0.09	63	0.334	0.014	5.19	0.08	0.11279	0.00053	101	1845	9
466.1	191	97	0.03	55	0.334	0.016	5.26	0.08	0.11428	0.00054	99	1869	8
467.1	92	53	-0.01	27	0.338	0.015	5.43	0.09	0.11644	0.00069	99	1902	11
468.1	119	33	-0.06	34	0.329	0.014	5.16	0.08	0.11387	0.00088	98	1862	14
469.1	108	42	0.02	32	0.344	0.014	5.42	0.08	0.11439	0.00065	102	1870	10
470.1	103	155	-0.09	32	0.361	0.014	5.78	0.09	0.11624	0.00072	104	1899	11
471.1	177	89	0.05	52	0.340	0.014	5.30	0.08	0.11320	0.00055	102	1851	9
472.1	182	63	-0.02	53	0.338	0.015	5.32	0.08	0.11421	0.00050	100	1868	8
473.1	229	168	-0.02	68	0.345	0.014	5.57	0.08	0.11695	0.00044	100	1910	7
474.1	114	67	0.00	34	0.342	0.014	5.51	0.09	0.11667	0.00089	100	1906	14
475.1	183	80	0.00	53	0.336	0.014	5.35	0.07	0.11550	0.00049	99	1888	8
476.1	67	108	0.11	19	0.335	0.015	5.40	0.10	0.11670	0.00109	98	1906	17
477.1	187	120	0.00	77	0.479	0.014	11.36	0.16	0.17190	0.00067	98	2576	7
478.1	72	89	-0.06	23	0.372	0.015	6.32	0.11	0.12327	0.00094	102	2004	14
479.1	167	123	-0.01	48	0.334	0.014	5.22	0.08	0.11329	0.00067	100	1853	11
480.1	190	116	0.04	55	0.337	0.014	5.30	0.08	0.11403	0.00052	100	1865	8
481.1	197	114	0.05	56	0.332	0.014	5.18	0.08	0.11303	0.00058	100	1849	9
482.1	153	82	-0.06	44	0.334	0.014	5.31	0.08	0.11514	0.00067	99	1882	10
483.1	119	52	0.03	34	0.334	0.014	5.21	0.08	0.11312	0.00083	100	1850	13
484.1	286	147	0.04	82	0.334	0.013	5.20	0.07	0.11303	0.00037	100	1849	6
485.1	107	86	-0.09	27	0.298	0.014	4.70	0.08	0.11444	0.00072	89	1871	11
486.1	334	154	0.02	95	0.332	0.013	5.25	0.07	0.11473	0.00041	98	1876	6
487.1	192	83	0.03	57	0.343	0.014	5.43	0.08	0.11485	0.00057	101	1878	9
488.1	200	111	0.01	58	0.339	0.014	5.33	0.07	0.11413	0.00048	101	1866	8
489.1	60	78	-0.03	18	0.350	0.016	5.65	0.14	0.11730	0.00235	101	1916	35
490.1	195	67	0.02	58	0.349	0.014	5.60	0.08	0.11649	0.00045	101	1903	7
491.1	203	116	0.00	60	0.342	0.014	5.41	0.08	0.11455	0.00045	101	1873	7
492.1	79	55	-0.07	23	0.338	0.018	5.43	0.10	0.11653	0.00078	99	1904	12
493.1	282	160	0.02	81	0.333	0.013	5.23	0.07	0.11406	0.00036	99	1865	6
494.1	81	90	0.01	33	0.473	0.014	10.42	0.16	0.15975	0.00072	102	2453	8
495.1	43	58	-0.09	15	0.395	0.016	7.09	0.13	0.13040	0.00100	102	2104	14

Data are 1σ precision. All Pb data are common Pb corrected based on measured ^{204}Pb (after Stacey and Kramer 1975).

200036 6137: meta-greywacke, Stuart Range

1:250,000 sheet: Kingoonya (SH5311)

1:100,000 sheet: Bon Bon (5937)

AMG: 513049 E 6679812 N

Location: The sample was taken from diamond drillhole SR9, depth interval 86-87 m (Figure 46). The diamond drillhole is located within the Stuart Range prospect of the Olympic Domain.

Description: The drill core sample has captured the contact between a grey sandy sedimentary lens or horizon, which interfingers with fine-grained dark grey meta-pelitic sediment. Cutting the rock are minor thin veinlets filled by white minerals. The sandy lens bubbles vigorously in reaction with dilute HCl, suggesting calcite is present in moderate amount. (NB: zircons were obtained only from the sandy material).

In thin section the sample displays a relatively well-preserved framework-supported clastic sedimentary texture, modified by metamorphic replacement and mild deformation. The sample is considered to have formed as a rapidly deposited arenaceous sediment (non-sorted, non-layered wacke) composed of lithic fragments of plagioclase (now albitised)-quartz-phyric dacite lava (50%), and crystals derived from that source (plagioclase 35%, magmatically corroded quartz crystals and angular crystal fragments 5%), in a fine matrix of comminuted materials derived from that source. A minor amount of clays might also have been deposited with the matrix materials. Trace amounts of apatite occur as microphenocrysts in the dacitic lava fragments. Small zircon crystals occur in the matrix areas, as small squat terminated crystals ~50-150 µm in size with prominent growth-zoning. The source of the zircon is uncertain: it is likely that they were derived from the principal contributing source (ie the dacitic volcanic source), but it remains possible that the zircon was derived from a different (possibly granitoid) source.

Following deposition and burial, the greywacke underwent low-grade regional metamorphism in the lower greenschist facies. This generated the new assemblage of albite (replacing original plagioclase) + sericite (5%)+ chlorite (3%) + minor quartz + calcite + leucoxene. Sericite flakes and aggregates are aligned in a moderately well-defined foliation, which wraps around the blocky crystal and lithic fragments. The only two primary minerals to survive this event were apatite (microphenocrysts in dacitic lava fragments) and zircon (discrete clastic grains).

See Appendix 1 for full petrographic report (Mason 2003).

Mount: Z3966

Description of zircons

The sample contains euhedral prismatic zircons ranging between 50 to 150 µm in size, with aspect ratios of about 2:1 (Figure 47). The grains have fairly sharp, low-angle pointed terminations. No obvious detrital textures are observed. The zircons are translucent brown in colour, due to oxide staining. Clarity is poor and most grains are obviously metamict. Brown, hematite-stained cracks are common. No obvious cores are visible. The zircons display very clear euhedral and concentric zoning in transmitted and reflected light photos, enhanced by the weathering of the grains. The CL response is weak and the grains appear dark, although concentric zoning is still visible. About 10% of the grains are clear and unstained and relatively free of cracks, with a few clear, bleb- to rod-shaped inclusions, and these grains were targeted for analysis.

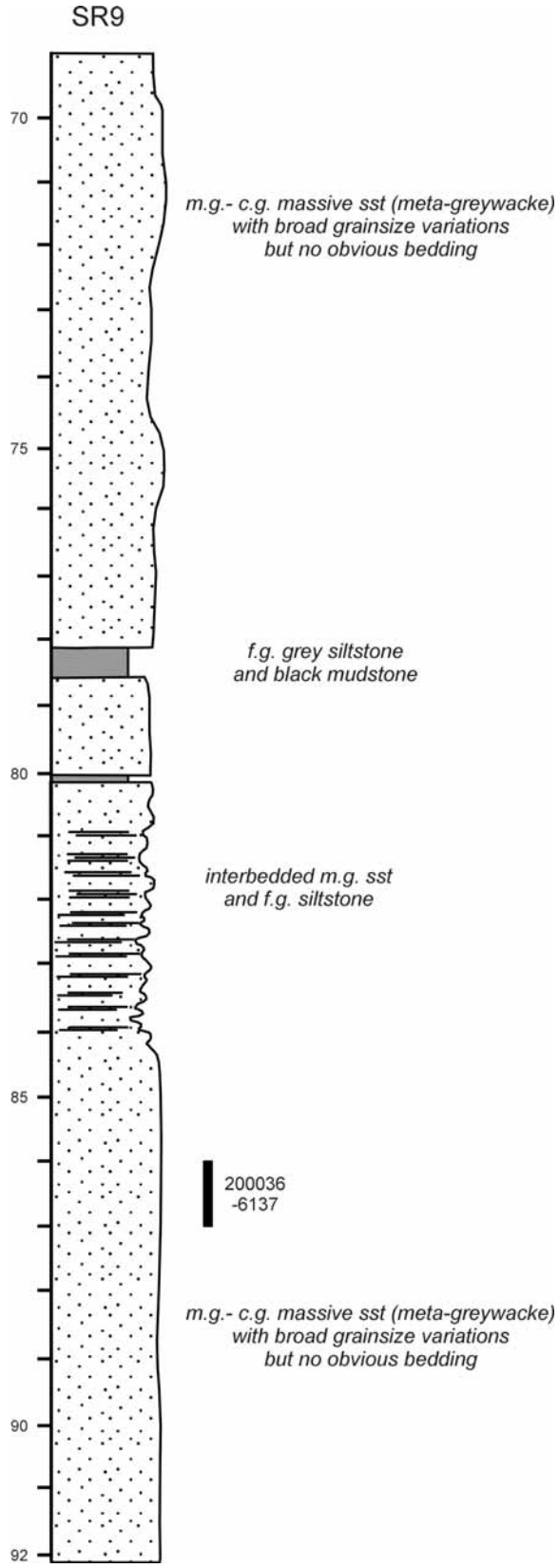

Figure 46. Stratigraphic log for diamond drill hole SR9*, showing the location of sample collected for SHRIMP dating.*

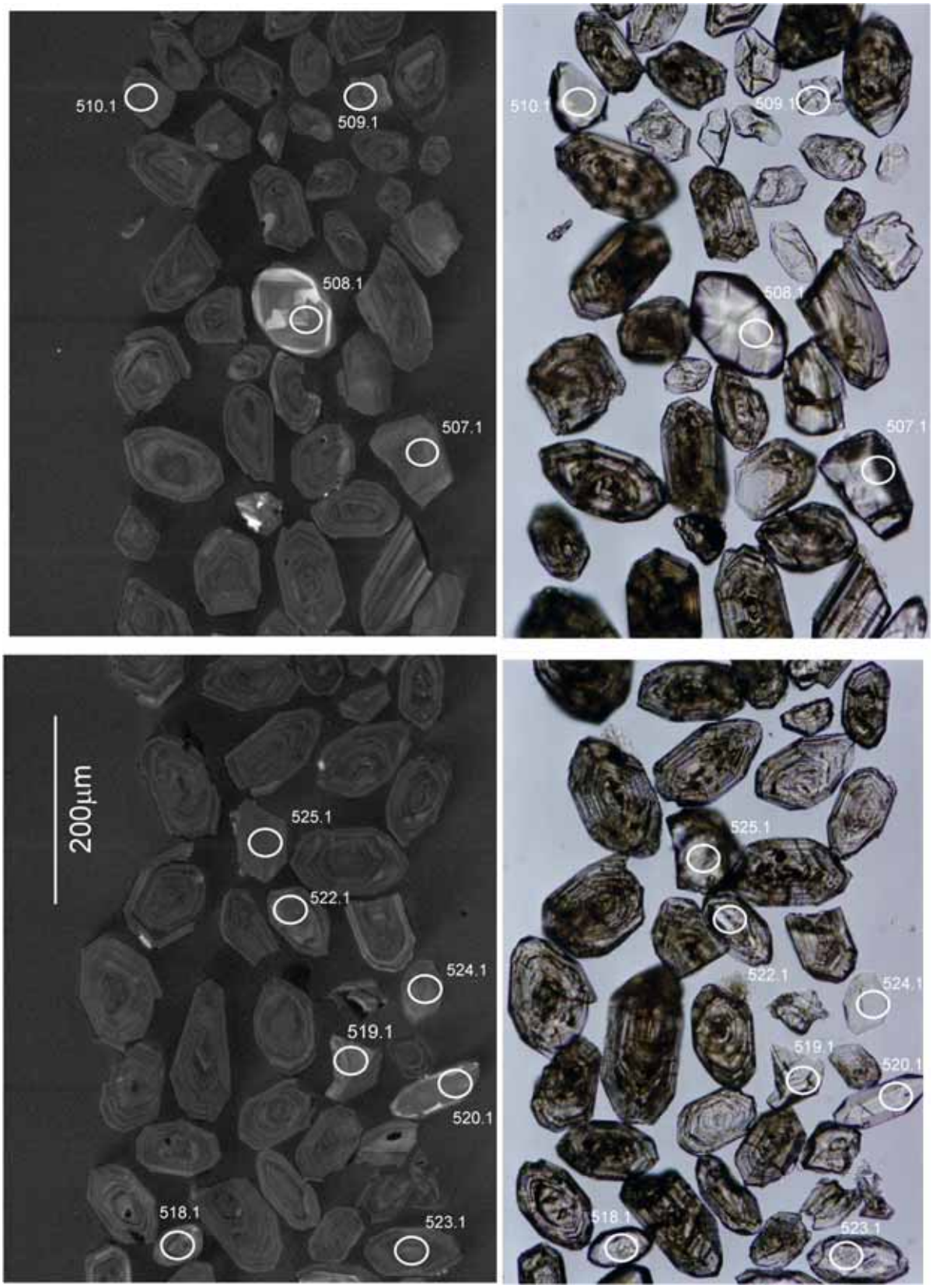

Figure 47. Representative CL (left) and transmitted light (right) images for sample 200036 6137: meta-greywacke, Stuart Range prospect. SHRIMP analysis spots are labelled. Scale bar is 200 µm.

Concurrent standard data

Data for the standard are presented in Appendix 3. The calibration exponent for this QGNG data set is 1.96, with an upper limit of 2.26 and a lower limit of 1.61 (at the 95% confidence level). Thus the nominal value of 2.0 has been used in data reduction. All analyses are used in the calibration. There are two outliers in $^{206}Pb/^{238}U$ (915.1 and 932.1) and these have been omitted, leaving 49 analyses with a 1σ scatter in $^{206}Pb/^{238}U$ of 3.58%. Element abundance calibration was based on SL13 (n = 1).

There is only one obvious outlier amongst the $^{207}Pb/^{206}Pb$ ages, (915.1) but the remaining 50 analyses do not conform to a normal distribution, yielding a weighted mean $^{207}Pb/^{206}Pb$ age of 1843 ± 6 Ma (MSWD = 2.5; probability of fit = 0). The analyses are corrected for overcounts at mass ^{204}Pb (after Black in press; calculated assuming $^{\mathbf{206}}Pb/^{238}U$-$^{207}Pb$-$^{235}U$ age concordance), which forces the weighted mean $^{207}Pb/^{206}Pb$ age for QGNG to the TIMS reference value. The sample data below are also corrected for overcounts at the ^{204}Pb mass peak.

The recalculated age for QGNG becomes 1851.9 ± 4.6 Ma (MSWD is 1.3; probability of fit is .09; n = 46 of 51). In this case, *SQUID* identifies 5 statistical outliers. Excluding the youngest analysis (915.1; age 1727 ± 15 Ma (1σ error)) from the age calculation is warranted, as the grain contains high common ^{206}Pb and is discordant, suggesting Pb loss may have occurred. However, there are no other obvious statistical outliers, and no geological reason for further culling of analyses. The remaining 50 analyses yield a weighted mean $^{207}Pb/^{206}Pb$ age of 1849 ± 6 Ma (MSWD = 2.2; probability of fit = 0). The high MSWD indicates the scatter in the analyses is greater than that predicted by counting statistics alone. The wide spread of ages is therefore attributed to a component of instrument uncertainty, and high MSWDs for the corresponding samples are also acceptable.

Sample data

Thirty four grains were analysed. The analyses define a chord of discordance that intersects concordia at about 2550 Ma and 0 Ma, indicating the Pb loss is recent (Figure 48). With a high MSWD of 2.3, the analyses do not fulfil the requirements of a simple population. A probability density curve of $^{207}Pb/^{206}Pb$ ages suggests some of the analysed zircons are older grains (Figure 49). Eliminating the three oldest analyses from the weighted mean age calculation results in a $^{207}Pb/^{206}Pb$ age of 2540 ±6 Ma. When the data are corrected for overcounts at mass ^{204}Pb, the age becomes 2543 ± 6 Ma (MSWD = 1.5; probability of fit = .045). The slightly high MSWD is acceptable given that the standard for this session also exhibits a scatter greater than that predicted by counting statistics alone.

Geochronological interpretation

The maximum age for the sandstone is considered to be 2543 ± 6 Ma. The provenance for detrital zircons appears to be a local igneous source, solely comprising material of this age.

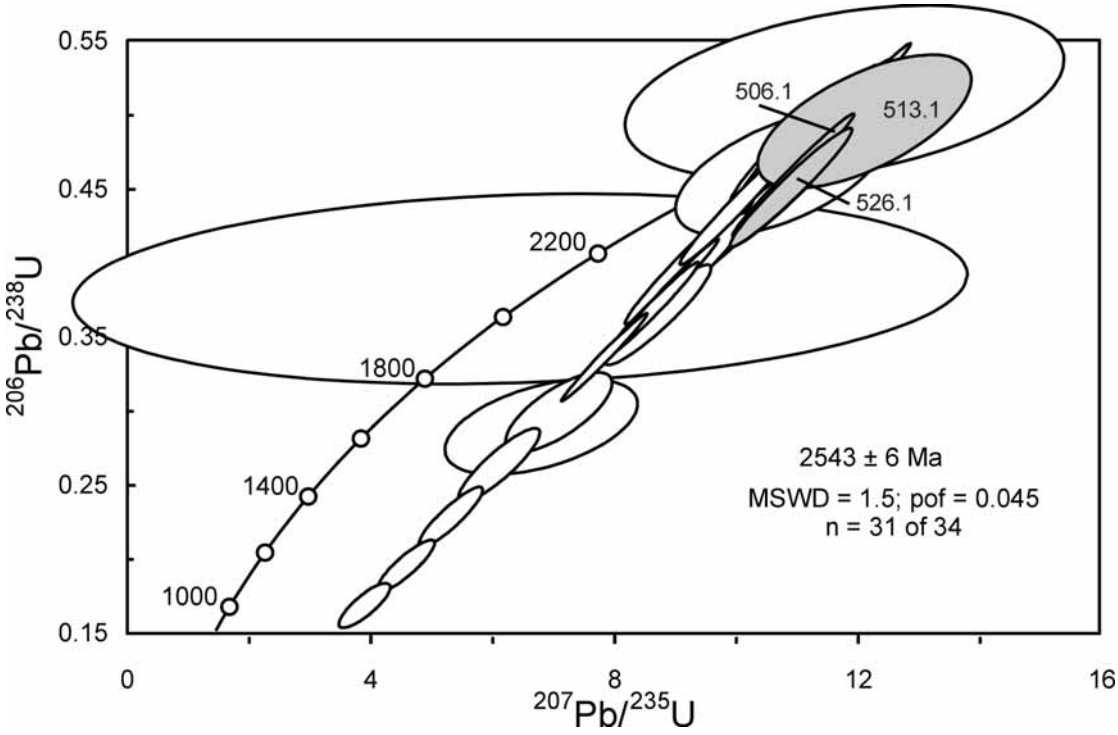

Figure 48. Concordia diagram for zircons in sample 200036 6137 showing the range of discordance of the analyses. White-filled symbols represent analyses used in the weighted mean age calculation. Light grey ellipses represent older grains.

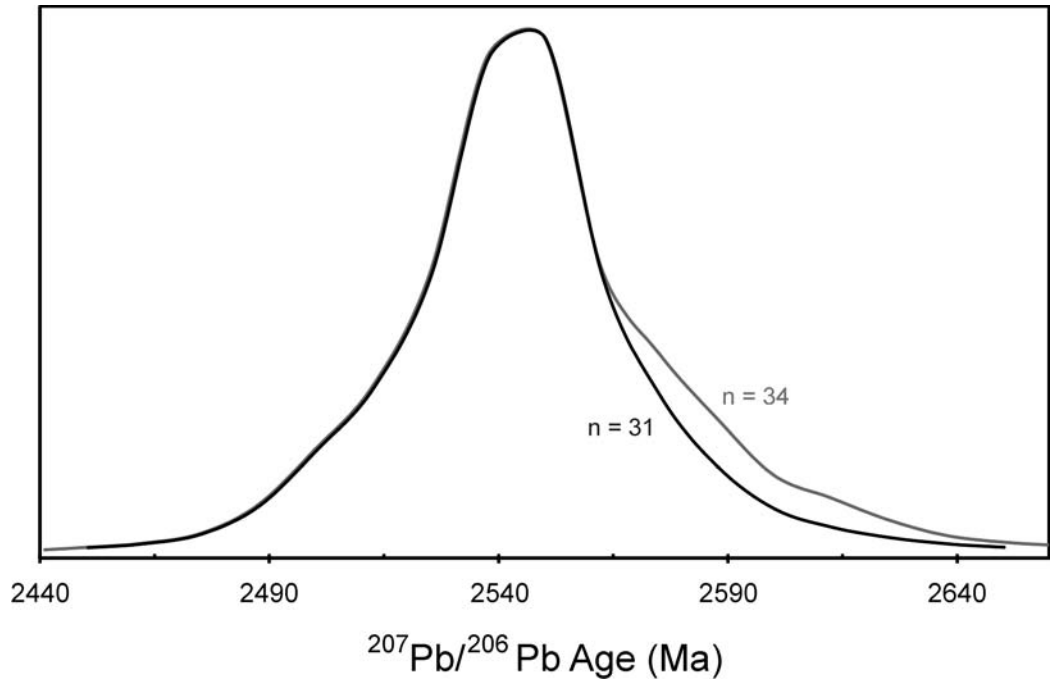

Figure 49. A probability density distribution of the $^{207}Pb/^{206}Pb$ ages shows the 34 analyses do not conform to a normal distribution. Eliminating the 3 oldest analyses improves the fit.

Table 15. SHRIMP analytical results for zircon from sample 200036 6137.

Spot	U (ppm)	Th (ppm)	$^{206}Pb_c$ (%)	$^{206}Pb^*$ (ppm)	$^{206}Pb^*/^{238}U$	±	$^{207}Pb^*/^{235}U$	±	$^{207}Pb^*/^{206}Pb^*$	±	conc (%)	207Pb/206Pb Age(Ma)	±
501.1	238	174	-0.03	99	0.483	0.018	11.30	0.42	0.16987	0.00097	99	2556	10
502.1	94	41	6.62	45	0.516	0.024	11.80	1.42	0.16500	0.01980	107	2511	190
503.1	131	66	-0.04	56	0.493	0.018	11.47	0.44	0.16870	0.00127	102	2545	13
504.1	192	92	-0.01	80	0.481	0.018	11.21	0.41	0.16897	0.00086	99	2547	9
505.1	126	71	0.11	43	0.395	0.015	9.00	0.34	0.16520	0.00124	86	2509	13
506.1	159	69	-0.12	63	0.460	0.017	10.92	0.40	0.17234	0.00098	94	2581	10
507.1	226	159	-0.05	98	0.504	0.019	11.78	0.44	0.16954	0.00078	103	2553	8
508.1	119	33	-0.06	49	0.476	0.018	10.96	0.46	0.16690	0.00284	99	2526	28
509.1	209	183	1.10	77	0.426	0.016	10.07	0.38	0.17120	0.00171	89	2569	17
510.1	180	40	-0.04	70	0.456	0.017	10.59	0.40	0.16860	0.00185	95	2544	18
511.1	332	384	2.98	67	0.228	0.008	5.31	0.22	0.16870	0.00304	52	2544	30
512.1	332	309	3.96	89	0.299	0.011	7.07	0.36	0.17160	0.00601	66	2573	58
513.1	110	36	0.18	47	0.496	0.018	12.09	0.71	0.17680	0.00813	99	2623	77
514.1	279	373	1.82	64	0.263	0.010	6.10	0.27	0.16800	0.00353	59	2537	35
515.1	198	155	1.22	69	0.399	0.014	9.32	0.35	0.16940	0.00203	85	2551	20
516.1	164	62	-0.04	66	0.467	0.017	10.82	0.40	0.16816	0.00087	97	2539	9
517.1	148	53	0.52	60	0.467	0.017	10.84	0.40	0.16840	0.00125	97	2542	12
518.1	294	725	3.73	51	0.195	0.007	4.58	0.19	0.17010	0.00340	45	2559	33
519.1	201	60	0.28	71	0.407	0.015	9.41	0.35	0.16780	0.00102	87	2536	10
520.1	158	106	0.00	64	0.470	0.017	10.92	0.40	0.16847	0.00076	98	2543	8
521.1	257	242	0.37	75	0.337	0.012	7.82	0.29	0.16844	0.00094	74	2542	9
522.1	183	147	5.90	77	0.461	0.017	10.72	0.71	0.16860	0.00910	96	2544	91
523.1	469	878	4.89	71	0.168	0.006	3.89	0.17	0.16770	0.00419	40	2535	42
524.1	228	223	4.52	59	0.289	0.013	6.79	0.65	0.17000	0.01411	64	2561	140
525.1	222	81	0.92	85	0.438	0.016	9.97	0.37	0.16500	0.00125	93	2507	13
526.1	166	100	0.76	65	0.451	0.017	10.89	0.41	0.17500	0.00161	92	2606	15
527.1	184	113	-0.08	72	0.454	0.016	10.76	0.40	0.17170	0.00101	94	2574	10
528.1	185	147	0.22	61	0.382	0.014	8.89	0.33	0.16867	0.00093	82	2544	9
529.1	91	41	-0.12	37	0.473	0.018	10.97	0.41	0.16804	0.00097	98	2538	10
530.1	209	94	0.20	88	0.490	0.018	11.25	0.42	0.16655	0.00077	102	2523	8
531.1	181	181	27.73	82	0.383	0.026	6.40	3.01	0.12200	0.05612	105	1986	820
531.2	151	126	1.66	48	0.365	0.014	8.69	0.36	0.17260	0.00259	78	2583	26
532.1	249	208	1.99	79	0.368	0.013	8.60	0.32	0.16930	0.00119	79	2551	12
533.1	164	70	0.16	69	0.482	0.018	11.06	0.43	0.16640	0.00216	101	2521	22

Data are 1σ precision. All Pb data are common Pb corrected based on measured ^{204}Pb (after Stacey and Kramer 1975).
Analysis date 11/6/2002; SHRIMP I

200036 6130: Hutchison Group, Lake Gilles
forsterite marble (high-grade calc-silicate)

1:250,000 sheet: Port Augusta (SI5304)

1:100,000 sheet: Uno (6232)

AMG: 656169 E 6371594 N

Location: The sample was taken from diamond drillhole LG-DDH2, depth interval 87.6-91.9 m (Figure 50). The diamond drillhole is located within the Lake Gilles prospect of the Olympic Domain.

Description: The hand specimen represents a pale grey granular crystalline rock, in which layering is defined by thin darker mauvish grey (mica-rich) laminae several millimetres thick. The sample effervesces vigorously in reaction with dilute HCl, confirming calcite is abundant throughout the rock.

In thin section, the sample displays a granoblastic metamorphic texture, with foliation defined by aligned mica flakes and indistinct mineralogical lamination, modified by selective retrogressive alteration. It comprises equant anhedral grains calcite (58%), well-shaped flakes of phlogopite (20%), large anhedral grains of retrogressively altered diopside (5%) that porphyroblastically enclose numerous smaller calcite and phlogopite flakes, and trace forsterite, spinel, zircon and opaques. Forsterite occurs as equant anhedral grains scattered sparsely through calcite-phlogopite-rich horizons. Most are completely replaced by fine-grained, fibrous, colourless to very pale yellow serpentine. Isotropic pale green spinel tends to occur in the mica-rich horizons. Some grains are mantled by microgranular forsterite aggregates. Opaques occur as very fine-grained dense aggregates and discontinuous trails. They appear to represent retrogressive fine-grained pyrite. Zircon occurs as rare tiny rounded grains ~50 mm in size, only in the phlogopite-rich laminae, not in the calcite-rich layers.

This sample formed as an impure calc-silicate sediment, composed of carbonate and lesser clay components. High-grade regional metamorphism in the upper amphibolite to granulite facies generated the foliated assemblage of calcite + phlogopite + forsterite + diopside + trace spinel. Indistinct mineralogical lamination of the metamorphic assemblage (ie mica-rich laminae, thicker calcite-forsterite-diopside-phlogopite layers) possibly reflects primary compositional layering in which thicker calc-silicate layers were interlayered with thinner clay-rich layers.

At a much later time, under much lower conditions of P and T, retrogressive alteration generated serpentine + opaques (?pyrite): the serpentine formed by hydration of forsterite, and the opaques formed as irregularly distributed small discontinuous trails and filamentous fracture fillings.

See Appendix 1 for full petrographic report (Mason 2003).

Mount: Z3966

Description of zircons

The sample contains abundant small zircons, mostly 30 µm to 50 µm in size but up to 200 µm (Figure 51). The grains are mostly euhedral, with blunt to round terminations and aspect ratios up to about 3:1 (2:1 is more common). Many zircons have an irregular morphology and a corroded appearance. The zircons are clear and a faint brown colour, with few cracks and inclusions. There are no visible cores. Concentric euhedral zoning is present in most grains, a few displaying more complex zoning or heterogeneous rims overgrowing zoned cores. A few grains have a very bright CL.

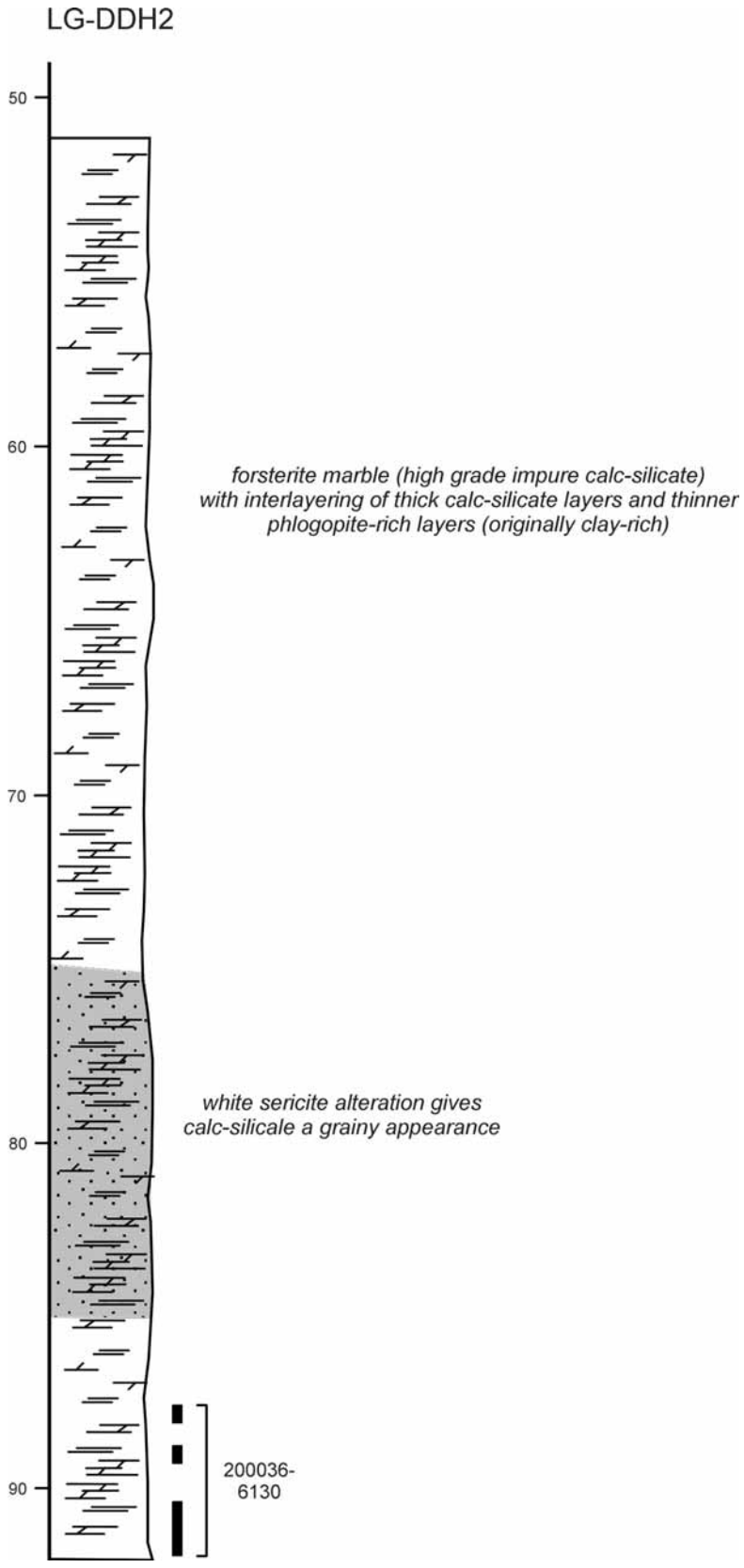

Figure 50. Stratigraphic log for diamond drill hole LG DDH02, showing the location of sample collected for SHRIMP dating.

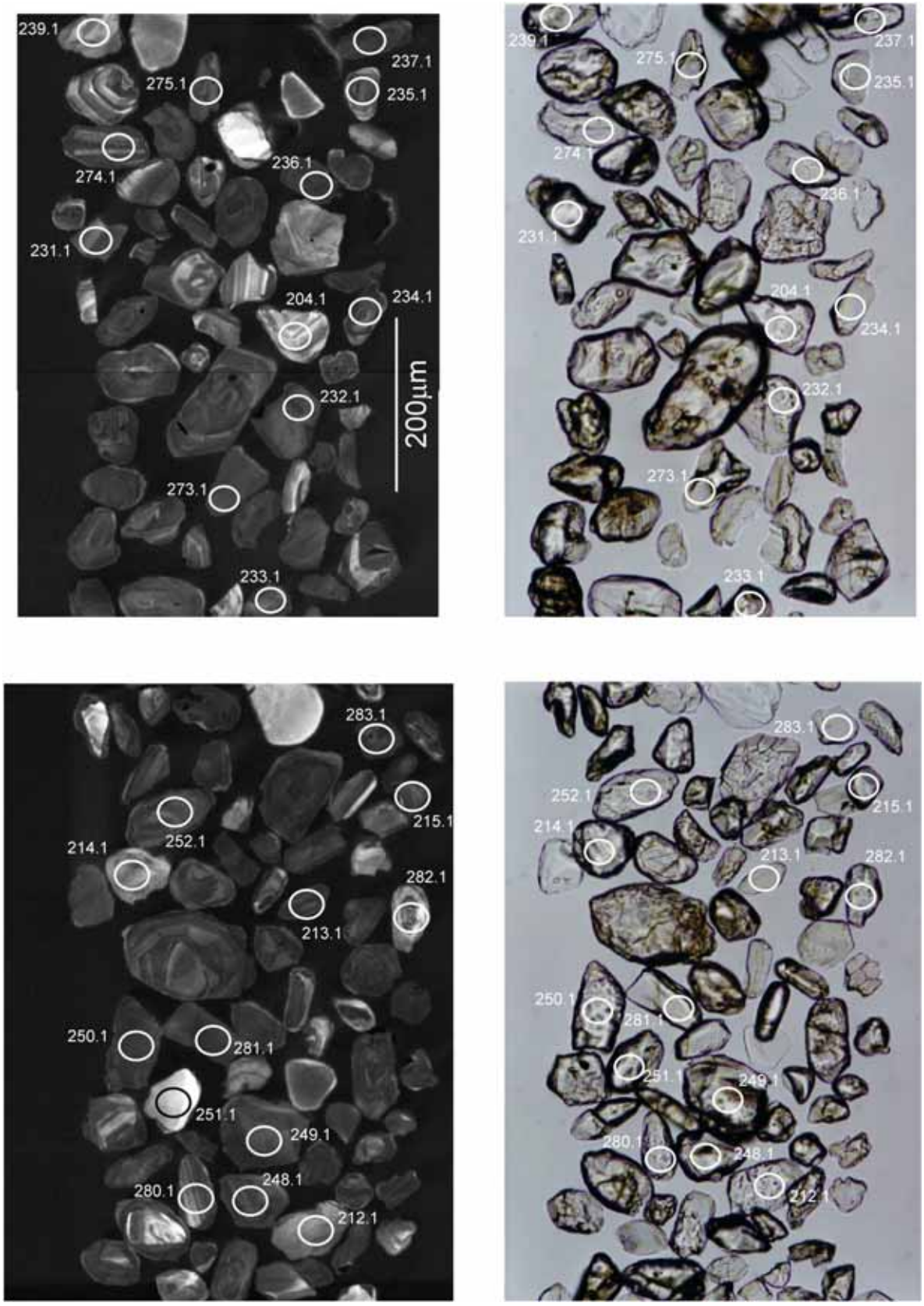

Figure 51. Representative CL (left) and transmitted light (right) images for sample 200036 6130: high grade calc-silicate (forsterite marble), Lake Gilles prospect. SHRIMP analysis spots are labelled. Scale bar is 200 µm.

Concurrent standard data

Data for the standard are presented in Appendix 3. The calibration exponent for this QGNG data set is 1.96, with an upper limit of 2.26 and a lower limit of 1.61 (at the 95% confidence level). Thus the nominal value of 2.0 has been used in data reduction. All analyses are used in the calibration. There are two outliers in $^{206}Pb/^{238}U$ (915.1 and 932.1) and these have been omitted, leaving 49 analyses with a 1σ scatter in $^{206}Pb/^{238}U$ of 3.58%. Element abundance calibration was based on SL13 (n = 1).

There is only one obvious outlier amongst the $^{207}Pb/^{206}Pb$ ages, (915.1) but the remaining 50 analyses do not conform to a normal distribution, yielding a weighted mean $^{207}Pb/^{206}Pb$ age of 1843 ± 6 Ma (MSWD = 2.5; probability of fit = 0). The analyses are corrected for overcounts at mass ^{204}Pb (after Black in press; calculated assuming $^{\mathbf{206}}Pb/^{238}U$-$^{207}Pb$-$^{235}U$ age concordance), which forces the weighted mean $^{207}Pb/^{206}Pb$ age for QGNG to the TIMS reference value. The sample data below are also corrected for overcounts at the ^{204}Pb mass peak.

The recalculated age for QGNG becomes 1851.9 ± 4.6 Ma (MSWD is 1.3; probability of fit is .09; n = 46 of 51). In this case, *SQUID* identifies 5 statistical outliers. Excluding the youngest analysis (915.1; age 1727 ± 15 Ma (1σ error)) from the age calculation is warranted, as the grain contains high common ^{206}Pb and is discordant, suggesting Pb loss may have occurred. However, there are no other obvious statistical outliers, and no geological reason for further culling of analyses. The remaining 50 analyses yield a weighted mean $^{207}Pb/^{206}Pb$ age of 1849 ± 6 Ma (MSWD = 2.2; probability of fit = 0). The high MSWD indicates the scatter in the analyses is greater than that predicted by counting statistics alone. The wide spread of ages is therefore attributed to a component of instrument uncertainty, and high MSWDs for the corresponding samples are also acceptable.

Sample data

A total of 93 grains were analysed, producing a wide spread of ages between *ca* 1720 Ma and 3400 Ma (Figure 52).

The largest group of analyses (n = 20) forms an alignment that intersects concordia at about 2000 Ma (Figure 53) and forms a distinct peak on a probability density curve of the $^{207}Pb/^{206}Pb$ ages. The analyses conform to a single population (Figure 54a) and yield a weighted mean age of 2000 ± 10 Ma. When the data are corrected for overcounts at mass ^{204}Pb, the age becomes 2009 ± 10 Ma (MSWD = 1.6; probability of fit = .055).

Three grains are younger than the 2009 Ma population, with $^{207}Pb/^{206}Pb$ ages of *ca* 1930, 1840 and 1740 Ma. As only 3 of 93 grains analysed yield these younger ages, laboratory contamination is the most likely origin of these grains. Cross contamination may have occurred between the samples on mount Z3966, which contain abundant zircons of similar age to the youngest grains.

Twenty seven analyses cluster close to concordia at about 2500 Ma. These analyses form a distinctive double peak on the probability density curve, indicating the analyses do not represent a single population (MSWD = 6). An inflection point in the data subset can be used to divide the analyses into the two age populations (Figure 54b), with weighted mean $^{207}Pb/^{206}Pb$ ages of 2478 ± 6 Ma and 2511 ± 6 Ma. .When the data are corrected for overcounts at mass ^{204}Pb, the ages become 2481 ± 6 Ma

(MSWD = 1.16; probability of fit = 0.31; n = 10) and 2514 ± 6 Ma (MSWD = 1.7; probability of fit = 0.034; n = 17).

There are insufficient data to distinguish any more age groups within the data set. There is a significant age peak at *ca* 2410 Ma and a possible *ca* 2460 Ma population (Figure 52). The spread of ages below the *ca* 2410 Ma peak (between 2100 and 2400 Ma) has no geological significance, as all analyses are highly discordant and/or have high common radiogenic Pb, strongly suggesting the U-Pb isotope systematics for these grains have been reset. Some of these grains may be part of the *ca* 2410 Ma population. Other possible age peaks occur at 2650, 2670, 2700 and 2740 Ma, with individual grains of ~ 3000, 3330 and 3400 Ma.

Geochronological interpretation

The maximum deposition age for the calc-silicate is considered to be 2009 ± 10 Ma. The three younger analyses may suggest a maximum age closer to 1745 Ma, but this is not considered to be a reliable limit due to the possibility of laboratory contamination in the sample. The provenance for detrital zircons is dominantly 2010-2750 Ma in age, but includes components as old as 3400 Ma.

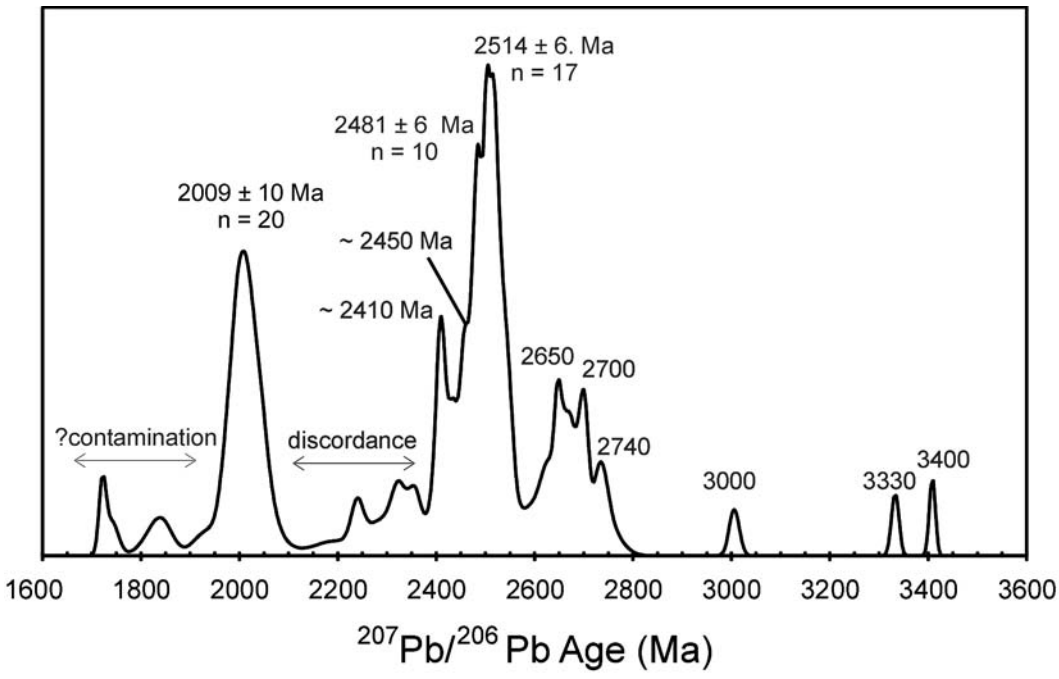

Figure 52. Probability density distribution of the $^{207}Pb/^{206}Pb$ ages for the zircons in sample 200036 6130 illustrating the full range of zircon ages.

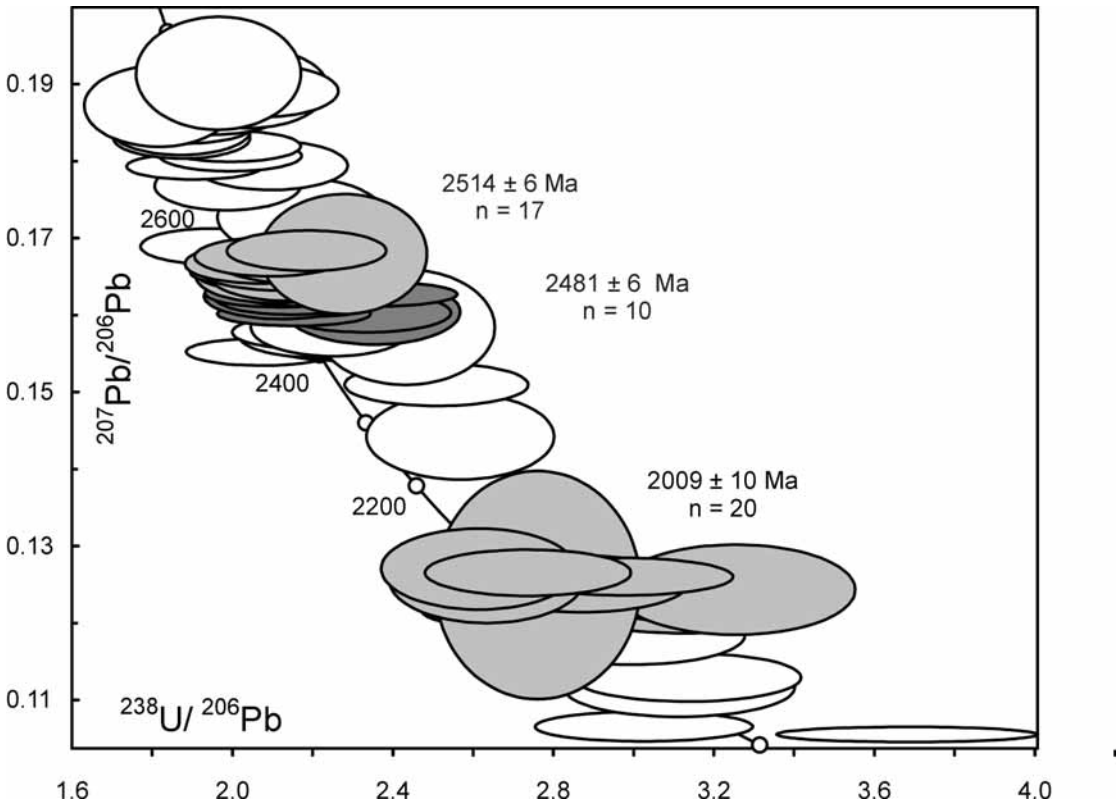

Figure 53. Concordia plot for zircons in sample 200036 6130. Grey-filled symbols represent analyses used in weighted mean estimates. Discordant analyses (>10%) are not displayed. The three oldest grains plot above the range of this diagram.

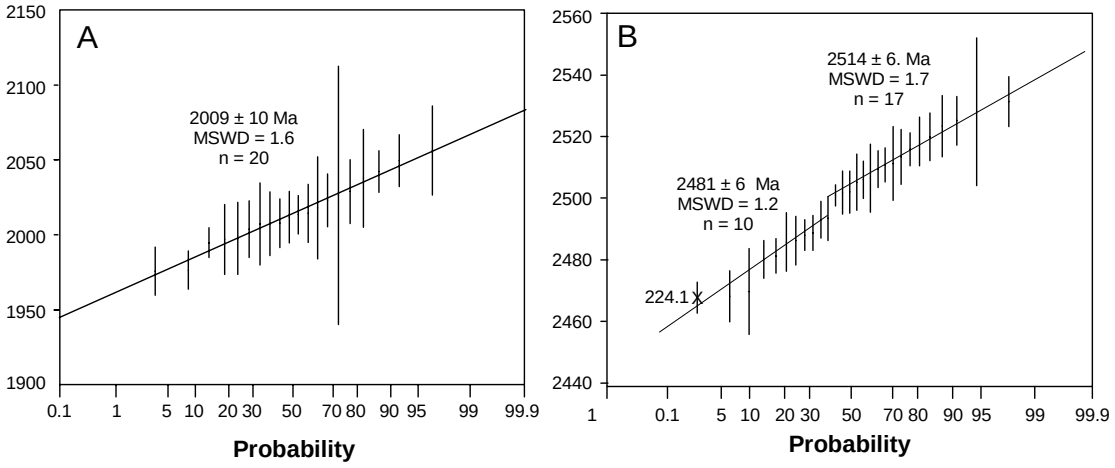

Figure 54a. Probability diagram for individual zircon ages for the ~ 2000 Ma data subset. 20 analyses delineate a single age population. Figure 54b. Probability diagram for individual zircon ages between 2460 and 2540 Ma. An inflection point occurs between the 11 youngest and 17 oldest analyses, suggesting the analyses divide into two age populations at this point.

Table 16. SHRIMP analytical results for zircon from sample 200036 6130.

Spot	U (ppm)	Th (ppm)	$^{206}Pb_c$ (%)	$^{206}Pb^*$ (ppm)	$^{206}Pb^*/^{238}U$	±	$^{207}Pb^*/^{235}U$	±	$^{207}Pb^*/^{206}Pb^*$	±	conc (%)	207Pb/206Pb Age(Ma)	±
201.1	168	149	-0.01	97	0.675	0.025	26.83	0.99	0.28830	0.00112	98	3408	6
202.1	218	107	-0.14	91	0.483	0.018	11.11	0.41	0.16670	0.00105	101	2525	11
203.1	165	126	0.02	75	0.531	0.020	13.54	0.51	0.18478	0.00096	102	2696	9
204.1	81	65	0.00	37	0.534	0.020	13.56	0.53	0.18410	0.00134	103	2690	12
205.1	116	60	-0.02	64	0.647	0.024	24.51	0.93	0.27470	0.00132	97	3333	8
206.1	148	114	0.00	43	0.336	0.012	5.83	0.22	0.12596	0.00100	91	2042	14
207.1	258	96	-0.02	106	0.481	0.018	10.97	0.41	0.16555	0.00078	101	2513	8
208.1	303	141	-0.05	123	0.472	0.017	10.59	0.39	0.16288	0.00073	100	2486	8
209.1	177	168	-0.06	55	0.362	0.013	6.12	0.24	0.12280	0.00160	100	1997	23
210.1	106	59	-0.08	34	0.379	0.014	6.57	0.28	0.12560	0.00226	102	2038	33
211.1	161	103	0.04	64	0.462	0.017	10.40	0.38	0.16342	0.00077	98	2491	8
212.1	100	38	-0.07	31	0.360	0.013	6.13	0.23	0.12350	0.00112	99	2008	16
213.1	213	125	0.11	68	0.370	0.014	7.89	0.31	0.15470	0.00102	85	2399	11
214.1	97	37	-0.02	30	0.359	0.013	6.14	0.23	0.12393	0.00089	98	2014	13
215.1	293	73	-0.06	122	0.483	0.017	10.34	0.38	0.15523	0.00071	106	2404	8
217.1	287	91	-0.02	105	0.425	0.015	9.54	0.34	0.16278	0.00065	92	2485	7
218.1	262	75	-0.02	104	0.463	0.017	10.63	0.38	0.16639	0.00070	97	2522	7
219.1	195	93	0.25	96	0.569	0.020	17.53	0.65	0.22350	0.00141	97	3006	10
220.1	163	166	-0.06	72	0.517	0.019	13.22	0.49	0.18558	0.00084	99	2703	7
221.1	191	120	0.21	82	0.501	0.018	12.59	0.47	0.18205	0.00082	98	2672	8
222.1	54	46	-0.53	18	0.383	0.015	6.70	0.27	0.12700	0.00216	102	2056	30
223.1	189	169	0.06	85	0.525	0.019	12.98	0.48	0.17939	0.00070	103	2647	7
224.1	280	44	0.07	112	0.464	0.017	10.26	0.37	0.16020	0.00064	100	2458	7
225.1	378	197	0.01	152	0.467	0.017	10.60	0.38	0.16444	0.00044	99	2502	5
226.1	84	29	-0.16	14	0.197	0.011	4.20	0.26	0.15420	0.00432	49	2393	48
227.1	155	77	0.12	48	0.357	0.014	6.13	0.24	0.12460	0.00123	97	2023	18
228.1	300	206	-0.04	132	0.514	0.019	11.96	0.44	0.16898	0.00095	105	2548	9
229.1	92	92	0.28	29	0.362	0.014	6.17	0.26	0.12350	0.00185	99	2007	27
230.1	220	140	0.16	76	0.399	0.015	8.79	0.33	0.15990	0.00131	88	2454	14
231.1	227	105	-0.06	68	0.348	0.013	6.00	0.23	0.12500	0.00150	95	2029	21
232.1	229	74	-0.12	91	0.462	0.017	10.51	0.40	0.16500	0.00119	98	2507	12
233.1	209	113	0.01	96	0.534	0.020	13.47	0.51	0.18310	0.00110	103	2681	10
234.1	291	106	0.40	112	0.445	0.016	9.71	0.37	0.15850	0.00155	97	2439	17
235.1	454	485	-0.05	129	0.330	0.012	4.85	0.18	0.10649	0.00079	106	1740	14
235.2	608	669	-0.01	142	0.271	0.010	3.94	0.14	0.10542	0.00040	90	1722	7
236.1	321	85	0.05	126	0.458	0.017	10.33	0.38	0.16347	0.00093	98	2492	10
237.1	454	245	-0.01	183	0.470	0.017	10.75	0.40	0.16574	0.00073	99	2515	7
238.1	133	124	-0.10	54	0.475	0.018	10.82	0.42	0.16520	0.00144	100	2509	15
239.1	113	53	0.10	36	0.369	0.014	6.24	0.26	0.12280	0.00172	101	1998	24
240.1	128	56	0.08	40	0.365	0.014	6.21	0.25	0.12330	0.00136	100	2004	19
241.1	192	99	-0.14	51	0.307	0.011	5.26	0.22	0.12430	0.00236	86	2018	34
242.1	72	66	-0.21	30	0.490	0.020	12.81	0.53	0.18960	0.00209	94	2739	19
243.1	357	52	-0.07	139	0.454	0.017	10.30	0.38	0.16459	0.00089	96	2503	9
244.1	145	92	-0.04	60	0.477	0.018	11.81	0.45	0.17950	0.00131	95	2648	12
245.1	37	19	0.10	16	0.509	0.022	13.44	0.62	0.19150	0.00306	96	2755	26
246.1	181	51	-0.06	73	0.470	0.017	10.74	0.41	0.16580	0.00158	99	2516	16
247.1	342	427	-0.01	147	0.501	0.019	12.49	0.46	0.18076	0.00083	98	2660	8

Spot	U (ppm)	Th (ppm)	$^{206}Pb_c$ (%)	$^{206}Pb^*$ (ppm)	$^{206}Pb^*/^{238}U$	±	$^{207}Pb^*/^{235}U$	±	$^{207}Pb^*/^{206}Pb^*$	±	conc (%)	207Pb/206Pb Age(Ma)	±
248.1	303	377	1.48	88	0.332	0.012	6.71	0.33	0.14670	0.00484	80	2307	56
249.1	167	65	-0.11	52	0.365	0.014	6.37	0.25	0.12650	0.00124	98	2049	17
250.1	373	223	0.01	119	0.370	0.014	6.26	0.23	0.12263	0.00067	102	1995	10
251.1	47	36	-0.02	22	0.551	0.023	14.22	0.61	0.18720	0.00225	104	2718	19
252.1	178	107	-0.07	55	0.362	0.014	6.23	0.39	0.12480	0.00612	98	2026	86
253.1	130	49	-0.08	52	0.464	0.018	10.70	0.42	0.16740	0.00132	97	2532	13
254.1	268	76	1.68	91	0.389	0.014	7.74	0.31	0.14420	0.00231	93	2278	27
255.1	126	63	-0.03	52	0.483	0.018	12.59	0.49	0.18920	0.00138	93	2735	12
256.1	168	871	0.07	46	0.320	0.012	5.35	0.21	0.12130	0.00109	90	1976	16
257.1	575	291	-0.02	216	0.437	0.016	9.40	0.35	0.15602	0.00069	97	2413	8
258.1	202	277	1.15	77	0.439	0.016	10.17	0.43	0.16800	0.00319	92	2538	32
259.1	434	107	-0.05	174	0.466	0.017	10.41	0.39	0.16192	0.00071	100	2476	8
260.1	267	198	0.14	98	0.428	0.016	9.47	0.35	0.16030	0.00103	93	2458	11
261.1	271	96	0.02	111	0.477	0.018	11.03	0.41	0.16760	0.00104	99	2534	10
262.1	162	44	-0.05	66	0.470	0.018	10.54	0.40	0.16250	0.00122	100	2482	13
263.1	139	66	0.07	44	0.367	0.014	6.28	0.24	0.12400	0.00136	100	2014	19
264.1	288	233	0.04	113	0.455	0.017	9.89	0.37	0.15776	0.00088	99	2432	10
265.1	333	81	1.42	64	0.219	0.008	4.14	0.18	0.13700	0.00315	58	2190	40
266.1	181	46	0.34	50	0.321	0.012	4.94	0.20	0.11150	0.00156	98	1824	25
266.2	158	43	0.54	44	0.319	0.012	4.96	0.19	0.11280	0.00124	97	1845	21
267.1	137	64	0.11	44	0.374	0.014	6.38	0.25	0.12380	0.00121	102	2012	17
269.1	191	162	0.04	74	0.449	0.017	10.49	0.40	0.16950	0.00144	94	2552	14
270.1	109	76	-0.01	41	0.434	0.018	10.71	0.45	0.17900	0.00177	88	2644	16
272.1	216	106	-0.08	88	0.475	0.018	10.87	0.41	0.16610	0.00116	99	2518	12
273.1	245	262	0.08	77	0.368	0.014	6.15	0.23	0.12138	0.00087	102	1977	13
274.1	221	221	-0.01	89	0.470	0.017	10.66	0.39	0.16456	0.00091	99	2503	9
275.1	226	60	0.07	89	0.457	0.017	10.62	0.40	0.16840	0.00108	96	2542	11
276.1	262	169	0.09	90	0.399	0.015	8.29	0.32	0.15090	0.00113	92	2356	13
277.1	100	46	0.33	40	0.460	0.018	10.97	0.45	0.17280	0.00207	94	2585	20
278.1	402	165	1.08	141	0.404	0.015	9.85	0.42	0.17660	0.00389	84	2621	37
279.1	141	78	-0.08	38	0.316	0.012	5.38	0.22	0.12350	0.00148	88	2008	21
280.1	181	227	0.08	72	0.465	0.017	10.43	0.40	0.16250	0.00101	99	2482	10
281.1	298	185	0.03	122	0.475	0.018	10.82	0.40	0.16510	0.00079	100	2509	8
282.1	131	86	0.17	57	0.503	0.019	12.27	0.47	0.17690	0.00131	100	2624	12
283.1	335	131	1.18	105	0.361	0.013	7.40	0.30	0.14870	0.00253	85	2331	29
284.1	116	93	0.34	42	0.422	0.016	10.21	0.41	0.17550	0.00193	87	2610	18
285.1	237	85	0.27	92	0.452	0.017	9.80	0.37	0.15740	0.00121	99	2428	13
286.1	304	132	0.13	95	0.363	0.013	7.06	0.27	0.14099	0.00100	89	2239	12
287.1	423	582	0.02	158	0.434	0.016	9.32	0.34	0.15580	0.00072	96	2411	8
288.1	433	197	-0.02	170	0.457	0.017	10.20	0.38	0.16177	0.00078	98	2474	8
289.1	556	265	1.65	181	0.373	0.014	7.65	0.43	0.14870	0.00625	88	2332	73
290.1	218	217	1.07	78	0.411	0.015	8.98	0.38	0.15850	0.00301	91	2439	33
291.1	334	318	0.12	133	0.462	0.017	10.62	0.39	0.16690	0.00102	97	2527	10
292.1	275	71	0.09	88	0.371	0.014	7.57	0.29	0.14800	0.00114	88	2323	13
293.1	246	215	0.52	71	0.333	0.013	5.43	0.22	0.11830	0.00154	96	1931	24
294.1	206	76	0.56	76	0.425	0.016	9.40	0.37	0.16050	0.00177	93	2460	18

Data are 1σ precision. All Pb data are common Pb corrected based on measured ^{204}Pb (after Stacey and Kramer 1975).
Analysis date 11/6/2002; SHRIMP I

200036 6131: Wandearah Metasiltstone, Moonta

1:250,000 sheet: Whyalla (SI5308)

1:100,000 sheet: Wiltunga (6430)

AMG: 776517 E 6247233 N

Location: The sample was taken from diamond drillhole BUTE5, depth interval 62-67.3 m. The diamond drillhole is located within the Moonta Region of the Yorke Peninsula.

Description: The BUTE5 diamond drillhole intersects intercalated finely laminated meta-siltstone (Wandearah Metasiltstone) and amphibolite (metadolerite-basalt; Bute Metadolerite). The metasediments are fine-grained, and planar bedded (45-70^{o} to core axis) to locally massive. The intercalated Bute Metadolerite is fine- to medium-grained and non-foliated, with a massive texture. Contacts between the metadolerite and metasediments are generally conformable, but not locally so. The metadolerite is possibly extrusive locally (drillhole description from Conor 1995).

The hand specimen represents a fine-grained dark greenish grey rock in which thin layering is defined by interlayered dark reddish brown and dark greenish grey materials. The sample fails to respond to the hand magnet, suggesting magnetite is absent. In thin section, the meta-siltstone displays a partly-preserved fine-grained matrix-supported silty clastic sedimentary texture, modified by selective pervasive metamorphic recrystallisation without foliation. The meta-siltstone formed as a fine silty pelitic sediment, composed of minor small crystal fragments (quartz (5%)>> plagioclase >> zircon) in a fine clay matrix. Small angular quartz fragments are sparsely scattered throughout the rock, but tend to be loosely concentrated in particular laminae (thin primary layers). Zircon is rare, occurring as subrounded to angular fragments ~50 µm in size, derived by comminution of small growth-zoned crystals.

Subsequent low-grade regional metamorphism in the lower greenschist facies caused complete recrystallisation of the finer clay materials, generating fine-grained sericite (35%) + chlorite (46%) + hematite (3%). Indistinct mineralogical lamination of these minerals is considered to reflect primary sedimentary layering. The phyllosilicate minerals show no preferred orientation, suggesting that recrystallisation occurred in the absence of a directed regional stress regime. Primary silty clastic particles (quartz, plagioclase, zircon) survived this event. A moderate amount of quartz (10%) occurs as tiny equant anhedral grains, in equilibrium contact with tiny chlorite and sericite flakes. This quartz appears to form part of the metamorphic assemblage, but is likely to have formed by grain modification of primary tiny clastic particles.

See Appendix 1 for full petrographic report (Mason 2003).

Mount: Z3966

Description of zircons

The sample contains well rounded detrital zircons, many of which exhibit finely pitted surfaces indicative of sedimentary transport (Figure 55). A few small grains preserve simple euhedral pyramidal and prismatic facets. The zircons vary between 50 to 200 µm in length, although most grains are small (~50 µm). Aspect ratios are variable, but generally < 3:1. The grains are light brown in colour and clear, with bleb-shaped brown inclusions, and a few hematite-stained brown cracks. Although it is rarely visible optically, cathodoluminescence shows that prismatic zoning is

ubiquitous, suggesting an initially igneous origin for the detrital grains. Some grains exhibit sector zoning. Possible cores are only present in a few grains. All available zircons from the methylene iodide density separation were mounted.

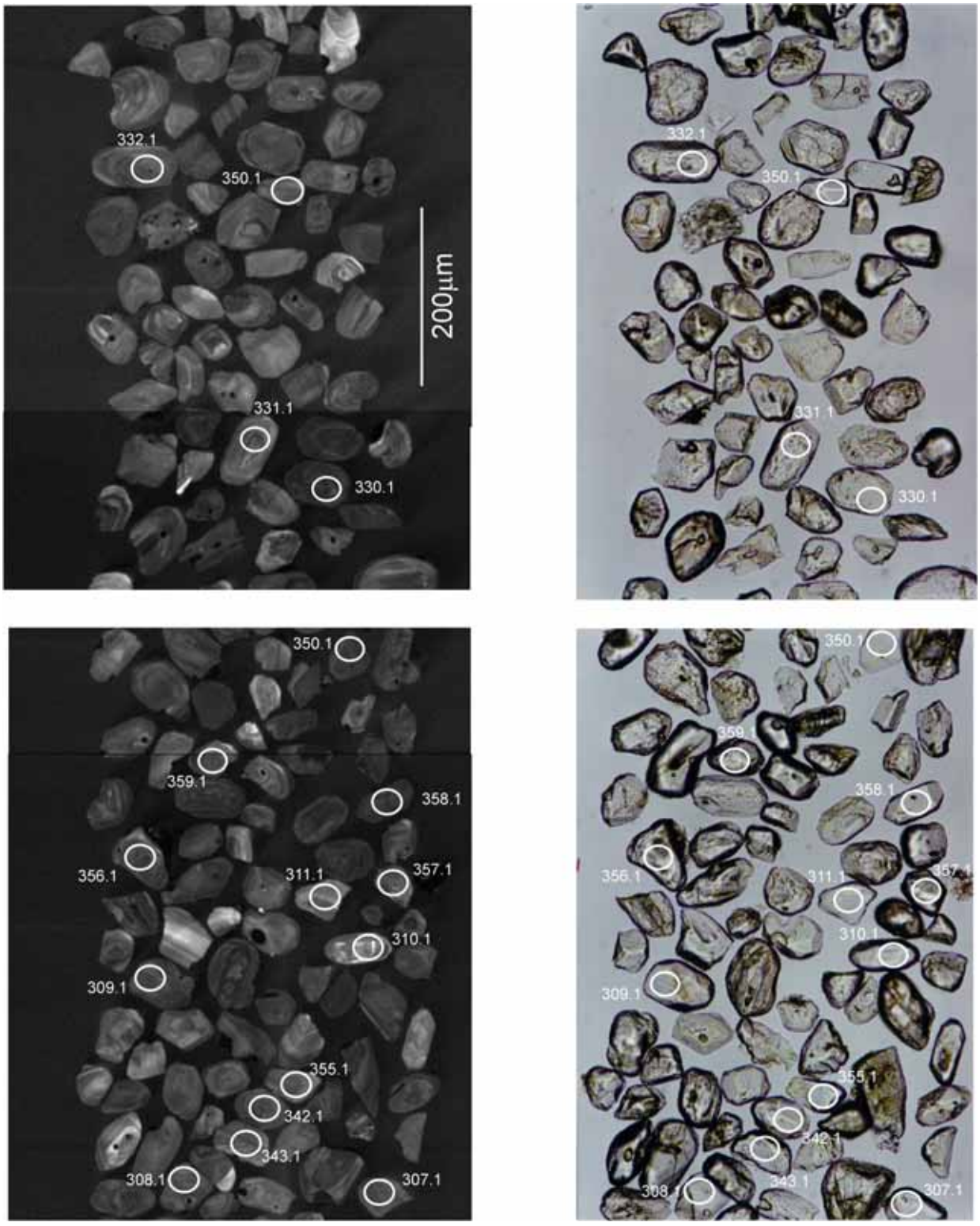

Figure 55. Representative CL (left) and transmitted light (right) images for sample 200036 6131: Wandearah Metasiltstone, Moonta. SHRIMP analysis spots are labelled. Scale bar is 200 µm.

Concurrent standard data

Data for the standard are presented in Appendix 3. The calibration exponent for this QGNG data set is 1.96, with an upper limit of 2.26 and a lower limit of 1.61 (at the 95% confidence level). Thus the nominal value of 2.0 has been used in data reduction. All analyses are used in the calibration. There are two outliers in $^{206}Pb/^{238}U$ (915.1 and 932.1) and these have been omitted, leaving 49 analyses with a 1σ scatter in $^{206}Pb/^{238}U$ of 3.58%. Element abundance calibration was based on SL13 (n = 1).

There is only one obvious outlier amongst the $^{207}Pb/^{206}Pb$ ages, (915.1) but the remaining 50 analyses do not conform to a normal distribution, yielding a weighted mean $^{207}Pb/^{206}Pb$ age of 1843 ± 6 Ma (MSWD = 2.5; probability of fit = 0). The analyses are corrected for overcounts at mass ^{204}Pb (after Black in press; calculated assuming $^{\mathbf{206}}Pb/^{238}U$-$^{207}Pb$-$^{235}U$ age concordance), which forces the weighted mean $^{207}Pb/^{206}Pb$ age for QGNG to the TIMS reference value. The sample data below are also corrected for overcounts at the ^{204}Pb mass peak.

The recalculated age for QGNG becomes 1851.9 ± 4.6 Ma (MSWD is 1.3; probability of fit is .09; n = 46 of 51). In this case, *SQUID* identifies 5 statistical outliers. Excluding the youngest analysis (915.1; age 1727 ± 15 Ma (1σ error)) from the age calculation is warranted, as the grain contains high common ^{206}Pb and is discordant, suggesting Pb loss may have occurred. However, there are no other obvious statistical outliers, and no geological reason for further culling of analyses. The remaining 50 analyses yield a weighted mean $^{207}Pb/^{206}Pb$ age of 1849 ± 6 Ma (MSWD = 2.2; probability of fit = 0). The high MSWD indicates the scatter in the analyses is greater than that predicted by counting statistics alone. The wide spread of ages is therefore attributed to a component of instrument uncertainty, and high MSWDs for the corresponding samples are also acceptable.

Sample data

A total of 75 grains were analysed. The main cluster of 61 analyses lie close to concordia, between *ca* 1700 and 1920 Ma (Figure 56). Two analyses are considerably younger (grains 322 and 334), plotting near concordia at about 580 Ma. The 12 oldest analyses produce a spread of ages between *ca* 1920 Ma and 3400 Ma (Figure 57).

A probability density curve shows two clear age peaks within the main group of data (Figure 58a.) An obvious inflection point in the data set is used to divide the analyses into the two separate age populations (Figure 58b). Using the uncorrected dataset, the oldest 14 analyses yield an age of 1853 ± 9 Ma and the youngest 47 analyses yield an age of 1753 ± 7 Ma. When the data are corrected for overcounts at mass ^{204}Pb, the 14 oldest analyses yield a weighted mean $^{207}Pb/^{206}Pb$ age of 1862 ± 8 Ma (MSWD = 0.87; probability of fit = 0.58). The youngest 47 analyses lie below the inflection point, and yield an age of 1762 ± 7 Ma (MSWD = 1.9; probability of fit = 0). Although the scatter is high, the probability density distribution for this younger age population is normal, and so there is no geological reason to discard any of the analyses. Based on robust statistics, *SQUID* suggests eliminating five analyses within the group (333.1, 331.1, 302.1, 311.1 and 313.1), to give an improved weighted mean age of 1761 ± 5 Ma (MSWD = 1.12; probability of fit = .0.27). However, the excess scatter in the QGNG analyses in this session indicates the less precise age of 1762 ± 7 Ma should be accepted as the age of the group. The mixture modelling algorithm of Sambridge and Compston (1994) applied to the data subset calculates the two component ages to be 1762.5 ± 4.6 Ma (79% of analyses) and 1862 ± 8.5 Ma (21% of

analyses; Figure 58a), which agree very well with the above weighted mean age calculations.

There are insufficient data to distinguish any more age groups within the data set, although they may be postulated to occur at about 1950, 2040 and 2590 Ma, with individual grains of *ca* 2510, 3000 and 3320 Ma (Figure 57). There appears to be a hiatus between about 2040 and 2500 Ma. The oldest zircon ages represent single-phase grains (as opposed to cores), and as all analyses are at least 90% concordant, their $^{207}Pb/^{206}Pb$ compositions should provide reliable age estimates.

The two analyses younger than the 1762 Ma population, plot near concordia at *ca* 580 Ma (322.1 and 334.1), with ^{204}Pb corrected $^{206}Pb/^{238}U$ ages of *ca* 590 and 520 Ma, respectively. However, independent geological constraints on the relative age of the Wandearah Metasiltstone indicate the unit cannot be of Cambrian/Adelaidean age. The possibility that the grains are laboratory contaminants was explored, but an inspection of Geoscience Australia laboratory records indicated that no samples of Cambrian/Adelaidean age had been processed in the months before sample 200036 6131 was handled. The $^{176}Hf/^{177}Hf$ ratio of analysis 334.1 suggests this grain should be considerably older (~ 2200 Ma), and that the U-Pb isotope system has been reset (E.Belousova pers. comm.; Figure 59). The same is likely to apply for grain 322.1.

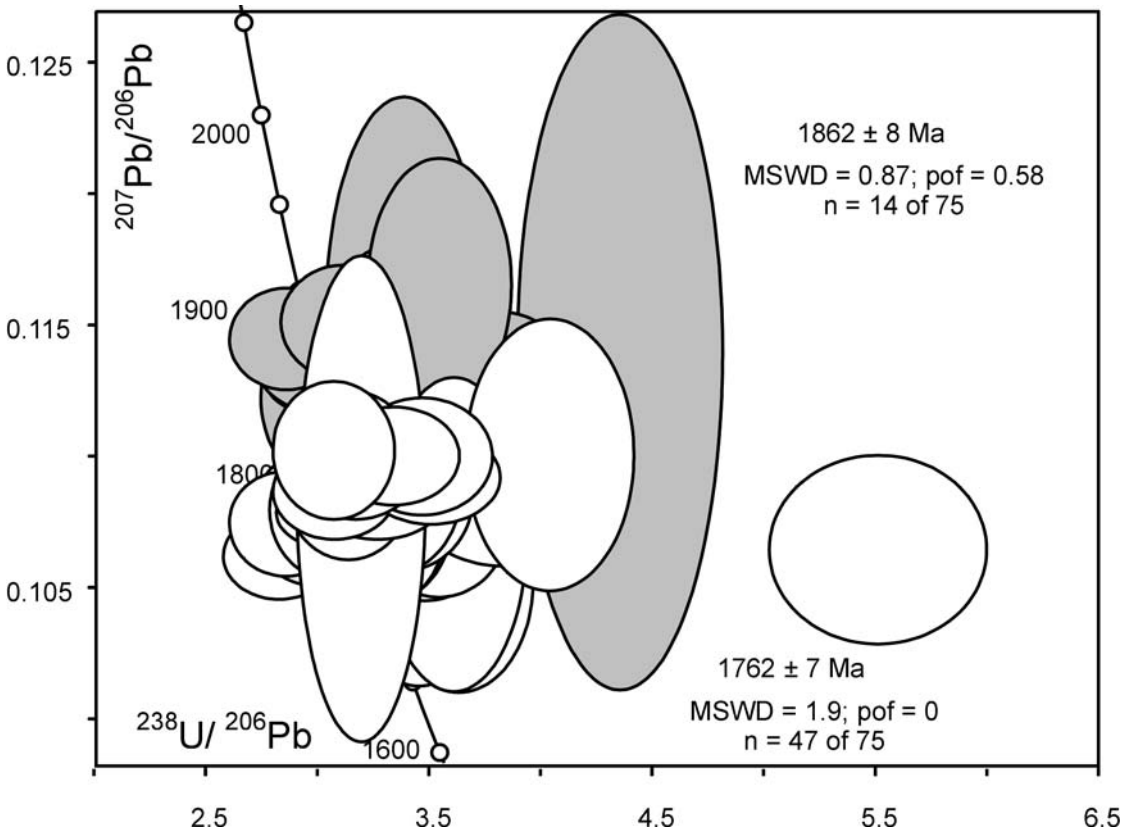

Figure 56. Concordia plot for zircons in sample 200036 6131. Only the main body of analyses are plotted (those between 1700 and 1920 Ma in age). The analyses can be divided into two distinct populations. The white filled error ellipses represent the 1762 Ma population and the grey represent the 1862 Ma population.

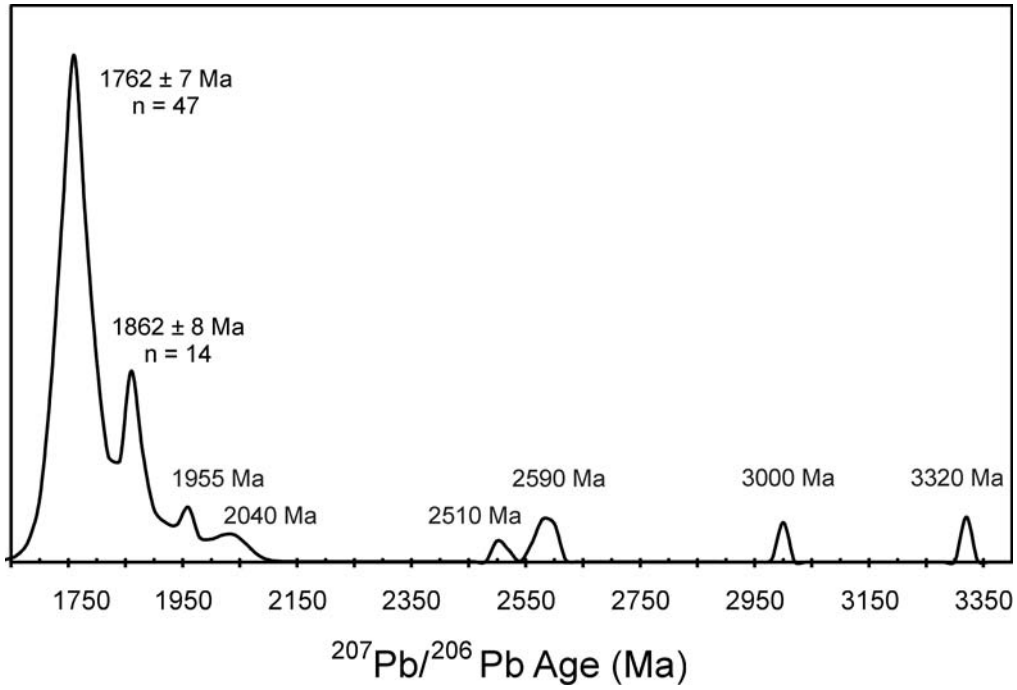

Figure 57. Probability density distribution of $^{207}Pb/^{206}Pb$ ages for sample 200036 6131 illustrating the full range of zircon ages. The two youngest grains are not included in the figure.

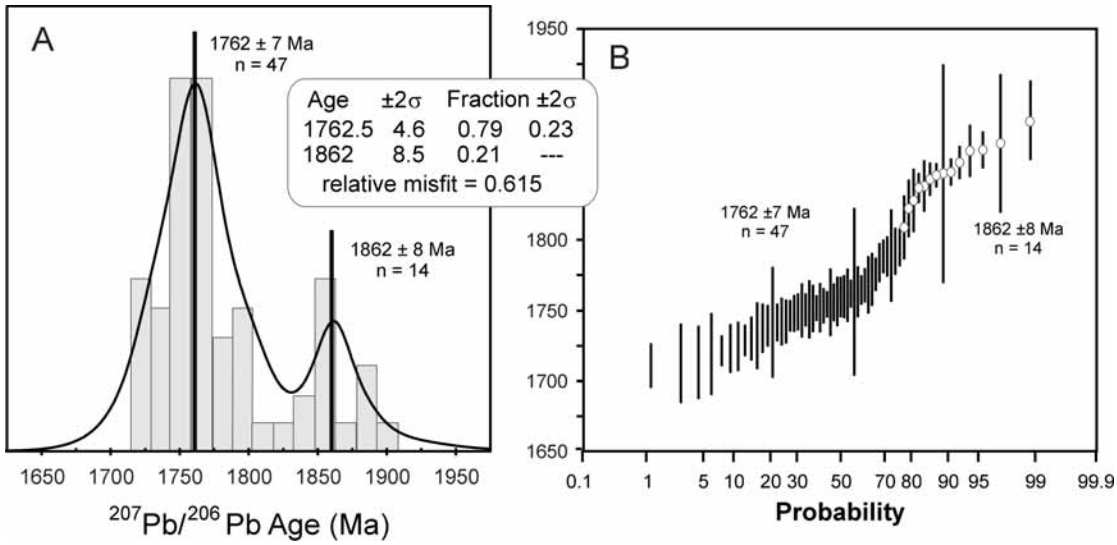

Figure 58a. Probability density distribution showing the main group of 61 analyses. The clear double peak indicates the existence of two age populations in the group. Ages in text box are calculated by the mixture modelling algorithm (Sambridge and Compston (1994). Ages at peaks are weighted mean $^{207}Pb/^{206}Pb$ age of the two components, subdivided into 2 groups using the inflection point illustrated in Figure 58b.

Figure 58b. Probability diagram for individual zircon ages between 1700 and 1920 Ma. An inflection point between the 47 youngest and 14 oldest analyses (denoted by filled circles) is used to separate the two age populations.

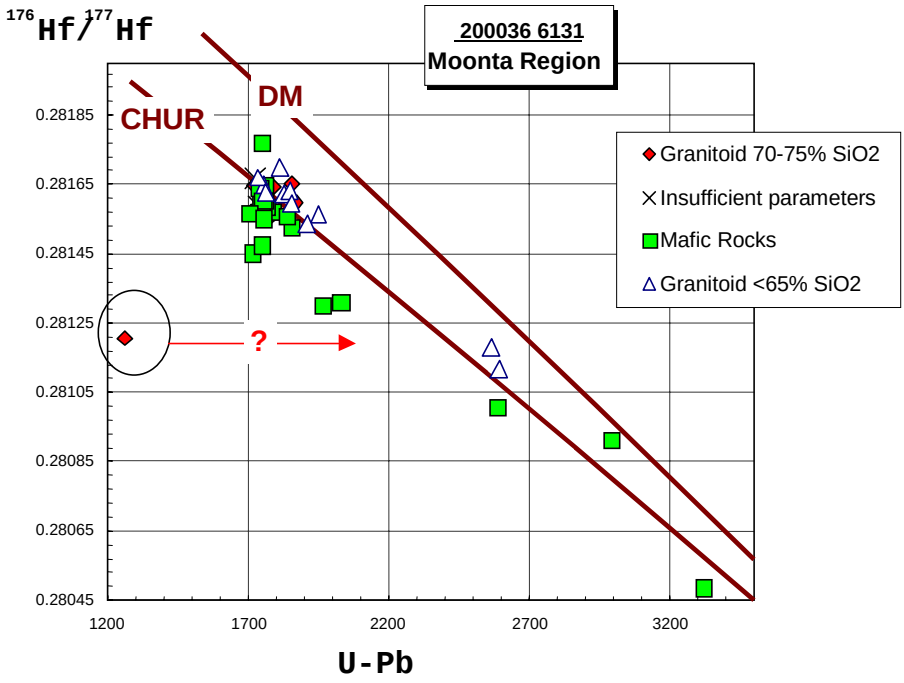

Figure 59. $^{176}Hf/^{177}Hf$ ratios vs $^{207}Pb/^{206}Pb$ age for selected zircon analyses. The Hf isotopes suggest that grain 334 (represented by a red diamond) should have a U-Pb age of ~ 2200 Ma, and that the U-Pb isotope systematics have been disturbed. Graph supplied by Dr Elena Belousova (unpublished data; Macquarie University).

Geochronological interpretation

The maximum deposition age for the Wandearah Metasiltstone is considered to be 1762 ± 7 Ma. The provenance for detrital zircons also includes an ~1860 Ma source, with a spread of older ages suggesting a multiple source region that includes components at least as old as 3300 Ma.

Table 17. SHRIMP analytical results for zircon from sample 200036 6131.

Spot	U (ppm)	Th (ppm)	$^{206}Pb_c$ (%)	$^{206}Pb^*$ (ppm)	$^{206}Pb^*/^{238}U$	±	$^{207}Pb^*/^{235}U$	±	$^{207}Pb^*/^{206}Pb^*$	±	conc (%)	207Pb/206Pb Age(Ma)	±
301.1	208	153	-0.07	54	0.304	0.027	4.50	2.93	0.10800	0.07020	97	1770	1200
302.1	171	103	-0.04	42	0.289	0.011	4.38	0.17	0.10998	0.00091	91	1799	15
303.1	147	97	0.17	40	0.312	0.012	4.56	0.17	0.10590	0.00106	101	1730	19
304.1	127	95	0.28	35	0.325	0.012	5.04	0.20	0.11260	0.00146	98	1842	24
305.1	196	99	-0.06	94	0.559	0.021	17.14	0.63	0.22225	0.00098	96	2997	7
306.1	229	125	-0.03	66	0.335	0.012	5.25	0.19	0.11364	0.00078	100	1858	13
307.1	190	113	-0.07	51	0.314	0.012	4.69	0.24	0.10840	0.00379	99	1772	64
308.1	200	135	-0.02	52	0.304	0.011	4.52	0.17	0.10790	0.00084	97	1764	14
309.1	164	135	-0.09	66	0.468	0.017	11.04	0.41	0.17130	0.00110	96	2570	11
310.1	105	28	-0.26	30	0.333	0.013	5.81	0.23	0.12650	0.00164	91	2049	23
311.1	115	66	-0.04	32	0.320	0.012	4.88	0.19	0.11040	0.00086	99	1806	14
312.1	207	109	0.06	84	0.473	0.017	10.77	0.40	0.16510	0.00069	100	2509	7
313.1	216	98	-0.10	56	0.300	0.011	4.55	0.17	0.10998	0.00077	94	1799	13
314.1	162	407	3.13	33	0.230	0.010	3.61	0.23	0.11390	0.00524	72	1863	84
315.1	235	148	-0.01	67	0.333	0.012	5.15	0.20	0.11220	0.00135	101	1836	22
316.1	436	354	1.21	69	0.182	0.007	2.67	0.10	0.10640	0.00149	62	1739	25
317.1	281	166	0.03	76	0.316	0.011	4.95	0.18	0.11383	0.00058	95	1861	9
318.1	177	156	0.03	48	0.314	0.012	4.65	0.17	0.10730	0.00070	100	1754	12
319.1	196	85	0.09	55	0.326	0.012	4.89	0.19	0.10866	0.00076	102	1777	13
320.1	235	161	-0.12	64	0.318	0.011	4.69	0.18	0.10704	0.00097	102	1750	17
321.1	194	95	-0.07	60	0.357	0.013	5.91	0.22	0.12016	0.00066	100	1959	10
322.1	740	463	0.15	61	0.096	0.003	0.79	0.03	0.05958	0.00060	100	588	22
323.1	219	211	0.11	62	0.332	0.012	5.18	0.19	0.11322	0.00071	100	1852	11
324.1	228	151	0.16	69	0.355	0.013	5.19	0.19	0.10619	0.00068	113	1735	12
325.1	183	123	-0.05	49	0.314	0.011	4.68	0.18	0.10815	0.00095	100	1768	16
326.1	154	67	-0.14	43	0.322	0.012	5.10	0.19	0.11507	0.00090	96	1881	14
327.1	144	103	-0.20	40	0.326	0.012	4.96	0.19	0.11020	0.00108	101	1803	18
328.1	186	120	-0.02	52	0.325	0.012	4.83	0.18	0.10782	0.00058	103	1763	10
329.1	190	177	-0.05	58	0.357	0.013	5.97	0.28	0.12110	0.00351	100	1973	51
330.1	288	180	0.15	76	0.307	0.011	4.58	0.17	0.10828	0.00061	97	1771	10
331.1	157	169	0.09	43	0.319	0.011	4.65	0.17	0.10573	0.00067	103	1727	12
332.1	388	247	0.41	96	0.286	0.010	4.30	0.16	0.10917	0.00073	91	1786	12
333.1	259	283	0.49	64	0.288	0.010	4.17	0.15	0.10508	0.00097	95	1716	17
334.1	250	1080	15.67	22	0.085	0.003	1.01	0.19	0.08600	0.01548	39	1346	350
335.1	252	247	0.08	107	0.496	0.018	11.84	0.43	0.17316	0.00059	100	2589	6
336.1	110	83	-0.15	28	0.300	0.011	4.50	0.18	0.10870	0.00130	95	1777	22
337.1	191	167	0.57	51	0.305	0.011	4.50	0.17	0.10670	0.00107	99	1744	19
338.1	158	106	-0.04	42	0.306	0.011	4.55	0.17	0.10775	0.00079	98	1762	13
339.1	140	135	0.04	79	0.661	0.024	24.87	0.92	0.27270	0.00115	99	3322	7
340.1	290	157	0.12	127	0.510	0.018	12.24	0.45	0.17410	0.00101	102	2597	10
341.1	198	163	0.21	53	0.309	0.011	4.52	0.17	0.10628	0.00097	100	1737	17
342.1	279	220	0.62	70	0.288	0.010	4.25	0.16	0.10700	0.00106	93	1750	18
343.1	166	158	0.05	50	0.350	0.013	5.53	0.20	0.11445	0.00079	103	1871	13
344.1	107	167	-0.15	30	0.323	0.019	4.80	1.82	0.10800	0.04104	102	1769	690
345.1	231	292	0.51	56	0.283	0.010	4.19	0.16	0.10750	0.00118	91	1758	21

Spot	U (ppm)	Th (ppm)	$^{206}Pb_c$ (%)	$^{206}Pb^*$ (ppm)	$^{206}Pb^*/^{238}U$	±	$^{207}Pb^*/^{235}U$	±	$^{207}Pb^*/^{206}Pb^*$	±	conc (%)	207Pb/206Pb Age(Ma)	±
346.1	377	115	0.11	87	0.267	0.010	4.20	0.16	0.11398	0.00064	82	1864	10
347.1	245	131	0.03	68	0.324	0.012	4.80	0.18	0.10764	0.00057	103	1760	10
348.1	345	401	0.23	104	0.351	0.013	5.20	0.19	0.10740	0.00082	110	1756	14
349.1	204	130	-0.05	54	0.306	0.011	4.58	0.17	0.10845	0.00064	97	1774	11
350.1	211	217	-0.24	59	0.324	0.012	4.78	0.18	0.10700	0.00083	104	1749	14
351.1	160	82	-0.06	47	0.342	0.013	5.89	0.24	0.12480	0.00162	94	2026	24
352.1	129	88	0.23	36	0.320	0.012	4.80	0.19	0.10890	0.00120	100	1782	20
353.1	247	220	0.32	63	0.297	0.011	4.72	0.18	0.11500	0.00127	89	1880	20
354.1	162	111	1.18	43	0.305	0.011	4.54	0.18	0.10790	0.00151	97	1764	25
355.1	227	284	0.05	55	0.278	0.010	4.10	0.18	0.10700	0.00246	90	1749	42
356.1	215	176	0.60	58	0.316	0.012	4.78	0.18	0.10970	0.00088	99	1794	15
357.1	218	473	0.15	53	0.282	0.010	4.53	0.19	0.11650	0.00198	84	1904	30
358.1	326	310	0.58	91	0.323	0.012	4.77	0.18	0.10685	0.00092	103	1746	16
359.1	276	407	0.06	66	0.276	0.010	4.00	0.16	0.10520	0.00168	91	1717	30
360.1	392	305	0.03	88	0.262	0.009	3.89	0.14	0.10756	0.00073	85	1759	12
361.1	237	226	-0.08	64	0.313	0.012	4.63	0.18	0.10747	0.00083	100	1757	14
362.1	173	187	0.17	49	0.327	0.012	4.86	0.19	0.10790	0.00108	103	1765	19
363.1	313	374	0.06	76	0.282	0.010	4.41	0.17	0.11330	0.00125	86	1853	20
364.1	204	157	0.30	59	0.337	0.012	5.00	0.20	0.10760	0.00105	106	1759	18
365.1	168	461	0.79	36	0.248	0.009	3.76	0.16	0.11000	0.00209	79	1800	35
366.1	359	181	0.30	86	0.278	0.010	4.26	0.17	0.11130	0.00145	87	1821	24
366.1	220	211	0.57	71	0.372	0.014	6.03	0.24	0.11780	0.00141	106	1923	21
367.1	239	245	0.09	60	0.290	0.011	4.23	0.17	0.10560	0.00180	95	1725	31
368.1	209	269	-0.13	51	0.286	0.011	4.17	0.16	0.10580	0.00106	94	1729	18
369.1	200	212	0.47	51	0.296	0.011	4.43	0.17	0.10840	0.00108	94	1772	19
370.1	320	633	0.26	84	0.303	0.012	4.39	0.18	0.10520	0.00158	99	1718	28
370.1	315	573	0.46	82	0.304	0.011	4.50	0.18	0.10760	0.00129	97	1759	22
371.1	56	89	0.03	14	0.295	0.013	4.70	0.24	0.11540	0.00335	88	1886	53
372.1	195	208	0.80	49	0.294	0.011	4.36	0.17	0.10770	0.00108	94	1760	19
373.1	188	206	0.04	59	0.364	0.014	6.08	0.26	0.12130	0.00206	101	1975	31

Data are 1σ precision. All Pb data are common Pb corrected based on measured ^{204}Pb (after Stacey and Kramer 1975).
Analysis date 11/6/2002; SHRIMP I

200036 6115: Moonabie Formation, Roopena (volcaniclastic sandstone)

1:250,000 sheet: Port Augusta (SI5304)

1:100,000 sheet: Roopena (6332)

AMG: 722867 E 6374155 N

Location: The sample was taken from diamond drillhole SOC8, depth interval 181.5-.75, 182.3-.6, 199-200 m (Figure 60). The diamond drillhole is located within the Roopena prospect of the Olympic Domain.

Description: In hand specimen the sample represents an arenaceous clastic sediment with little or no layering, composed of closely-packed small particles with overall mauvish colour from pervasive hematite alteration. Sparsely scattered slightly larger ragged patches several millimetres in size are cream in colour and appear to be 'grains', but under the hand lens they are observed to represent clastic sediment that lacks the pervasive hematite staining.

In thin section the sample displays a well-preserved framework-supported, sorted but non-layered, arenaceous clastic sedimentary texture that has been modified by pervasive alteration. It is composed of abundant (54%) lithic fragments (mainly felsic volcanic fragments, minor recrystallised metamorphic quartz fragments, now replaced by fine-grained massive quartz mosaics and pervasive hematite alteration) and lesser (35%) crystal fragments (equant subrounded to subangular crystal fragments of quartz, some polycrystalline quartz displaying sutured lineated metamorphic textures, rare zircon). Zircon occurs as uncommon fragments of prismatic terminated crystals up to ~0.2 mm long. Interparticle pores are filled with microgranular aggregates of quartz and hematite, and rare sericite, forming fine-grained flakes that have replaced precursor flakes up to ~0.5 mm long (probably biotite, as inferred from the presence of tiny leucoxene granules sprinkled through the sericite mat).

The lithic (volcaniclastic) sandstone formed as a coarse sandy deposit. Two different source terrains are inferred: (i) a coarsely crystalline ?metamorphic terrane contributed at least some of the quartz crystal fragments (specifically the polycrystalline quartz fragments, and possibly some of the larger quartz crystal fragments); and ii) a felsic volcanic source contributed glassy to partly-crystallised lava fragments, and some of the crystal fragments. Some of the lava fragments contain quartz phenocrysts, which suggests that some of the quartz crystal fragments most likely were derived from the felsic volcanic source.

The sediment underwent strong pervasive alteration under low P-T conditions, generating abundant quartz + hematite, both by replacement of the felsic volcanic fragments and by filling of the interparticle pores.

See Appendix 1 for full petrographic report (Mason 2003).

Mount: Z3966

Description of zircons

The sample contains predominantly euhedral zircons ranging between 50 µm to 150 µm in size, with aspect ratios up to about 2:1. The zircons are clear and light brown in colour, with few cracks and inclusions. Sharp, angular prismatic terminations and crystal facets are well preserved. Only a few grains exhibit evidence of abrasion, attesting to a detrital origin. There are no visible cores. Well-defined

concentric zoning is present in most grains, as seen in the CL images (Figure 61), suggesting an igneous origin for the zircons.

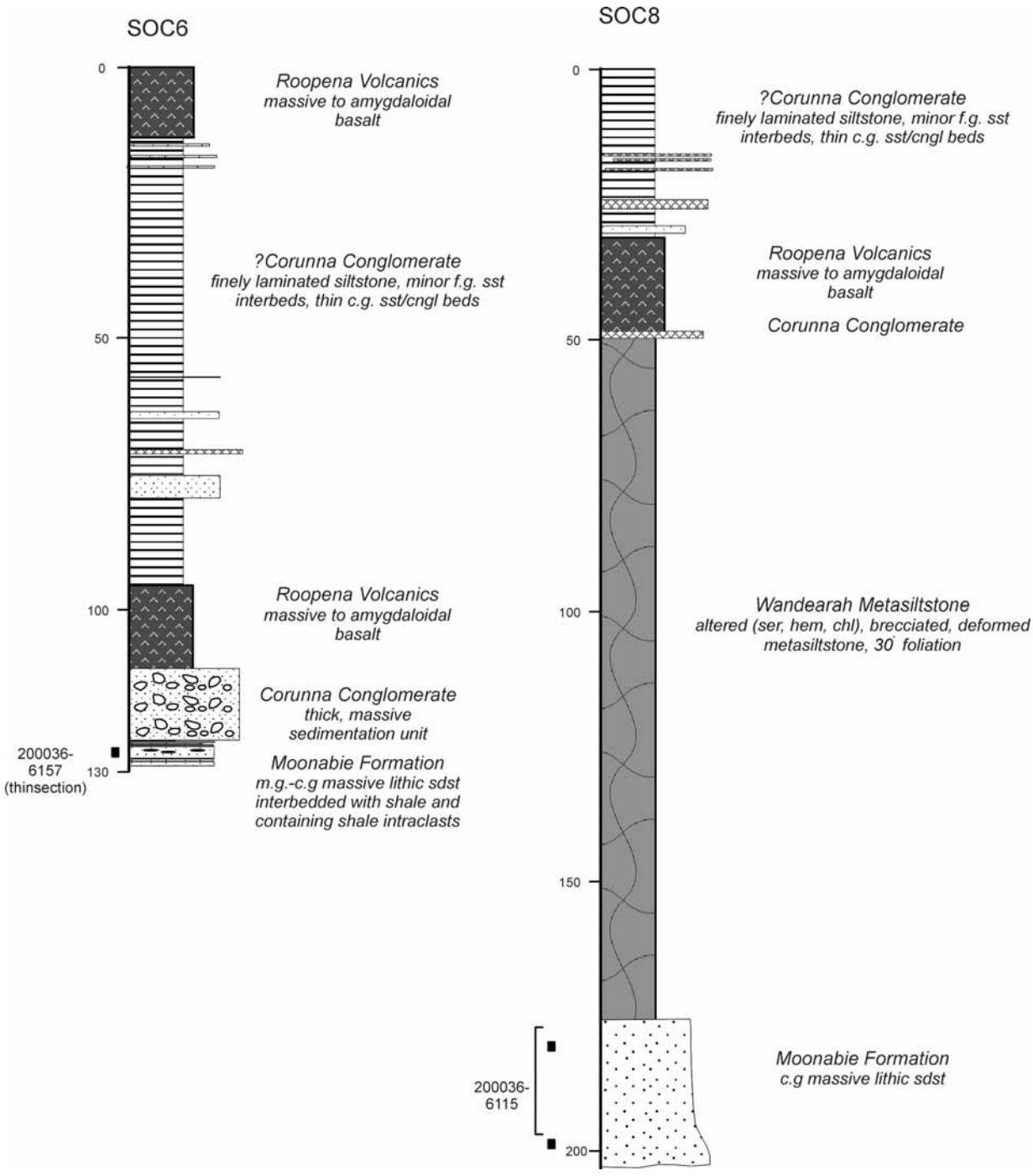

Figure 60. Stratigraphic log for diamond drill holes from Roopena prospect, showing the location of sample collected for SHRIMP dating and petrographic analysis.

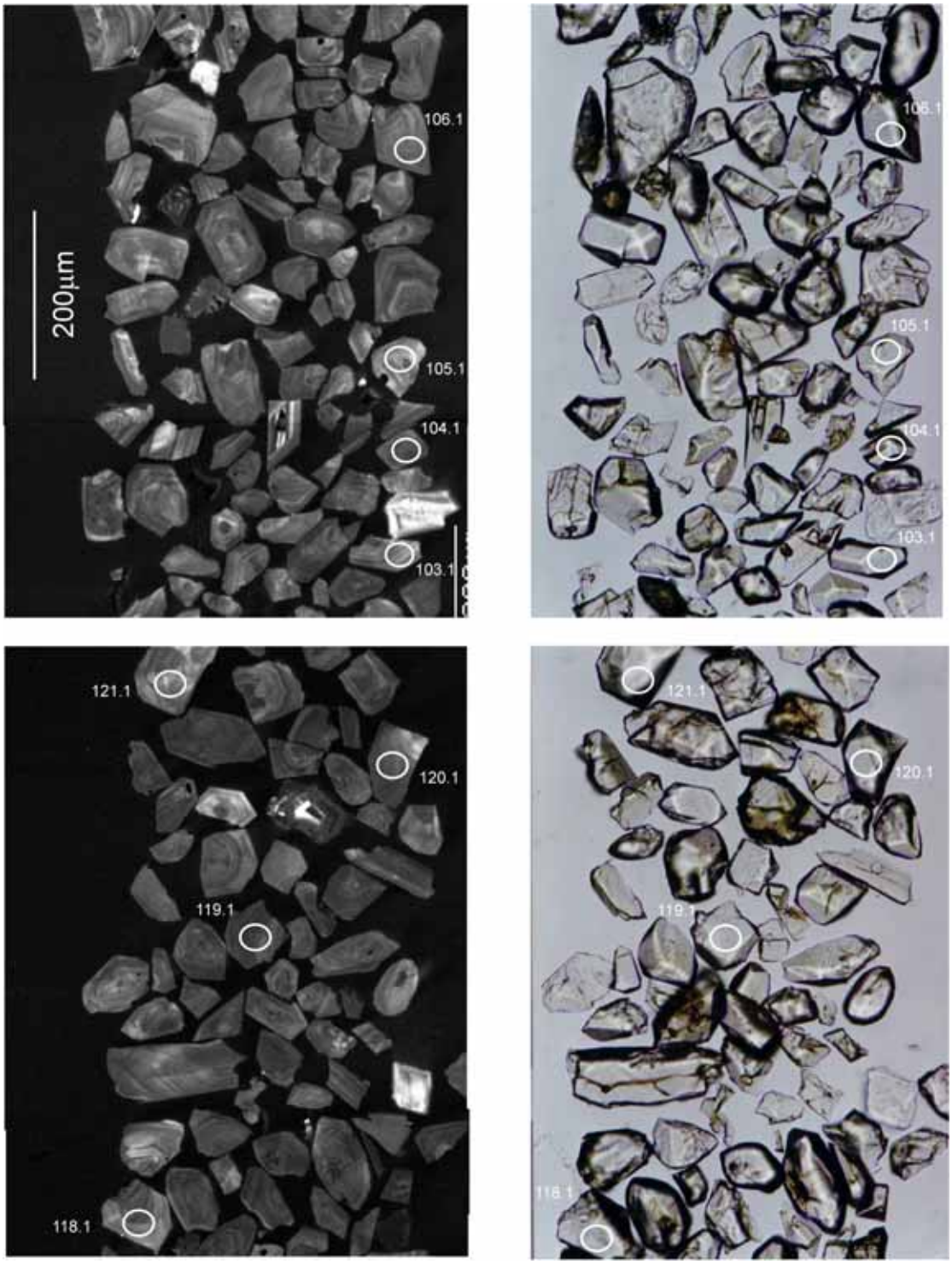

Figure 61. Representative CL (left) and transmitted light (right) images for sample 200036 6115: volcaniclastic sandstone, Moonabie Formation, Roopena prospect. SHRIMP analysis spots are labelled. Scale bar is 200 µm.

Concurrent standard data

Data for the standard are presented in Appendix 3. The calibration exponent for this QGNG data set is 1.96, with an upper limit of 2.26 and a lower limit of 1.61 (at the 95% confidence level). Thus the nominal value of 2.0 has been used in data reduction. All analyses are used in the calibration. There are two outliers in $^{206}Pb/^{238}U$ (915.1 and 932.1) and these have been omitted, leaving 49 analyses with a 1σ scatter in $^{206}Pb/^{238}U$ of 3.58%. Element abundance calibration was based on SL13 (n = 1).

There is only one obvious outlier amongst the $^{207}Pb/^{206}Pb$ ages, (915.1) but the remaining 50 analyses do not conform to a normal distribution, yielding a weighted mean $^{207}Pb/^{206}Pb$ age of 1843 ± 6 Ma (MSWD = 2.5; probability of fit = 0). The analyses are corrected for overcounts at mass ^{204}Pb (after Black in press; calculated assuming $^{\mathbf{206}}Pb/^{238}U$-$^{207}Pb$-$^{235}U$ age concordance), which forces the weighted mean $^{207}Pb/^{206}Pb$ age for QGNG to the TIMS reference value. The sample data below are also corrected for overcounts at the ^{204}Pb mass peak.

The recalculated age for QGNG becomes 1851.9 ± 4.6 Ma (MSWD is 1.3; probability of fit is .09; n = 46 of 51). In this case, *SQUID* identifies 5 statistical outliers. Excluding the youngest analysis (915.1; age 1727 ± 15 Ma (1σ error)) from the age calculation is warranted, as the grain contains high common ^{206}Pb and is discordant, suggesting Pb loss may have occurred. However, there are no other obvious statistical outliers, and no geological reason for further culling of analyses. The remaining 50 analyses yield a weighted mean $^{207}Pb/^{206}Pb$ age of 1849 ± 6 Ma (MSWD = 2.2; probability of fit = 0). The high MSWD indicates the scatter in the analyses is greater than that predicted by counting statistics alone. The wide spread of ages is therefore attributed to a component of instrument uncertainty, and high MSWDs for the corresponding samples are also acceptable.

Sample data

Thirty grains were analysed. Most analyses cluster close to concordia at about 1750 Ma (Figure 62). Three grains are clearly older, with near concordant ages of *ca* 2610, 2000 and 1860 Ma (Figure 63). The remaining 27 analyses yield a weighted mean $^{207}Pb/^{206}Pb$ age of 1748 ± 8 Ma. When the data are corrected for overcounts at mass ^{204}Pb, tha age becomes 1756 ± 8 Ma, with an acceptable MSWD of 1.3 (probability of fit = 0.11).

Geochronological interpretation

The maximum age for the sandstone is considered to be 1756 ± 8 Ma. The provenance for detrital zircons appears to be a local igneous source, solely comprising material of this age, with the few older grains that may represent inheritance within the igneous source, rather than indicating a multiple source region.

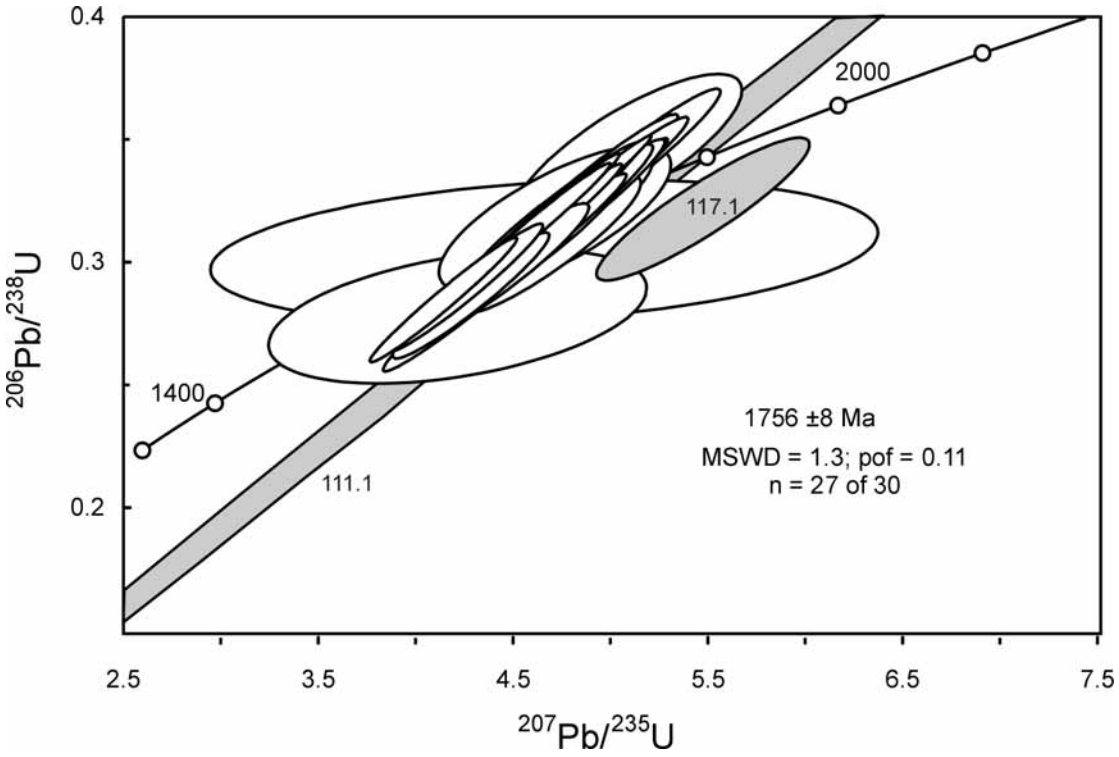

Figure 62. Concordia plot for zircons in sample 200036 6115. White-filled symbols represent analyses used in the weighted mean age calculation. One outlier (108.1) plots above the range of the diagram (see Figure 63). The remaining outliers are shaded light grey.

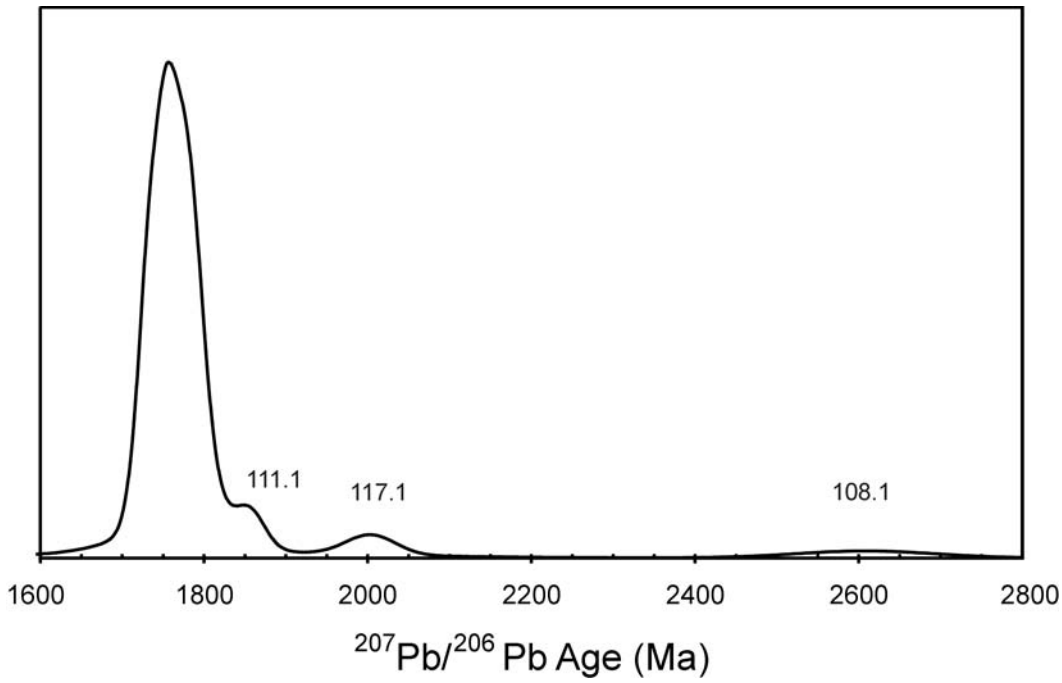

Figure 63. Probability density distribution of $^{207}Pb/^{206}Pb$ ages illustrating the full range of zircon ages. Outliers are labelled.

Table 18. SHRIMP analytical results for zircon from sample 200036 6115.

Spot	U (ppm)	Th (ppm)	$^{206}Pb_c$ (%)	$^{206}Pb^*$ (ppm)	$^{206}Pb^*/^{238}U$	±	$^{207}Pb^*/^{235}U$	±	$^{207}Pb^*/^{206}Pb^*$	±	conc (%)	207Pb/206Pb Age(Ma)	±
101.1	179	146	-0.17	46	0.297	0.011	4.45	0.17	0.10860	0.00152	94	1776	25
102.1	108	83	-0.14	29	0.308	0.011	4.62	0.18	0.10870	0.00152	94	1777	25
103.1	109	61	0.14	30	0.319	0.012	4.71	0.18	0.10700	0.00118	101	1748	20
104.1	228	158	0.45	56	0.286	0.011	4.28	0.16	0.10830	0.00130	102	1772	21
105.1	96	80	-0.13	26	0.318	0.012	4.71	0.24	0.10740	0.00376	102	1756	64
106.1	167	94	-0.08	46	0.316	0.012	4.69	0.19	0.10740	0.00150	103	1756	25
107.1	130	98	-0.22	36	0.321	0.012	4.84	0.18	0.10921	0.00093	110	1786	15
108.1	319	168	-0.03	136	0.497	0.019	12.02	0.77	0.17530	0.00894	101	2609	86
109.1	135	80	-0.01	36	0.308	0.011	4.64	0.18	0.10915	0.00095	105	1785	16
110.1	167	113	-0.07	45	0.315	0.012	4.73	0.19	0.10890	0.00196	104	1781	32
111.1	61	77	-0.47	17	0.320	0.122	5.00	1.90	0.11350	0.01135	101	1857	18
112.1	151	63	-0.26	38	0.293	0.015	4.40	0.23	0.10900	0.00109	103	1782	19
113.1	194	97	-0.11	55	0.330	0.012	4.94	0.18	0.10856	0.00096	100	1775	16
114.1	173	161	6.59	48	0.305	0.012	4.65	0.70	0.11100	0.01665	101	1813	260
115.1	147	100	-0.08	40	0.319	0.012	4.76	0.18	0.10810	0.00130	97	1767	21
116.1	288	457	12.24	78	0.278	0.011	4.21	0.40	0.10980	0.00933	107	1797	160
117.1	108	67	0.08	30	0.322	0.012	5.47	0.22	0.12320	0.00209	92	2004	30
118.1	112	77	0.13	28	0.290	0.011	4.25	0.16	0.10648	0.00098	95	1740	17
119.1	233	119	-0.01	65	0.323	0.012	4.77	0.18	0.10717	0.00057	104	1752	10
120.1	155	82	-0.23	43	0.321	0.012	4.82	0.18	0.10880	0.00109	101	1780	19
121.1	80	78	-0.26	21	0.307	0.011	4.67	0.19	0.11050	0.00199	99	1807	33
122.1	201	196	0.20	49	0.285	0.010	4.14	0.15	0.10542	0.00078	93	1722	14
123.1	94	70	0.25	27	0.328	0.012	4.86	0.19	0.10760	0.00129	97	1759	21
124.1	126	95	0.23	35	0.320	0.012	4.71	0.18	0.10676	0.00100	101	1745	17
125.1	143	98	0.92	43	0.346	0.013	5.08	0.24	0.10670	0.00309	95	1744	53
126.1	178	119	-0.03	48	0.312	0.011	4.63	0.17	0.10748	0.00072	88	1757	12
127.1	114	75	0.22	33	0.331	0.012	4.88	0.19	0.10710	0.00107	95	1751	18
128.1	182	119	0.06	49	0.313	0.011	4.58	0.17	0.10610	0.00064	96	1734	11
129.1	194	137	0.16	53	0.316	0.011	4.63	0.17	0.10606	0.00064	90	1733	11
130.1	162	105	0.50	48	0.340	0.013	5.08	0.19	0.10830	0.00119	100	1771	20

Data are 1σ precision. All Pb data are common Pb corrected based on measured ^{204}Pb (after Stacey and Kramer 1975).
Analysis date 11/6/2002; SHRIMP I

200036 6103: gneiss, Saddle Hill

1:250,000 sheet: Andamooka (SH5312)

1:100,000 sheet: Yarrawurta (6337)

AMG: 692756 E 6658936 N

Location: The sample was taken from diamond drillhole SHD1, depth interval 935-937 m (Figure 64). The diamond drillhole is located within the Saddle Hill prospect of the Olympic Domain.

Description: The sample is a well-foliated gneiss with pegmatoidal lenses and disseminated alkali feldspar. The gneiss has foliations to 2 mm wide with various proportions of well-foliated biotite (20%), granular quartz (50%), fresh to sericitised plagioclase (10%) and fresh orthoclase (10%). Garnet (5%) occurs as grains to 2 mm in diameter, weakly elongate parallel to foliation, and there are discrete lenses of fibrolitic sillimanite (5%) also elongate parallel to the foliation but locally knotted and partially altered to sericite. The pegmatoidal lenses are variously rich in orthoclase or in quartz + sericitised, coarse plagioclase ± biotite (to 3 mm in grainsize) Lenses rich in garnet and biotite also occur within the pegmatoidal zones. Metamorphic grade is upper amphibolite facies.

Locally the gneiss retrogresses to schist, a grey foliated rock with pale lenses and spots. The schist comprises predominantly fine-grained quartz-biotite-plagioclase, with some albite- to sericite-altered plagioclase to 1 mm in grainsize. Lenses of quartzofeldspathic material occur with plagioclase to albite- to sericite-altered 2 mm in grainsize. Large lenses of sericite also occur, locally enclosing residual patches of garnet. Highly contorted lenses of fibrolitic sillimanite are also disseminated, to 6 cm long.

Purvis (1999) interprets the gneiss to be a paragneiss, and suggests a fine-grained sandstone as a possible protolith based on the fine grainsize (up to .05 mm) of the accessory minerals, apatite, zircon and monazite. R.Uppill (in Paterson and Muir 1986) suggests a possible sedimentary precursor could have been a muddy arkosic sandstone, or, alternatively, dacitic or rhyodacitic volcanic rock.

Purvis, 1999.

Mount: Z3931

Description of zircons

The sample contains zircons crystals and crystal fragments ranging between 30 to 200 µm in length (Figure 65). They vary in shape from equant, sub-rounded grains to tabular grains with blunt or rounded terminations with aspect ratios up to 2:1. Many grains exhibit finely pitted surfaces indicative of sedimentary transport. The grains have poor clarity and are light brown in colour due to oxide staining caused by weathering. Brown, hematite-stained cracks are common. Bleb- and rod-shaped clear inclusions and blebby brown inclusions are present in some grains. No cores are visible. Zoning is visible optically in many grains, and cathodoluminescence shows that zoning is ubiquitous, suggesting an initially igneous origin for the detrital grains. There is no evidence of a metamorphic origin for any of the grains.

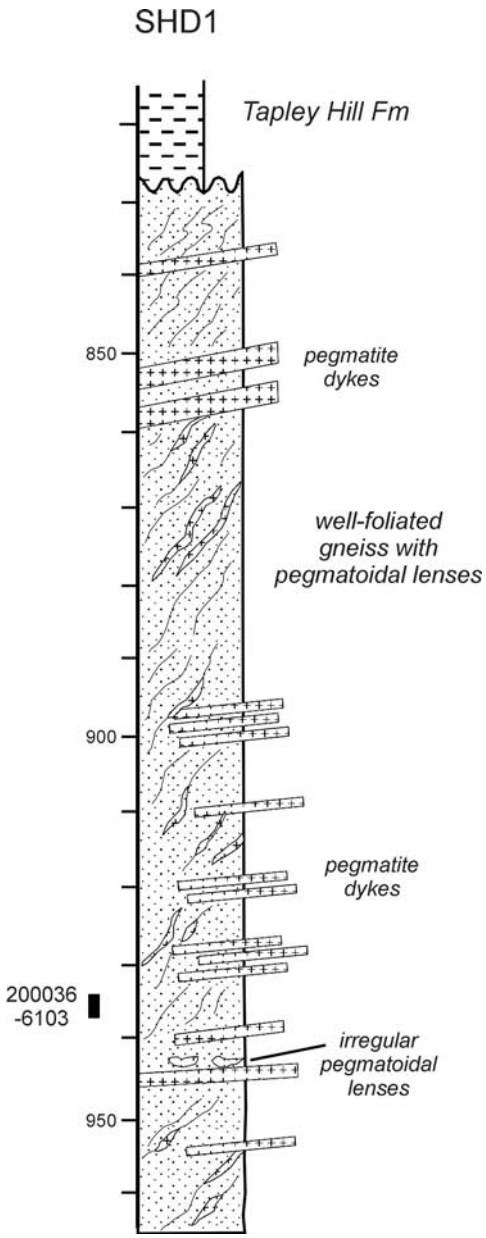

Figure 64. Stratigraphic log for diamond drill hole SHD1, showing the location of sample collected for SHRIMP dating.

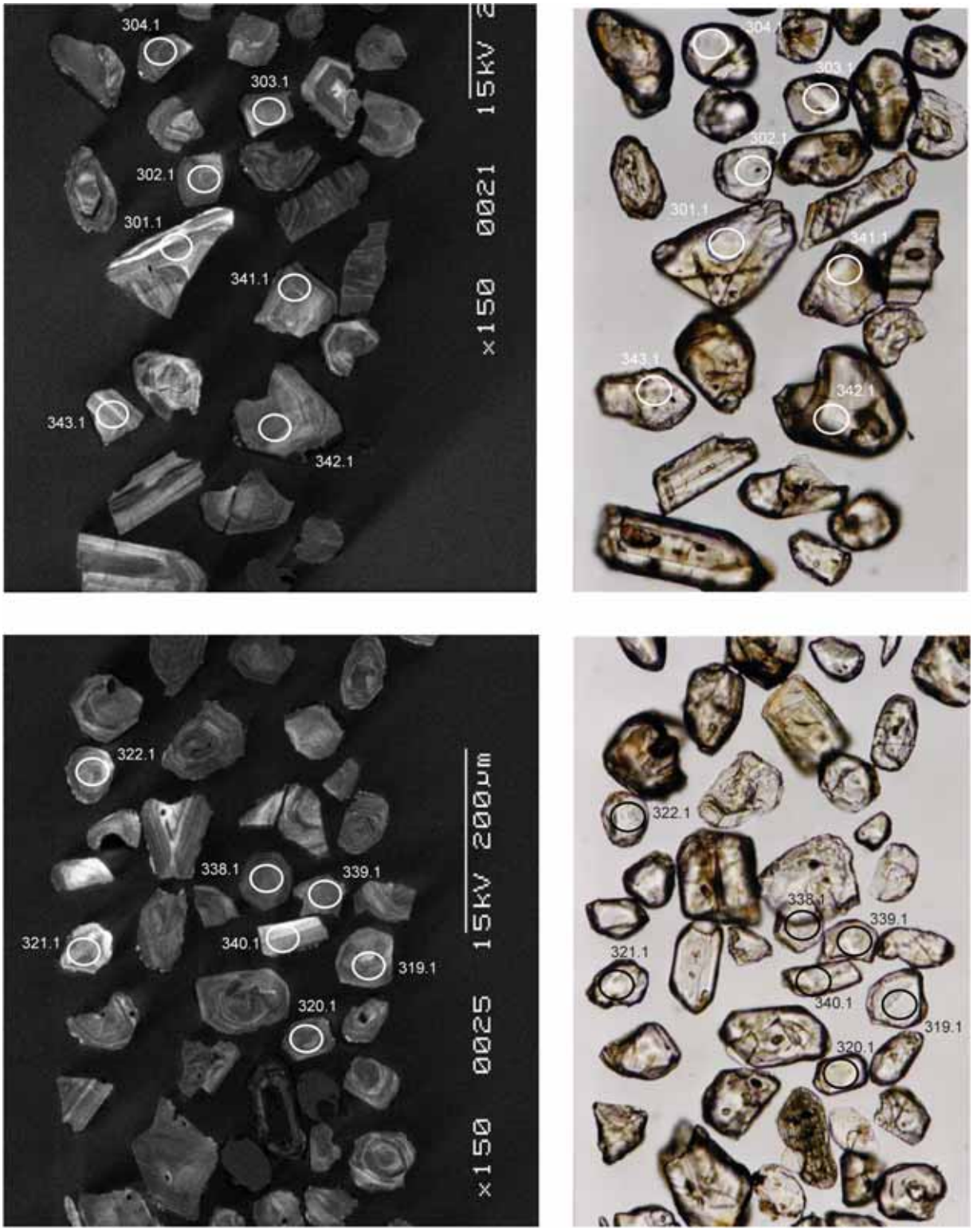

Figure 65. Representative CL (left) and transmitted light (right) images for sample 200036 6103: gneiss, Saddle Hill prospect. SHRIMP analysis spots are labelled. Scale bar is 200 µm.

Session 1: SHRIMP I

Concurrent standard data

Data for the standard are presented in Appendix 3. All $^{206}Pb/^{238}U$ QGNG analyses were included in the calibration, to give a calibration exponent of 1.73, with an upper limit of 2.0 and lower limit of 1.5 (at 95% confidence level). Thus the nominal value of 2.0 has been used in data reduction. The 37 $^{206}Pb/^{238}U$ analyses have a 1σ scatter of 2.64%. Element abundance calibration was based on SL13 (n = 1).

The weighted mean $^{207}Pb/^{206}Pb$ age for all 37 analyses is 1846.3 ± 3.9 Ma (MSWD is 1.5; probability of fit = .024). The analyses are corrected for overcounts at mass ^{204}Pb (after Black in press, calculated assuming $^{\mathbf{206}}Pb/^{238}U$-$^{207}Pb$-$^{235}U$ age concordance), which forces the weighted mean $^{207}Pb/^{206}Pb$ age for QGNG to the TIMS reference value. The recalculated age for QGNG becomes 1851.8 ± 3.5 Ma (MSWD = 1.3; probability of fit = .09; n = 37 of 37). The sample data below are also corrected for overcounts.

Sample data

A total of 51 grains were analysed. Most of the analyses lie on a chord that intersects concordia at *ca* 1750 Ma. Five grains are clearly much older (grains 321, 318, 344, 301 and 326), with ages ranging between *ca* 1800 and 2680 Ma (Figure 66a). The oldest zircon ages represent single-phase grains (as opposed to cores), and as all analyses except one are at least 90% concordant, their $^{207}Pb/^{206}Pb$ compositions should provide reliable age estimates. The exception is analysis 301.1. There appears to be a hiatus between about 2200 and 2700 Ma.

The main cluster of 46 analyses does not conform to a normal distribution (MSWD is 3.1). A probability density distribution of the ages shows the youngest 11 analyses have elevated common ^{206}Pb, and define a tail of Pb loss (Figure 66b). Eight of these analyses are highly discordant (Figure 67). When these analyses are omitted from the age determination, the remaining 35 analyses yield a weighted mean $^{207}Pb/^{206}Pb$ age 1740 ± 6 Ma. When the data are corrected for overcounts at mass ^{204}Pb, the age becomes 1750 ± 6 Ma (MSWD is 2; probability of fit is 0.001). Although the MSWD indicates there is still an unacceptable statistical scatter in the ages, the probability density distribution of the remaining 35 analyses appears normal (Figure 66b), and there are no other obvious statistical outliers, and no geological reason to discard any other analyses. The mixture modelling algorithm of Sambridge and Compston (1994) applied to the data subset calculates the age of this component of the dataset to be 1753 ± 7 Ma (Figure 66b), which agrees well with the above weighted mean age calculation.

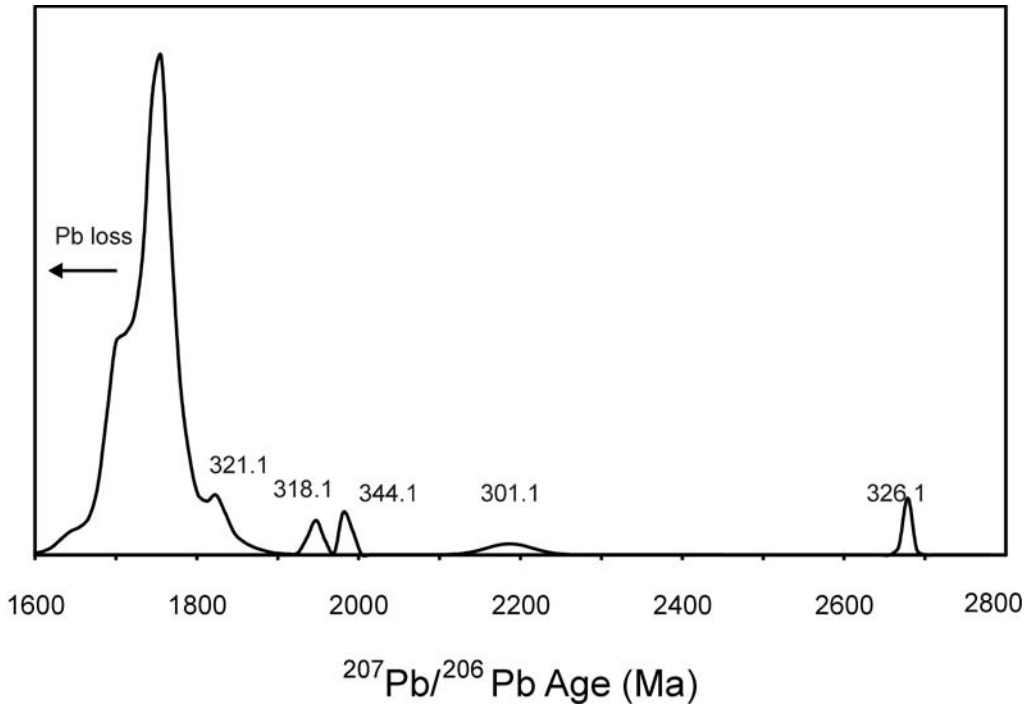

Figure 66a. Probability density distribution of $^{207}Pb/^{206}Pb$ ages illustrating the full range of zircon ages (session 1).

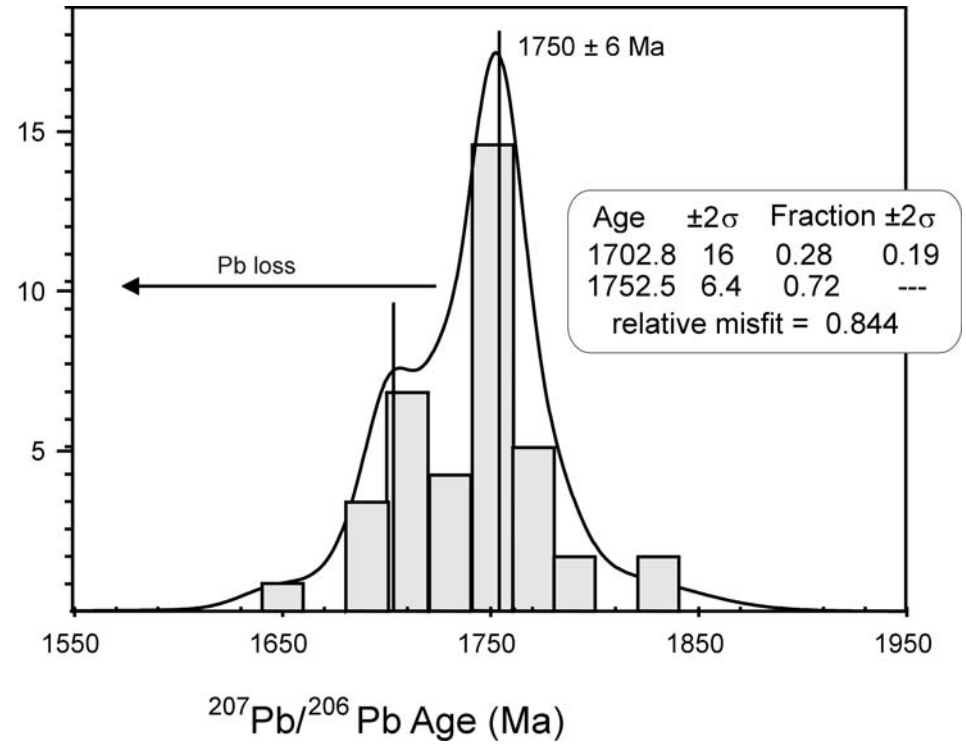

*Figure 66b. Probability density distribution of the main data group showing a tail that reflects the discordance and/or high common ^{206}**Pb** of the youngest analyses. Ages in the text box are calculated using the mixture modelling algorithm of Sambridge and Compston (1994), assuming two components within the dataset.*

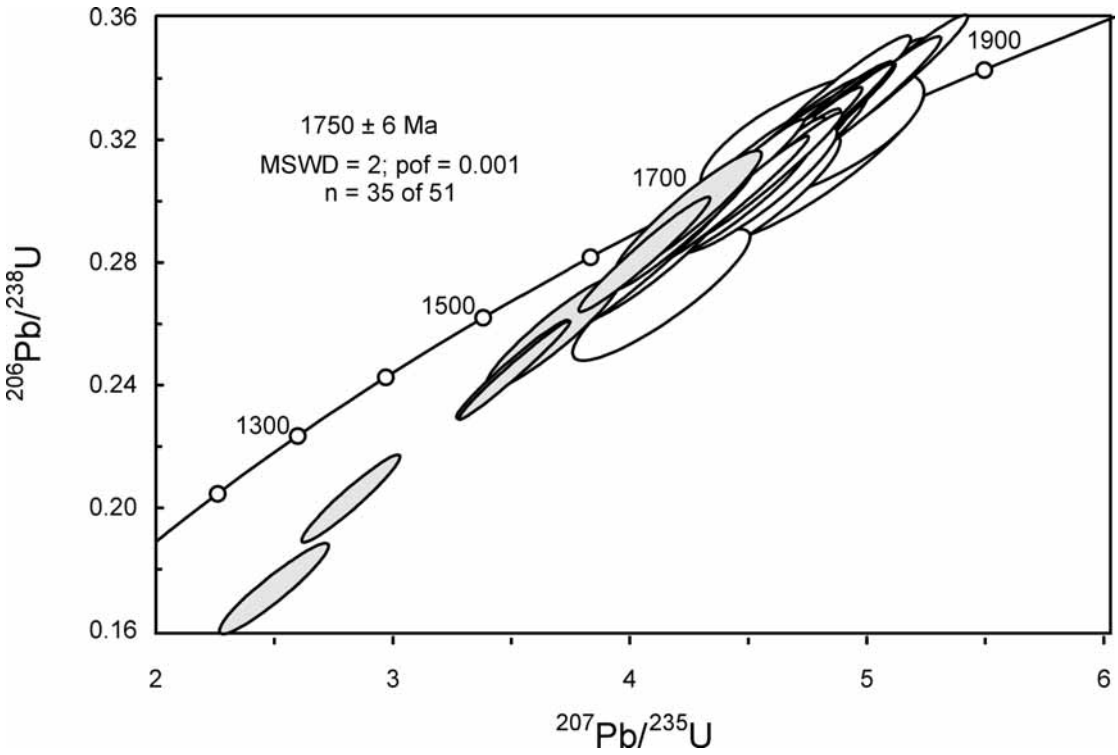

Figure 67. Concordia plot for zircons in sample 200036 6103. White-filled symbols represent analyses used in the weighted mean age calculation. Discordant and/or high common Pb analyses are light grey.

Session 2: SHRIMP IIA

Sample 200036 6103 was re-analysed in January 2005 on SHRIMP II (A) at Curtin University in Perth, in order to test whether the youngest analyses collected during the SHRIMP I session could be recording a 'real' geological event at ~1700 Ma, or if it is more likely that they represent radiogenic Pb loss within ~1750 Ma grains. Where possible, the grains yielding the youngest analyses in session 1 were re-analysed (some grains had been subsequently destroyed through laser ablation and could not be re-analysed).

Concurrent standard data

Data for the standard are presented in Appendix 3. No data were excluded from the Pb/U calibration, to give a calibration exponent of 2.00, with a lower limit of 1.85 and an upper limit of 2.09 (at the 95% confidence level). Thus the nominal value of 2.0 has been used in data reduction. There are three outliers in $^{206}Pb/^{238}U$ (Q.1, Q7.1 and Q52.1) and these have been omitted, leaving 49 analyses with a 1σ scatter in $^{206}Pb/^{238}U$ of 1.28%. The 52 analyses yield a weighted mean $^{207}Pb/^{206}Pb$ age of 1850.9 ± 2.5 Ma (MSWD = 1.4; probability of fit = 0.026). The slightly high MSWD indicates a slight scatter beyond that predicted by counting statistics alone. One grain (Q34) is younger than the others and has higher common ^{206}Pb, suggesting Pb loss may have occurred. When analysis Q34.1 is eliminated from the data set, the remaining 51 analyses yield an age of 1851.2 ± 2.4 Ma (MSWD = 1.2; probability of fit = 0.14).

The analyses are corrected for overcounts at mass ^{204}Pb (after Black in press, calculated assuming ^{206}Pb/^{238}U-^{207}Pb-^{235}U age concordance), which forces the weighted mean ^{207}Pb/^{206}Pb age for QGNG to the TIMS reference value. The sample data for session 2 are also corrected for overcounts.

Element abundance calibration was based on SL13 (n = 2).

Sample data

Forty six new analyses of sample 200036 6103 were obtained in session 2 (Figure 68a), resulting in a total of 97 analyses obtained over the two sessions.

Four analyses are notably younger than the main group at ~1750 Ma (353.1, 367.1, 372.1 and 345.2). The analyses are discordant (Figure 69), with high common Pb and/or U, and define a tail of Pb loss on a Probability density curve (Figure 68a). These analyses are not included in the weighted mean age calculations below.

Three grains (385, 377 and 376) are clearly older than the bulk of the analyses (Figure 68a) and are also excluded from the following calculations. A probability density distribution of the remaining 39 analyses shows a distinctive double peak, indicating two age components within the group (Figure 68b). The mixture modelling algorithm of Sambridge and Compston (1994) applied to the uncorrected data subset calculates the two components to be 1746.8 ± 3.4 Ma and 1783 ± 8 Ma. When the data are corrected for overcounts at mass ^{204}Pb, the algorithm yields near-identical ages of 1748.9 ± 3.3 Ma and 1784 ± 8 Ma.

Geochronological interpretation

Nine of the 16 grains that gave apparent ages younger than 1720 Ma in session 1 were re-analysed in session 2. Eight of the duplicated analyses fall within the main population at *ca* 1750 Ma, and in each case, the analysis is more precise. The only exception (grain 345) yields a more discordant analysis, with high common Pb. This result strongly suggests that the cluster of *ca* 1700 Ma ages obtained in session 1 reflects discordance caused by non-recent radiogenic Pb loss, rather than a younger age population in the gneiss.

The age of 1748.9 ± 3.3 Ma accords with 1750 ± 6 Ma obtained in the first SHRIMP I session. As the SHRIMP II age is more precise, 1748.6 ± 3.3 Ma is taken to be the crystallisation age of the youngest population of grains in the sample, and the maximum age of deposition of the paragneiss protolith. The spread of ages suggests a multiple source region with components as old as 2700 Ma, including a source *ca* 1780 Ma old, delineated in session 2, but not session 1. The analyses measured on SHRIMP I are less precise than those measured in session 2 on SHRIMP II (A), which may explain why the *ca* 1780 Ma grains could not be distinguished from the 1750 Ma population in session 1.

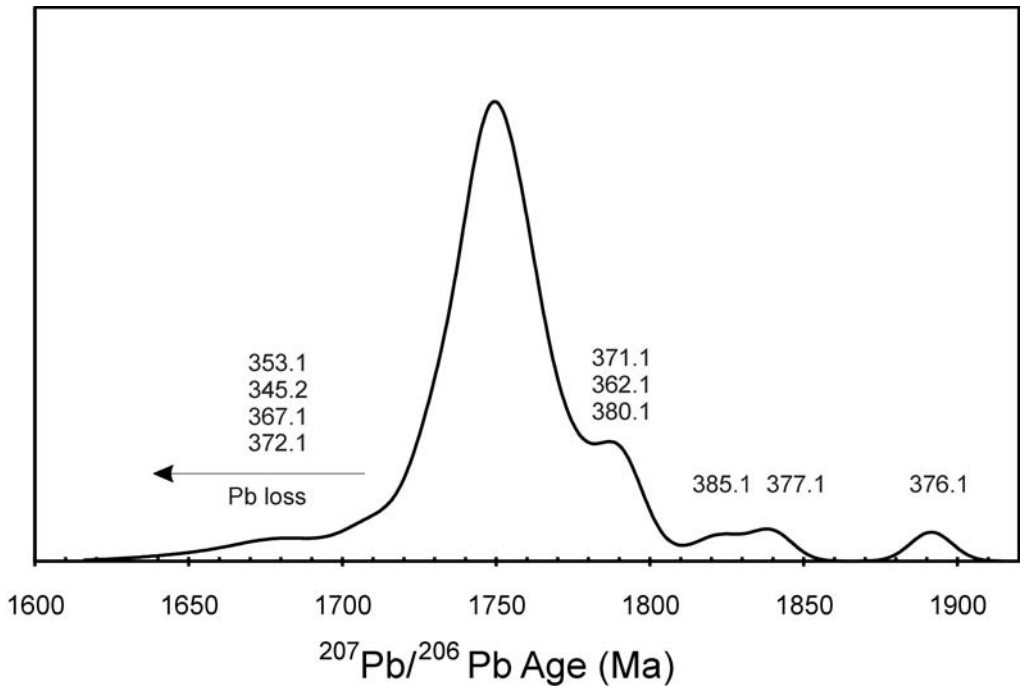

Figure 68a. Probability density distribution of $^{207}Pb/^{206}Pb$ ages illustrating the full range of zircon ages (session 1).

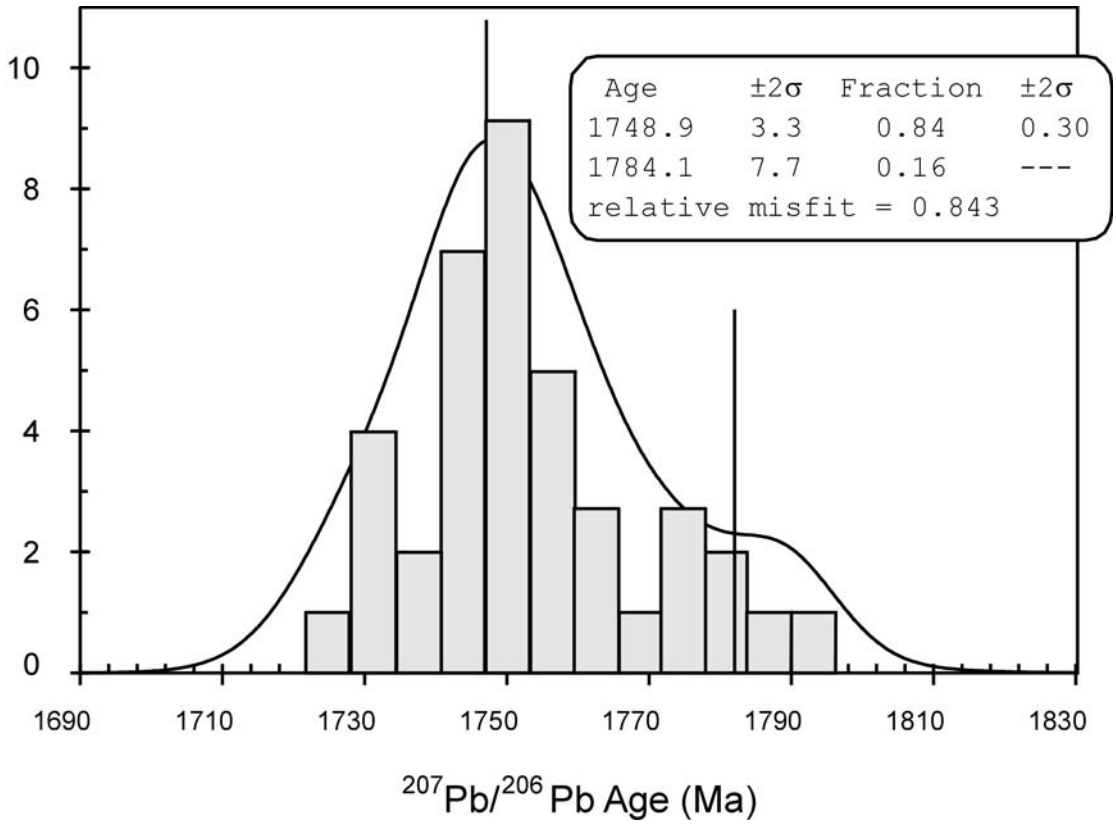

Figure 68b. Probability density distribution of the main data group. The mixture modelling algorithm of Sambridge and Compston (1994) calculates the above ages, assuming two components within the dataset.

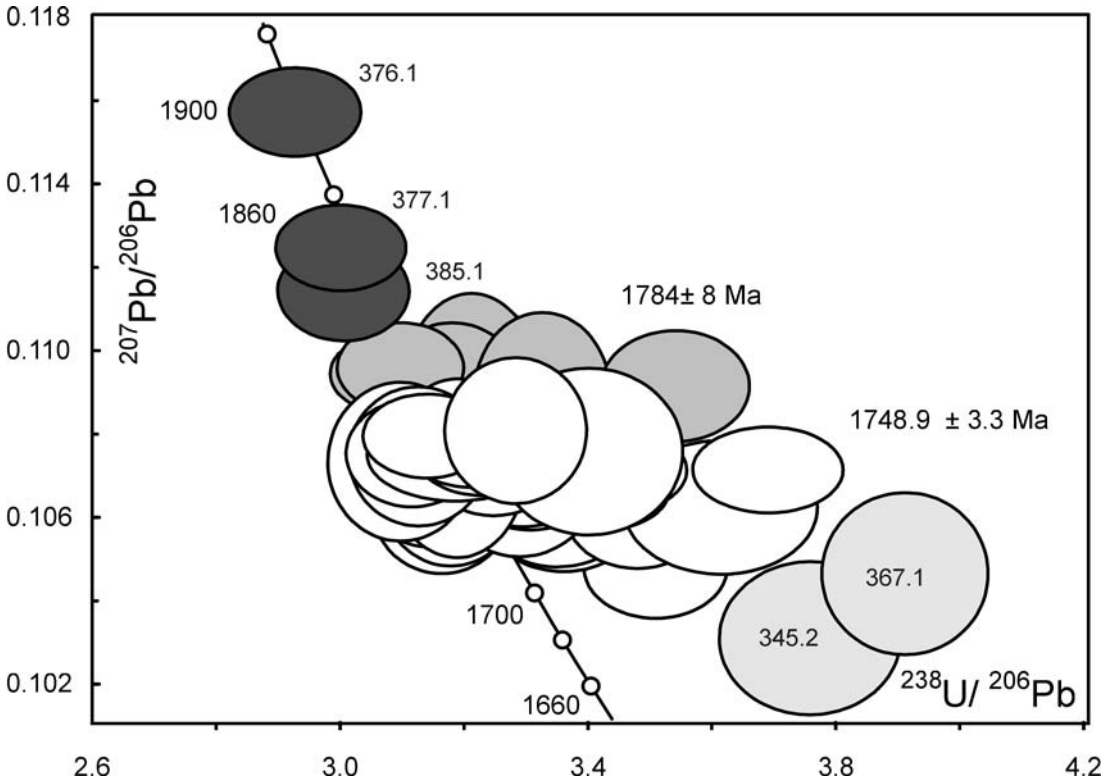

Figure 69. Concordia plot for zircons in sample 200036 6103 (session 2). The two main populations are represented by grey (1784 Ma) and white (1749 Ma) error ellipses. Discordant analyses are light grey. Older grains are black.

Table 19. SHRIMP analytical results for zircon from sample 200036 6103.

Spot	U (ppm)	Th (ppm)	$^{206}Pb_c$ (%)	$^{206}Pb^*$ (ppm)	$^{206}Pb^*/^{238}U$	±	$^{207}Pb^*/^{235}U$	±	$^{207}Pb^*/^{206}Pb^*$	±	conc (%)	207Pb/206Pb Age(Ma)	±
Session 1: analysis date 26/4/2002; SHRIMP I													
301.1	222	108	1.44	49	0.254	0.007	4.78	0.15	0.1367	0.0022	67	2185	28
302.1	187	145	0.12	51	0.319	0.009	4.67	0.14	0.1063	0.0009	103	1736	16
303.1	130	105	-0.08	34	0.309	0.009	4.59	0.14	0.1078	0.0012	98	1762	21
304.1	230	44	0.27	59	0.296	0.008	4.25	0.13	0.1041	0.0010	99	1698	19
305.1	161	141	-0.17	41	0.299	0.009	4.50	0.16	0.1091	0.0019	95	1784	31
306.1	121	79	0.46	33	0.313	0.010	4.81	0.18	0.1114	0.0019	96	1822	31
307.1	368	163	0.19	89	0.281	0.008	4.11	0.13	0.1060	0.0012	92	1732	21
308.1	240	65	-0.14	56	0.269	0.009	4.14	0.15	0.1114	0.0019	84	1823	32
309.1	194	87	0.08	55	0.331	0.009	4.97	0.14	0.1088	0.0008	104	1780	13
310.1	171	99	0.03	50	0.338	0.009	5.08	0.14	0.1090	0.0007	105	1783	12
311.1	232	63	-0.07	64	0.324	0.009	4.77	0.13	0.1069	0.0007	103	1747	12
312.1	271	75	0.02	71	0.307	0.009	4.52	0.13	0.1068	0.0006	99	1745	10
313.1	107	78	-0.02	29	0.309	0.009	4.60	0.13	0.1079	0.0009	98	1765	15
314.1	110	60	0.02	31	0.331	0.009	4.84	0.14	0.1061	0.0009	106	1734	15
315.1	170	67	0.12	43	0.297	0.008	4.31	0.13	0.1052	0.0012	98	1718	20
316.1	201	58	-0.03	55	0.321	0.009	4.74	0.13	0.1073	0.0007	102	1754	12
317.1	226	71	-0.03	62	0.320	0.009	4.73	0.13	0.1073	0.0007	102	1754	12
318.1	256	188	-0.02	77	0.351	0.009	5.78	0.16	0.1194	0.0006	100	1947	9

Spot	U (ppm)	Th (ppm)	$^{206}Pb_c$ (%)	$^{206}Pb^*$ (ppm)	$^{206}Pb^*/^{238}U$	±	$^{207}Pb^*/^{235}U$	±	$^{207}Pb^*/^{206}Pb^*$	±	conc (%)	207Pb/206Pb Age(Ma)	±
Session 1: analysis date 26/4/2002; SHRIMP I													
319.1	171	61	-0.03	48	0.324	0.009	4.79	0.13	0.1072	0.0006	103	1752	9
320.1	239	63	-0.04	62	0.301	0.008	4.45	0.13	0.1072	0.0013	97	1753	21
321.1	128	60	-0.03	37	0.335	0.009	5.15	0.14	0.1115	0.0006	102	1824	10
322.1	143	67	-0.07	40	0.324	0.009	4.80	0.13	0.1076	0.0006	103	1759	11
323.1	273	67	0.49	68	0.290	0.008	4.14	0.12	0.1035	0.0010	97	1687	17
324.1	189	174	-0.04	51	0.316	0.009	4.66	0.13	0.1071	0.0006	101	1751	11
325.1	184	89	0.01	51	0.319	0.009	4.73	0.14	0.1076	0.0006	101	1759	11
326.1	358	126	0.00	146	0.477	0.014	12.01	0.35	0.1828	0.0006	94	2678	5
327.1	300	110	0.26	63	0.245	0.007	3.51	0.09	0.1039	0.0006	83	1696	11
328.1	190	84	0.36	52	0.316	0.009	4.67	0.14	0.1072	0.0013	101	1752	22
329.1	71	50	0.06	20	0.329	0.010	4.88	0.15	0.1076	0.0008	104	1760	14
330.1	103	107	-0.09	28	0.321	0.009	4.77	0.19	0.1079	0.0031	102	1765	54
331.1	203	135	0.02	56	0.323	0.009	4.79	0.13	0.1075	0.0005	103	1758	9
332.1	341	107	0.12	72	0.245	0.007	3.52	0.09	0.1042	0.0005	83	1701	9
333.1	213	65	0.05	55	0.301	0.008	4.46	0.12	0.1074	0.0005	97	1755	9
334.1	149	149	0.02	40	0.309	0.009	4.58	0.13	0.1073	0.0007	99	1754	12
335.1	213	80	-0.05	56	0.304	0.009	4.55	0.14	0.1085	0.0013	96	1775	23
336.1	149	91	0.13	37	0.291	0.008	4.23	0.12	0.1057	0.0007	95	1726	12
337.1	118	100	0.24	31	0.306	0.009	4.42	0.13	0.1048	0.0009	101	1711	15
338.1	274	80	0.08	72	0.307	0.009	4.47	0.13	0.1058	0.0005	100	1728	8
339.1	181	64	0.10	48	0.306	0.008	4.44	0.12	0.1051	0.0006	100	1716	11
340.1	157	80	0.59	24	0.174	0.006	2.51	0.09	0.1049	0.0014	60	1712	23
341.1	355	303	7.79	131	0.397	0.015	4.40	1.54	0.0810	0.0284	179	1220	690
342.1	277	147	0.02	67	0.280	0.008	4.11	0.12	0.1067	0.0004	91	1743	7
343.1	102	87	0.15	28	0.314	0.010	4.64	0.14	0.1072	0.0008	100	1753	14
344.1	306	287	0.01	93	0.354	0.010	5.96	0.16	0.1220	0.0004	98	1985	6
345.1	142	67	0.14	35	0.283	0.008	4.07	0.11	0.1044	0.0007	94	1703	12
346.1	195	78	2.01	18	0.106	0.007	1.53	0.12	0.1051	0.0044	38	1717	77
347.1	236	86	0.57	61	0.297	0.008	4.27	0.12	0.1042	0.0009	99	1700	16
348.1	329	55	0.72	73	0.257	0.007	3.68	0.11	0.1040	0.0012	87	1697	21
349.1	90	76	-0.03	24	0.309	0.009	4.55	0.13	0.10673	0.0007	100	1744	12
350.1	385	211	0.62	68	0.203	0.006	2.83	0.08	0.1012	0.0009	72	1646	16
351.1	152	94	0.11	40	0.308	0.008	4.59	0.13	0.1080	0.0006	98	1766	11
Session 2: analysis date 20/1/2005; SHRIMP IIA													
307.2	389	150	0.03	102	0.304	0.014	4.48	0.07	0.10679	0.00049	98	1745	8
314.2	174	119	0.00	46	0.304	0.014	4.48	0.07	0.10702	0.00051	98	1749	9
334.2	114	80	-0.07	30	0.305	0.014	4.54	0.07	0.10808	0.00071	97	1767	12
336.2	148	98	-0.03	41	0.318	0.014	4.68	0.07	0.10668	0.00058	102	1743	10
337.2	136	96	0.09	37	0.314	0.014	4.64	0.07	0.10717	0.00088	100	1752	15
339.2	207	62	-0.03	56	0.316	0.015	4.66	0.07	0.10703	0.00050	101	1750	9
340.2	96	54	0.11	18	0.220	0.018	3.28	0.07	0.10840	0.00119	72	1773	20
345.2	196	114	0.24	45	0.266	0.016	3.78	0.07	0.10308	0.00075	91	1680	13
346.2	76	75	0.01	21	0.323	0.016	4.78	0.08	0.10733	0.00078	103	1755	13

Spot	U (ppm)	Th (ppm)	$^{206}Pb_c$ (%)	$^{206}Pb^*$ (ppm)	$^{206}Pb^*/^{238}U$	±	$^{207}Pb^*/^{235}U$	±	$^{207}Pb^*/^{206}Pb^*$	±	conc (%)	207Pb/206Pb Age(Ma)	±
Session 2: analysis date 20/1/2005; SHRIMP IIA													
347.2	248	77	0.00	66	0.309	0.014	4.55	0.06	0.10683	0.00043	99	1746	7
352.1	220	48	0.10	53	0.277	0.018	4.06	0.08	0.10623	0.00066	90	1736	11
353.1	343	128	0.63	59	0.198	0.015	2.79	0.06	0.10210	0.00123	70	1662	23
354.1	210	119	-0.01	53	0.294	0.018	4.36	0.09	0.10757	0.00082	95	1759	14
355.1	138	115	0.08	36	0.304	0.016	4.49	0.08	0.10709	0.00084	98	1751	14
356.1	117	73	-0.05	32	0.320	0.015	4.74	0.08	0.10746	0.00069	102	1757	12
357.1	340	100	0.03	79	0.271	0.013	4.01	0.06	0.10713	0.00042	88	1751	7
358.1	158	110	0.01	41	0.303	0.014	4.46	0.07	0.10699	0.00053	97	1749	9
359.1	188	134	-0.04	52	0.320	0.015	4.73	0.07	0.10715	0.00050	102	1752	9
360.1	323	49	0.20	84	0.301	0.014	4.52	0.07	0.10890	0.00083	95	1781	14
361.1	215	129	0.09	53	0.288	0.014	4.21	0.06	0.10610	0.00054	94	1733	9
362.1	286	179	-0.05	80	0.324	0.013	4.90	0.07	0.10944	0.00039	101	1790	7
363.1	324	104	0.04	82	0.293	0.013	4.30	0.06	0.10663	0.00039	95	1743	7
365.1	339	132	0.02	91	0.312	0.013	4.60	0.06	0.10687	0.00037	100	1747	6
366.1	218	124	0.05	59	0.315	0.015	4.72	0.08	0.10877	0.00078	99	1779	13
367.1	152	86	0.17	34	0.256	0.014	3.69	0.06	0.10463	0.00080	86	1708	14
368.1	250	67	0.00	62	0.290	0.014	4.29	0.06	0.10713	0.00042	94	1751	7
369.1	290	67	0.02	78	0.312	0.013	4.63	0.06	0.10771	0.00041	99	1761	7
370.1	154	122	-0.01	41	0.312	0.015	4.67	0.08	0.10870	0.00109	98	1778	18
371.1	219	71	0.01	53	0.283	0.014	4.25	0.06	0.10914	0.00055	90	1785	9
372.1	400	173	0.10	98	0.285	0.013	4.12	0.06	0.10479	0.00050	95	1711	9
373.1	132	61	0.10	36	0.315	0.014	4.63	0.07	0.10655	0.00070	101	1741	12
374.1	214	142	0.04	57	0.312	0.015	4.57	0.07	0.10636	0.00046	101	1738	8
375.1	160	110	-0.03	44	0.321	0.014	4.76	0.07	0.10753	0.00053	102	1758	9
376.1	231	109	0.00	68	0.342	0.015	5.46	0.08	0.11574	0.00044	100	1892	7
377.1	264	121	-0.03	76	0.334	0.014	5.17	0.08	0.11247	0.00043	101	1840	7
378.1	229	113	-0.03	63	0.319	0.014	4.77	0.07	0.10843	0.00043	101	1773	7
379.1	191	86	-0.04	51	0.314	0.018	4.66	0.09	0.10750	0.00045	100	1758	8
380.1	247	163	-0.04	69	0.323	0.014	4.88	0.07	0.10960	0.00044	101	1793	7
381.1	146	141	0.02	39	0.308	0.014	4.56	0.07	0.10732	0.00053	99	1754	9
382.1	241	66	-0.04	64	0.310	0.014	4.59	0.07	0.10751	0.00041	99	1758	7
383.1	265	67	0.05	68	0.298	0.013	4.34	0.06	0.10579	0.00045	97	1728	8
384.1	268	79	0.06	69	0.299	0.013	4.36	0.06	0.10589	0.00044	97	1730	8
385.1	316	193	-0.07	90	0.333	0.014	5.12	0.08	0.11143	0.00049	102	1823	8
386.1	121	38	0.13	33	0.316	0.014	4.63	0.07	0.10613	0.00060	102	1734	11
387.1	127	61	-0.02	34	0.311	0.017	4.58	0.08	0.10691	0.00053	100	1747	9
388.1	197	112	0.03	54	0.319	0.014	4.74	0.07	0.10794	0.00042	101	1765	7

Data are 1σ precision. All Pb data are common Pb corrected based on measured ^{204}Pb (after Stacey and Kramer 1975).

Part 3: Hiltaba Suite and contemporary mafic rocks

200036 6000: quartz monzonite, Horn Ridge

1:250,000 sheet: Andamooka (SH5312)

1:100,000 sheet: Mattaweara (6237)

AMG: 689740 E 6628312 N

Location: The sample was taken from diamond drillhole HRD1, depth interval 383.3-384.8m. The diamond drillhole is located within the Horn Ridge prospect, near Olympic Dam.

Description: The sample is an equigranular, medium- to coarse-grained quartz monzonite. It contains 32.6% plagioclase, 38.7% alkali feldspar, 16.8% quartz, and 11.9% mafic minerals. Mafics comprise 3.3% amphibole, 1.9% biotite, 1.2% chlorite 3% opaques, 0.4% titanite, 0.2% zircon, 0.4% apatite and trace allanite. Plagioclase occurs as euhedral crystals up to 8 mm in size, exhibiting sericite alteration. Alkali feldspar crystals occur as larger subhedral to euhedral grains, and quartz occurs interstitially. Apatite crystals are typically large and euhedral and occur in clusters with opaque minerals. Zircons are large and have concentric growth zones. Allanite is a late-crystallising, interstitial phase and is always metamict (description and modal analysis from Creaser 1989).

Mount: Z3677

Description of zircons

The zircons from sample 200036 6000 are euhedral grains averaging about 100 μm in length, with blunt to normal pyramidal terminations (Figure 70). Aspect ratios lie mostly between 1.5 to 2:1. Most grains have continuous prismatic zoning, visible optically and/or under cathodoluminescence. None of the grains appear to contain cores. Some grains contain round fluid inclusions or rod-like silicate inclusions. Some contain clear or hematite-stained cracks, which were avoided during analysis.

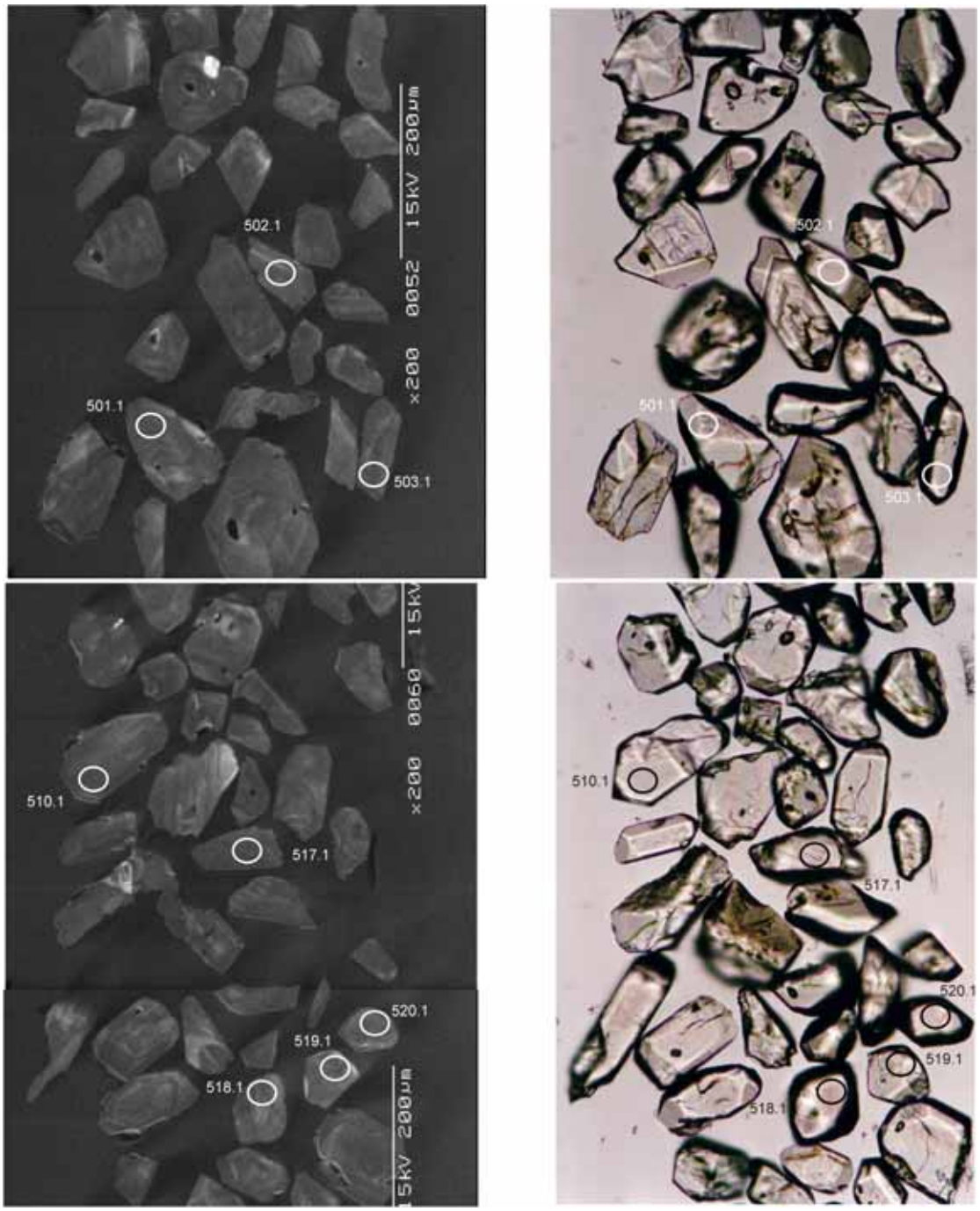

Figure 70. Representative CL (left) and transmitted light (right) images for sample 200036 6000: quartz monzonite, Horn Ridge prospect. SHRIMP analysis spots are labelled. Scale bar is 200 µm.

Concurrent standard data

Z3677 and sample 200036 6029 on mount Z3678 were analysed over the 4 day session. Data for the standard are presented in Appendix 3. Twenty six QGNG analyses for Z3677 give a calibration exponent of 2.08, with an upper limit of 2.26 and lower limit of 1.85 (at 95% confidence level). The weighted mean $^{207}Pb/^{206}Pb$ age for all 26 analyses is 1851.7 ± 2.4 Ma (MSWD = 1.12; probability of fit =0.31). Nine QGNG analyses for Z3678 give a calibration exponent of 2.29 with an upper limit of 2.98 and lower limit of 1.61. The weighted mean $^{207}Pb/^{206}Pb$ age for all 9 analyses is 1848.9 ± 3.5 Ma (MSWD = 1.05; probability of fit = 0.39). Because no significant calibration shift is observed between the two data batches, both have been combined for data processing. This yields a calibration exponent of 2.08, with an upper limit of 2.22 and lower limit of 1.86. Thus the nominal value of 2.0 has been used in data reduction. The $^{206}Pb/^{238}U$ reproducibility for QGNG is 1.34% (1σ; n = 35 of 35). The weighted mean $^{207}Pb/^{206}Pb$ age for all 35 analyses is 1850.7 ± 1.9 (MSWD = 1.09; probability of fit = 0.33).

The analyses are corrected for overcounts at mass ^{204}Pb (after Black in press, calculated assuming $^{206}Pb/^{238}U$-^{207}Pb-^{235}U age concordance), which forces the weighted mean $^{207}Pb/^{206}Pb$ age for QGNG to the TIMS reference value. The recalculated age for QGNG becomes 1851.6 ± 2.2 Ma (MSWD = 1.13; probability of fit = .27; n = 35 of 35). The sample data below are also corrected for overcounts.

Element abundance calibration was based on SL13 (n = 1).

Sample data

Twenty four of the 25 analyses combine to yield a wighted mean crystallisation age of 1593.2 ± 3.4 Ma. When corrected for overcounts at mass ^{204}Pb, the age becomes 1594.4 ± 3.4 Ma (MSWD = 1.26; probability of fit = 0.18; Figure 71). The outlier (525.1) is discordant (Figure 72) and has anomalously high radiogenic ^{204}Pb (Table 20), which would explain the young age (*ca* 1520 Ma) as resulting from non-recent radiogenic Pb loss.

Geochronological interpretation

The $^{207}Pb/^{206}Pb$ age of 1594.4 ± 3.4 Ma is considered to be the crystallisation age of the quartz monzonite.

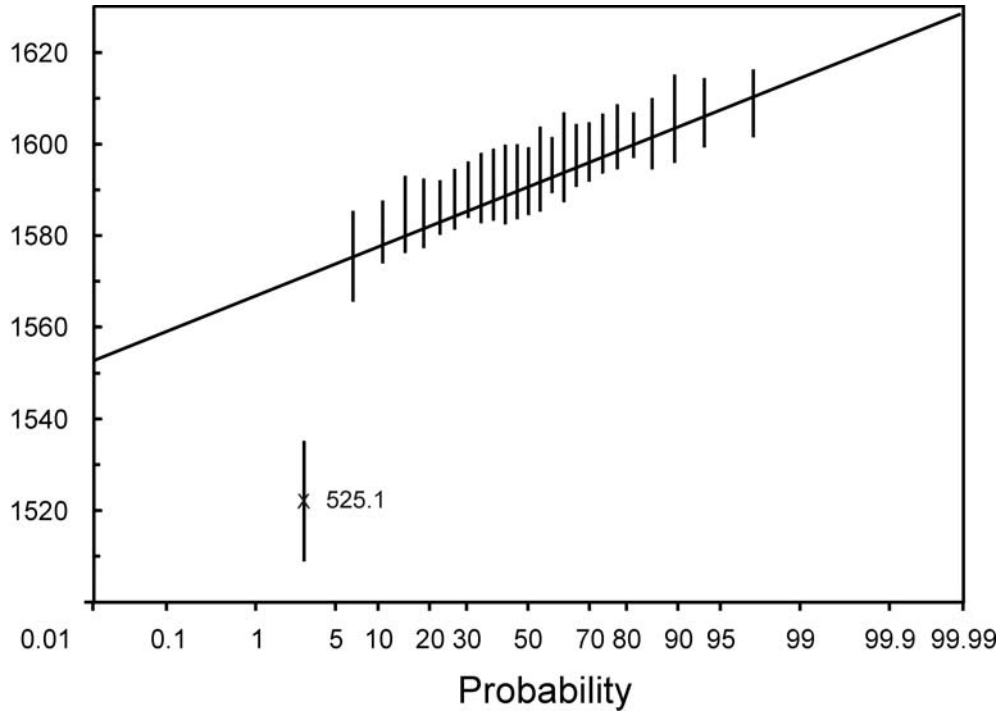

Figure 71. Probability diagram for individual zircon ages for sample 200036 6000. Analysis 5.25 clearly represents an outlier from the main population.

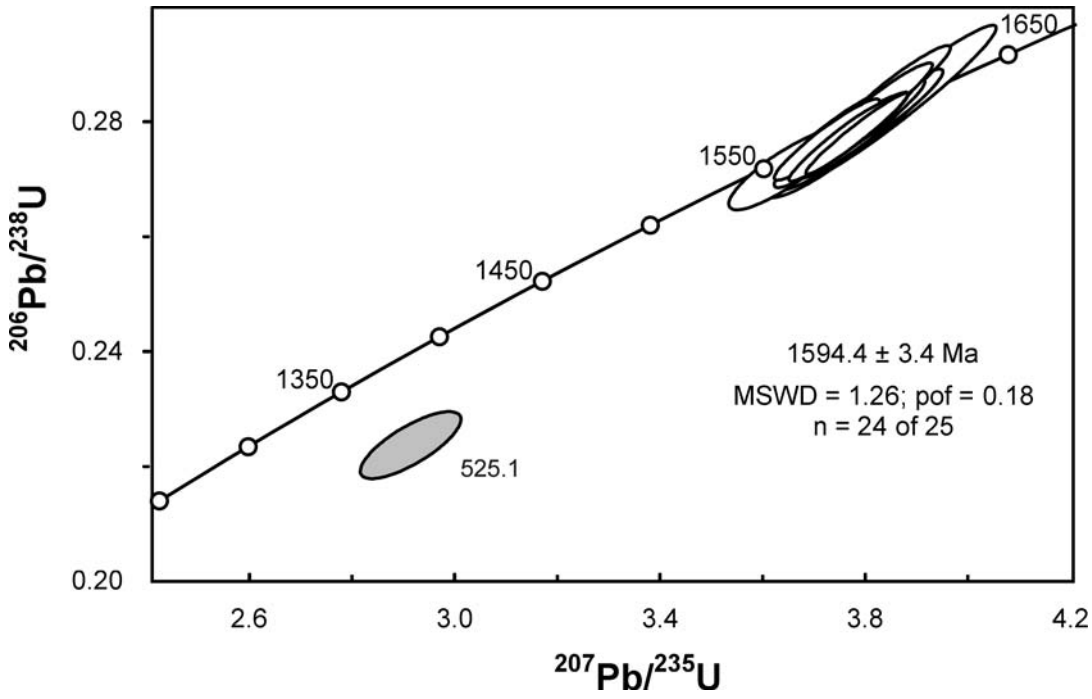

Figure 72. Concordia diagram for zircons in sample 200036 6000 showing radiogenic Pb compositions. White-filled symbols represent analyses used in the weighted mean age calculation. Discordant, high common Pb analysis is light grey.

Table 20. SHRIMP analytical results for zircon from sample 200036 6000.

Spot	U (ppm)	Th (ppm)	$^{206}Pb_c$ (%)	$^{206}Pb^*$ (ppm)	$^{206}Pb^*/^{238}U$	±	$^{207}Pb^*/^{235}U$	±	$^{207}Pb^*/^{206}Pb^*$	±	conc (%)	207Pb/206Pb Age(Ma)	±
501.1	192	137	-0.01	46	0.281	0.004	3.84	0.06	0.09908	0.00040	99	1607	8
502.1	205	144	0.07	49	0.279	0.004	3.78	0.06	0.09825	0.00045	100	1591	9
503.1	273	206	0.00	66	0.282	0.004	3.82	0.05	0.09819	0.00032	101	1590	6
504.1	212	140	0.07	51	0.278	0.004	3.75	0.06	0.09791	0.00044	100	1585	8
505.1	249	177	0.07	60	0.280	0.004	3.79	0.05	0.09829	0.00038	100	1592	7
506.1	194	134	0.02	46	0.278	0.004	3.80	0.06	0.09919	0.00039	98	1609	7
507.1	185	140	0.02	44	0.275	0.004	3.73	0.06	0.09825	0.00041	98	1591	8
508.1	326	259	0.03	77	0.276	0.004	3.75	0.05	0.09847	0.00032	98	1595	6
509.1	440	364	0.00	105	0.277	0.004	3.78	0.05	0.09882	0.00026	99	1602	5
510.1	276	189	-0.01	66	0.278	0.004	3.78	0.05	0.09872	0.00035	99	1600	7
511.1	225	161	0.24	53	0.275	0.004	3.73	0.06	0.09843	0.00048	98	1595	9
512.1	211	170	0.05	50	0.275	0.004	3.71	0.06	0.09792	0.00039	99	1585	8
513.1	218	143	0.06	52	0.279	0.004	3.78	0.06	0.09821	0.00040	100	1590	8
514.1	332	217	0.02	79	0.277	0.004	3.77	0.05	0.09858	0.00035	99	1598	7
515.1	214	205	0.01	52	0.283	0.006	3.86	0.08	0.09901	0.00050	100	1606	10
516.1	273	189	0.05	64	0.274	0.004	3.72	0.06	0.09856	0.00051	98	1597	10
517.1	278	215	0.06	66	0.276	0.004	3.72	0.05	0.09771	0.00035	99	1581	7
518.1	238	252	0.00	58	0.285	0.004	3.86	0.05	0.09808	0.00034	102	1588	7
519.1	231	206	-0.03	56	0.280	0.004	3.81	0.05	0.09880	0.00038	99	1602	7
520.1	196	148	0.02	47	0.278	0.004	3.76	0.06	0.09828	0.00042	99	1592	8
521.1	319	252	0.00	77	0.282	0.004	3.81	0.05	0.09799	0.00030	101	1586	6
522.1	284	222	0.04	68	0.277	0.004	3.77	0.06	0.09862	0.00034	99	1598	6
523.1	242	177	0.28	57	0.271	0.004	3.64	0.05	0.09743	0.00052	98	1575	10
524.1	260	166	0.11	62	0.277	0.004	3.77	0.06	0.09884	0.00041	98	1602	8
525.1	287	124	0.48	55	0.223	0.003	2.92	0.05	0.09470	0.00065	85	1522	13

Data are 1σ precision. All Pb data are common Pb corrected based on measured ^{204}Pb (after Stacey and Kramer 1975).
Analysis date 8/4/2001; SHRIMP II

200036 6006: monzodiorite, Snake Gully

1:250,000 sheet: Andamooka (SH5312)

1:100,000 sheet: Yarrawurta (6337)

AMG: 701560 E 6637500 N

Location: The sample was taken from diamond drillhole SGD5, depth interval 780-785 m. The diamond drillhole is located within the Snake Gully prospect northeast of Olympic Dam (Figure 5).

Description: The sample is albitised and undeformed. It varies from fine grained and equigranular in the upper parts of the drillhole, to medium grained and porphyritic at the base. It contains about 75% probable albite to 2 mm in grainsize and 12-13% interstitial quartz + granophyre, with albitised possible K-feldspar. Some of the albite has a checkerboard pattern and may have replaced K-feldspar, partly as independent laths and partly as rims on plagioclase. Calcite and chlorite are disseminated as interstitial patches to 2 mm in diameter (8%). Ilmenite plates to 1.5 mm long are disseminated as well as minor titanite or anatase to 0.5 mm in grainsize and disseminated probable magnetite and apatite (4%). There is possibly trace zircon to 0.05 mm in grainsize, but this is clouded and fractured and difficult to distinguish from fine-grained anatase. The original lithology seems to have been a quartz microdiorite or micromonzodiorite, depending on the original K-feldspar content.

(Purvis 2003, Creaser 1989)

Mount: Z3677

Description of zircons

Sample 200036 6006, from an undeformed, medium-grained, equigranular granite from drill hole SGD5, yielded only 8 zircons. Six of these produce an incoherent suite of ages with variable degrees of discordance (Table 21). The large grains (100-200 μm) are igneous in character. Most are broken grain fragments. The whole grains are elongate, with blunt to sharp terminations. All reveal internal zoning under cathodoluminescence (Figure 73).

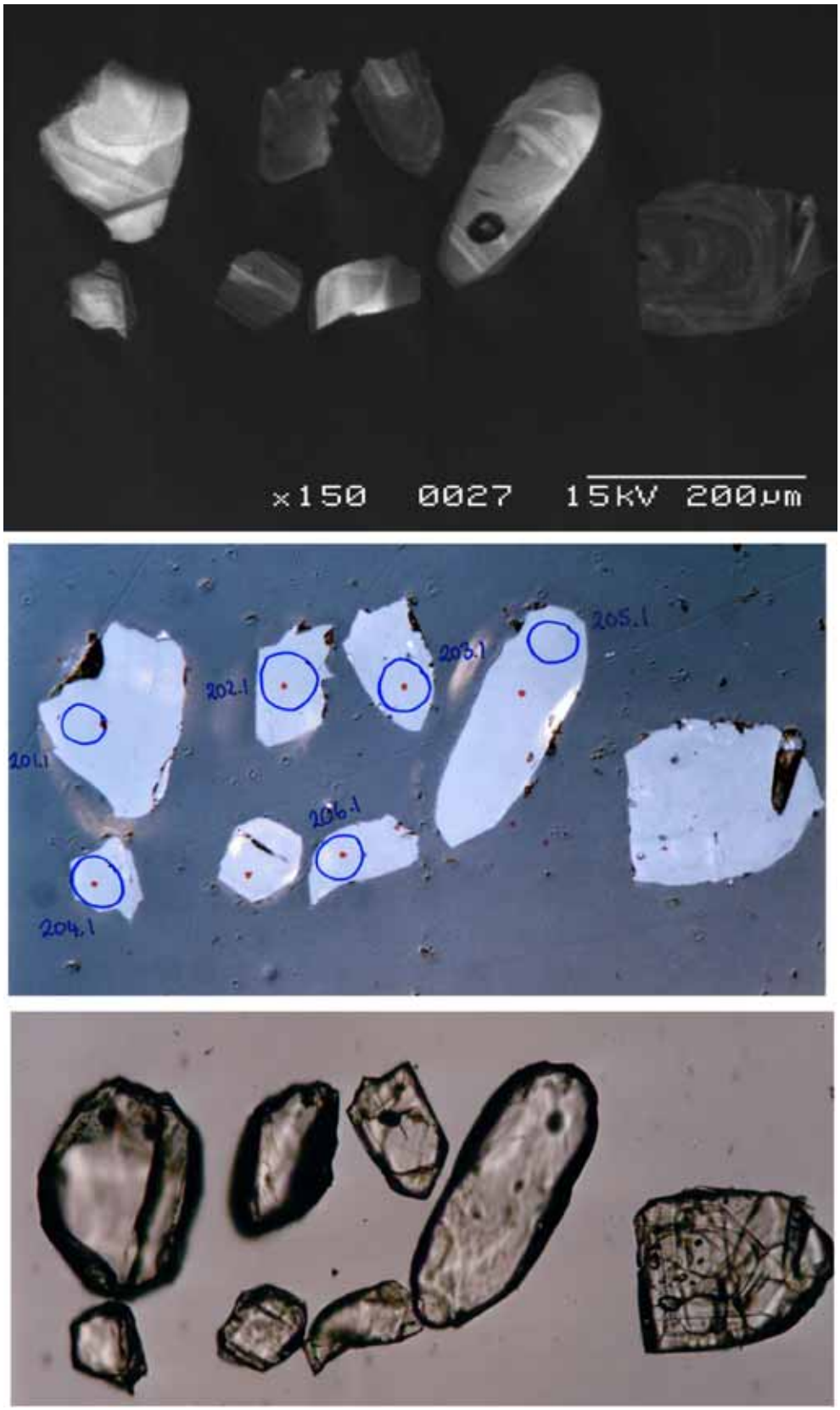

Figure 73. Representative CL (left) and transmitted light (right) images for sample 200036 6006: monzodiorite, Snake Gully prospect (SGD5). SHRIMP analysis spots are labelled. Scale bar is 200 µm.

Concurrent standard data

Z3677 and sample 200036 6029 on mount Z3678 were analysed over the 4 day session. Data for the standard are presented in Appendix 3. Twenty six QGNG analyses for Z3677 give a calibration exponent of 2.08, with an upper limit of 2.26 and lower limit of 1.85 (at 95% confidence level). The weighted mean $^{207}Pb/^{206}Pb$ age for all 26 analyses is 1851.7 ± 2.4 Ma (MSWD = 1.12; probability of fit =0.31). Nine QGNG analyses for Z3678 give a calibration exponent of 2.29 with an upper limit of 2.98 and lower limit of 1.61. The weighted mean $^{207}Pb/^{206}Pb$ age for all 9 analyses is 1848.9 ± 3.5 Ma (MSWD = 1.05; probability of fit = 0.39). Because no significant calibration shift is observed between the two data batches, both have been combined for data processing. This yields a calibration exponent of 2.08, with an upper limit of 2.22 and lower limit of 1.86. Thus the nominal value of 2.0 has been used in data reduction. The $^{206}Pb/^{238}U$ reproducibility for QGNG is 1.34% (1σ; n = 35 of 35). The weighted mean $^{207}Pb/^{206}Pb$ age for all 35 analyses is 1850.7 ± 1.9 (MSWD = 1.09; probability of fit = 0.33).

The analyses are corrected for overcounts at mass ^{204}Pb (after Black in press, calculated assuming $^{206}Pb/^{238}U$-^{207}Pb-^{235}U age concordance), which forces the weighted mean $^{207}Pb/^{206}Pb$ age for QGNG to the TIMS reference value. The recalculated age for QGNG becomes 1851.6 ± 2.2 Ma (MSWD = 1.13; probability of fit = .27; n = 35 of 35). The sample data below are also corrected for overcounts.

Element abundance calibration was based on SL13 (n = 1).

Sample data

Two grains contain high common Pb (Table 21) and are highly discordant, with 1σ errors of 100 Ma. Two analyses (202.1 and 205.1) yielded near-concordant ages of about 1600 Ma (Figure 74). The remaining two analyses yield older ages of about 1770 Ma.

Geochronological interpretation

It is impossible to extract a crystallisation age for the granite from this limited dataset. The low zircon yield and the isotopic inhomogeneity of the grains suggest they are inherited, and that the granite did not crystallise zircon. Foliated megacrystic granite, similar in character to the *ca* 1854 Ma granite in SGD4, occurs at the top of SGD5, and as clasts within the medium-grained granite near its top contact (Figure 5). These features indicate that the undeformed granite intrudes *ca* 1850 Ma basement. The most likely interpretation of the data is that the 1600 Ma grains provide a maximum age for the granite, suggesting it is a member of the Hiltaba Suite, as suggested by Creaser (1989). The *ca* 1765 Ma grains suggest that basement material of this age may also occur within the Snake Gully prospect area. This is supported by the presence of similar-aged grains in sample 200036 6008 (see Part 2).

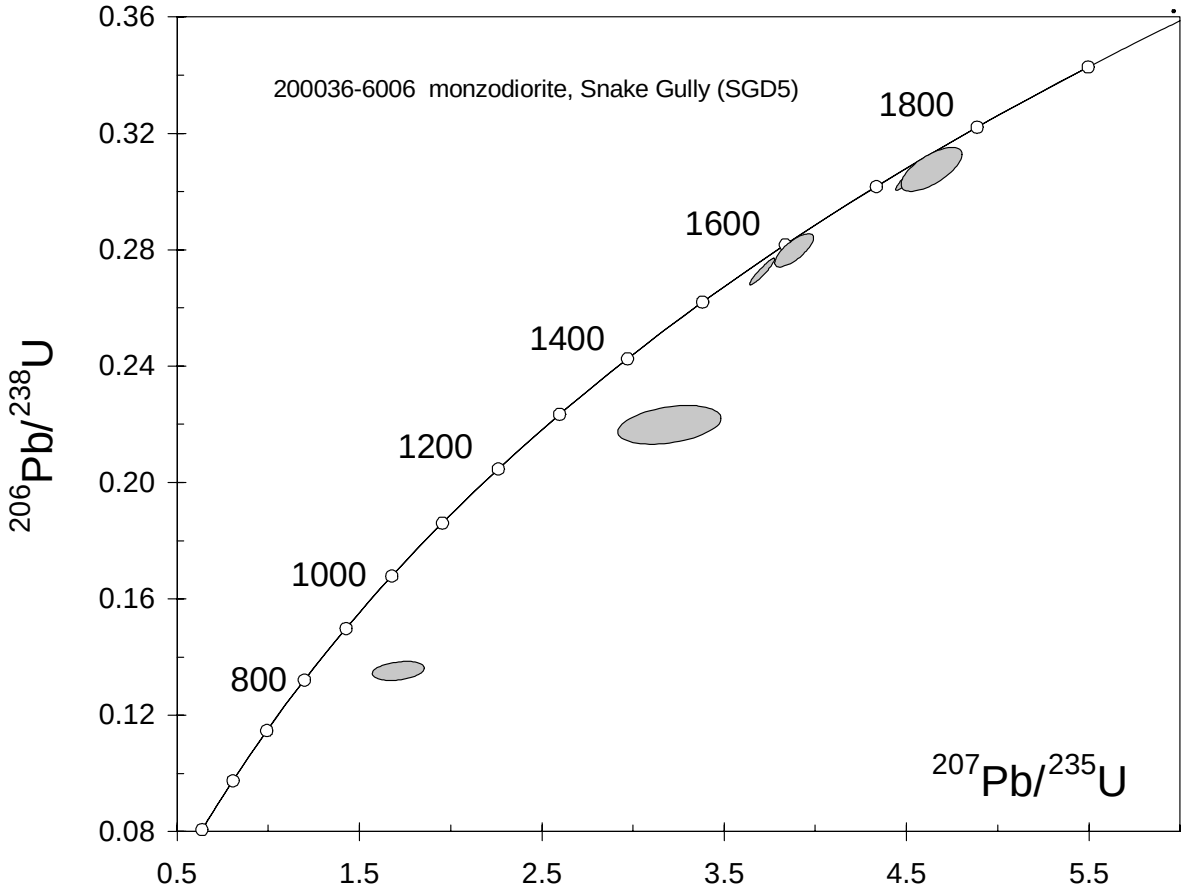

Figure 74. Concordia diagram for zircons in sample 200036-6006 showing radiogenic Pb compositions.

Table 21. SHRIMP analytical results for zircon from sample 200036 6006.

Spot	U (ppm)	Th (ppm)	$^{206}Pb_c$ (%)	$^{206}Pb^*$ (ppm)	$^{206}Pb^*/^{238}U$	±	$^{207}Pb^*/^{235}U$	±	$^{207}Pb^*/^{206}Pb^*$	±	conc (%)	207Pb/206Pb Age(Ma)	±
201.1	22	10	0.23	6	0.309	0.006	4.70	0.11	0.11020	0.00154	96	1803	26
202.1	220	171	0.03	52	0.274	0.004	3.73	0.06	0.09879	0.00040	97	1601	7
203.1	200	103	0.03	53	0.307	0.005	4.56	0.07	0.10753	0.00043	98	1758	7
204.1	174	172	3.19	21	0.136	0.002	1.72	0.09	0.09160	0.00467	57	1459	97
205.1	46	35	-0.02	11	0.281	0.004	3.92	0.07	0.10120	0.00111	97	1645	20
206.1	68	55	3.23	13	0.215	0.004	3.15	0.18	0.10620	0.00563	72	1736	98

Data are 1σ precision. All Pb data are common Pb corrected based on measured ^{204}Pb (after Stacey and Kramer 1975).
Analysis date 8/4/2001; SHRIMP II

200036 6005: microgabbro dyke, Snake Gully

1:250,000 sheet: Andamooka (SH5312)

1:100,000 sheet: Mattaweara (6237)

AMG: 689940 E 6634800 N

Location: The sample was taken from diamond drillhole SGD4, depth interval 402.9-404.8, 414.5-417, 422.8-423.5, 425-427, 432.6-433.6, 442-443m. The diamond drillhole is located within the Snake Gully prospect northeast of Olympic Dam.

Description: At SGD4, the Donington Suite megacrystic granite is intruded by an undeformed and unaltered microgabbro dyke (Figure 5). The dyke has fine-grained chilled margins, coarsening towards the middle of the 60 m thick body. It contains irregular-shaped inclusions of megacrystic granite with evidence of resorption at their margins. The microgabbro contains albite, biotite and magnetite, with minor alkali feldspar and about 2% quartz. The presence of visible quartz in thin section, suggested the microgabbro may contain zircon or badellyite, providing the first opportunity to directly analyse mafic material in the Olympic Domain.

Mount: Z3677

Description of zircons

Sample 200036 6005 (microgabbro dyke) yielded 33 zircons, of which 26 were analysed. The grains are equant, uniform in size (60 μm) and exhibit pyramidal and prismatic facets that are characteristic of an igneous origin (Figure 75). All of the grains are clear, optically homogeneous with no visible cores, and virtually free of inclusions. Zoning is uncommon, and only revealed under cathodoluminescence. Although the grain yield is low, the simple euhedral morphology and uniform appearance of the zircons (and uniform isotopic systematics described below) suggests they are a cogenetic suite of magmatic zircons, and not inherited grains or laboratory contaminants. The zircons have a distinctly different morphology to zircons extracted from the megacrystic granite hosting the dyke, which also supports the interpretation that the grains are not xenocrysts.

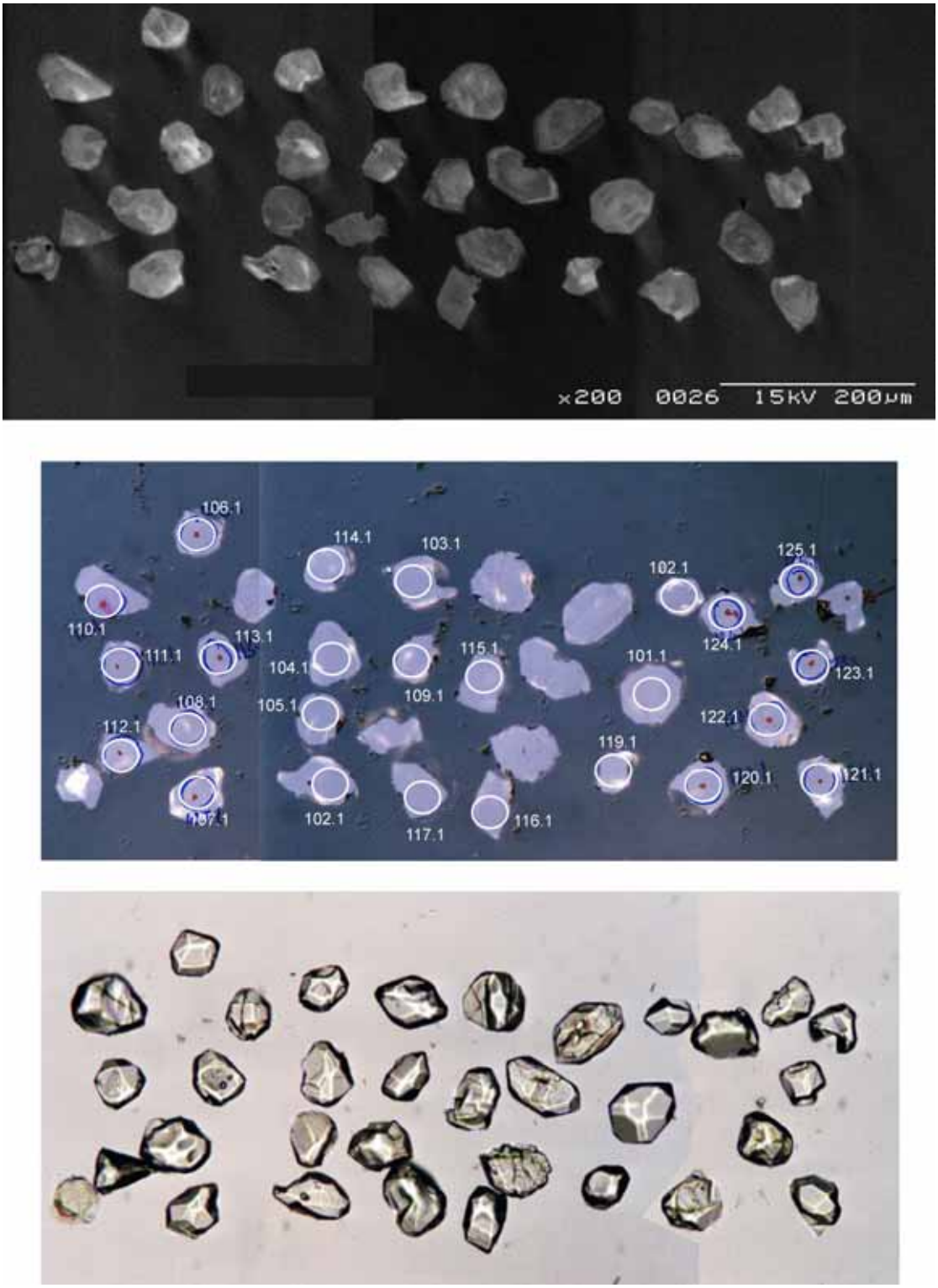

Figure 75. Representative CL (left) and transmitted light (right) images for sample 200036 6005: microgabbro dyke, Snake Gully prospect (SGD4). SHRIMP analysis spots are labelled. Scale bar is 200 µm.

Concurrent standard data

Z3677 and sample 200036 6029 on mount Z3678 were analysed over the 4 day session. Data for the standard are presented in Appendix 3. Twenty six QGNG analyses for Z3677 give a calibration exponent of 2.08, with an upper limit of 2.26 and lower limit of 1.85 (at 95% confidence level). The weighted mean $^{207}Pb/^{206}Pb$ age for all 26 analyses is 1851.7 ± 2.4 Ma (MSWD = 1.12; probability of fit =0.31). Nine QGNG analyses for Z3678 give a calibration exponent of 2.29 with an upper limit of 2.98 and lower limit of 1.61. The weighted mean $^{207}Pb/^{206}Pb$ age for all 9 analyses is 1848.9 ± 3.5 Ma (MSWD = 1.05; probability of fit = 0.39). Because no significant calibration shift is observed between the two data batches, both have been combined for data processing. This yields a calibration exponent of 2.08, with an upper limit of 2.22 and lower limit of 1.86. Thus the nominal value of 2.0 has been used in data reduction. The $^{206}Pb/^{238}U$ reproducibility for QGNG is 1.34% (1σ; n = 35 of 35). The weighted mean $^{207}Pb/^{206}Pb$ age for all 35 analyses is 1850.7 ± 1.9 (MSWD = 1.09; probability of fit = 0.33).

The analyses are corrected for overcounts at mass ^{204}Pb (after Black in press, calculated assuming $^{206}Pb/^{238}U$-^{207}Pb-^{235}U age concordance), which forces the weighted mean $^{207}Pb/^{206}Pb$ age for QGNG to the TIMS reference value. The recalculated age for QGNG becomes 1851.6 ± 2.2 Ma (MSWD = 1.13; probability of fit = .27; n = 35 of 35). The sample data below are also corrected for overcounts.

Element abundance calibration was based on SL13 (n = 1).

Sample data

Twenty three of the 24 analyses conform to a single population (MSWD = 1.24) with a mean age of 1594.0 ± 3.9 Ma. When corrected for overcounts at mass ^{204}Pb, the age becomes 1595.6 ± 3.8 Ma (probability of fit = 0.2). Analysis 112.1 yields a younger age (*ca* 1465 Ma) than the main population (Figure 76). Morphologically, this grain is similar to the other clear zircons, but the analysis reveals a relatively high U content and some discordance (Table 22; Figure 77), suggesting lead loss has occurred.

Geochronological interpretation

The $^{207}Pb/^{206}Pb$ age of 1595.6 ± 3.8 Ma is considered to be the intrusive age of the microgabbro dyke.

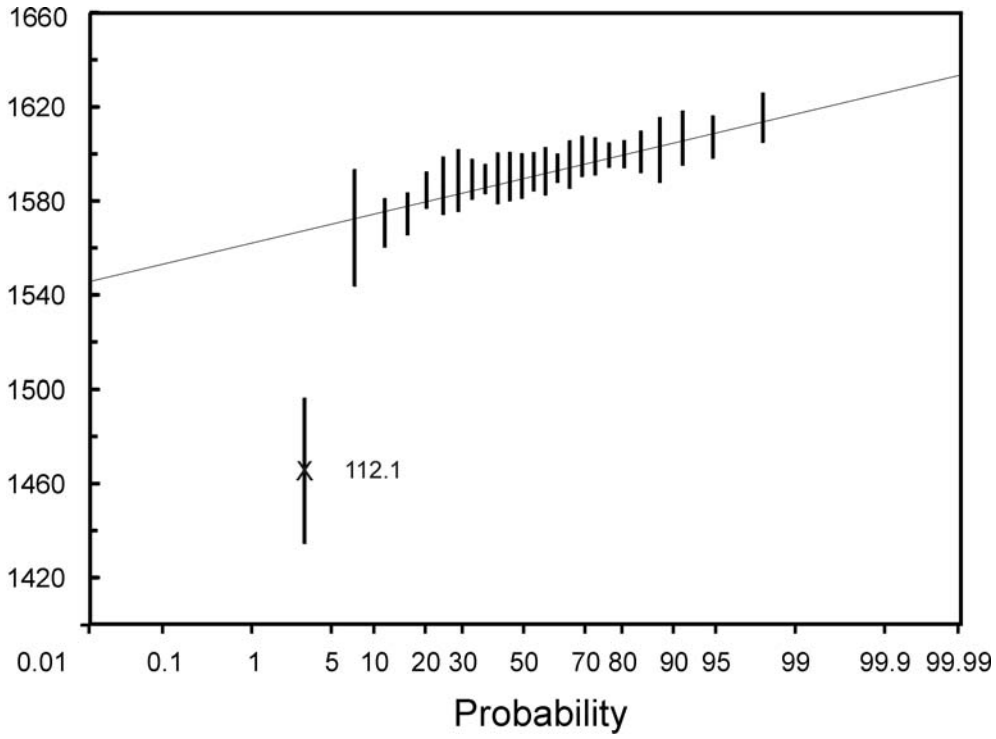

Figure 76. Probability diagram for individual zircon ages for sample 200036 6005. 112.1 clearly represents an outlier from the main population.

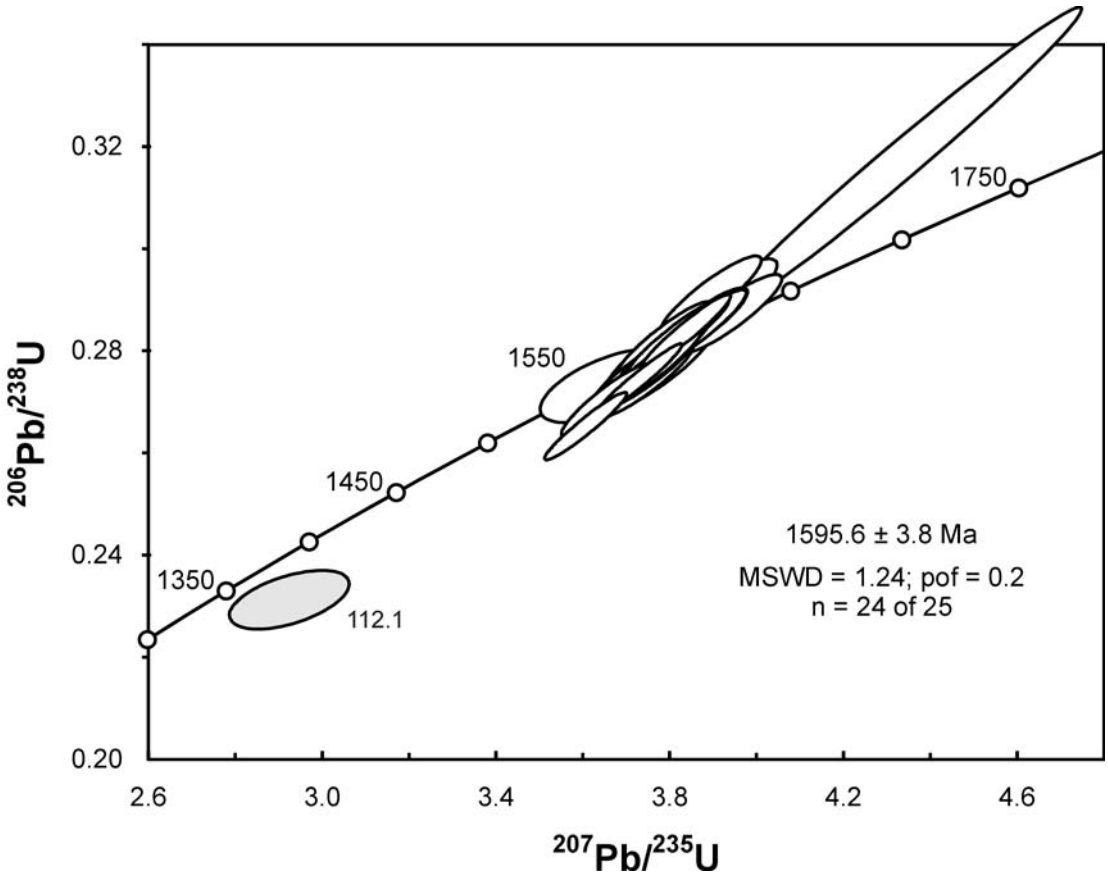

Figure 77. Concordia diagram for zircons in sample 200036 6005 showing radiogenic Pb compositions. White-filled symbols represent analyses used in the weighted mean age calculation. The light grey symbol represents one discordant, high U and common Pb analysis.

Table 22. SHRIMP analytical results for zircon from sample 200036 6005.

Spot	U (ppm)	Th (ppm)	$^{206}Pb_c$ (%)	$^{206}Pb^*$ (ppm)	$^{206}Pb^*/^{238}U$	±	$^{207}Pb^*/^{235}U$	±	$^{207}Pb^*/^{206}Pb^*$	±	conc (%)	207Pb/206Pb Age(Ma)	±
101.1	161	25	0.05	38	0.274	0.004	3.72	0.06	0.09846	0.00050	98	1595	10
102.1	170	32	0.15	42	0.288	0.004	3.91	0.06	0.09823	0.00066	103	1591	13
103.1	158	36	0.04	38	0.281	0.004	3.78	0.06	0.09749	0.00044	101	1577	8
104.1	201	42	0.00	47	0.269	0.004	3.65	0.05	0.09824	0.00038	97	1591	7
105.1	494	107	0.03	116	0.273	0.004	3.72	0.05	0.09872	0.00027	97	1600	5
106.1	164	30	0.08	39	0.276	0.004	3.76	0.06	0.09877	0.00045	98	1601	9
107.1	134	30	0.07	32	0.275	0.004	3.73	0.06	0.09830	0.00053	98	1592	10
108.1	147	30	0.09	35	0.275	0.004	3.72	0.06	0.09833	0.00051	98	1593	10
109.1	239	75	0.50	56	0.272	0.004	3.65	0.07	0.09710	0.00117	99	1570	22
110.1	165	30	0.03	40	0.283	0.004	3.86	0.06	0.09876	0.00042	100	1601	8
111.1	197	44	0.06	48	0.282	0.004	3.80	0.06	0.09799	0.00040	101	1586	8
112.1	535	224	1.19	107	0.230	0.003	2.92	0.05	0.09195	0.00089	91	1466	18
113.1	101	19	0.10	24	0.276	0.004	3.76	0.06	0.09902	0.00067	98	1606	13
114.1	131	40	0.07	32	0.286	0.004	3.93	0.06	0.09966	0.00052	100	1618	10
115.1	185	39	0.12	46	0.290	0.004	3.89	0.06	0.09729	0.00051	104	1573	10
116.1	369	85	0.06	89	0.281	0.004	3.82	0.06	0.09844	0.00031	100	1595	6
117.1	172	31	0.03	42	0.284	0.004	3.86	0.06	0.09858	0.00048	101	1597	9
118.1	323	68	0.02	79	0.283	0.004	3.83	0.05	0.09821	0.00031	101	1590	6
119.1	120	17	0.12	29	0.279	0.004	3.77	0.06	0.09815	0.00060	100	1589	11
120.1	173	31	-0.04	41	0.275	0.004	3.75	0.06	0.09886	0.00048	98	1603	9
121.1	183	33	0.03	44	0.279	0.004	3.78	0.06	0.09832	0.00047	100	1592	9
122.1	513	79	0.07	116	0.264	0.004	3.60	0.05	0.09875	0.00030	94	1601	6
123.1	200	27	0.12	55	0.316	0.013	4.32	0.17	0.09915	0.00058	110	1608	11
124.1	235	43	0.06	55	0.272	0.004	3.68	0.06	0.09840	0.00041	97	1594	8
125.1	165	31	0.01	39	0.273	0.004	3.74	0.06	0.09921	0.00044	97	1609	8

Data are 1σ precision. All Pb data are common Pb corrected based on measured ^{204}Pb (after Stacey and Kramer 1975).
Analysis date 8/4/2001; SHRIMP II

200136 8015f: leucogranite, Mount Woods Inlier

1:250,000 sheet: Billakalina (SH5307)

1:100,000 sheet: Peak (5938)

MGA: 533729 E 6719692 N

Location: The sample was taken from diamond drillhole DD86EN26. The collar site is located within the Bluebird Cu-Au prospect of the Mount Woods Inlier.

Description: In PIRSA's database (SA Geodata) the sample is described as a quartz-magnetite-Kfeldspar-chlorite gneiss with some pegmatite veins.

Mount: Z3962

Description of zircons

The sample contains euhedral, prismatic zircons and zircon fragments, with sharp to simple (blunt) terminations. Some grains exhibit well preserved crystal facets. They are predominantly medium-sized crystals and fragments (80 to 200µm long) with aspect ratios up to 4:1. The grains are light brown in colour and clear, and hematite-stained cracks are common. Acicular and blebby inclusions are rare, and difficult to see among the cracks. The grains contain few visible cores. The grains emit a strong CL response. Some grains are homogenous, but most display a pronounced concentric zoning typical of igneous crystallisation (Figure 78). Some grains exhibit darker, homogenous rims. In many grains, zoning and core-rim relationships are also visible in transmitted light photographs.

Concurrent standard data

Data for the standard are presented in Appendix 3. The data were analysed in two concurrent sessions. In the first session, containing standards 909.1-928.1, a large spot-size (and correspondingly higher beam strength) was used to target predominantly grain centres. The spot size (and beam strength) were then reduced in order to target the thinner homogeneous rims in the second session, which contains standards 929.1-937.1. The first batch of data yielded a Pb/U calibration (observed Ln(Pb/U)-Ln(UO/U) slope) of 1.73. The second batch of data yielded a slope of 1.78. The weighted mean $^{207}Pb/^{206}Pb$ age for QGNG data in the first batch is 1850.6 ± 2.3 Ma (n = 19 of 22; MSWD = 0.86), and for the second batch is 1850.6 ± 3.8 Ma (n = 7 of 8; MSWD = 1.1). Because no significant calibration shift is observed between the two data batches, both have been combined for data processing.

All $^{206}Pb/^{238}U$ QGNG analyses were included in the calibration, to give a calibration exponent of 1.77, with an upper limit of 2.01 and lower limit of 1.38 (at 95% confidence level). Thus the nominal value of 2.0 has been used in data reduction. There are two outliers amongst the $^{206}Pb/^{238}U$ analyses (920.1 and 927.1). When omitted, the remaining 28 analyses have a 1σ scatter of 2.24%. Three young outliers were eliminated from the $^{207}Pb/^{206}Pb$ analyses to give a weighted mean age of 1850.0 ± 2.1 Ma (n=27; MSWD = 1.14; probability of fit =0.28).

Element abundance calibration was based on SL13 (n = 1).

Figure 78. Representative CL (left) and transmitted light (right) images for sample 200136 8015f: leucogranite, Mount Woods Inlier. SHRIMP analysis spots are labelled. Scale bar is 200 µm.

Sample data

Thirty nine analyses were made on 33 grains. Some of the darker, homogenous rims were analysed separately. The rims have a lower Th/U ratio than the centre of the grains (Figure 79), suggesting secondary recrystallisation has occurred. However, their ages are indistinguishable from the zoned centres (Figure 80). The data distribution is simple, with most analyses clustering in a tight group near concordia (Figure 81). Omitting one analysis with high ^{204}Pb (332.2) produces a weighted mean ^{207}Pb/^{206}Pb age of 1586.9 ± 3.4 Ma (MSWD = 1.44; probability of fit is .042). Based on robust statistics, *SQUID* also identifies the oldest analysis (323.1) as an outlier (Figure 81). Its elimination from the dataset yields a weighted mean ^{207}Pb/^{206}Pb age of 1586.3 ± 2.8 Ma, with an improved MSWD of 1.17 (probability of fit is 0.22).

Geochronological interpretation

The ^{207}Pb/^{206}Pb age of 1586.3 ± 2.8 Ma is considered to be the crystallisation age of the granite.

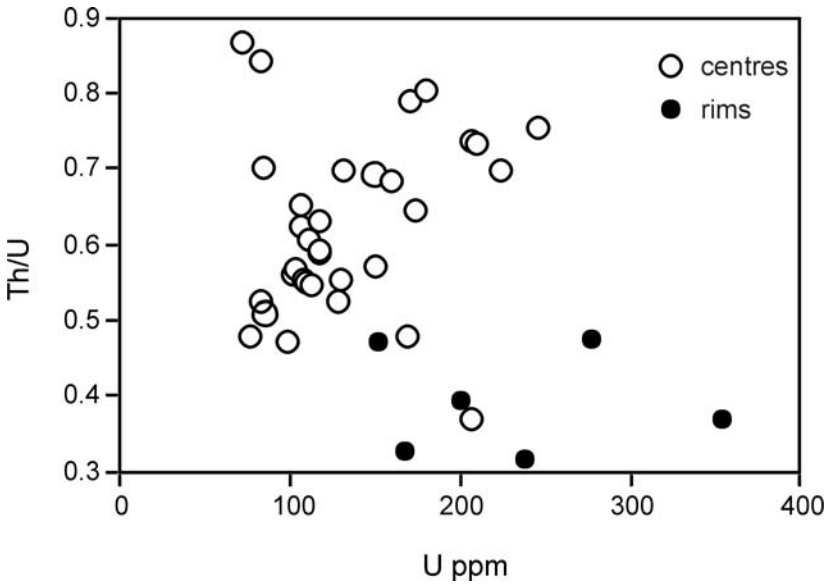

Figure 79. Comparison of the Th/U content of grain rims and grain centres for zircons in sample 200136 8015f showing the rims have lower Th/U contents overall.

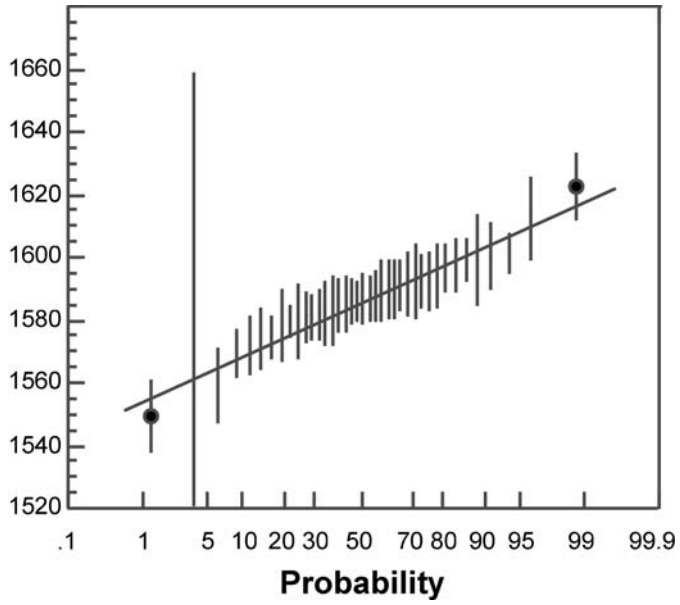

Figure 80. Probability diagram for individual zircon ages for sample 200136 8015f. SQUID identifies two analyses as outliers, which are marked with filled circles. The cores and rims define a single age population.

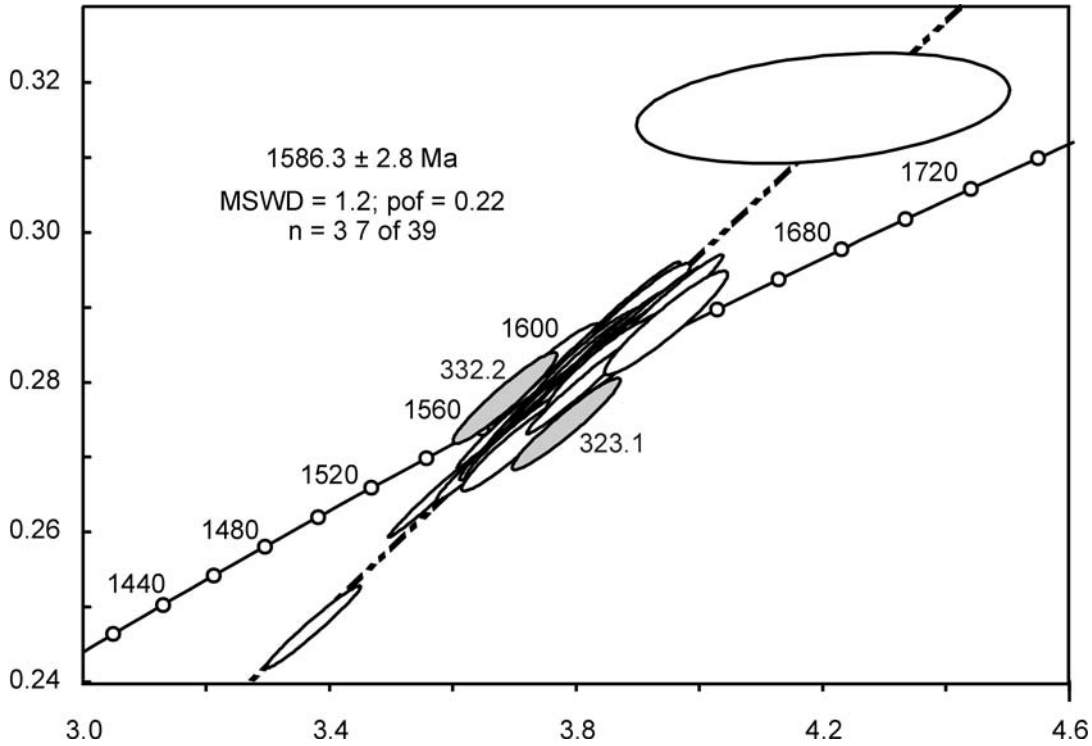

Figure 81. Concordia diagram for zircons in sample 200136 8015f showing radiogenic Pb compositions. White-filled symbols represent analyses used in the weighted mean age calculation. Outliers are shaded grey.

Table 23. SHRIMP analytical results for zircon from sample 200036 8015f.

Spot	U (ppm)	Th (ppm)	$^{206}Pb_c$ (%)	$^{206}Pb^*$ (ppm)	$^{206}Pb^*/^{238}U$	±	$^{207}Pb^*/^{235}U$	±	$^{207}Pb^*/^{206}Pb^*$	±	conc (%)	207Pb/206Pb Age(Ma)	±
316.1	129	69	0.05	31	0.276	0.005	3.74	0.07	0.09823	0.00043	99	1591	8
316.2	278	128	0.12	59	0.248	0.004	3.37	0.06	0.09867	0.00037	89	1599	7
317.1	102	55	0.11	25	0.280	0.005	3.76	0.07	0.09737	0.00052	101	1574	10
317.2	237	72	0.09	58	0.282	0.005	3.80	0.07	0.09772	0.00037	101	1581	7
318.1	117	67	-0.18	29	0.288	0.006	3.95	0.08	0.09937	0.00071	101	1612	13
319.1	128	65	0.02	32	0.289	0.005	3.92	0.07	0.09832	0.00049	103	1593	9
320.1	108	58	0.11	26	0.282	0.005	3.81	0.07	0.09777	0.00053	101	1582	10
321.1	103	57	0.07	25	0.279	0.005	3.77	0.07	0.09793	0.00047	100	1585	9
322.1	109	58	0.19	27	0.282	0.005	3.75	0.07	0.09658	0.00062	103	1559	12
323.1	113	59	0.01	27	0.275	0.005	3.79	0.07	0.09991	0.00058	96	1622	11
324.1	84	41	0.02	20	0.283	0.005	3.85	0.08	0.09867	0.00076	100	1599	14
325.1	170	129	0.05	40	0.277	0.005	3.73	0.07	0.09776	0.00041	100	1582	8
326.1	83	68	0.04	20	0.285	0.005	3.86	0.07	0.09832	0.00062	101	1592	12
327.1	106	64	0.00	26	0.285	0.005	3.86	0.07	0.09832	0.00046	101	1593	9
328.1	84	57	0.04	20	0.272	0.005	3.70	0.07	0.09872	0.00056	97	1600	11
329.1	106	67	0.06	26	0.285	0.005	3.83	0.07	0.09725	0.00049	103	1572	9
330.1	117	67	0.00	28	0.278	0.005	3.76	0.07	0.09819	0.00048	99	1590	9
331.1	72	60	0.07	18	0.290	0.005	3.90	0.07	0.09758	0.00060	104	1578	12
332.1	111	65	0.00	27	0.283	0.005	3.85	0.07	0.09859	0.00045	101	1598	9
332.2	151	69	0.24	36	0.278	0.005	3.69	0.07	0.09608	0.00059	102	1549	11
333.1	180	140	-0.01	44	0.284	0.005	3.84	0.07	0.09798	0.00035	102	1586	7
334.1	159	105	0.01	39	0.282	0.005	3.81	0.07	0.09803	0.00038	101	1587	7
334.2	168	53	0.09	42	0.291	0.005	3.95	0.07	0.09853	0.00041	103	1597	8
335.1	207	147	0.05	49	0.275	0.005	3.69	0.07	0.09738	0.00035	99	1575	7
335.2	354	126	0.03	81	0.265	0.005	3.57	0.06	0.09763	0.00026	96	1579	5
336.1	210	150	0.03	51	0.282	0.005	3.80	0.07	0.09803	0.00043	101	1587	8
337.1	246	180	0.04	59	0.278	0.005	3.75	0.07	0.09769	0.00042	100	1581	8
338.1	170	79	0.05	40	0.273	0.005	3.69	0.07	0.09807	0.00042	98	1588	8
339.1	206	73	0.03	48	0.271	0.005	3.65	0.07	0.09797	0.00037	97	1586	7
340.1	224	152	0.00	54	0.279	0.005	3.81	0.07	0.09877	0.00034	99	1601	6
341.1	131	89	0.08	32	0.284	0.005	3.82	0.07	0.09783	0.00058	102	1583	11
342.1	99	45	2.30	27	0.317	0.006	4.20	0.25	0.09630	0.00539	114	1553	110
343.1	117	71	0.00	28	0.282	0.005	3.81	0.07	0.09816	0.00049	101	1590	9
344.1	148	100	0.01	37	0.290	0.005	3.88	0.07	0.09713	0.00040	105	1570	8
345.1	173	108	0.04	41	0.273	0.005	3.71	0.07	0.09840	0.00054	98	1594	10
345.2	200	76	0.13	49	0.286	0.005	3.87	0.07	0.09792	0.00045	102	1585	9
346.1	151	83	0.17	37	0.285	0.005	3.85	0.07	0.09814	0.00052	102	1589	10
347.1	77	35	0.03	19	0.281	0.005	3.81	0.07	0.09827	0.00055	100	1591	11
348.1	82	42	0.13	20	0.284	0.005	3.82	0.07	0.09765	0.00062	102	1580	12

Data are 1σ precision. All Pb data are common Pb corrected based on measured ^{204}Pb (after Stacey and Kramer 1975). Analysis date 22/4/2003; SHRIMP II

200236 8028b: leucogabbro, Mount Woods Inlier

1:250,000 sheet:

1:100,000 sheet:

MGA: 538128E 6730169 N

Location: The sample was taken from diamond drillhole PK1, depth interval 326.7-328.8 m. The collar site is located within the Peculiar Knob North iron ore prospect of the Mount Woods Inlier.

Description: The sample consists of a fine-grained mafic host cut by pegmatoidal leucogabbro segregations. The host is either noritic microgabbro (clinopyroxene > orthopyroxene) or gabbroic micronorite (orthopyroxene > clinopyroxene) consisting of plagioclase, subequal amounts of orthopyroxene and clinopyroxene, magnetite and minor red-brown biotite, ilmenite and apatite. Mineralogical layering consistent with primary igneous layering, is present in the host phase. The pegmatoidal leucogabbro segregations have a similar mineralogy, with more abundant red-brown biotite and small euhedral zircon, and some pyrrhotite, pyrite and chalcopyrite. The zircons commonly occur in or adjacent to the biotite and opaques. These segregations are clearly a late magmatic phase related to the fine-grained host. The association of zircon grains with the pegmatoidal segregations suggests that their formation is coeval with this late magmatic phase of the mafic rocks.

Both host and segregations have a mature granoblastic texture with well-developed triple junctions and smooth, curved grain boundaries. Exsolution textures are present in the plagioclase and pyroxene. Plagioclase phenocrysts are commonly sub-rounded with sutured margins due to solid state recrystallisation against pyroxene and opaques. These features indicate that both host and segregations have been recrystallised after solidification. The combination of fine grainsize and mature granoblastic texture suggests relatively brief reheating (hornfelsing), most likely caused by a separate nearby intrusive event.

The veining and recrystallisation have been overprinted by a later alteration event characterised by narrow veins of blue-green tourmaline and yellow-brown biotite. The same minerals are present in a surrounding halo.

(Unpublished Geoscience Australia report by Dr Morrie Duggan).

Mount: Z3962

Description of zircons

The sample contains abundant euhedral prismatic zircons with slightly rounded edges and terminations. They are predominantly small- to medium-sized crystals (100 µm to 200 µm long), with aspect ratios up to about 4:1. Most grains are colourless to pink and have good clarity, with few cracks and scarce clear, round inclusions. The grains emit a strong CL response. Most grain centres display a pronounced concentric zoning typical of igneous crystallisation (Figure 82). Highly cathodoluminescent homogenous rims cross-cut the concentric zoning in many grains. The zoning and core-rim relationships are generally not visible in transmitted light photographs.

Figure 82. Representative CL (left) and transmitted light (right) images for sample 200236 8028b: leucogabbro, Mt Woods Inlier. SHRIMP analysis spots are labelled. Scale bar is 200 µm.

Concurrent standard data

Data for the standard are presented in Appendix 3. The data were analysed in two concurrent sessions. In the first session, containing standards 909.1-928.1, a large spot-size (and correspondingly higher beam strength) was used to target predominantly grain centres. The spot size (and beam strength) were then reduced in order to target the thinner homogeneous rims in the second session, which contains standards 929.1-937.1. The first batch of data yielded a Pb/U calibration (observed Ln(Pb/U)-Ln(UO/U) slope) of 1.73. The second batch of data yielded a slope of 1.78. The weighted mean $^{207}Pb/^{206}Pb$ age for QGNG data in the first batch is 1850.6 ± 2.3 Ma (n = 19 of 22; MSWD = 0.86), and for the second batch is 1850.6 ± 3.8 Ma (n = 7 of 8; MSWD = 1.1). Because no significant calibration shift is observed between the two data batches, both have been combined for data processing.

All $^{206}Pb/^{238}U$ QGNG analyses were included in the calibration, to give a calibration exponent of 1.77, with an upper limit of 2.01 and lower limit of 1.38 (at 95% confidence level). Thus the nominal value of 2.0 has been used in data reduction. There are two outliers amongst the $^{206}Pb/^{238}U$ analyses (920.1 and 927.1). When omitted, the remaining 28 analyses have a 1σ scatter of 2.24%. Three young outliers were eliminated from the $^{207}Pb/^{206}Pb$ analyses to give a weighted mean age of 1850.0 ± 2.1 Ma (n=27; MSWD = 1.14; probability of fit =0.28).

Element abundance calibration was based on SL13 (n = 1).

Sample data

Sixty seven analyses were made on 50 grains. The zoned grain centres and brighter homogeneous rims were analysed separately. Overall, as with sample 200136 8015f, the rims have a lower Th/U ratio than the centre of the grains (Figure 83), suggesting secondary recrystallisation has occurred. However, in this case some grain centres also have low Th/U ratios and the distinction is less clear.

Forty four zoned cores were analysed. The analyses do not conform to a single population (MSWD = 3.46). A probability diagram of the zircon ages reveals one clear outlier: grain 440.1 is clearly older than the main population (Figure 84a). The remaining 43 analyses combine to yield a mean crystallisation age of 1586.8 ± 4.1 Ma (Figure 85) The MSWD of 1.71 is somewhat high (probability of fit = .003), but appears to be a true indication of the wide spread of $^{207}Pb/^{206}Pb$ ages within the dataset. No other obvious outliers are indicated by the probability diagram, and the removal of other analyses as possible statistical outliers reduces the MSWD and improves the probability of fit, without significantly affecting the weighted mean age. The age spread may reflect some overlap onto younger areas of zircon grains (rims) during analysis.

Twenty three rims were analysed. The analyses do not conform to a single population (MSWD = 2.33). The two youngest analyses (440.3 and 453.2) contain high common Pb and are rejected as outliers (Figure 84b). Analysis 456.1 is also rejected as a statistical outlier, and may reflect drilling of the primary beam into an older core. The remaining 20 analyses combine to yield a mean crystallisation age of 1576.2 ± 7.0 Ma (MSWD = 1.23, probability of fit is 0.22; Figure 86).

Geochronological interpretation

The greater error in the age of the rims reflects both their lower U content, and the smaller spot size used in their analysis. The older analyses included in the wide spread

of rim ages, may also reflect analytical overlap, as the primary beam burns through the thin rims and into the zircon cores. However, the age difference between the cores and rims of the zircons appears to be real (Figure 87). The $^{207}Pb/^{206}Pb$ age of 1586.8 ± 4.1 Ma is considered to be the crystallisation age of the microgabbro. This is identical to the age of the Hiltaba Granite analysed from the Mt Woods Inlier (1586.3 ± 2.8; sample 200136-8015f). The *ca* 10 m.y. younger age of the rims may reflect recrystallisation during a slightly later, relatively brief contact metamorphic event, for which there is petrographic evidence.

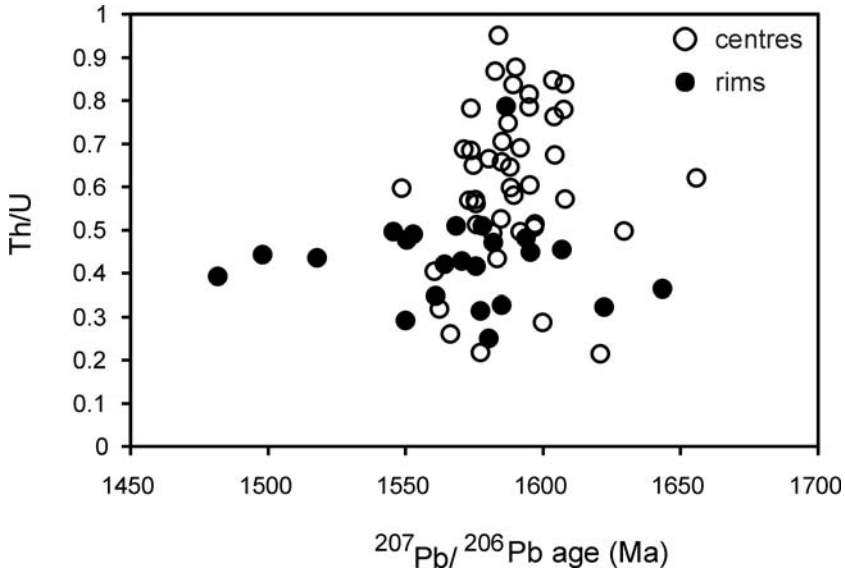

Figure 83. Comparison of the Th/U content of grain centres and rims for zircons in sample 200236 8028b showing the rims have lower Th/U contents overall.

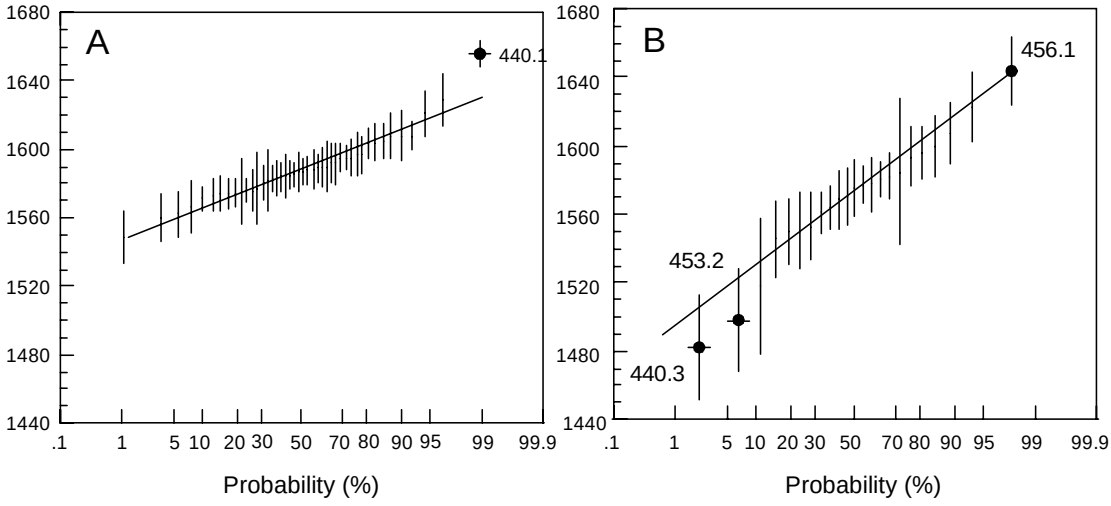

Figure 84 (A) Probability diagram for ages of zircon cores, sample 200236 8028b. (B) Probability diagram for ages of zircon rims, sample 200236 8028b (scale is the same as for (A), to allow comparison with core ages).

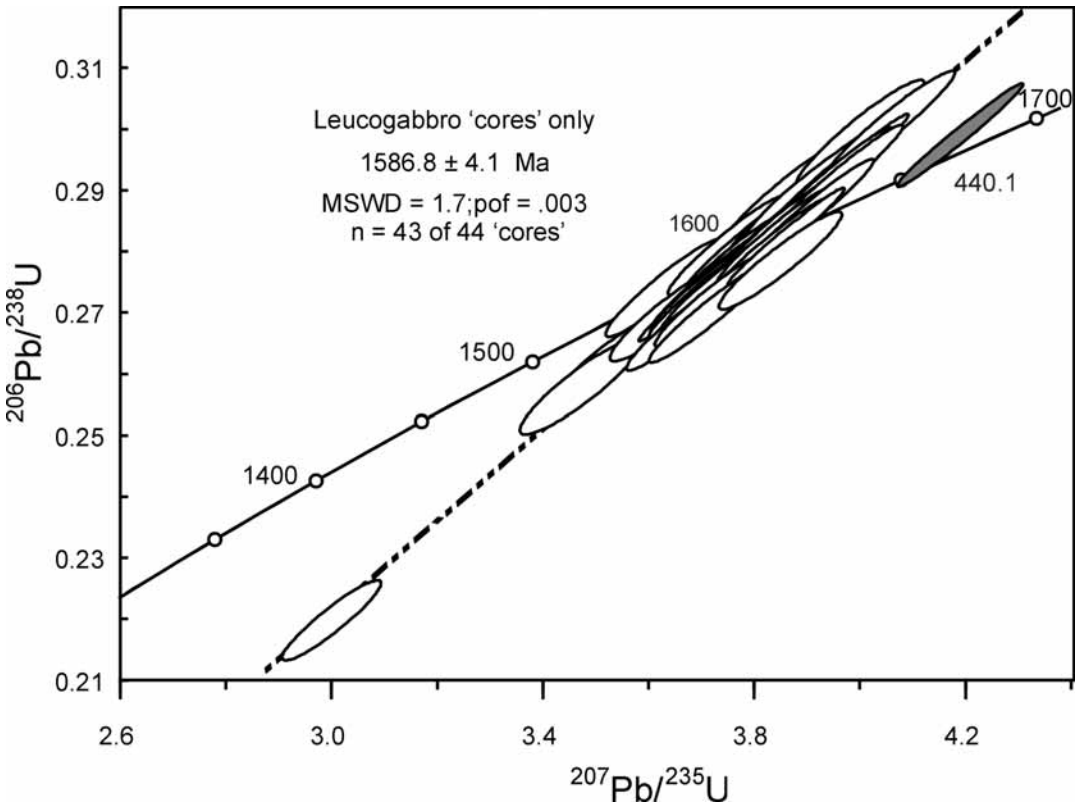

Figure 85. Concordia diagram for zircon cores in sample 200236 8028b.

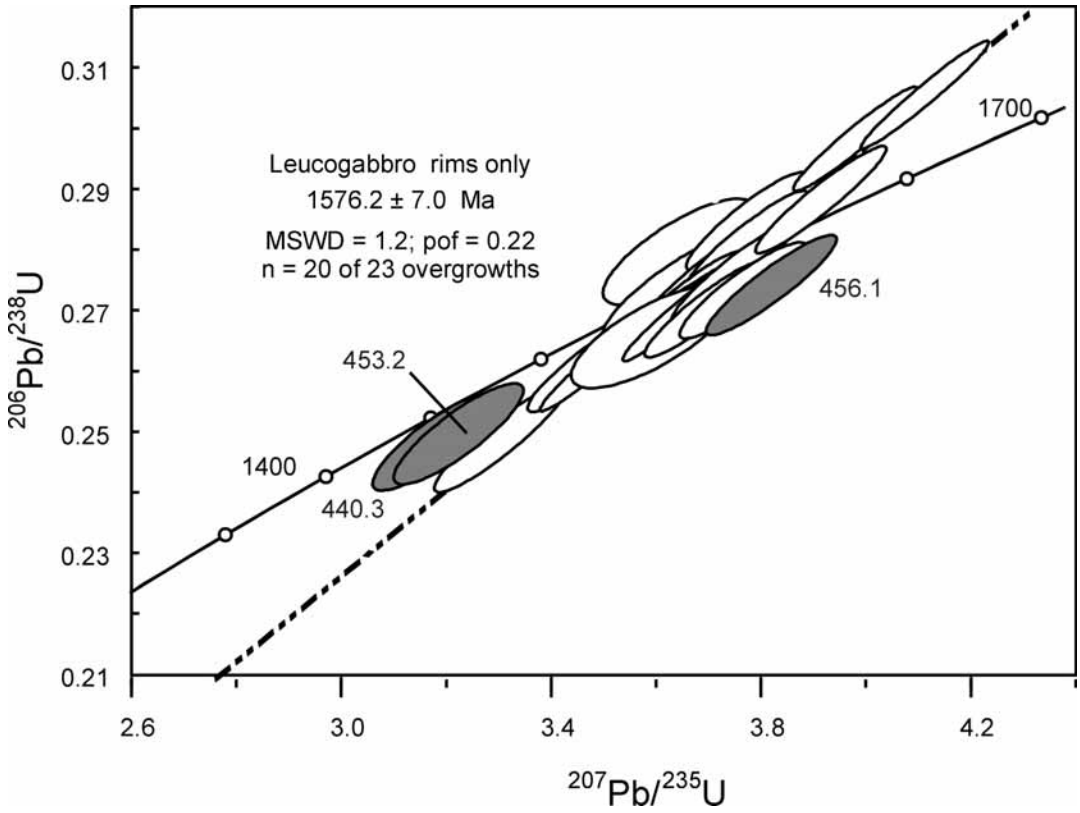

Figure 86. Concordia diagram for zircon rims in sample 200236 8028b.

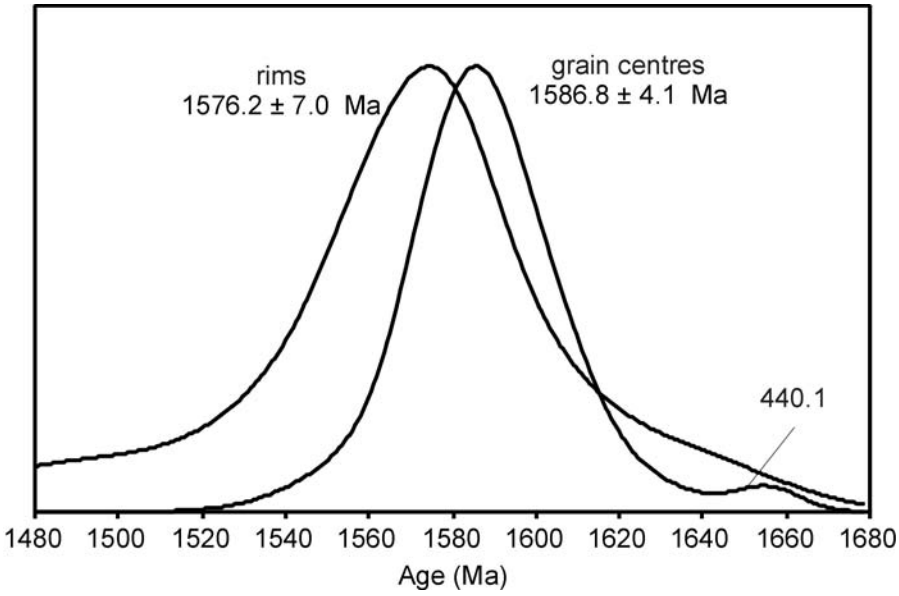

Figure 87. Probability density plot comparing the weighted mean $^{207}Pb/^{206}Pb$ ages of zircon cores and rims in sample 200236 8028b.

Table 24. SHRIMP analytical results for zircon from sample 200036 8015f.

Spot		U (ppm)	Th (ppm)	$^{206}Pb_c$ (%)	$^{206}Pb^*$ (ppm)	$^{206}Pb^*/^{238}U$	±	$^{207}Pb^*/^{235}U$	±	$^{207}Pb^*/^{206}Pb^*$	±	conc (%)	207Pb/206Pb Age(Ma)	±
401.2	rim	29	12	0.50	7	0.280	0.007	3.65	0.12	0.09450	0.00198	105	1518	39
413.1	centre	150	97	0.11	36	0.278	0.006	3.75	0.09	0.09768	0.00053	100	1580	10
414.1	centre	83	54	-0.02	20	0.281	0.006	3.83	0.09	0.09894	0.00053	99	1604	10
415.1	centre	114	75	0.02	28	0.288	0.007	3.86	0.09	0.09734	0.00046	104	1574	9
416.1	centre	167	90	0.00	41	0.288	0.007	3.87	0.09	0.09743	0.00036	104	1576	7
417.1	centre	148	93	0.04	36	0.284	0.007	3.84	0.09	0.09808	0.00044	101	1588	8
418.1	centre	124	69	0.03	30	0.283	0.006	3.86	0.09	0.09913	0.00045	100	1608	8
418.2	rim	59	25	0.15	14	0.282	0.006	3.78	0.09	0.09717	0.00086	102	1571	17
419.1	centre	87	49	0.00	22	0.292	0.007	3.95	0.09	0.09815	0.00062	104	1589	12
420.1	centre	72	35	-0.12	17	0.279	0.006	3.85	0.10	0.10028	0.00082	97	1629	15
421.1	centre	89	44	0.11	22	0.291	0.007	3.90	0.09	0.09744	0.00062	104	1576	12
422.1	centre	124	72	0.01	30	0.278	0.006	3.76	0.09	0.09809	0.00061	100	1588	12
423.1	centre	81	69	0.02	19	0.275	0.006	3.72	0.09	0.09818	0.00076	98	1590	14
424.1	centre	176	120	0.04	42	0.277	0.006	3.74	0.09	0.09793	0.00037	99	1585	7
425.1	centre	154	98	0.02	38	0.286	0.007	3.87	0.09	0.09792	0.00044	102	1585	8
426.1	centre	87	58	0.05	21	0.285	0.007	3.85	0.09	0.09827	0.00066	101	1592	12
427.1	centre	195	154	0.05	46	0.278	0.006	3.77	0.09	0.09845	0.00038	99	1595	7
428.1	centre	118	90	0.01	29	0.285	0.007	3.87	0.09	0.09845	0.00045	101	1595	9
429.1	centre	105	58	0.03	25	0.282	0.006	3.79	0.09	0.09731	0.00049	102	1573	9
430.1	centre	108	63	-0.03	27	0.292	0.007	3.97	0.10	0.09846	0.00056	104	1595	11
430.2	rim	69	28	0.03	18	0.298	0.007	3.98	0.10	0.09684	0.00067	108	1564	13
431.1	centre	72	53	-0.05	18	0.287	0.007	3.91	0.09	0.09892	0.00056	101	1604	11
431.2	rim	90	25	0.30	22	0.285	0.007	3.78	0.09	0.09611	0.00095	104	1550	19
432.1	centre	69	33	-0.04	16	0.274	0.006	3.71	0.09	0.09827	0.00060	98	1592	11

432.2	rim	45	14	-0.11	11	0.274	0.007	3.77	0.10	0.09990	0.00110	96	1622	21
433.1	centre	135	110	0.05	34	0.294	0.007	3.98	0.09	0.09814	0.00043	105	1589	8
433.2	rim	52	20	0.16	13	0.290	0.007	3.86	0.10	0.09664	0.00071	105	1560	14
434.1	centre	148	93	0.07	37	0.293	0.007	3.93	0.09	0.09739	0.00044	105	1575	8
434.2	rim	52	21	0.07	12	0.272	0.006	3.66	0.09	0.09743	0.00089	98	1576	17
435.1	centre	148	122	0.04	36	0.285	0.007	3.89	0.09	0.09890	0.00050	101	1604	10
436.1	centre	172	145	0.00	43	0.293	0.007	3.95	0.09	0.09780	0.00039	105	1583	7
437.1	centre	109	82	-0.05	25	0.268	0.006	3.67	0.09	0.09911	0.00072	95	1607	14
438.1	centre	194	129	0.09	47	0.282	0.006	3.77	0.09	0.09720	0.00039	102	1571	8
439.1	centre	104	78	0.05	25	0.282	0.006	3.78	0.09	0.09733	0.00053	102	1574	10
439.2	rim	65	16	0.12	17	0.300	0.007	4.01	0.10	0.09695	0.00079	108	1566	15
440.1	centre	129	77	-0.02	33	0.299	0.007	4.19	0.10	0.10172	0.00043	102	1656	8
440.2	rim	157	38	0.22	41	0.306	0.007	4.12	0.10	0.09768	0.00055	109	1580	11
440.3	rim	60	23	0.63	13	0.249	0.006	3.18	0.10	0.09270	0.00148	97	1482	31
440.4	rim	55	15	0.00	10	0.220	0.005	3.00	0.08	0.09871	0.00094	80	1600	18
441.1	centre	100	51	-0.01	26	0.301	0.007	4.06	0.10	0.09790	0.00066	107	1585	13
442.1	rim	101	31	0.15	24	0.270	0.006	3.63	0.09	0.09752	0.00059	98	1577	11
442.2	centre	39	22	0.12	9	0.263	0.006	3.53	0.09	0.09742	0.00097	95	1575	19
443.1	centre	139	100	0.00	33	0.275	0.006	3.72	0.09	0.09804	0.00041	99	1587	8
444.1	centre	89	44	0.01	22	0.283	0.007	3.84	0.09	0.09856	0.00057	101	1597	11
444.2	centre	79	24	0.19	19	0.281	0.006	3.75	0.09	0.09675	0.00070	102	1562	13
445.1	centre	136	103	0.07	32	0.270	0.006	3.64	0.09	0.09800	0.00061	97	1586	12
445.2	centre	203	187	-0.01	48	0.273	0.006	3.69	0.09	0.09787	0.00044	98	1584	8
446.1	rim	50	25	0.10	12	0.276	0.007	3.69	0.10	0.09706	0.00087	100	1568	17
447.1	rim	92	42	0.10	21	0.269	0.006	3.62	0.09	0.09776	0.00070	97	1582	14
447.2	rim	94	41	0.08	23	0.288	0.007	3.92	0.10	0.09847	0.00081	102	1595	15
448.1	rim	61	30	0.08	14	0.268	0.006	3.61	0.09	0.09755	0.00084	97	1578	16
449.1	rim	61	27	-0.08	14	0.271	0.006	3.70	0.10	0.09908	0.00094	96	1607	18
450.1	rim	61	29	0.09	15	0.276	0.007	3.75	0.10	0.09839	0.00089	99	1594	17
451.1	rim	112	38	0.06	25	0.261	0.006	3.48	0.08	0.09668	0.00062	96	1561	12
452.1	centre	162	68	0.05	38	0.276	0.006	3.72	0.09	0.09783	0.00054	99	1583	10
453.1	rim	38	17	0.09	8	0.249	0.007	3.30	0.10	0.09610	0.00115	93	1550	22
453.2	rim	26	11	0.39	6	0.250	0.007	3.22	0.10	0.09350	0.00150	96	1498	30
454.1	centre	66	14	-0.04	15	0.270	0.007	3.72	0.10	0.09982	0.00071	95	1621	13
455.1	centre	63	51	0.06	15	0.273	0.007	3.73	0.09	0.09913	0.00076	97	1608	14
456.1	rim	41	15	-0.13	10	0.274	0.007	3.82	0.10	0.10100	0.00111	95	1643	20
457.1	centre	38	8	0.24	8	0.258	0.006	3.47	0.09	0.09750	0.00117	94	1577	22
458.1	centre	63	37	0.21	15	0.274	0.007	3.63	0.09	0.09604	0.00078	101	1549	15
458.2	centre	80	39	0.07	19	0.275	0.006	3.73	0.09	0.09855	0.00067	98	1597	13
459.1	centre	65	31	0.20	15	0.270	0.006	3.64	0.09	0.09775	0.00093	98	1582	18
460.1	rim	64	31	0.27	15	0.274	0.007	3.62	0.10	0.09590	0.00115	101	1545	23
460.2	rim	62	30	0.14	14	0.261	0.006	3.47	0.09	0.09630	0.00096	96	1553	20
461.1	rim	23	7	0.07	5	0.266	0.007	3.59	0.13	0.09790	0.00225	96	1585	43

Data are 1σ precision. All Pb data are common Pb corrected based on measured ^{204}Pb (after Stacey and Kramer 1975).

Analysis date 22/4/2003; SHRIMP II

Part 4: The Olympic Dam deposit

200036 6163: dolerite, Olympic Dam

1:250,000 sheet: Andamooka (SH5312)

1:100,000 sheet: Mattaweara (6237)

MGA: 681735 E 6630758 N

Location: The sample was taken from Western Mining Corporation diamond drillhole RD160, depth interval. 684.6-900 m.

Description: This sample is an altered dolerite with abundant plagioclase as unoriented laths to 3 mm long, partly altered to sericite. There is possibly 4-5% sericite in this thin section as well as 55% plagioclase, including fine-grained plagioclase in interstitial areas of mesostasis with opaque oxides and quartz. Probable clinopyroxene has been altered to chlorite and carbonate, possibly calcite, as the geochemistry indicates a reasonably high CaO content. Patches of skeletal opaque oxides to 3 mm in diameter have been altered to hematite. Trace apatite is present as small needles and accessory leucoxene or sphene is seen in the chlorite, but no radioactive grains were noted.

Narrow fractures cutting the rock are filled by hematite.

(Purvis 2003).

Mount: Z4125

Description of zircons

This sample yielded only 9 zircons. The grains are all small (30 μm) with aspect ratios < 2:1, and predominantly rounded terminations. The zircons are mostly colourless and clear, with few inclusions. One grain contains a large clear inclusion that appears opaque in reflected light. The grains emit a strong CL response. Two emit a homogenous signature. The remainder display pronounced oscillatory zoning typical of igneous crystallisation (Figure 88).

Concurrent standard data

Data for the standard are presented in Appendix 3. No data were excluded from the Pb/U calibration. The calibration exponent for this QGNG data set is 1.65, with a lower limit of 1.27 and an upper limit of 2.13 (at the 95% confidence level). Thus the nominal value of 2.0 has been used in data reduction. The 26 analyses have a 1σ scatter in $^{206}Pb/^{238}U$ of 1.63%. Element abundance calibration is based on SL13 (n = 1).

The weighted mean $^{207}Pb/^{206}Pb$ age for all 26 analyses is 1848.4 ± 2.5 Ma (MSWD = 1.8; probability of fit = .007). Experiments by Black (in press) show that where SHRIMP II sessions deliver young $^{207}Pb/^{206}Pb$ ages for zircon standards, the age discrepancy is always consistent with interferences at the ^{204}Pb mass peak, and not with mass fractionation, as previously presumed. The analyses are corrected for overcounts at mass ^{204}Pb (calculated assuming $^{206}Pb/^{238}U$-^{207}Pb-^{235}U age concordance), which forces the weighted mean $^{207}Pb/^{206}Pb$ age for QGNG to the TIMS reference value. The sample data below are also corrected for overcounts at the ^{204}Pb mass peak.

The recalculated age for QGNG becomes 1851.6 ± 2.2 Ma (MSWD = 1.3; probability of fit = .16; n = 25 of 26). In this case, *SQUID* identifies one statistical outliers, but there is no geological reason for culling this analysis (eg Pb loss). The weighted mean $^{207}Pb/^{206}Pb$ age for all 26 analyses is 1850.7 ± 2.5 Ma (MSWD = 1.6; probability of fit = .04). The slightly high MSWD indicates the scatter in the analyses is greater than that predicted by counting statistics alone. The wide spread of ages is therefore attributed to a component of instrument uncertainty, and high MSWDs for the corresponding samples are also acceptable.

Sample data

Eight of the 9 zircons were analysed. Six analyses cluster near concordia at ~ 1840 Ma, but with considerable excess scatter (MSWD is 3.7), which disallows a weighted mean $^{207}Pb/^{206}Pb$ age to be determined for the group (Figure 89). Analysis 401.1 is younger, intersecting concordia at 1725 Ma, and analysis 403.3 is older, with a $^{207}Pb/^{206}Pb$ age of 1975 Ma.

Geochronological interpretation

Given the low zircon yield for this medium-grained mafic intrusion, all grains are interpreted to be xenocrysts. The analyses suggest a maximum age of 1725 Ma for the dolerite, but with only one analysis it is impossible to rule out sample contamination, and the dolerite may be older. The ~ 1835 Ma grains could be inherited from ~ 1850 Ma foliated granitoids of the Donington Suite, which are intersected in many prospects surrounding the Olympic Dam deposit, and throughout the Olympic Domain.

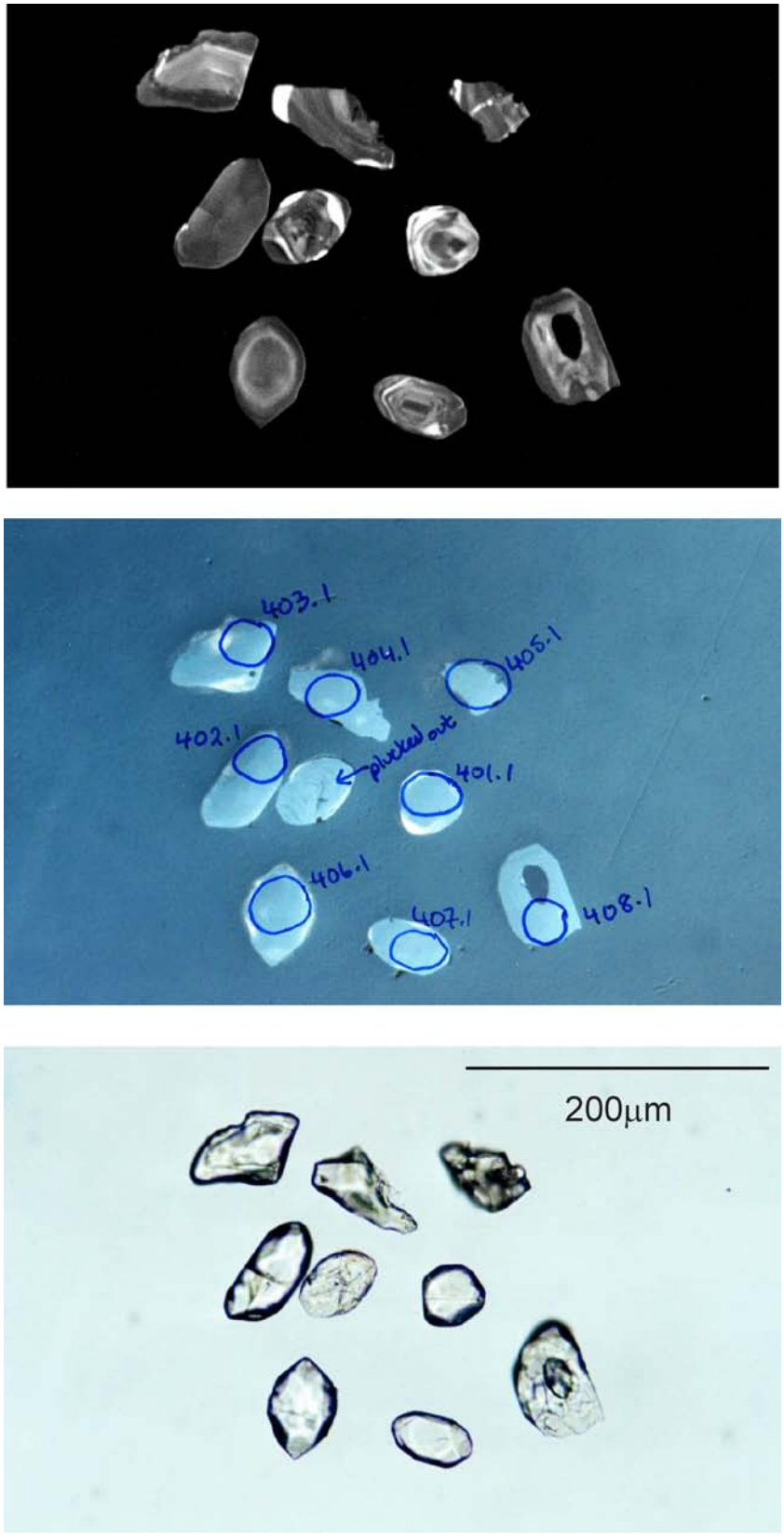

Figure 88. Representative CL (left) and transmitted light (right) images for sample 200036 6163: altered dolerite, Olympic Dam. SHRIMP analysis spots are labelled. Scale bar is 200 µm.

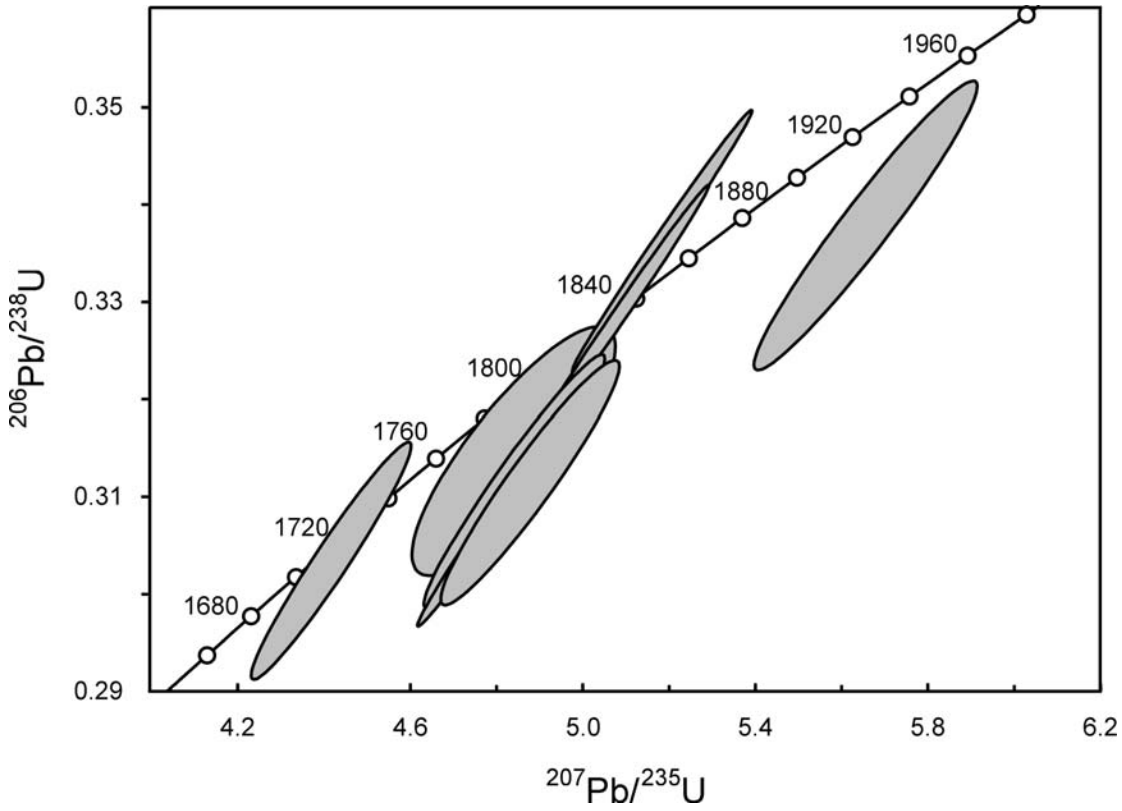

Figure 89. Concordia diagram for zircons in sample 200036 6163 showing radiogenic Pb compositions.

Table 25. SHRIMP analytical results for zircon from sample 200036 6163.

Spot	U (ppm)	Th (ppm)	$^{206}Pb_c$ (%)	$^{206}Pb^*$ (ppm)	$^{206}Pb^*/^{238}U$	±	$^{207}Pb^*/^{235}U$	±	$^{207}Pb^*/^{206}Pb^*$	±	conc (%)	207Pb/206Pb Age(Ma)	±
401.1	199	121	0.31	52	0.303	0.005	4.42	0.08	0.10560	0.00045	99	1725	8
402.1	635	120	0.11	184	0.336	0.005	5.18	0.08	0.11183	0.00019	102	1829	3
403.1	305	61	0.23	89	0.338	0.006	5.66	0.11	0.12145	0.00062	95	1978	9
404.1	378	180	0.08	100	0.309	0.005	4.81	0.08	0.11292	0.00024	94	1847	4
405.1	366	203	0.13	98	0.312	0.005	4.84	0.09	0.11271	0.00051	95	1844	8
406.1	542	92	0.01	153	0.329	0.005	5.09	0.08	0.11223	0.00018	100	1836	3
407.1	406	254	1.43	111	0.315	0.005	4.84	0.10	0.11160	0.00123	97	1825	20
408.1	410	162	0.84	111	0.311	0.005	4.88	0.08	0.11362	0.00061	94	1858	10

Data are 1σ precision. All Pb data are common Pb corrected based on measured ^{204}Pb (after Stacey and Kramer 1975).
Analysis date 30/4/2003; SHRIMP II

200036 6164: volcaniclastic sandstone, Olympic Dam

1:250,000 sheet: Andamooka (SH5312)

1:100,000 sheet: Mattaweara (6237)

MGA: 681194 E 6629479 N

Location: The sample was taken from Western Mining Corporation diamond drillhole RU 38-2625, depth interval 422-425 m and 440-445 m.

Mount: Z4125

Description: Geological context: Heterolithic breccias of the Olympic Dam Breccia Complex (ODBC) locally contain abundant surficial volcaniclastic clasts that occur as small fragments to very large blocks (up to 50 m; see photograph). The fine-grained, layered clasts are interpreted to derive from laminated ash, lapilli tuff and conglomerate, and reworked hydrothermal breccias that accumulated in phreatic and phreatomagmatic craters above the breccia system (Cross et al. 1993). They are commonly plastically deformed, indicating only partial lithification before disruption and incorporation into the host breccia during crater collapse. Block margins are commonly irregular and gradational due to partial disaggregation during emplacement, and/or ongoing brecciation. They are strongly affected by sericite and/or hematite alteration. Sample 200036 6164 is taken from a thick drillcore intersection of this volcaniclastic material.

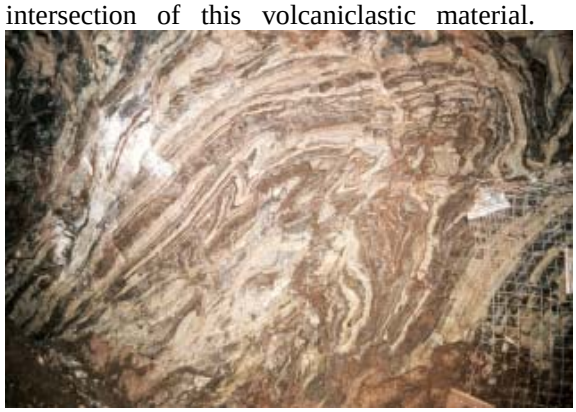

Large block of highly-contorted, laminated mafic volcaniclastics (?ash fall tuff) in ODBC, consisting of intensely sericitised layers (pale) and partially haematised layers (dark). Width of view is ~ 4 m across. (Photo 48174 MESA Journal 23; L.Reynolds 2001).

Petrographic description (slightly modified from Purvis 2003): The thin section labelled 5719 comprises fine- to coarse-grained volcaniclastic sandstone and interbedded siltstone. The sandstone contains felsic and lesser mafic clasts, and rare single-crystal quartz grains. Grains range from 0.25mm to 2mm in size and are rounded to elongate in shape. Siltstone layers also contain lithic detritus, but much finer-grained. Single-crystal quartz grains are rare (1-2%), and mostly of medium sand size, with even rarer aggregates of granular to prismatic quartz. The quartz is unstrained. Most grains are mafic to felsic volcanic lithic clasts. The more mafic clasts are mostly chlorite-rich with minor leucoxene, but some have possibly albitic plagioclase laths about 0.1-0.2 mm long as well as chlorite and leucoxene. Largely chloritised clasts, with or without diffuse leucoxene, may represent hydrothermally altered mafic or intermediate glassy fragments and include some with chlorite-filled small flattened vesicles. Intermediate clasts are more plagioclase-rich and have little or no chlorite, with hydrothermal sericite in some clasts. Pale quartz-rich or quartzofeldspathic clasts may be of felsic origin and have mostly minor sericite and leucoxene, as well as mostly fine-grained quartz and/or probably albitised feldspar. The matrix to clasts is composed of mainly chlorite, giving an overall rather melanocratic appearance to the mixed felsic-mafic volcaniclastic rock. The siltstone lenses contain detritus largely altered to sericite, quartz, chlorite and leucoxene, but these grains are too small for adequate interpretation. Iron oxides are rare, with 0.1% hematite as fine blocky grains. Patches of chalcopyrite (0.2%) and less abundant pyrite are disseminated within the matrix of the rock, but no radioactive grains were seen. No zircons are readily visible in the thin section. The presence of variably chloritised and sericitised volcanic clasts, and chlorite and sulfides in the matrix, suggest that the rock incorporated variably altered rock fragments, and was also subjected to hydrothermal processes after its clastic deposition.

Description of zircons

The sample contains abundant euhedral prismatic zircons and some fragments, with mostly sharp terminations and crystal facets. They are predominantly small- to medium-sized crystals (50 to 150 µm long), with aspect ratios up to about 3:1. The grains are brown in colour and clear, with a few hematite-stained cracks and small blebby clear and opaque (brown) inclusions. There are no visible cores. The grains emit a strong CL response (Figure 90). Most grain centres display a pronounced oscillatory zoning typical of igneous crystallisation, which is commonly also visible in transmitted light photographs. Many grains also exhibit sector zoning.

Concurrent standard data

Data for the standard are presented in Appendix 3. No data were excluded from the Pb/U calibration. The calibration exponent for this QGNG data set is 1.65, with a lower limit of 1.27 and an upper limit of 2.13 (at the 95% confidence level). Thus the nominal value of 2.0 has been used in data reduction. The 26 analyses have a 1σ scatter in $^{206}Pb/^{238}U$ of 1.63%. Element abundance calibration is based on SL13 (n = 1).

The weighted mean $^{207}Pb/^{206}Pb$ age for all 26 analyses is 1848.4 ± 2.5 Ma (MSWD = 1.8; probability of fit = .007). Experiments by Black (in press) show that where SHRIMP II sessions deliver young $^{207}Pb/^{206}Pb$ ages for zircon standards, the age discrepancy is always consistent with interferences at the ^{204}Pb mass peak, and not with mass fractionation, as previously presumed. The analyses are corrected for overcounts at mass ^{204}Pb (calculated assuming $^{\mathbf{206}}Pb/^{238}U$-$^{207}Pb$-$^{235}U$ age concordance), which forces the weighted mean $^{207}Pb/^{206}Pb$ age for QGNG to the TIMS reference value. The sample data below are also corrected for overcounts at the ^{204}Pb mass peak.

The recalculated age for QGNG becomes 1851.6 ± 2.2 Ma (MSWD = 1.3; probability of fit = .16; n = 25 of 26). In this case, *SQUID* identifies one statistical outliers, but there is no geological reason for culling this analysis (eg Pb loss). The weighted mean $^{207}Pb/^{206}Pb$ age for all 26 analyses is 1850.7 ± 2.5 Ma (MSWD = 1.6; probability of fit = .04). The slightly high MSWD indicates the scatter in the analyses is greater than that predicted by counting statistics alone. The wide spread of ages is therefore attributed to a component of instrument uncertainty, and high MSWDs for the corresponding samples are also acceptable.

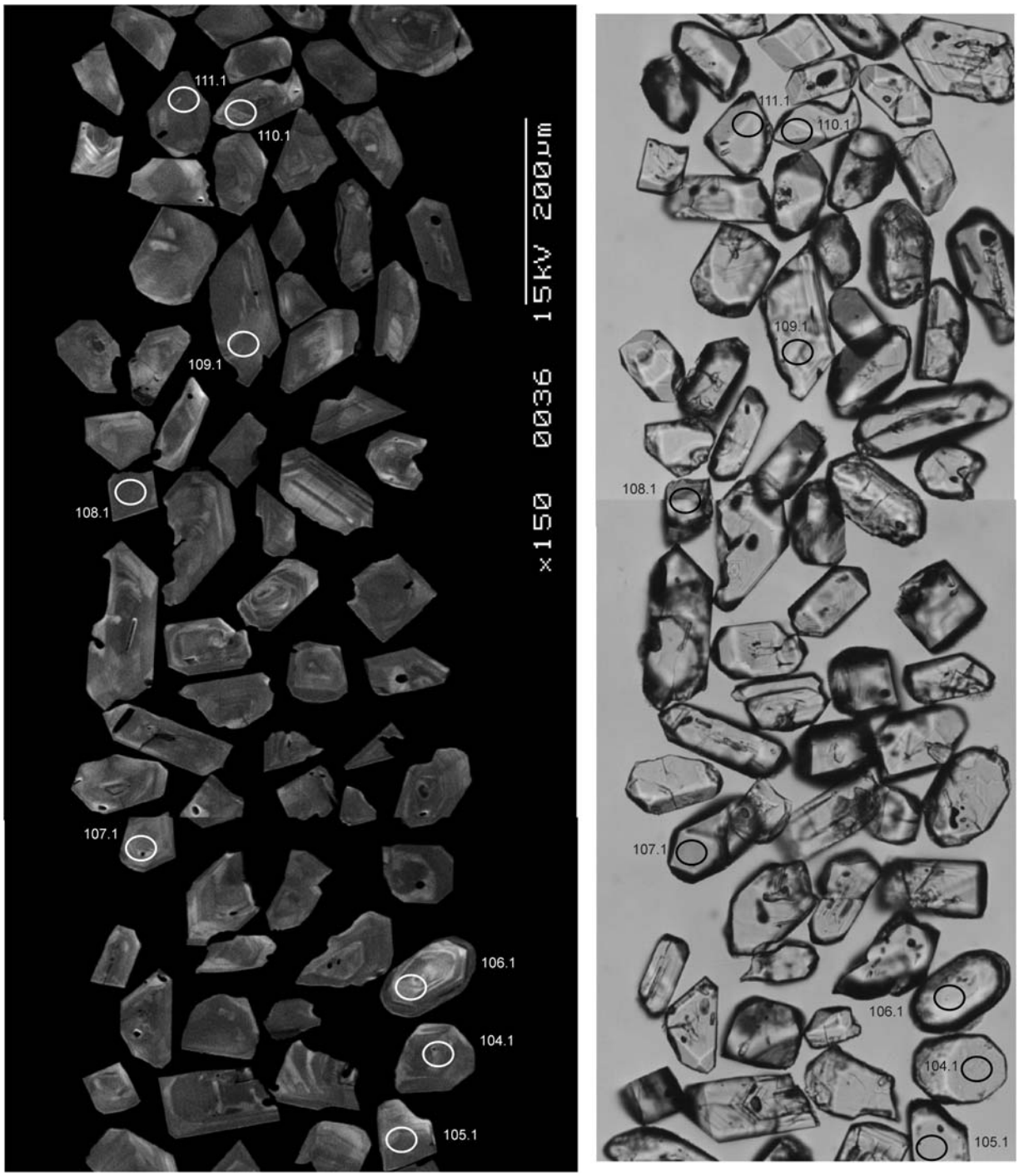

Figure 90. Representative CL (left) and transmitted light (right) images for sample 200036 6164: a block of sediment (volcaniclastic sandstone and interbedded siltstone) within the Olympic Dam Breccia Complex, Olympic Dam. SHRIMP analysis spots are labelled. Scale bar is 200 µm.

Sample data

Twenty two grains were analysed. Grain 106, with a comparatively low Th/U content and a $^{207}Pb/^{206}Pb$ age of 2677 Ma, is clearly older than the rest. A probability diagram suggests analysis 118.1 is also an outlier (Figure 91). The remaining 20 analyses yield a weighted mean $^{207}Pb/^{206}Pb$ age of 1589.4 ± 3.3 Ma. When corrected for overcounts at mass ^{204}Pb, the age becomes 1594.5 ± 3.3 Ma (MSWD = 1.4; probability of fit = 0.12; Figure 92).

Geochronological interpretation

These zircons are characterised by an unusually high percentage of solid inclusions. Some inclusions (e.g. those with apatite) are melt inclusions but some containing hematite or anatase appear to be related to the mineralising event at Olympic Dam and suggest that some of the zircons precipitated via hydrothermal processes. LA-ICPMS analyses confirm that these zircons contain very high enrichments of heavy REEs, and the Y vs Ce anomaly plot suggests a felsic igneous source (T. Mernagh, pers. comm., 2005). These observations suggest that both igneous and hydrothermal zircons (or hydrothermally altered igneous zircons) were analysed in sample 2000366164.

The $^{207}Pb/^{206}Pb$ age of 1594.5 ± 3.3 Ma is considered to be the age of crystallisation of zircon in felsic (and mafic?) igneous rocks from which the epiclastic volcanogenic sediment was partially derived. This age also may record the precipitation of zircon from metal-bearing hydrothermal fluids, if an hydrothermal origin of some of the zircons is confirmed.

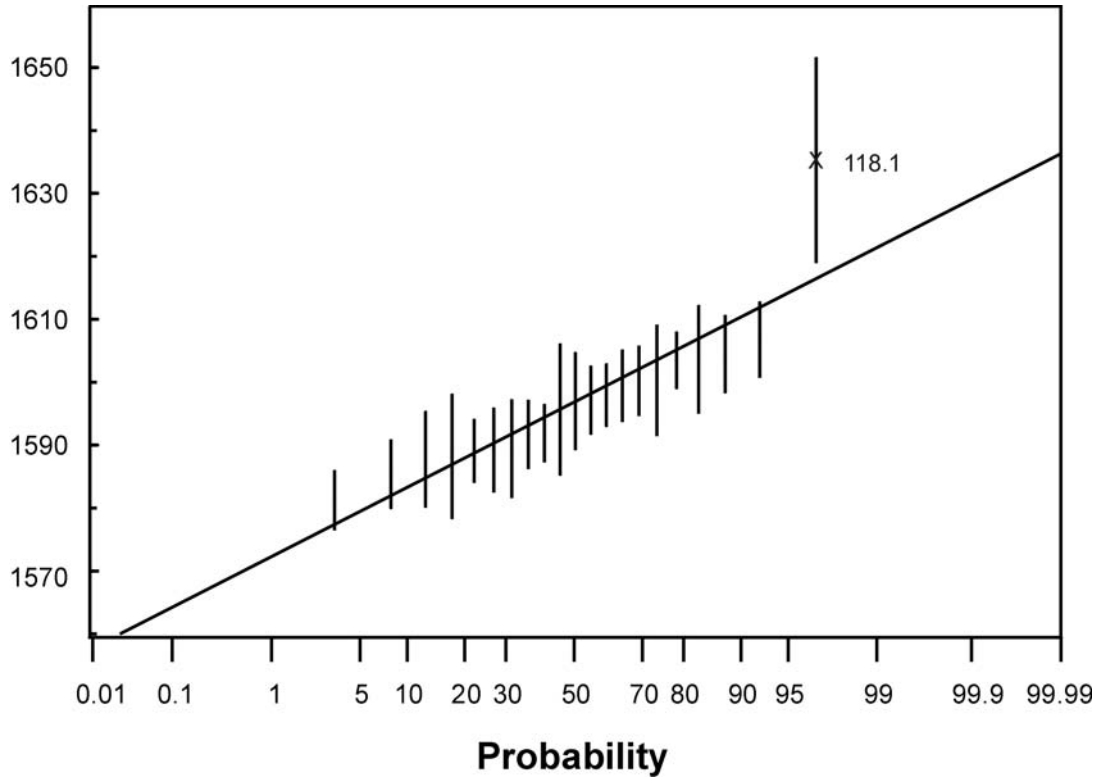

Figure 91. Probability diagram for individual zircon ages for sample 200036 6164. The oldest grain (106.1) plots above the range of this diagram. Analysis 118.1 clearly represents an outlier from the main population.

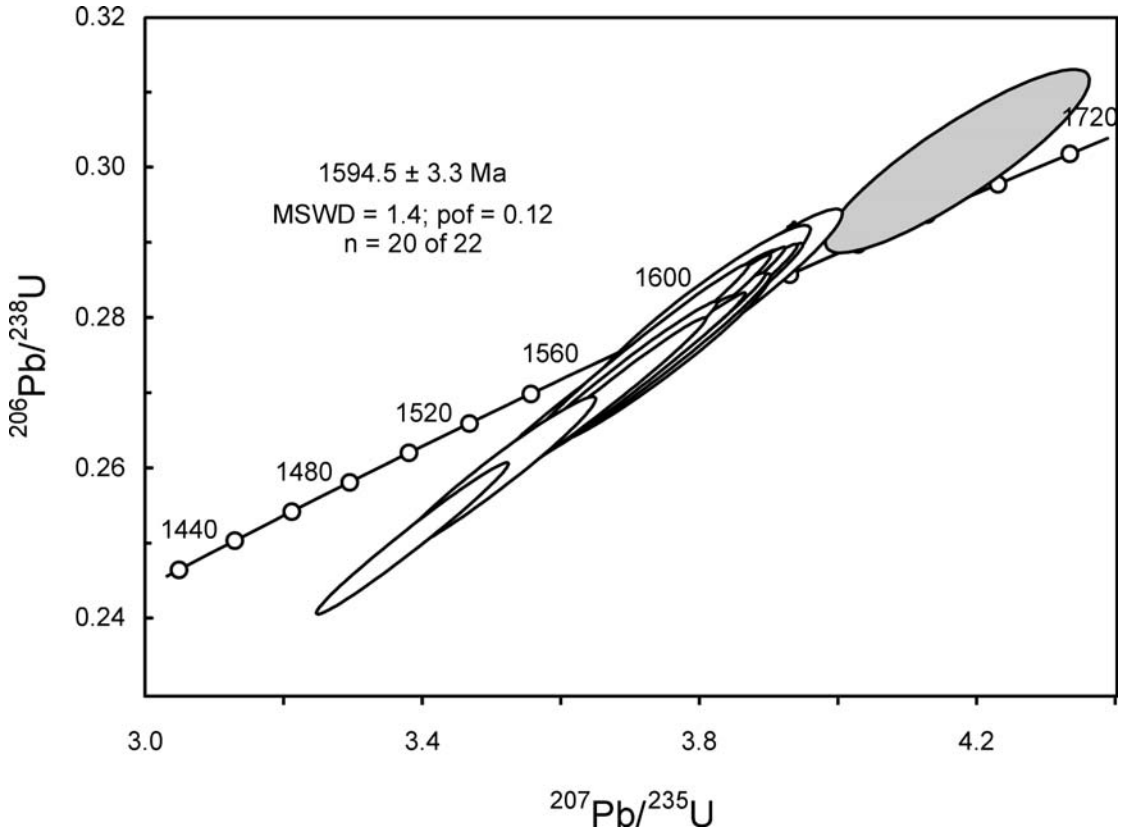

Figure 92. Concordia diagram for zircons in sample 200036 6164 showing radiogenic Pb compositions. The oldest grain (106.1) plots above the range of this diagram. Outlier 118.1 is shaded light grey.

Table 26. SHRIMP analytical results for zircon from sample 200036 6164.

Spot	U (ppm)	Th (ppm)	$^{206}Pb_c$ (%)	$^{206}Pb^*$ (ppm)	$^{206}Pb^*/^{238}U$	±	$^{207}Pb^*/^{235}U$	±	$^{207}Pb^*/^{206}Pb^*$	±	conc (%)	207Pb/206Pb Age(Ma)	±
102.1	249	212	0.00	61	0.283	0.005	3.84	0.07	0.09849	0.00055	101	1596	10
103.1	190	132	0.03	45	0.275	0.004	3.74	0.06	0.09873	0.00030	98	1600	6
104.1	203	168	0.03	49	0.279	0.004	3.79	0.06	0.09856	0.00029	99	1597	5
105.1	162	109	0.03	38	0.275	0.005	3.75	0.06	0.09895	0.00033	98	1605	6
106.1	198	92	0.06	80	0.468	0.007	11.78	0.20	0.18265	0.00035	92	2677	3
107.1	184	123	0.07	43	0.274	0.004	3.74	0.06	0.09891	0.00045	97	1604	9
108.1	221	181	0.01	52	0.275	0.005	3.75	0.07	0.09873	0.00046	98	1600	9
109.1	195	141	0.01	47	0.281	0.004	3.80	0.06	0.09809	0.00052	100	1588	10
110.1	226	175	0.08	49	0.251	0.004	3.38	0.06	0.09795	0.00028	91	1585	6
111.1	285	181	0.04	68	0.276	0.004	3.72	0.06	0.09773	0.00024	99	1581	5
112.1	326	281	0.13	75	0.269	0.004	3.66	0.06	0.09861	0.00027	96	1598	5
113.1	282	227	0.02	67	0.277	0.004	3.75	0.06	0.09814	0.00026	99	1589	5
114.1	196	159	0.03	46	0.272	0.004	3.70	0.06	0.09869	0.00030	97	1599	6
115.1	193	128	0.00	46	0.279	0.005	3.81	0.27	0.09910	0.00684	99	1600	6
116.1	323	255	0.02	76	0.272	0.004	3.71	0.06	0.09890	0.00024	97	1604	5
117.1	264	187	0.05	63	0.278	0.004	3.76	0.06	0.09815	0.00035	99	1589	7
118.1	183	130	0.95	48	0.301	0.005	4.17	0.08	0.10061	0.00089	104	1635	16
119.1	151	76	0.08	36	0.274	0.005	3.73	0.06	0.09856	0.00040	98	1597	8
120.1	419	241	0.10	93	0.259	0.004	3.50	0.06	0.09807	0.00040	93	1588	8
121.1	319	253	0.03	76	0.278	0.004	3.77	0.06	0.09829	0.00024	99	1592	5
122.1	172	122	0.21	40	0.269	0.005	3.64	0.06	0.09816	0.00041	97	1589	8

Data are 1σ precision. All Pb data are common Pb corrected based on measured ^{204}Pb (after Stacey and Kramer 1975).
Analysis date 30/4/2003; SHRIMP II

200036 6165: chloritised mafic-ultramafic dyke, Olympic Dam

1:250,000 sheet: Andamooka (SH5312)

1:100,000 sheet: Mattaweara (6237)

MGA: 681641 E 6629439 N

Location: The sample was taken from Western Mining Corporation diamond drillhole RD 1408, depth interval 704-708 m.

Mount: Z4125

Description: Geological context: The Olympic Dam Breccia Complex (ODBC) is intruded by a variety of ultramafic, mafic and felsic dykes. In the upper part of the ODBC, dykes are typically narrow (<1 m), coherent bodies with irregular, tentacular or wispy morphologies (Reeve et al., 1990: see photograph). The more mafic dykes have undergone intense, texturally-destructive sericite and haematite alteration, and their intrusive origins are generally interpreted from morphology, geometry and geochemistry. Alteration and local mineralisation of dykes, quench-fragmentation textures, reworked equivalents within breccia zones, juvenile fragments, and preservation of dykes within the root zones of diatreme structures indicate that intrusive activity was probably contemporaneous with hydrothermal activity (Reynolds 2001). Sample 200036 6165 is from drillcore intersecting what is interpreted to be one of these mafic-ultramafic dykes that has been intensely chloritised (K. Ehrig pers. comm.).

Intensely sericitised mafic dyke (yellowish brown) within a haematite-rich breccia. View is ~ 2 m high. (Photo 48175 MESA Journal 23; L. Reynolds 2001).

Petrographic description: The thin section labelled 5718 is a laminated volcaniclastic rock with early chlorite-filled fractures and microfaults (Purvis, 2004). It is likely that this thin section is from an interval nearby but not within the interval of the analysed zircon sample, which is a strongly chloritised dyke rock of originally mafic/ultramafic composition (similar to the dyke in the figure, above). For this reason the petrographic description of thin section 5718 is not included here.

Description of zircons

The sample contains euhedral prismatic zircons with sharp to rounded edges and terminations. Zircons were scarce in the least magnetic fractions, and their abundance increased in the more magnetic fractions. The sample contains abundant apatite, with about one zircon per several thousand apatite grains. The zircons are small (30 to 100 µm long), with aspect ratios up to about 3:1. The grains are a light purple-brown colour and clear, with bleb-shaped clear and opaque (brown) inclusions, and a few hematite-stained cracks. They contain no visible cores. The grains emit a strong CL response. Some grains emit a homogenous signature, but most display a pronounced oscillatory zoning typical of igneous crystallisation (Figure 93). In many grains, zoning is also visible in transmitted light photographs.

Concurrent standard data

Data for the standard are presented in Appendix 3. No data were excluded from the Pb/U calibration. The calibration exponent for this QGNG data set is 1.65, with a lower limit of 1.27 and an upper limit of 2.13 (at the 95% confidence level). Thus the nominal value of 2.0 has been used in data reduction. The 26 analyses have a 1σ scatter in $^{206}Pb/^{238}U$ of 1.63%. Element abundance calibration is based on SL13 (n = 1).

The weighted mean $^{207}Pb/^{206}Pb$ age for all 26 analyses is 1848.4 ± 2.5 Ma (MSWD = 1.8; probability of fit = .007). Experiments by Black (in press) show that where SHRIMP II sessions deliver young $^{207}Pb/^{206}Pb$ ages for zircon standards, the age discrepancy is always consistent with interferences at the ^{204}Pb mass peak, and not with mass fractionation, as previously presumed. The analyses are corrected for overcounts at mass ^{204}Pb (calculated assuming $^{\mathbf{206}}Pb/^{238}U$-$^{207}Pb$-$^{235}U$ age concordance), which forces the weighted mean $^{207}Pb/^{206}Pb$ age for QGNG to the TIMS reference value. The sample data below are also corrected for overcounts at the ^{204}Pb mass peak.

The recalculated age for QGNG becomes 1851.6 ± 2.2 Ma (MSWD = 1.3; probability of fit = .16; n = 25 of 26). In this case, *SQUID* identifies one statistical outliers, but there is no geological reason for culling this analysis (eg Pb loss). The weighted mean $^{207}Pb/^{206}Pb$ age for all 26 analyses is 1850.7 ± 2.5 Ma (MSWD = 1.6; probability of fit = .04). The slightly high MSWD indicates the scatter in the analyses is greater than that predicted by counting statistics alone. The wide spread of ages is therefore attributed to a component of instrument uncertainty, and high MSWDs for the corresponding samples are also acceptable.

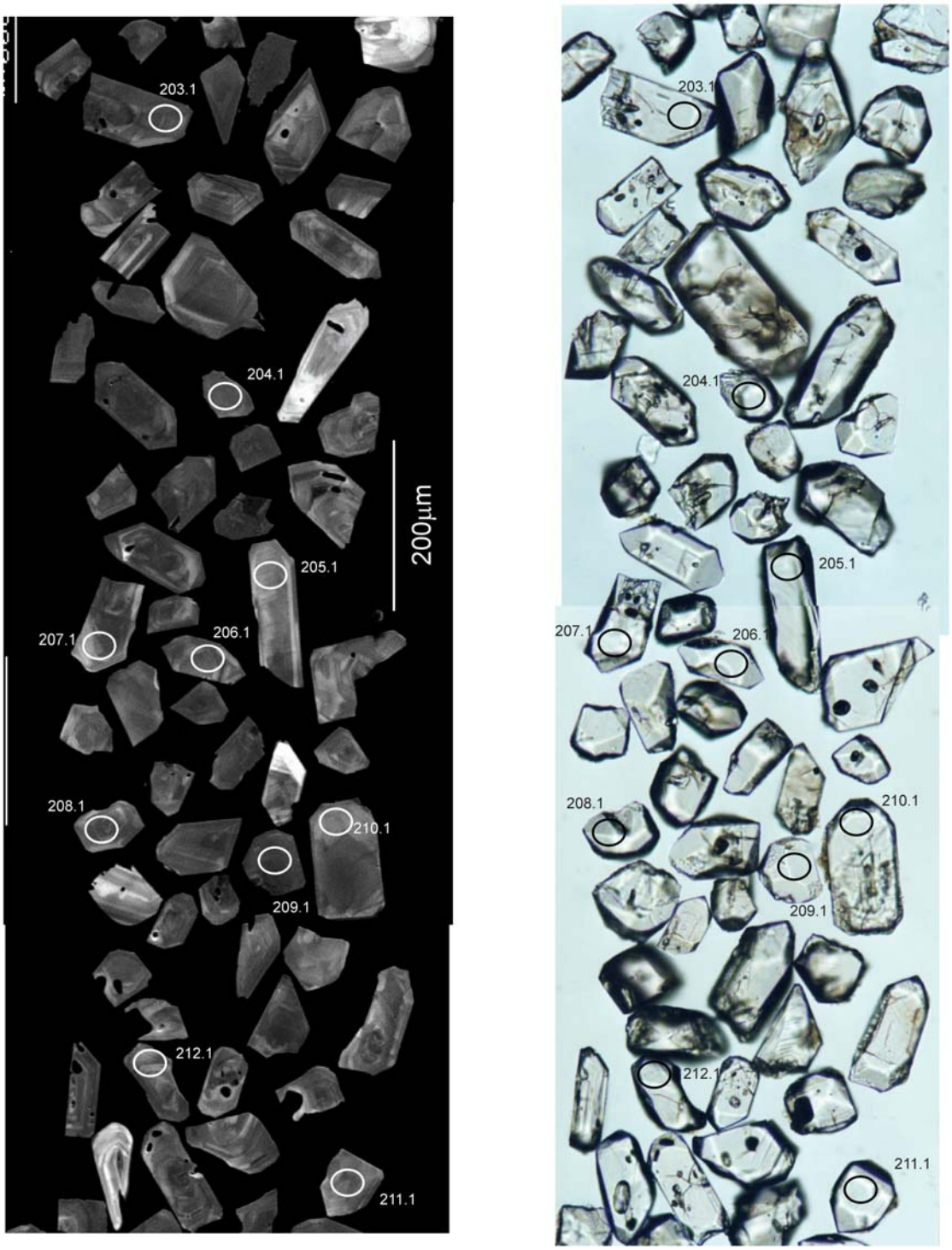

Figure 93. Representative CL (left) and transmitted light (right) images for sample 200036 6165: a block of laminated basaltic sediment within the Olympic Dam Breccia Complex, Olympic Dam. SHRIMP analysis spots are labelled. Scale bar is 200 µm.

Sample data

Twenty two grains were analysed. The data distribution is simple, with all analyses clustering in a tight group near concordia (Figure 94). The analyses yield a weighted mean $^{207}Pb/^{206}Pb$ age of 1592.4 ± 3.5 Ma. When corrected for overcounts at mass ^{204}Pb, the age becomes 1597.4 ± 3.6 Ma (MSWD = 1.6; probability of fit = .04). The slightly high MSWD is acceptable, as it accords with the excess scatter in the standard recorded during this session.

Geochronological interpretation

These zircons are characterised by melt inclusions of apatite and vesuvianite but some contain hematite + carbon or anatase or chalcopyrite. Rare fluid inclusions were also observed in a few zircons. These observations suggest that some of the zircon precipitated via hydrothermal processes. LA-ICPMS analyses confirm that these zircons contain very high enrichments of heavy REEs and the Y vs Ce anomaly plot suggests a felsic source (T. Mernagh, pers. comm., 2005).

The $^{207}Pb/^{206}Pb$ age of 1597.4 ± 3.6 Ma is is considered to be the crystallisation age of zircon in the altered mafic/ultramafic dyke, although it is not clear whether the zircons crystallised from the mafic/ultramafic magma or were inherited. This age also may record the precipitation of zircon from metal-bearing hydrothermal fluids, if an hydrothermal origin of some of the zircons is confirmed.

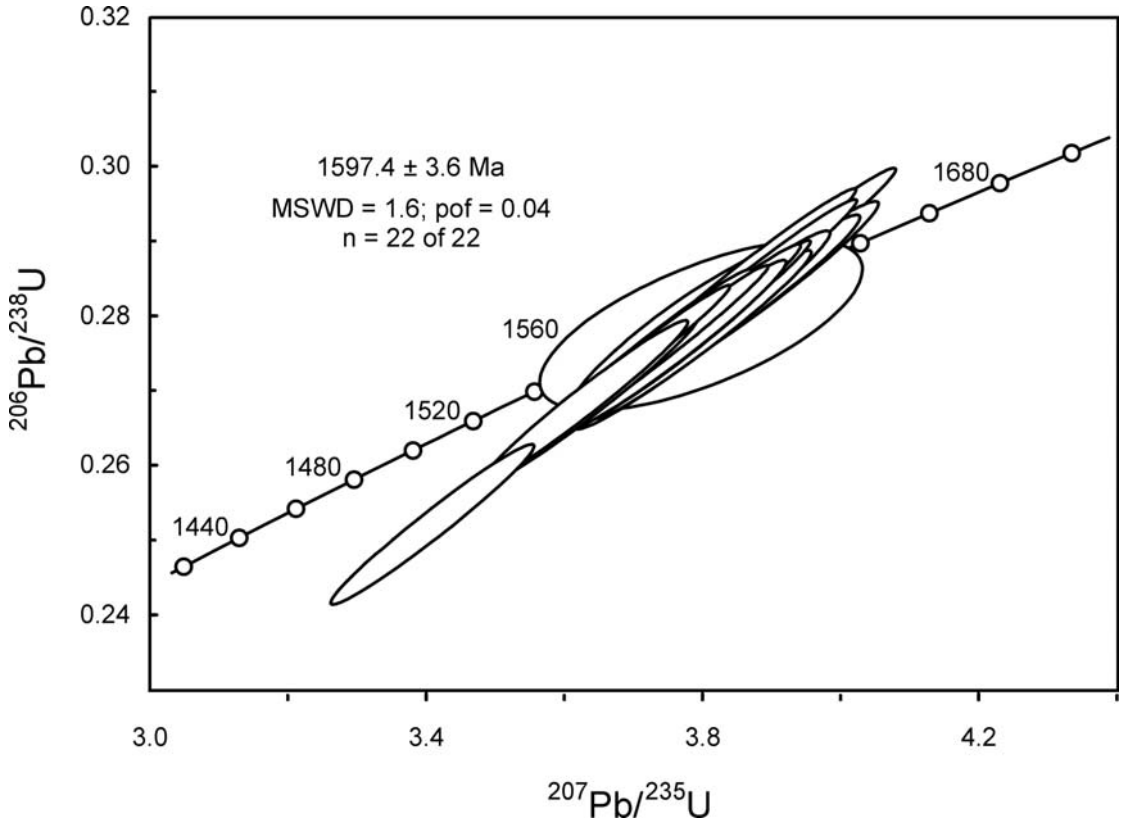

Figure 94. Concordia diagram for zircons in sample 200036 6165 showing radiogenic Pb compositions.

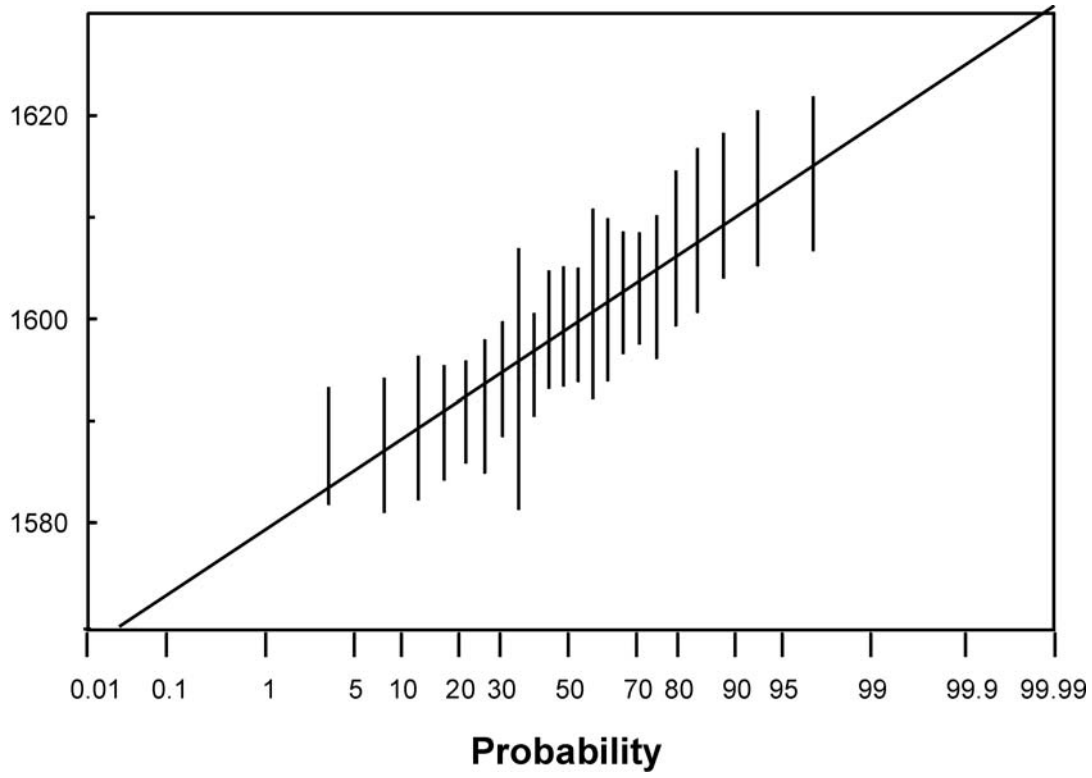

Figure 95. Probability diagram for individual zircon ages for sample 200036 6165.

Table 27. SHRIMP analytical results for zircon from sample 200036 6165.

Spot	U (ppm)	Th (ppm)	$^{206}Pb_c$ (%)	$^{206}Pb^*$ (ppm)	$^{206}Pb^*/^{238}U$	±	$^{207}Pb^*/^{235}U$	±	$^{207}Pb^*/^{206}Pb^*$	±	conc (%)	207Pb/206Pb Age(Ma)	±
201.1	99	88	0.05	23	0.276	0.005	3.78	0.07	0.09918	0.00043	98	1609	8
202.1	174	110	0.03	43	0.288	0.005	3.92	0.07	0.09866	0.00031	102	1599	6
203.1	236	141	0.02	56	0.276	0.004	3.74	0.06	0.09848	0.00027	98	1596	5
204.1	182	112	0.04	44	0.284	0.005	3.87	0.07	0.09868	0.00030	101	1599	6
205.1	136	83	--	33	0.282	0.005	3.87	0.07	0.09940	0.00041	99	1613	8
206.1	204	153	0.02	49	0.279	0.005	3.80	0.06	0.09887	0.00029	99	1603	6
207.1	176	116	0.04	42	0.278	0.005	3.79	0.06	0.09868	0.00031	99	1599	6
208.1	218	167	--	51	0.275	0.004	3.73	0.06	0.09840	0.00030	98	1594	6
209.1	256	151	0.00	60	0.273	0.005	3.70	0.21	0.09820	0.00520	98	1586	5
210.1	149	99	0.08	34	0.269	0.005	3.63	0.06	0.09806	0.00034	97	1588	7
211.1	230	206	0.00	55	0.278	0.004	3.78	0.07	0.09840	0.00068	99	1594	13
212.1	171	111	0.04	40	0.269	0.005	3.64	0.06	0.09826	0.00034	96	1591	7
213.1	233	166	0.01	57	0.284	0.005	3.89	0.07	0.09947	0.00041	100	1614	8
214.1	216	154	0.08	51	0.275	0.005	3.72	0.06	0.09806	0.00030	99	1588	6
215.1	152	142	0.01	37	0.281	0.005	3.83	0.07	0.09879	0.00049	100	1602	9
216.1	176	120	0.01	42	0.276	0.005	3.76	0.06	0.09882	0.00042	98	1602	8
217.1	201	147	0.02	49	0.285	0.005	3.86	0.07	0.09818	0.00029	102	1590	6
218.1	212	146	--	51	0.280	0.004	3.83	0.07	0.09908	0.00041	99	1607	8
219.1	235	137	0.01	56	0.278	0.005	3.80	0.06	0.09931	0.00038	98	1611	7
220.1	200	144	0.04	47	0.276	0.005	3.77	0.06	0.09888	0.00038	98	1603	7
221.1	212	133	0.00	51	0.279	0.005	3.80	0.09	0.09890	0.00188	99	1596	6
222.1	241	218	0.09	52	0.252	0.004	3.41	0.06	0.09815	0.00037	91	1589	7

Data are 1σ precision. All Pb data are common Pb corrected based on measured ^{204}Pb (after Stacey and Kramer 1975).
Analysis date 30/4/2003; SHRIMP II

200036 6166: sericitised feldspathic dyke, Olympic Dam

1:250,000 sheet: Andamooka (SH5312)

1:100,000 sheet: Mattaweara (6237)

MGA: 680209 E 6631024 N

Location: The sample was taken from Western Mining Corporation diamond drillhole RU45-4425, depth interval 100.5-102.2 m.

Description: Geological context: Sample 200036 6166 is from drillcore intersecting what is interpreted to be a mafic-ultramafic dyke (as described above for sample 20036 6165), which has been intensely sericitised (K. Ehrig, pers. comm.). In drillcore, sericitised dykes of this type are a distinctive light green colour and disintegrate rapidly following surface exposure.

Petrographic description (modified after Purvis 2003): This sample is a sericitised dyke, possibly derived from a feldspathic pegmatite or diorite to syenite dyke. Unlike the field interpretation of a mafic/ultramafic dyke, there is no petrographic evidence in this sample for the former presence of abundant mafic minerals. The geochemistry of the sample permits as much as 85% sericite as the main mineral apart from iron and /or titanium-rich minerals, quartz and minerals containing REE, Zr and P. Pale yellow, probably phengitic sericite is the most abundant mineral in this sample, with possible microcrystalline quartz. There are areas to 10 x 8 mm rich in iron-stained granular to prismatic K-spar, possibly Ba-rich as well as mostly minor quartz. The K-spar is 0.5 to 4 mm in grainsize and commonly fractured, veined and replaced by sericite. Separate quartz-rich lenses occur, with prismatic quartz to 1 mm in grainsize. Rare carbonate was noted, as rhombs 0.05 mm to 0.2 mm long intergrown with the K-spar. The geochemistry suggests 0.5-0.6% uranium-rich monazite and 0.1% zircon (~0.33% total REE and 0.08% Zr). Zircon is present in clusters of relatively coarse (up to 0.3 mm), clear, euhedral crystals within the sericite. Traces of chalcopyrite and pyrite are present in the sample, and ten zircon grains in the thin section were observed to contain inclusions of chalcopyrite within growth zones. The original lithology is uncertain but the sericite is probably after feldspar, suggesting a feldspathic pegmatite or a feldspar-rich igneous lithology such as diorite, monzonite or syenite.

Mount: Z4125

Description of zircons

This sample contains mostly fragments of larger prismatic zircon grains. Where terminations are preserved, they are sharp to rounded. The zircon yield was not abundant, and the sample also contains abundant apatite and barite in the non-magnetic fraction. The zircon fragments range from 50 µm to 300 µm in size. They are brown in colour, with good clarity and few cracks. They contain rare bleb-shaped clear and opaque (brown) inclusions, and no visible cores. The grains emit a strong CL response. Some grains are homogenous, but most display a pronounced oscillatory zoning typical of igneous crystallisation (Figure 96). This zoning is rarely visible in transmitted light photographs.

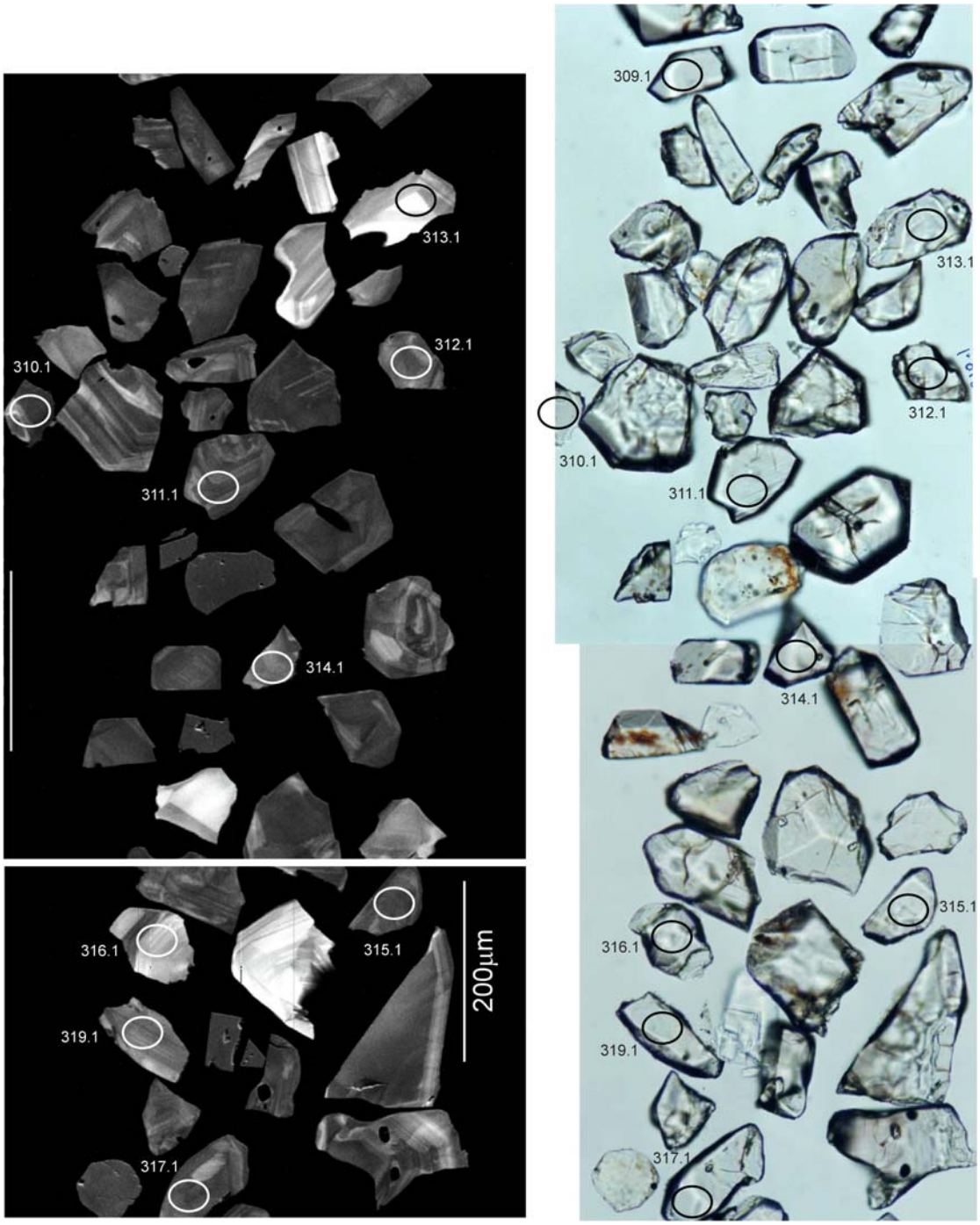

Figure 96. Representative CL (left) and transmitted light (right) images for sample 200036 6166: a sericitised dyke intruding the Olympic Dam Breccia Complex, Olympic Dam. SHRIMP analysis spots are labelled. Scale bar is 200 µm.

Concurrent standard data

Data for the standard are presented in Appendix 3. No data were excluded from the Pb/U calibration. The calibration exponent for this QGNG data set is 1.65, with a lower limit of 1.27 and an upper limit of 2.13 (at the 95% confidence level). Thus the nominal value of 2.0 has been used in data reduction. The 26 analyses have a 1σ scatter in $^{206}Pb/^{238}U$ of 1.63%. Element abundance calibration is based on SL13 (n = 1).

The weighted mean $^{207}Pb/^{206}Pb$ age for all 26 analyses is 1848.4 ± 2.5 Ma (MSWD = 1.8; probability of fit = .007). Experiments by Black (in press) show that where SHRIMP II sessions deliver young $^{207}Pb/^{206}Pb$ ages for zircon standards, the age discrepancy is always consistent with interferences at the ^{204}Pb mass peak, and not with mass fractionation, as previously presumed. The analyses are corrected for overcounts at mass ^{204}Pb (calculated assuming $^{\mathbf{206}}Pb/^{238}U$-$^{207}Pb$-$^{235}U$ age concordance), which forces the weighted mean $^{207}Pb/^{206}Pb$ age for QGNG to the TIMS reference value. The sample data below are also corrected for overcounts at the ^{204}Pb mass peak.

The recalculated age for QGNG becomes 1851.6 ± 2.2 Ma (MSWD = 1.3; probability of fit = .16; n = 25 of 26). In this case, *SQUID* identifies one statistical outliers, but there is no geological reason for culling this analysis (eg Pb loss). The weighted mean $^{207}Pb/^{206}Pb$ age for all 26 analyses is 1850.7 ± 2.5 Ma (MSWD = 1.6; probability of fit = .04). The slightly high MSWD indicates the scatter in the analyses is greater than that predicted by counting statistics alone. The wide spread of ages is therefore attributed to a component of instrument uncertainty, and high MSWDs for the corresponding samples are also acceptable.

Sample data

Twenty nine grains were analysed. With a high MSWD of 5.6, the analyses do not conform to a normal distribution. A probability diagram suggests the two youngest, analyses (320.1 and 312.1) lie below the main data group (Figure 97). These analyses are discordant (Figure 98), suggesting the grains are affected by Pb loss. The probability diagram also suggests three analyses are older than the main data cluster (317.1, 327.1 and 304.1). The remaining 24 analyses yield a weighted mean $^{207}Pb/^{206}Pb$ age of 1590.8 ± 3.7 Ma. When corrected for overcounts at mass ^{204}Pb, the age becomes 1596.0 ± 4.4 Ma (MSWD = 2.0; probability of fit = .002). The high MSWD indicates there is still excess scatter in the population, but there are no other obvious statistical outliers.

Geochronological interpretation

These zircons are characterised by an unusually high percentage of solid inclusions. Some inclusions are hematite or anatase or chalcopyrite, suggesting that at least some of the zircon precipitated via hydrothermal processes. LA-ICPMS analyses confirm that these zircons contain very high enrichments of heavy REEs. The Y vs Ce anomaly plot show a very large scatter in Ce/Ce* values which differ from the ratios of common mafic or felsic igneous rocks (T. Mernagh, pers. comm., 2005).

The $^{207}Pb/^{206}Pb$ age of 1596.0 ± 4.4 Ma is considered to be either the age of precipitation of the zircons from metal-bearing hydrothermal fluids, or the age of igneous zircons that were hydrothermally modified during sericitisation of the feldspathic dyke.

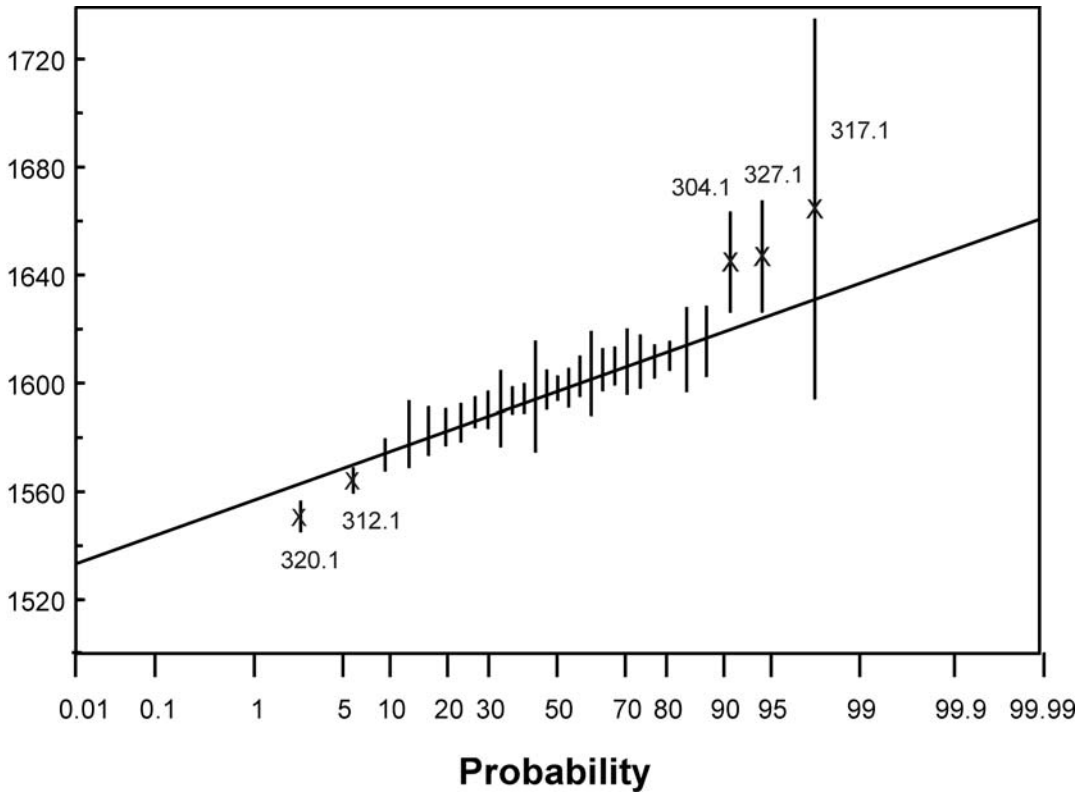

Figure 97. Probability diagram for individual zircon ages for sample 200036 6166. Outliers are marked by a cross.

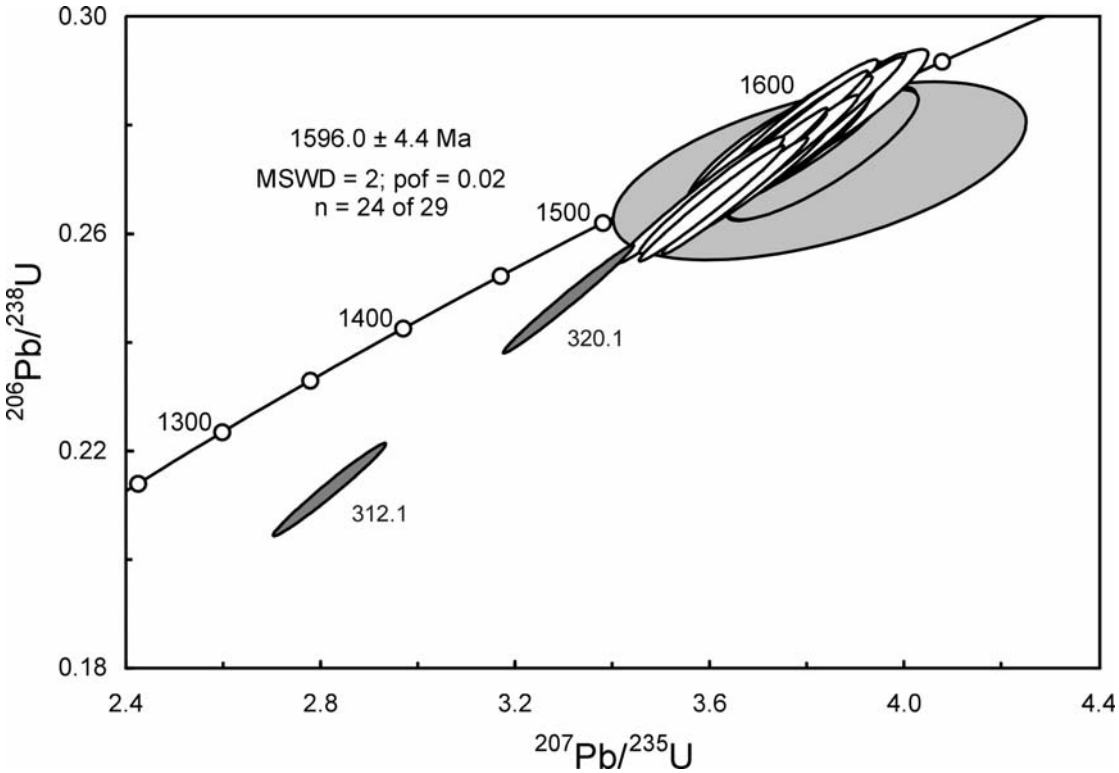

Figure 98. Concordia diagram for zircons in sample 200036 6166 showing radiogenic Pb compositions. White ellipses represent analyses used in the weighted mean age calculation. Discordant analyses are dark grey. Inherited grains are light grey.

Table 28. SHRIMP analytical results for zircon from sample 200036 6166.

Spot	U (ppm)	Th (ppm)	$^{206}Pb_c$ (%)	$^{206}Pb^*$ (ppm)	$^{206}Pb^*/^{238}U$	±	$^{207}Pb^*/^{235}U$	±	$^{207}Pb^*/^{206}Pb^*$	±	conc (%)	207Pb/206Pb Age(Ma)	±
301.1	127	102	0.09	30	0.276	0.005	3.73	0.06	0.09795	0.00037	99	1586	7
302.1	206	202	0.03	47	0.267	0.005	3.65	0.06	0.09925	0.00029	95	1610	5
303.1	40	44	0.19	9	0.275	0.005	3.71	0.07	0.09773	0.00065	99	1581	12
304.1	20	33	0.27	5	0.275	0.005	3.83	0.08	0.10120	0.00111	95	1647	21
305.1	79	101	0.03	19	0.283	0.005	3.88	0.07	0.09954	0.00070	99	1615	13
306.1	230	205	0.04	52	0.265	0.005	3.56	0.06	0.09734	0.00031	96	1574	6
307.1	168	133	0.01	40	0.281	0.005	3.79	0.06	0.09779	0.00047	101	1582	9
308.1	185	134	0.03	45	0.282	0.005	3.84	0.07	0.09885	0.00040	100	1603	8
309.1	155	99	--	37	0.275	0.005	3.75	0.06	0.09914	0.00033	97	1608	6
310.1	251	226	0.00	59	0.276	0.004	3.76	0.07	0.09891	0.00082	98	1604	16
311.1	248	156	0.02	58	0.272	0.004	3.69	0.06	0.09838	0.00027	97	1594	5
312.1	314	229	0.06	67	0.248	0.004	3.31	0.06	0.09684	0.00024	91	1564	5
313.1	66	53	0.05	16	0.276	0.005	3.78	0.07	0.09914	0.00064	98	1608	12
314.1	166	118	0.09	40	0.280	0.005	3.80	0.07	0.09859	0.00038	99	1598	7
315.1	350	229	--	83	0.276	0.005	3.73	0.06	0.09820	0.00036	99	1590	7
316.1	55	60	0.10	13	0.280	0.005	3.79	0.07	0.09822	0.00074	100	1591	14
317.1	129	103	0.00	30	0.272	0.007	3.83	0.17	0.10220	0.00388	93	1606	7
317.1	195	146	--	47	0.281	0.005	3.84	0.07	0.09905	0.00038	99	1606	7
318.1	216	184	0.05	52	0.279	0.004	3.77	0.06	0.09815	0.00029	100	1589	6
319.1	130	86	0.05	31	0.281	0.005	3.83	0.07	0.09898	0.00042	99	1605	8
320.1	493	299	0.11	90	0.213	0.004	2.82	0.05	0.09616	0.00029	80	1551	6
321.1	67	58	0.04	16	0.278	0.005	3.81	0.07	0.09938	0.00082	98	1612	16
322.1	157	119	0.02	38	0.278	0.005	3.78	0.06	0.09863	0.00037	99	1598	7
323.1	98	106	0.01	23	0.275	0.005	3.74	0.07	0.09850	0.00108	98	1595	20
324.1	223	179	0.03	51	0.266	0.005	3.61	0.06	0.09842	0.00029	95	1594	5
325.1	336	222	0.01	77	0.267	0.004	3.60	0.06	0.09786	0.00036	96	1584	7
326.1	356	240	0.00	83	0.271	0.005	3.69	0.06	0.09862	0.00024	97	1598	5
327.1	47	49	0.05	11	0.275	0.005	3.83	0.08	0.10110	0.01011	95	1645	19
328.1	142	158	0.01	33	0.270	0.005	3.70	0.06	0.09914	0.00053	96	1608	10

Data are 1σ precision. All Pb data are common Pb corrected based on measured ^{204}Pb (after Stacey and Kramer 1975).
Analysis date 30/4/2003; SHRIMP II

Discussion of results

The following section evaluates the existing TIMS and SHRIMP ages for the Burgoyne Batholith and Olympic Dam Breccia Complex (ODBC) in the context of the new age determinations for magmatism and mineralisation at Olympic Dam presented in this report (Table 29).

Figure 99 shows probability density plots of U-Pb ages available for the Hiltaba Suite (including the ODBC) and Gawler Range Volcanics in the Olympic Dam region. The ages range between 1584 and 1613 Ma, and do not conform to a normal distribution. This pattern might suggest magmatism occurred over a prolonged period involving several distinct emplacement events. However, the historical data span this age range for the Roxby Downs Granite alone (Figure 99), and prolonged magmatism (over *ca* 40 m.y.) is highly unlikely within a single small pluton. The spread of ages is more likely to reflect disturbance in the isotope systematics of material within the hydrothermal system.

Analyses of the hydrothermally altered and brecciated Roxby Downs Granite are less precise than those of less altered plutons within the Burgoyne Batholith (Figure 99). The oldest crystallisation ages from drill holes RD80 and RD87 (1606 ± 7 Ma and 1613 ± 20 Ma, respectively) derive from extremely altered samples that yielded notably discordant and reversely discordant zircon fractions. The discordance reflects problems with barite contamination and high common Pb levels (Mortimer et al. 1988a), and the TIMS analyses are probably inaccurate, with their inclusion giving a misleading representation of the duration of felsic magmatism. The remaining ages lie within a narrower range (1588-1598 Ma). The age distribution is biased towards the most precise analysis at 1588 ± 4 Ma (TIMS), which Creaser and Cooper (1993) interpreted as the crystallisation age of the Roxby Downs Granite. This age falls below the weighted mean age of the ODBC (Figure 99), whereas field relationships demonstrate that components of the ODBC cannot be older than the granite.

Johnson (1993) suggested the apparent age discrepancy between the 1588 ± 4 Ma TIMS age for the Roxby Downs Granite and his older SHRIMP I ages (1595 ± 11 and 1598 ± 14 Ma) may relate to a hydride contribution to ^{207}Pb counts during SHRIMP I analysis (although there is no evidence of this in the zircon standard). However, in light of the new ages presented in this study, it seems likely that the older SHRIMP analyses are a better estimate of the crystallisation age of the pluton. The SHRIMP technique allows for careful selection of grains to avoid areas of lattice damage and the subsequent effects of Pb loss, whereas the younger TIMS age of 1588 ± 4 Ma may reflect a component of Pb loss, even though the analysed zircons were heavily abraded. The SHRIMP ages are in better agreement with the more tightly constrained ages from unmineralised and comparatively unaltered plutons and dykes within the Burgoyne Batholith.

Ages for the unmineralised plutons lie within a narrower range (between 1590 and 1598 Ma; Figure 99). The 1598 Ma age of quartz monzonite from Wirrda Well (WRD6) is nominally older than all other granitoids within this group at the 95% confidence level. This TIMS U-Pb age is based on a single titanite fraction (Creaser and Cooper 1993). The remaining ages range between 1590 and 1596 Ma and combine to yield a weighted mean age of 1593.3±1.7 (MSWD = 0.87, probability of fit = 0.50; n=6). Given that the U-Pb isotope systematics should be least disturbed in

these less altered samples, this narrower age range of about 6 Ma may represent more accurately the period of magmatic activity in the Olympic Dam region. The age of magmatism cannot be distinguished from the age of hydrothermal zircons within the ODBC (1596.1±2.2 Ma; MSWD = 0.56, probability of fit = 0.57; n=3 samples).

The microdiorite dyke is the first mafic component of Hiltaba Suite age to be dated directly, confirming empirically, the association of mafic and felsic magmatism in the Olympic Dam region. Statistically, its age of 1595.6 ± 3.8 Ma is indistinguishable from 1594.4 ± 3.4 Ma, obtained from the quartz monzonite at Horn Ridge. Both analyses lie within the existing body of data for the Burgoyne Batholith, confirming they are contemporary with the Roxby Downs Granite. The result extends the known limit of mafic magmatism associated with the Hiltaba Suite, beyond the perimeters of the orebody.

Table 29: Summary of available U-Pb zircon ages for the Hiltaba Suite in the Olympic Dam region.

Sample/Drillhole	Lithology	Age	Method	Reference
Hiltaba Suite: Roxby Downs Granite				
RD161	Roxby Downs Granite	1588±4	TIMS	Creaser & Cooper 1993
RD80	quartz syenite	1606±7	TIMS	Mortimer et al 1988a
RD87	quartz syenite	1613±20	TIMS	Mortimer et al 1988a
29NB49SDr	granite microbreccia	1595±11	SHRIMP	Johnson 1993
32LK58NWD	granite microbreccia	1598±14	SHRIMP	Johnson 1993
Olympic Dam Breccia Complex				
200036 6164	hydrothermal zircons	1594.8±3.5	SHRIMP	this study
200036 6165	hydrothermal zircons	1597.5±3.7	SHRIMP	this study
200036 6166	hydrothermal zircons	1596.0±4.0	SHRIMP	this study
dykes and diatremes intruding the ODBC				
33NB53WDr	lapilli tuff in diatreme	1597±8	SHRIMP	Johnson 1993
RD647	felsic 'peperite' dyke	1584±20	SHRIMP	Johnson 1993
RD32	felsic 'peperite' dyke	1592±8	SHRIMP	Johnson 1993
Hiltaba Suite: regional data from the Burgoyne Batholith				
WRD6	quartz monzonite	1598±2.3	TIMS	Creaser & Cooper 1993
OFD3	quartz monzonite	1590±10	TIMS	Creaser & Cooper 1993
PD3	quartz monzodiorite	1590±5	TIMS	Mortimer et al 1988a
BLD2	quartz monzonite	1590±5	TIMS	Creaser & Cooper 1993
WRD3	quartz monzodiorite	1593±3.4	TIMS	Creaser & Cooper 1993
200036 6000	quartz monzonite	1594.4±3.4	SHRIMP	this study
200036 6005	mafic dyke	1595.6±3.8	SHRIMP	this study
Gawler Range Volcanics				
ACD5	quartz latite	1591±10	TIMS	Mortimer et al 1988a, Creaser & Cooper 1993

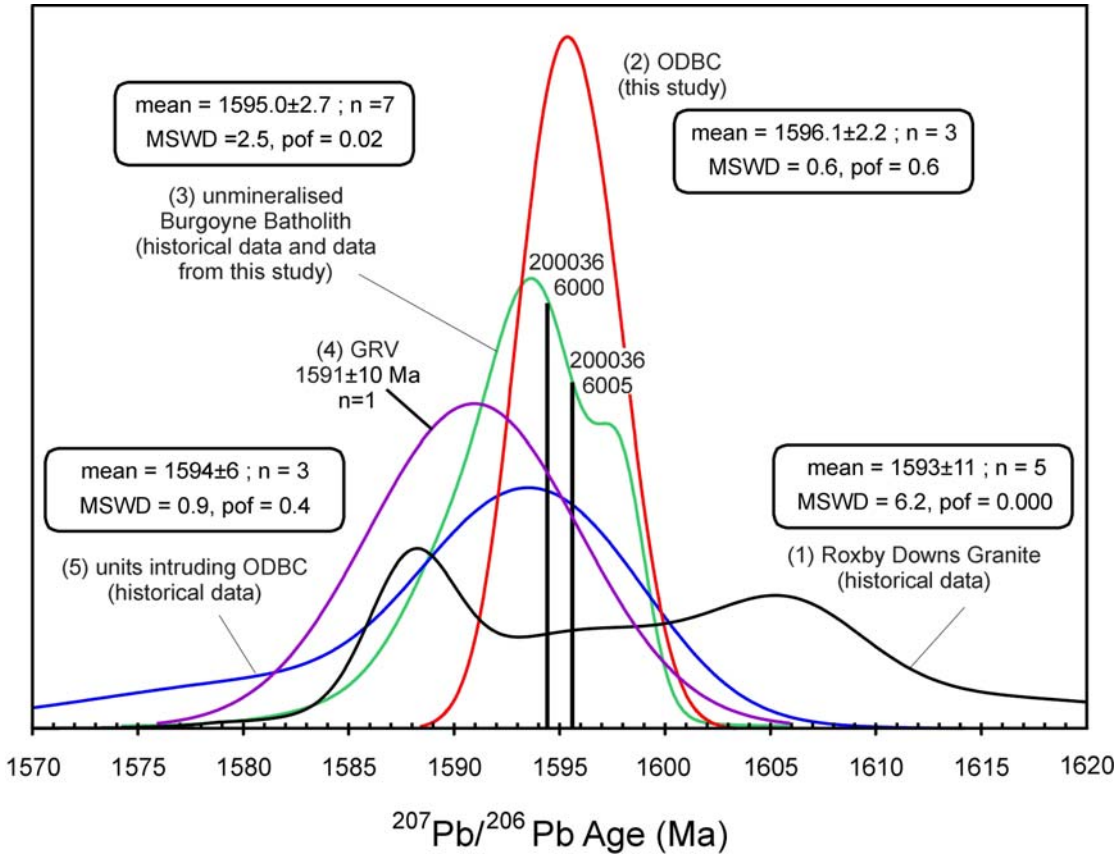

Figure 99. Probability density plots comparing available $^{207}Pb/^{206}Pb$ ages for; (1) the Roxby Downs Granite (2) Olympic Dam Breccia Complex (3) unmineralised plutons and dykes within the Burgoyne Batholith (4), and units intruding the ODBC (historical data) (5).

Acknowledgments

Thanks to Western Mining Corporation for permission to analyse samples from Olympic Dam, and to Dr Kathy Ehrig for advice and assistance in sampling strategy and sample provision. Samples from the Mount Woods Inlier were provided by Tony Belperio of Minotaur Exploration.

Mineral separation was undertaken by Gerald Kuehlich, Tas Armstrong, Stephen Ridgway at the mineral separation laboratories at Geoscience Australia. Chris Foudoulis selected zircons for mounting, and prepared mineral mounts, including all photography and SEM (cathodoluminescence) imaging.

SHRIMP analyses were undertaken under the technical guidance of Chris Foudoulis, who took responsibility for machine maintenance, optimising running conditions and troubleshooting during the sessions. Dr Lance Black provided advice and instruction on sample processing techniques, where required.

Terry Mernagh carried out LA-ICPMS and fluid inclusion studies of zircon inclusions in the samples from Olympic Dam described in Part 4, in order to ascertain the nature of the grains being analysed (i.e. hydrothermal vs magmatic). Roger Skirrow carried out complementary petrographic studies on the samples.

References

Black, L.P. The use of multiple reference standards for the monitoring of ion microprobe performance during zircon 207Pb/206Pb age determinations *Journal of Geostandards and Geoanalysis, in press.*

Black, L.P., Kamo, S.L., Williams, I.S., Mundil, R., Davis, D.W., Korsch, R.J. and Foudoulis, C. 2003. The application of SHRIMP to Phanerozoic geochronology; a critical appraisal of four zircon standards. *Chemical Geology 200*: 171-188.

Compston, W., Williams, I.S. and Meyer, C. 1984. U-Pb geochronology of zircons from lunar breccia 73217 using a sensitive high mass-resolution ion-microprobe. In: Boynton-William V. and Schubert, G. (eds) *Proceedings of the 14th Lunar Science Conference*, pp. B525-534. Journal of Geophysical Research 89.

Conor, C.H.H. 1995. Moonta-Wallaroo Region. An interpretation of the geology of the Maitland and Wallaroo 1:100 000 sheet areas. *South Australian Department of Mines and Energy, Open File Envelope 8886* (DME 588/93).

Cowley, W., Conor, C.H.H. and Zang W. 2003. New and revised Proterozoic stratigraphic units on northern Yorke Peninsula. *MESA Journal 29*: 46-58.

Creaser, R.A. 1989. The geology and petrology of middle Proterozoic felsic magmatism of the Stuart Shelf, South Australia. *Unpublished PhD thesis, Latrobe University.*

Creaser, R.A. 1995. Neodymium isotopic constraints for the origin of Mesoproterozoic felsic magmatism, Gawler Craton, South Australia. *Canadian Journal of Earth Sciences* 32: 460-471.

Creaser, R.A., and Cooper, J.A. 1993. U-Pb geochronology of middle Proterozoic felsic magatism surrounding the Olympic Dam Cu-U-Au-Ag and Moonta Cu-Au-Ag deposits, South Australia. *Economic Geology* 88: 186-197.

Cross, K.C., Daly, S.J. and Flint, R.B. 1993. Mineralisation associated with the GRV and Hiltaba Suite Granitoids. Olympic Dam Deposit. *In:* Drexel, J.F., Preiss, W.V. and Parker, A.J. (Eds) *The Geology of South Australia. Volume 1. The Precambrian*. Mines and Energy South Australia. Bulletin 54.

Daly, S.J., Fanning, C.M. and Fairclough, M.C. 1998. Tectonic evolution and exploration potential of the Gawler Craton, South Australia. *AGSO Journal of Australian Geology and Geophysics* 17: 145-168.

Fanning, C.M. 1997. Geological synthesis of South Australia. Part II: the Gawler craton. South Australian Department of Mines and Energy, Open File Envelope 8918 (unpublished).

Fanning, C.M., Flint, R.B., Parker, A.J., Ludwig, K.R. and Blissett, A.H. 1988. Refined Proterozoic tectonic evolution of the Gawler Craton, South Australia, through U-Pb zircon geochronology. *Precambrian Research* 40/41: 363-386.

Ferris, G.M., Schwarz, M.P. and Heithersay, P., 2002. The geological framework, distribution and controls of Fe-oxide and related alteration, and Cu-Au mineralisation in the Gawler Craton, South Australia: Part 1: geological and tectonic framework. *In:* Porter, T.M. (Ed.), *Hydrothermal iron oxide copper-gold and related deposits: a global perspective. Vol. 2*. PGC Publishing, Adelaide, pp.9-32.

Jaffey, A.H., Flynn, K.F., Glendenin, L.F., Bentley, W.C. and Essling, A.M. 1971. Precision measurements of half-lives and specific activities of 235U and 238U. *Physical Review C4*: 1889-1906.

Johnson, J.P. 1993. The geochronology and radiogenic isotope systematics of the Olympic Dam Copper-Uranium-Gold Silver deposit, South Australia. *Unpublished PhD thesis, Australian National University.*

Johnson, J.P. and Cross, K.C. 1991. Geochronological and Sm-Nd isotopic constraints on the Olympic Dam Cu-U-Au-Ag deposit, South Australia. *In*: Pagel, M. and Leroy, J.L. eds. *Source Transport and Deposition of Metals. Proceedings of the 25 Years S.G.A. Anniversary Meeting, Nancy.* Rotterdam, Balkema, 841p.

Ludwig, K.R. 1999. Using Isoplot/Ex, Version 2, a Geochronological Toolkit for Microsoft Excel. *Berkeley Geochronology Center Special Publication* number 1a: 47 pp.

Ludwig, K.R. 2001. SQUID 1.02. A User's Manual. *Berkeley Geochronology Center Special Publication* number 2: 21 pp.

Mason, D. 2003. Petrographic Descriptions for Seven Radiometrically Dated Rock Samples. Report no. 2905; Mason Geoscience Pty Ltd. *Unpublished report.*

Mortimer, G.E., Cooper, J.A, Paterson, H.L., Cross, K., Hudson, G.R.T. and Uppill, R.K. 1988a. Zircon U-Pb dating in the vicinity of the Olympic Dam Cu-U-Au deposit, Roxby Downs, South Australia. *Economic Geology* 83: 694-709.

Mortimer, G.E., Cooper, J.A and Oliver, R.L. 1988b. The geochemical evolution of Proterozoic granitoids near Port Lincoln in the Gawler Orogenic Domain of South Australia. *Precambrian Research* 40/41: 387-406.

Oliver, R.L. and Fanning, C.M. 1997. Australia and Antarctica: precise correlation of Palaeoproterozoic terrains. *In*: Ricci, C.A. (ed.) *The Antarctic Region: geological evolution and processes.* 7th International Conference on Antarctic Earth Sciences, Sienna, Italy, 1995. Proceedings 4(1): 163-172.

Paterson, H.L. and Muir, P.M. 1986. Report on part relinquishment of EL1316, Stuart Shelf. *South Australia Depsrtment of Mines and Energy. Open File Envelope,* 6562 (*unpublished*).

Purvis, A.C. 1999. Mineralogical Report No. 7770; Pontifex and Associates Pty. Ltd. *Unpublished report.*

Purvis, A.C. 2003. Mineralogical Report No. 8389; Pontifex and Associates Pty. Ltd. *Unpublished report.*

Reeve, J.S., Cross, K.C., Smith, R.N. and Oreskes, N. 1990. The Olympic Dam copper-uranium-gold-silver deposit, South Australia. *Australian Institute of Mining and Metallury Monograph* 14.

Reynolds, L. 2001. Geology of the Olympic Dam Cu–U–Au–Ag–REE deposit. *MESA Journal 23*: 4-11.

Sambridge, M. and Compston, W. 1994. Mixture modeling of multi-component data sets with application to ion-probe zircon ages: *Earth and Planetary Science Letters* 128: 373-390.

Schwarz, M.P. (2003) Lincoln 1:250 000 Explanatory Notes.

Stacey, J.S. and Kramers, J.D. 1975. Approximation of terrestrial lead isotope evolution by a two-stage model. *Earth and Planetary Science Letters 26*: 207-221

Steiger, R.H. and Jäger, E. 1977. Subcommission of geochronology: Convention on the use of decay constants in geo- and cosmochronology. *Earth and Planetary Science Letters* 36: 359-362.

Appendix 1

Mason Geoscience Pty Ltd

Petrological Services for the
Minerals Exploration and Mining Industry

ABN 64 140 231 481 ACN 063 539 686

Postal: PO Box 78 Glenside SA 5065 Australia
Delivery: 141 Yarrabee Rd Greenhill SA 5140 Australia
Ph: +61-8-8390-1507 Fax: +61-8-8390-1194
e-mail: masongeo@ozemail.com.au

Petrographic Descriptions for Seven Radiometrically Dated Rock Samples

REPORT # **2905**

CLIENT **Primary Industries and Resources SA**

ORDER NO **Office Visit, L. Jagodzinksi, 4 September 2003**

CONTACT **Ms Liz Jagodzinski**

REPORT BY **Dr Douglas R Mason**

SIGNED

for Mason Geoscience Pty Ltd

DATE **25 September 2003**

Petrographic Descriptions for Seven Radiometrically Dated Rock Samples

SUMMARY

1. Rock Samples

- Seven drill core rock samples from diverse prospects in South Australia have been studied using routine petrographic methods. Zircon from each of the samples had previously been dated by SHRIMP methods.

2. Brief Results

- *A summary of rock names and mineralogy* is provided in TABLE 1.

- *Zircon occurrence*

  - Accessory zircon grains have been optically identified in each of the samples.

  - Zircon grain size is commonly related to the primary particle size of the sedimentary host. Most grains tend to be quite small (~0.05-0.2 mm).

  - All of the zircon is interpreted to be of primary clastic origin. This is consistent with the relatively low grade of metamorphic modification displayed by most of the samples. A single high-grade sample (200036-6130, forsterite marble) contains rare tiny rounded zircon grains in phlogopite-rich laminae that are inferred to represent recrystallised primary argillaceous laminae: the contained zircons, therefore, may also be of relict clastic origin.

TABLE 1: SUMMARY OF ROCK NAMES AND MINERALOGY

SAMPLE	ROCK NAME	MINERALOGY*		
		Primary**	**Metamorphic / Alteration*****	**Veins**
200036-6137 (SR9, 86.0m)	Meta-crystal-lithic wacke	Qtz, zir, apa	Alb, fls, ser, chl, cal, leu	-
AD8, 940.1	Medium-intensity sericite-hematite altered, laminated cataclasite (meta-arkosic sandstone)	Kf, qtz, mus, tou, zir	Ser, hem, leu	-
SX9491 (SGD6, 493m)	Thinly dolomite-chlorite fractured and sericite-chlorite-?magnetite altered meta-siltstone	Qtz, pla, zir	Ser, chl, opq(?mt, ?hem)	Dol, hem, chl
6157 (SOC6, 128.2m)	Quartz-hematite altered lithic arenite	Qtz, zir	Qtz, hem, ser, leu	-
200036-6110 (SAE6, 1110.3m)	Meta-arkosic sandstone	Qtz, Kf, mus, tou, apa, zir	Opq(?hem), ser, dol	Qtz, hem, chl
200036-6130 (LGDDH2, 87.6m)	Partly retrogressed, calcite-phlogopite-diopside-forsterite marble (high-grade meta-calc-silicate sediment)	Zir?	Ca, phlg, diop, for, sp; Serp, opq(?py)	-
200036-6131 (BUTE5, 62m)	Chlorite-sericite-hematite meta-siltstone	Qtz, pla, zir	Chl, ser, qtz, opq(?hem), leu	-

NOTES:
*: Minerals are listed in each paragenesis according to approximate decreasing abundance.
**: Only primary minerals currently present in the rock are listed. Others may have been present, but are altered.
***: Earlier parageneses are separated from later parageneses by a semicolon.

Mineral abbreviations:
Alb = albite; apa = apatite; cal = calcite; chl = chlorite; diop = diopsidic clinopyroxene; dol = dolomitic carbonate; fls = felsic mosaic (mainly albite, minor quartz); for = forsteritic olivine; hem = hematite; Kf = K-feldspar; leu = leucoxene (indeterminate Ti-phase, possibly rutile, anatase or sphene); mt = magnetite; mus = muscovite (coarser-grained white mica); opq = undifferentiated opaque minerals (possible mineral indicated in brackets); phlg = phlogopitic mica; pla = plagioclase; py = pyrite; qtz = quartz; ser = sericite (fine-grained white mica); serp = serpentine mineral; sp = spinel; tou = tourmaline; zir = zircon; ?min = uncertain mineral identification; min? = uncertain mineral paragenesis.

1 INTRODUCTION

A number of samples were provided by Ms Liz Jagodzinski (Geological Survey Branch, PIRSA, Adelaide) during an office visit to Mason Geoscience Pty Ltd on 4 September 2003. The samples included:

i) Three thin sections and accompanying remnant samples.

ii) Four samples for which thin sections should be prepared.

Background notes on the geological occurrence of the samples were provided by the client, indicating that the samples had been dated radiometrically.

Particular requests were to provide a petrographic description for each sample.

Excerpts from this report were provided by email to Ms Jagodzinski on 25 September 2003. This report contains the full results of this work.

2 METHODS

Four samples were submitted for thin section preparation at an external commercial laboratory (Pontifex & Associates Pty Ltd, Rose Park, South Australia).

At Mason Geoscience Pty Ltd conventional transmitted polarised light microscopy was used to prepare the routine petrographic descriptions. Additional mineragraphic observations are provided where a polished thin section is available. SHRIMP zircon ages provided by the client are mentioned with petrographic observations of zircon.

3 PETROGRAPHIC DESCRIPTIONS

The petrographic descriptions are provided in the following pages. A combined petrographic and mineragraphic description is provided where a polished thin section is available.

SAMPLE : 200036-6137 (Metagreywacke, metasiltstone; SR9, 86.0m; Stuart Range Prospect, SA)

SECTION NO : 6173 (The section has captured only the sandy horizon, not the pelitic horizon)

HAND SPECIMEN : The drill core sample has captured the contact between grey sandy sedimentary lens or horizon which interfingers with fine-grained dark grey meta-pelitic sediment. Cutting the rock are minor thin veinlets filled by white minerals.

The sandy lens bubbles vigorously in reaction with dilute HCl, suggesting calcite is present in moderate amount.

ROCK NAME : Meta-crystal-lithic wacke

PETROGRAPHY :

A visual estimate of the modal mineral abundances gives the following:

Mineral	Vol %	Origin
Quartz	5	Primary crystal particles
Zircon	Tr	Primary crystals
Apatite	Tr	Primary microphenocrysts (in lithic frag's)
Albite	35	Metamorphic (after plag. crystals, frag's)
Felsic mosaic (albite, minor quartz)	50	Metamorphic (after matrix, lithic frag's)
Sericite	5	Metamorphic
Chlorite	3	Metamorphic
Carbonate (calcite)	<1	Metamorphic alteration
Leucoxene	Tr	Metamorphic

In thin section, this sample displays a relatively well-preserved framework-supported clastic sedimentary texture, modified by metamorphic replacement and mild deformation.

Albitic plagioclase is abundant, and occurs in two forms:

i) Much occurs as optically continuous twinned replacements of blocky prismatic crystals and angular crystal fragments that range widely in size from ~0.1 mm up to ~2.0 mm. The blocky prismatic crystals occur mainly as discrete crystal particles, but a small proportion also occur as phenocrysts in dacitic lava fragments.

ii) Much albite occurs as very fine-grained massive microgranular felsic mosaics that occupy the altered groundmass of dacitic lava fragments. Similar fine-grained felsic mosaic material also occupies the matrix areas between the crystal and lithic fragments, but varies in abundance from place to place such that in places the texture is matrix supported but mainly is framework-supported.

Sericite is moderately abundant. Most occurs as tiny flakes and small aggregates of flakes that are distributed more-or-less uniformly through the matrix areas. The flakes and aggregates are aligned in a moderately well-defined foliation, which wraps around the blocky crystal and lithic fragments. A trace amount of sericite also occurs as tiny replacement flecks in the albite-altered plagioclase crystals.

Chlorite is present in minor amount as small pleochroic drab green flakes that occur mainly in the matrix areas with associated sericite.

Quartz occurs mainly as magmatically corroded crystals (ie phenocrysts from lava) and angular crystal fragments that display a size range comparable with the plagioclase crystals and crystal fragments. A small amount of quartz is present in the fine-grained felsic mosaic material.

Carbonate (calcite) occurs in minor amount as small ragged grains concentrated in ragged aggregates scattered sparsely and irregularly through the matrix areas, as fillings in local brittly-fractured quartz grains, and as small ragged replacement aggregates in some of the albite-altered plagioclase crystals.

Leucoxene is present in minor amount as turbid cloudy material that occupies

Zircon is uncommon, occurring as small squat terminated crystals ~50-150 µm in size with prominent growth-zoning. They occur in the matrix areas. [SHRIMP zircon age is 2553.6 ± 4.7 Ma, as indicated by the client.]

Apatite occurs as uncommon small stumpy crystals (microphenocrysts) in the dacitic lava fragments.

INTERPRETATION :

This sample is considered to have formed as a rapidly deposited arenaceous sediment (non-sorted, non-layered wacke) composed of lithic fragments of plagioclase-quartz-phyric dacite lava, and crystals derived from that source (plagioclase, quartz), in a fine matrix of comminuted materials derived from that source. A minor amount of clays might also have been deposited with the matrix materials. The source of the small zircon crystals remains uncertain: it is likely that they were derived from the principal contributing source (ie the dacitic volcanic source), but it remains possible that the zircon was derived from a different (possibly granitoid) source.

Following deposition and burial, the rock body suffered low-grade regional metamorphism in the lower greenschist facies. This generated the new assemblage of albite + sericite + chlorite + minor quartz + calcite + leucoxene. The only two primary minerals to survive this event were apatite (microphenocrysts in dacitic lava fragments) and zircon (discrete clastic grains).

SAMPLE : AD8, 940.1 (Arkosic arenite, AD8, 940.1; Arcoona Station Prospect, SA)

SECTION NO : AD8, 940.1

HAND SPECIMEN : [No material supplied]

ROCK NAME : Medium-intensity sericite-hematite altered, laminated cataclasite (meta-arkosic sandstone)

PETROGRAPHY AND MINERAGRAPHY :

A visual estimate of the modal mineral abundances gives the following:

Mineral	Vol %	Origin
K-feldspar	44	Primary clastic particles
Quartz	20	Primary clastic particles
Muscovite	10	Primary clastic particles
Tourmaline	Tr	Primary clastic particles
Zircon	Tr	Primary clastic particles
Sericite	20	Metamorphic alteration
Hematite	5	Metamorphic alteration
Leucoxene	Tr	Metamorphic alteration

In polished thin section, this sample displays a fine-grained framework-supported arenaceous clastic sedimentary texture with mica-defined primary bedding plane orientation, modified by strong cataclastic deformation and selective pervasive alteration.

K-feldspar is abundant, and occurs throughout the rock as small subrounded grains ~0.2 mm in size, with some local larger grains up to ~0.6 mm in size. All of the K-feldspar grains are relatively fresh despite minor dull brownish staining from incipient hematite alteration.

Quartz occurs in significant amount as small subrounded to angular crystal fragments mostly ~0.2 mm in size. Like the K-feldspar, some larger grains up to ~0.6 mm in size are present and display polycrystalline (sutured, partly-recrystallised) textures.

Two textural types of white mica are distinguished:

i) Some occurs as well-shaped large flakes (muscovite) ~0.2-0.4 mm long. Their large size and distribution confirms that they are primary clastic particles, and their strong preferred orientation defines the primary bedding plane orientation.

ii) Tiny randomly oriented flecks of white mica (sericite) occur as dense monominerallic mats that occupy interstices between the well-defined clastic particles of K-feldspar, quartz and muscovite. Some of these sericitic mats have blocky shapes, suggestive of primary feldspar grains (possibly ?plagioclase but none is preserved for confirmation).

Tourmaline is present in trace amount as equant subrounded grains, pleochroic in drab greens or pale mauves to dark drab greens.

Zircon occurs in trace amount as small subrounded grains ~0.1-0.2 mm in size. They appear to have formed initially as stumpy euhedral prismatic crystals. Locally, numbers of zircon grains are concentrated in thin

(~0.1-0.2 mm wide) bands of inferred heavy mineral sedimentary origin (also see hematite below). [SHRIMP zircon age is 1850.4 ± 5.9 Ma].

Hematite is moderately abundant, and is distributed in different sites throughout the rock:

i) Much occurs as minute (micron-sized) specks that are concentrated in subparallel anastomosing bands of cataclastic origin ~0.2-1.0 mm wide. The fine-grained hematite in these bands forms a matrix which encloses small angular to rounded quartz grains that represent disaggregated particles from the wallrock.

ii) Some hematite occurs as dense microgranular laminae that are limited to particular lenses that have suffered partial rotation between cataclastic bands. These laminae also contain zircon grains that are more abundant than elsewhere in the rock; hence these hematite-zircon-rich laminae are interpreted as modified primary heavy-mineral-rich laminae.

iii) A significant amount of hematite occurs as very fine-grained dense replacement clouds that occupy thin folia or patches aligned in the trace of the bedding plane (ie subparallel to the aligned muscovite flakes). This hematite is considered to have formed by replacement of precursor Mg-Fe phase (probably biotite but none is preserved for confirmation).

Leucoxene is present in trace amount as turbid yellowish-brown material which occupies small grains and aggregates sparsely scattered through the rock.

INTERPRETATION :

This sample is considered to have evolved through the following events:

1. Sedimentation
Partly-sorted but compositionally immature clastic materials (K-feldspar > quartz > ?plagioclase > muscovite > ?biotite > tourmaline > zircon) were deposited as part of a sedimentary sequence. Primary bedding was pervasively defined by aligned muscovite flakes, and locally by thin heavy-mineral-rich laminae composed of Fe-Ti oxide grains and zircon. The clastic materials are inferred to have been derived from a felsic crystalline source.

2. Burial and diagenesis
The sedimentary sequence is assumed to have suffered burial and low-grade diagenetic processes, including grain suturing, but little or no metamorphic modification of the rock appears to have occurred at this stage.

3. Cataclastic deformation and retrogressive alteration
The rock body suffered severe brittle deformation, with development of subparallel to anastomosing granulated bands. Partial rotation of primary lamination occurred between closely-spaced cataclastic bands. Pervasive low-grade alteration affected the rock, probably at this time, generating moderately abundant sericite + hematite. The sericite formed pervasively through the rock, both as matrix within the cataclastic bands and pervasively elsewhere possibly by preferential replacement of ?plagioclase grains. The hematite formed as matrix in the cataclastic bands, as replacements of precursor Fe-rich materials in the heavy-mineral-rich laminae, and as replacements of primary ?biotite flakes.

SAMPLE : SX9491 (Volcanosedimentary unit, SGD6, 493m; Snake Gully Prospect, SA)

SECTION NO : SGD6, 493m; SX9491

HAND SPECIMEN : The drill core sample represents a fine-grained thinly laminated meta-sedimentary rock composed mainly of drab greenish layers with lesser paler drab brownish cream layers.

The sample responds weakly to the hand magnet, suggesting minor magnetite is present.

ROCK NAME : Thinly dolomite-chlorite fractured and sericite-chlorite-?magnetite altered meta-siltstone

PETROGRAPHY :

A visual estimate of the modal mineral abundances gives the following:

Mineral	Vol %	Origin
Quartz	52	Primary clastic particles / metamorphic
Plagioclase	15	Primary clastic particles / metamorphic
Zircon	Tr	Primary clastic particles
Sericite	25	Metamorphic / metamorphic alteration
Chlorite	5	Metamorphic / fracture fillings
Opaques (?magnetite, ?hematite-altered)	2	Relict metamorphic
Carbonate (dolomite)	Tr	Fracture fillings
Hematite	Tr	Fracture fillings

In thin section, this sample displays a uniformly fine-grained clastic sedimentary texture, modified by weak metamorphic grain suturing, fracturing, and pervasive alteration.

Quartz is abundant, occurring as small equant anhedral grains 0.05-0.1 mm in size. They are distributed more-or-less uniformly throughout the rock, with suturing of quartz-quartz grain contacts.

Plagioclase occurs in moderate amount as small anhedral grains and small microgranular aggregates. They are distributed throughout the rock, but tend to be more abundant in indistinct horizons inferred to represent primary layering.

Sericite is moderately abundant, forming small flakes whose preferred orientation defines a moderate foliation subparallel to the weak mineralogical layering defined by plagioclase-quartz abundances (see above). The sericite tends to be concentrated in subparallel laminae, but also forms thick selvedges on the millimetre scale marginal to discordant fracture fillings of sparry anhedral dolomite and fine-grained chlorite.

Chlorite occurs in minor amount as small flakes whose preferred orientation contributes to definition of the foliation through the rock. Pleochroism from dark green to virtually colourless confirms that the chlorite has an Fe-rich composition.

Opaques occur as small equant crystals of cubic morphology. They may have formed as magnetite but have suffered partial to complete replacement by hematite. This cannot be confirmed in the absence of reflected light observations, but the interpretation is supported by the observation that some of the grains display dark red margins appropriate for hematite, and the rock responds weakly to the hand magnet.

Zircon occurs as uncommon small subrounded grains ~0.1-0.2 mm in size. [SHRIMP zircon age is 1852.4 ± 4.2 Ma; possible younger grains at ~1770 Ma.]

INTERPRETATION :

This sample formed as a fine-grained silty clastic sediment composed of abundant small crystal fragments (quartz >> plagioclase >> zircon) accompanied by fine argillaceous materials. Subsequent recrystallisation in response to a low-grade regional metamorphic event generated the new foliated assemblage of sericite + chlorite + minor opaques (?magnetite). Quartz and plagioclase remained stable from the primary clastic assemblage, and suffered grain suturing and incipient recrystallisation. At this time, or toward the end of this event, thin fractures were filled by dolomite + chlorite (the chlorite identical to that disseminated through the rock as foliated flakes), and fine sericite formed as selvedges marginal to the fractures. Hematite formed as tiny grains in the fracture-filling dolomite, and as replacements of ?magnetite.

SAMPLE : 6157 (Moonabie Formation quartzite/?volcaniclastic; SOC6, 128.2m; Roopena Prospect, SA)

SECTION NO : 6157

HAND SPECIMEN : The drill core rock slice represents an arenaceous clastic sediment with little or no layering, composed of closely-packed small particles with overall mauvish colour from pervasive alteration hematite. Sparsely scattered slightly larger ragged patches several millimetres in size are cream in colour and appear to be 'grains', but under the hand lens they are observed to represent clastic sediment that lacks the pervasive hematite staining.

ROCK NAME : Quartz-hematite altered lithic arenite

PETROGRAPHY :

A visual estimate of the modal mineral abundances gives the following:

Mineral	Vol %	Origin
Quartz	35	Primary clastic particles
Zircon	Tr	Primary clastic particles
Quartz	54	Alteration (after lithics, matrix filling)
Hematite	10	Alteration
Sericite	Tr	Alteration
Leucoxene	Tr	Alteration

In thin section, this sample displays a well-preserved framework-supported, sorted but non-layered, arenaceous clastic sedimentary texture that has been modified by pervasive alteration.

Quartz dominates the rock and occurs in different forms:

i) Some occurs as equant subrounded to subangular crystal fragments mostly ~0.4-1.0 mm in size. Most of these are fragments of single crystals whose origin remains uncertain, but some polycrystalline fragments display sutured lineated metamorphic textures.

ii) Much quartz occurs as fine-grained massive replacement mosaics after lithic fragments. The quartz displays varied textures suggestive of precursor felsic volcanic rock fragments: fine-grained massive microgranular texture, coarser-grained equigranular texture ('snowflake' texture) reminiscent of devitrification, uncommon relict massive to felted feldspar crystallite textures consistent with holohyalline (wholly glassy) to hemihyalline (partly glassy, partly crystalline) textures, and uncommon quartz-phyric lava textures.

iii) A small amount of quartz occurs as clear anhedral grains and microgranular aggregates that fill interstices between some lithic fragments, and locally forms optically continuous overgrowths on some quartz clastic particles.

iv) Rare blocky magmatically corroded crystals occur as phenocrysts in some of the altered felsic lithic fragments.

Hematite is the other principal phase, occurring as cryptocrystalline reddish specks and aggregates that pervade the altered lithic fragments, and also occurs as denser aggregates in the matrix areas. Hematite is

virtually absent from some indistinct ovoid areas several millimetres in size; these are the paler ‘grains’ observed in the hand specimen.

Sericite is uncommon, forming fine-grained flakes that have replaced precursor flakes up to ~0.5 mm long (probably biotite, as inferred from the presence of tiny leucoxene granules sprinkled through the sericite mat).

Zircon occurs as uncommon fragments of prismatic terminated crystals up to ~0.2 mm long. [SHRIMP zircon age is 1761.4 ± 6.8 Ma].

INTERPRETATION :

This sample formed as a coarse sandy deposit composed of abundant lithic fragments (mainly felsic volcanic fragments, minor recrystallised metamorphic quartz fragments) and lesser crystal fragments (quartz, rare zircon).

Two different source terrains are inferred:

i) A coarsely crystalline ?metamorphic terrane contributed at least some of the quartz crystal fragments (specifically the polycrystalline quartz fragments, and possibly some of the larger quartz crystal fragments), and possibly the zircon crystal fragments.

ii) A felsic volcanic source contributed glassy to partly-crystallised lava fragments, and some of the crystal fragments. Some of the lava fragments contain quartz phenocrysts, which suggests that some of the quartz crystal fragments most likely were derived from the felsic volcanic source.

The sediment suffered strong pervasive replacement under low P-T conditions, generating abundant quartz + hematite, both by replacement of the felsic volcanic fragments and by filling of the interparticle pores.

SAMPLE : 200036-6110 (Arkose, SAE6, 1110.3m; Emmie Bluff Prospect, SA)

SECTION NO : 200036-6110

HAND SPECIMEN : The drill core sample represents a pinkish arenaceous clastic sedimentary rock, in which indistinct lamination is defined by weak preferred orientation of slightly more elongate particles and weak particle size-layering. Rare small lustrous pyrite aggregates are observed under the hand lens. Uncommon thin dark reddish (hematite-filled) fractures cut the rock.

The sample fails to react with dilute HCl, suggesting calcite is absent.

ROCK NAME : Meta-arkosic sandstone

PETROGRAPHY :

A visual estimate of the modal mineral abundances gives the following:

Mineral	Vol %	Origin
Quartz	53	Primary clastic particles
K-feldspar	35	Primary clastic particles
Muscovite	<1	Primary clastic particles
Tourmaline	Tr	Primary clastic particles
Apatite	Tr	Primary clastic particles
Zircon	Tr	Primary clastic particles
Opaques (mainly ?hematite)	5	Alteration
Sericite	3	Alteration (metamorphic)
Carbonate (dolomite)	Tr	Alteration (metamorphic)
Hematite	Tr	Fracture fillings
Quartz	Tr	Fracture fillings
Chlorite	Tr	Fracture fillings

In thin section, this sample displays a well-preserved framework-supported arenaceous clastic sedimentary texture, modified by grain boundary suturing and selective pervasive alteration effects.

Quartz is abundant, forming rounded grains mostly ~0.4-0.6 mm in size, but also ranging down to ~0.1 mm and up to ~1 mm. Most are fragments of single crystals with weak shadowy strain extinction. Some fragments display sutured polycrystalline textures suggestive of a metamorphic origin.

K-feldspar is the other principal phase, forming rounded particles and subrounded blocky crystals similar in size to the quartz grains. Most display well-developed combined albite and pericline twinning (ie ‘tartan’ twinning), and many are rendered turbid by clouds of submicron-sized hematite specks.

Two types of white mica are identified:

i) Some occurs as well-crystallised flakes mostly ~0.4-0.6 mm long (muscovite) that are sparsely scattered through the rock. These flakes occur at quartz-quartz or quartz-feldspar grain boundaries and display kinking that reflects compaction during sedimentation or grain boundary migration. Clearly these muscovite flakes are of clastic origin. A preferred orientation of these flakes contributes to definition of the primary bedding plane attitude, and is further supported by preferred orientation of the larger more elongate fragments of quartz and K-feldspar.

ii) A moderate amount of white mica occurs as tiny randomly oriented flecks (sericite) that form loose aggregates in the interstitial areas between the quartz and K-feldspar fragments. This sericite clearly has formed by metamorphic recrystallisation of fine matrix materials.

Opaque material occurs as fine-grained dense aggregates scattered throughout the rock. Some are blocky in overall shape, and possibly may be ?pyrite (rare lustrous pyrite aggregates are observed in the hand specimen). Other opaque aggregates are more elongated or lenticular in shape, and tend to be moulded around the margins of quartz of K-feldspar fragments. These opaque lenticles appear to be composed of fine-grained hematite.

Tourmaline is present in trace amount as rounded clastic particles, strongly pleochroic in greens, blues and pale mauves.

Apatite is uncommon, forming small equant subrounded grains of clastic origin.

Zircon occurs in trace amount as small equant subrounded grains ~0.05-0.1 mm in size, very sparsely scattered through the rock. [SHRIMP zircon age is 1853.0 ± 4.4 Ma].

Carbonate occurs in trace amount as small rhombic crystals that tend to form local small aggregates scattered through the rock.

Cutting the rock are uncommon thin fractures that are filled by clear anhedral quartz grains, dense clouds of dark reddish brown hematite, and minor small patches of very fine-grained drab green chlorite.

INTERPRETATION :

This sample formed as a poorly sorted arkosic sediment composed of subrounded to rounded crystal fragments of quartz and K-feldspar, with minor to trace muscovite, tourmaline, Fe-Mg grains (?opaques, ?biotite), apatite and zircon. All of the clastic detritus is considered to have been derived from a felsic crystalline source.

The sediment suffered low-grade metamorphic effects up to lower greenschist facies. All of the quartz and K-feldspar remained stable during this event, with generation of new sericite + hematite + trace dolomite. Uncommon thin fractures were filled by quartz + hematite + trace chlorite. The development of pervasive hematitic staining of the K-feldspar grains during this event is responsible for the pink colour of the hand sample.

SAMPLE : 200036-6130 (?Calcsilicate rock, LG-DDH2, 87.6m; Hutchison Group, Lake Gilles Prospect, SA)

SECTION NO : 200036-6130

HAND SPECIMEN : The drill core sample represents a pale grey granular crystalline rock, in which layering is defined by thin darker mauvish grey (mica-rich) laminae several millimetres thick.

The sample effervesces vigorously in reaction with dilute HCl, confirming calcite is abundant throughout the rock.

ROCK NAME : Partly retrogressed, calcite-phlogopite-diopside-forsterite marble (high-grade meta-calc-silicate sediment)

PETROGRAPHY :

A visual estimate of the modal mineral abundances gives the following:

Mineral	Vol %	Origin
Zircon	Tr	?Relict clastic grains
Calcite	58	Metamorphic
Phlogopite	20	Metamorphic
Clinopyroxene (diopsidic)	5	Metamorphic
Forsterite	Tr	Relict metamorphic
Spinel (green)	Tr	Metamorphic
Serpentine	15	Retrogressive alteration (after ?forsterite)
Opaques	Tr	Retrogressive alt'n / filamentous fractures

In thin section, this sample displays a granoblastic metamorphic texture, with foliation defined by aligned mica flakes and indistinct mineralogical lamination, modified by selective retrogressive alteration.

Calcite dominates the rock, forming equant anhedral grains of wide size range (~0.2-3.0 mm). Grain size is mainly equigranular in some horizons, and coarser-grained in others.

Phlogopite is moderately abundant, occurring as well-shaped flakes mostly ~0.2-0.4 mm long but locally ranging up to ~4 mm long. Pleochroism varies from place to place, with most flakes displaying weak pale yellow to colourless pleochroism, increasing in absorption intensity to orange-brown to pale yellow in some mica-rich horizons.

Clinopyroxene forms large anhedral grains up to ~4 mm in size that porphyroblastically enclose numerous smaller calcite and phlogopite flakes. Most of the clinopyroxene is rendered turbid by drab brownish retrogressive alteration, but relict clinopyroxene is preserved in most grain sites.

Forsterite formed equant anhedral grains mostly ~0.2-0.6 mm in size scattered sparsely through calcite-phlogopite-rich horizons. Most of the grain sites have suffered complete replacement by fine-grained, fibrous, colourless to very pale yellow serpentine, but relict forsterite (colourless, high relief, high birefringence, parallel extinction) is preserved in some grain sites.

A spinel phase occurs in trace amount, forming blocky pale green grains that are perfectly isotropic. They tend to occur in the mica-rich horizons. Some are mantled by microgranular forsterite aggregates.

Opaques occur in trace amount as very fine-grained dense aggregates and discontinuous trails. They appear to represent retrogressive fine-grained pyrite, but reflected light observations are not available.

Zircon is observed as rare tiny rounded grains ~50 mm in size. They occur only in the phlogopite-rich laminae, not in the calcite-rich layers. [SHRIMP zircon ages are varied: 2013.5 ± 7.7 Ma (n = 20), 2497.9 ± 5.7 Ma (n = 8), 2525.8 ± 4.5 Ma (n = 14), and many grains up to 3500 Ma.]

INTERPRETATION :

This sample formed as an impure calc-silicate sediment, composed of carbonate and lesser clay components. High-grade regional metamorphism in the upper amphibolite to granulite facies generated the foliated assemblage of calcite + phlogopite + forsterite + diopside + trace spinel. Indistinct mineralogical lamination of the metamorphic assemblage (ie mica-rich laminae, thicker calcite-forsterite-diopside-phlogopite layers) possibly reflects primary compositional layering in which thicker calc-silicate layers were interlayered with thinner clay-rich layers.

At a much later time, under much lower conditions of P and T, retrogressive alteration generated serpentine + opaques (?pyrite): the serpentine formed by hydration of forsterite, and the opaques formed as irregularly distributed small discontinuous trails and filamentous fracture fillings.

SAMPLE : 200036-6131 (Wandearah Metasiltstone, BUTE5, 62m; Bute Prospect, near Moonta, SA)

SECTION NO : 200036-6131

HAND SPECIMEN : The drill core sample represents a fine-grained dark greenish grey rock in which thin layering is defined by interlayered dark reddish brown and dark greenish grey materials.

The sample fails to respond to the hand magnet, suggesting magnetite is absent.

ROCK NAME : Chlorite-sericite-hematite meta-siltstone

PETROGRAPHY :

A visual estimate of the modal mineral abundances gives the following:

Mineral	Vol %	Origin
Quartz	5	Primary clastic particles
Plagioclase	Tr	Primary clastic particles
Zircon	Tr	Primary clastic particles
Chlorite	46	Metamorphic
Sericite	35	Metamorphic
Quartz	10	?Metamorphic / ?recryst. clastic particles
Opaques (mainly hematite)	3	Metamorphic
Ti-phase (leucoxene, ?anatase, ?sphene)	Tr	Metamorphic

In thin section, this sample displays a partly-preserved fine-grained matrix-supported silty clastic sedimentary texture, modified by selective pervasive metamorphic recrystallisation without foliation.

Quartz occurs in two forms:

i) Some occurs as small angular crystal fragments ~0.05-0.1 mm in size. They are sparsely scattered throughout the rock, but tend to be loosely concentrated in particular laminae (thin primary layers).

ii) A moderate amount of quartz occurs as tiny equant anhedral grains, in equilibrium contact with tiny chlorite and sericite flakes. This quartz appears to form part of the metamorphic assemblage, but is likely to have formed by grain modification of primary tiny clastic particles.

Chlorite is abundant, forming randomly oriented small flakes pleochroic from dark green to almost colourless. An Fe-rich composition is inferred. Although distributed throughout the rock, slightly larger flakes tend to be concentrated in thin indistinct discontinuous laminae.

Sericite is abundant, occurring as tiny randomly oriented poorly-shaped flakes. Like chlorite, they are distributed abundantly throughout the rock, but tend to be more abundant in particular horizons.

Opaque materials (mainly hematite, as supported by ragged grain shapes and deep red colour of grains in thin edges) are distributed throughout the rock as tiny ragged grains. Like chlorite and sericite, the hematite is loosely concentrated in particular horizons.

Plagioclase is uncommon, forming small twinned angular crystal fragments comparable in size with the larger quartz particles.

Zircon is rare, occurring as subrounded to angular fragments ~50 µm in size, derived by comminution of small growth-zoned crystals. [SHRIMP zircon age is 1853.0 ± 4.4 Ma, and 1761 Ma.]

INTERPRETATION :

This sample formed as a fine silty pelitic sediment, composed of minor small crystal fragments (quartz >> plagioclase >> zircon) in a fine clay matrix. Subsequent low-grade regional metamorphism in the lower greenschist facies caused complete recrystallisation of the finer clay materials, generating fine-grained sericite + chlorite + hematite. Indistinct mineralogical lamination of these minerals is considered to reflect primary sedimentary layering. Primary silty clastic particles (quartz, plagioclase, zircon) survived this event. Note the absence of preferred orientation of the phyllosilicate minerals (chlorite, sericite): this suggests that the recrystallisation occurred in the absence of a directed regional stress regime.

Appendix 2

Geochemical Analyses

Sample #	200036-6004	200036-6005	200036-6006	200036-6008	200036-6020a	200036-6020b	200036-6020c	200036-6020d
Drill hole	SGD4	SGD4	SGD5	SGD6	BHD1	BHD1	BHD1	BHD1
Suite	Donington	Hiltaba	Hiltaba?		Donington	Donington	Donington	Donington
Lith								
SiO2	68.74	44.52	66.79	70.64	65.83	69.93	61.15	63.42
TiO2	0.8	1.81	0.48	0.59	0.36	0.32	0.94	0.71
Al2O3	15.11	15.03	15.53	12.76	16.52	14.59	16.09	15.28
Fe2O3tot	3.15	15.13	3.44	4.79	3.02	3.15	7.49	5.61
Fe2O3	1.86	6.02	2.06	2.99	1.24	1.4	4.11	2.62
FEO	1.16	8.19	1.24	1.62	1.6	1.57	3.04	2.69
MnO	0.05	0.16	0.04	0.04	0.05	0.05	0.11	0.07
MgO	1.18	7.8	1.37	1.76	1.66	1.59	2.44	1.97
CaO	1.03	7.01	1.39	0.8	1.85	1.7	3.69	2.65
Na2O	5.07	2.06	8.5	0.76	4.6	3.58	3.68	3.93
K2O	3.14	2.83	0.2	4.73	2.9	3.5	2.78	2.4
P2O5	0.08	0.28	0.15	0.16	0.1	0.08	0.26	0.18
SO3	0.06	0.24	0.1	–	–	–	–	–
LOI	0.13	0.91	0.14	–	–	–	–	–
Total	98.39	96.85	97.99	97.06	96.92	98.5	98.55	96.13
Ag	0.06	0.07	0.03	0.05	0.03	0.03	0.06	0.03
Ba	661	632	22	767	790	618	470	355
Be	5	2.4	4.8	2.5	1.7	1.9	2.8	2
Bi	0.1	0.1	0.1	0.3	0.1	–	0.1	0.1
Cd	–	0.18	-0.05	0.15	0.2	0.05	–	–
Ce	201	50.1	41	114	29.5	43.5	68.8	44.9
Cr	30	107	100	53	14	10	8	9
Cs	2.45	4.01	0.29	2.46	1.49	1.49	3.43	2.61
Cu	40	191	48	24	10	15	55	26
Dy	13.8	5.64	5.21	6.86	1.5	1.48	4.03	2.93
Er	7.86	3.48	3.1	4.19	0.85	0.76	2.12	1.58
Eu (ppb)	3137	1820	1076	1800	744	714	1214	904
F	1024	1793	230	1457	584	618	1014	929
Ga	19.8	19.9	16.1	17.4	21.5	18.9	23.8	22.1
Ge	1.6	2	1.2	1.6	1.1	1.3	1.6	1.4
Gd	17.2	6.12	5.69	8.31	1.96	2.16	5.46	3.82
Hf	9.8	3.1	5.9	11.7	4.6	4	5.8	4.8
Ho	2.77	1.21	1.06	1.43	0.32	0.3	0.79	0.58
La	76.4	24.3	20.7	54.9	15.6	23	28.8	21.4
Lu	1.05	0.49	0.49	0.66	0.13	0.12	0.29	0.28
Mo	3.3	2	3.9	2.2	1.7	1.7	2	1
Nb	26.5	10.9	15.3	19.3	6.4	6.1	17.2	11.1
Nd	101	24.6	18.8	46.3	11.4	14.9	28	19.6
Ni	12	126	7	16	18	10	15	11
Pb	9.5	23.5	7.5	2.2	10.9	27.8	28.1	24.5
Pr	25.4	6.01	4.57	12.2	3.01	4.19	7.01	4.91
Rb	129	181	12.7	200	119	122	134	125
Sb	0.3	0.3	0.3	0.5	0.2	0.1	0.1	0.1
Sc	15	39	7	12	6	6	19	13
Sm	19.7	5.43	4.54	9	2.29	2.45	5.73	4.19
Sn	6	3.9	2.7	6	2.2	1.7	3.1	2.2
Sr	184	178	23.9	36	301	242	308	279
Ta	1.9	0.7	1.3	1.6	0.5	0.5	1.1	0.8
Tb	2.74	1.04	1.01	1.3	0.27	0.28	0.79	0.57
Th	24.4	1.6	25.5	18.1	3.9	6.5	4.3	4
U	5.74	1.33	8.35	3.98	0.82	0.73	2.22	1.12
V	40	310	45	49	38	32	108	79
Y	75.7	34	31	43.8	9.5	8.9	18.7	17.5
Yb	7.31	3.21	3.23	4.25	0.78	0.63	1.84	1.46
Zn	29.5	97.5	10.3	17.6	66.2	72.3	113	93.1
Zr	327	123	226	455	156	147	179	164

Sample #	200036-6004	200036-6005	200036-6006	200036-6008	200036-6020a	200036-6020b	200036-6020c	200036-6020d
Sample #								
Drill hole	SGD4	SGD4	SGD5	SGD6	BHD1	BHD1	BHD1	BHD1
Suite	Donington	Hiltaba	Hiltaba?		Donington	Donington	Donington	Donington
Lith								
Q	24.09	-	12.75	45.94	21.91	29.89	18.35	23.57
C	1.9	-	-	5.77	2.81	2.11	1.09	2.05
Z	0.07	0.02	0.05	0.09	0.03	0.03	0.04	0.03
Or	18.94	17.54	1.21	28.94	17.77	21.09	16.77	14.83
Ab	43.68	18.21	73.57	6.64	40.25	30.81	31.68	34.67
An	4.21	24.46	3.71	2.26	8.77	7.9	16.56	12.12
Ne	-	-	-	-	-	-	-	-
Di	-	7.3	1.83	-	-	-	-	-
Di(CaMg)	-	5.49	1.83	-	-	-	-	-
Hd	-	1.81	-	-	-	-	-	-
Hy	2.99	4.74	2.64	4.53	5.73	5.34	7.02	6.91
En	2.99	3.44	2.64	4.53	4.27	4.03	6.18	5.11
Fs	-	1.3	-	-	1.46	1.31	0.84	1.8
Ol	-	14.21	-	-	-	-	-	-
Fo	-	10.03	-	-	-	-	-	-
Fa	-	4.18	-	-	-	-	-	-
Mt	1.61	9.19	2.78	3.75	1.87	2.07	6.09	3.98
Cm	0.01	0.02	0.02	0.01	-	-	-	-
Hm	0.79	-	0.2	0.51	-	-	-	-
Il	1.55	3.59	0.93	1.16	0.71	0.62	1.82	1.41
Ap	0.2	0.7	0.36	0.41	0.25	0.2	0.63	0.45
Fr	0.2	0.32	-	0.28	0.1	0.11	0.16	0.16
Cc	-	-	-	-	-	-	-	-
Diff. Index	86.7	35.75	87.53	81.51	79.92	81.79	66.8	73.08
Colour Index	6.94	39.05	8.4	9.95	8.31	8.03	14.93	12.3
Pl	47.89	42.67	77.28	8.9	49.02	38.71	48.24	46.79
Norm Plag Comp	8.79	57.32	4.8	25.36	17.9	20.41	34.33	25.9
100An/(An+Ab^)	8.79	57.32	4.8	25.36	17.9	20.41	34.33	25.9
Ab^	43.68	18.21	73.57	6.64	40.25	30.81	31.68	34.67
Q"	24.98	1.33	13.54	47.29	23.52	31.4	20.39	25.51
Ol^	2.1	17.63	1.85	3.17	4.12	3.83	4.98	4.97
Ne^	23.67	9.87	39.87	3.6	21.81	16.7	17.17	18.79
Q^	44.99	9.67	47.23	50.33	41.95	45.51	34.9	41.39
mg number	64.45	62.92	66.32	65.94	64.9	64.35	58.85	56.62

Sample #	200036-6020e	200036-6020f	200036-6021	200036-6022	200036-6023	200036-6024	200036-6025	200036-6026
Drill hole	BHD1	BHD1	BHD1	BHD2	BHD2	BHD2	BHD2	BHD2
Suite	Donington	Donington		Donington	Donington	Donington	Donington	
Lith			dlt dyke					dlt dyke
SiO2	67.98	58.16	47.95	67.73	67.53	70.05	61.93	46.44
TiO2	0.38	1.07	3.16	0.49	0.57	0.54	0.45	2.21
Al2O3	15.78	16.7	12.47	15.56	15.17	14.55	17.59	13.49
Fe2O3tot	3.21	8.52	17.46	4.55	4.95	4.52	4.99	21.21
Fe2O3	1.42	4.3	5.81	1.19	1.72	1.2	1.1	7.08
FEO	1.61	3.8	10.49	3.02	2.91	2.98	3.5	12.72
MnO	0.06	0.12	0.22	0.03	0.04	0.04	0.06	0.19
MgO	1.54	2.83	5.41	1.77	1.85	1.66	2.11	6.16
CaO	2.41	4.31	7.45	1.15	1.04	1.25	3.4	1.82
Na2O	4.48	3.35	2.1	1.38	1.96	1.68	2.45	0.48
K2O	2.17	3.17	1.81	4.01	3.83	3.65	4.1	4.91
P2O5	0.1	0.29	0.39	0.07	0.07	0.06	1.08	0.26
SO3	–		0.18	0.15	0.07	0.05	0.05	0.06
LOI	–		1.17	0.34	0.32	0.33	0.39	1.42
Total	98.08	98.38	98.6	96.89	97.08	98.05	98.18	97.21
Ag	0.04	0.06	0.05	0.05	0.03	0.02	0.06	0.04
Ba	306	566	331	919	826	959	246	949
Be	2.7	2.3	1.3	5.2	3.6	3	1.6	2.4
Bi	0.1	0.1	0.2	0.1	0	0	0.1	0.2
Cd	–	–	0.06	–	–	–	–	0.24
Ce	42	61.1	60.6	82.6	92.5	96.3	435	57.9
Cr	12	11	98	70	74	71	35	107
Cs	2.19	3.98	3.59	2.12	1.76	2.38	4.07	7.58
Cu	10	44	161	26	22	11	53	140
Dy	1.53	4.51	8.61	5.04	4.66	4.64	16	7.92
Er	0.8	2.39	5.28	3.23	2.76	2.66	7.81	4.79
Eu (ppb)	872	1601	2403	1207	1377	1249	2832	1677
F	674	1044	1384	596	665	613	1286	1470
Ga	21.8	23.7	23.6	20.6	19.7	19.1	20.1	21.7
Ge	1.2	1.7	2.3	1.6	1.6	1.6	1.8	2
Gd	2.21	5.96	8.83	5.55	5.79	6.02	20.9	8.03
Hf	4.4	5.7	5.5	5.9	6	6.2	2.7	5.5
Ho	0.3	0.87	1.79	1.05	0.91	0.88	2.86	1.63
La	22.8	27.4	26.9	40.5	45.5	47	202	25.2
Lu	0.1	0.31	0.69	0.4	0.28	0.34	0.85	0.58
Mo	2	2.1	4	5.7	8.2	7.3	3.6	2.4
Nb	7.2	20.3	15.6	9	10.6	9.7	13.3	14.9
Nd	14.8	29.5	31.9	32.9	36.5	38.1	168	29.9
Ni	10	16	50	20	23	18	16	65
Pb	11.5	15.4	17.3	12	15.3	13.2	18.3	7.9
Pr	4.11	7.14	7.27	8.79	9.8	10.2	44.9	6.85
Rb	111	184	121	111	117	113	133	248
Sb	0.2	0.2	0.3	0.1	0	0.1	0.1	0.3
Sc	6	17	50	9	12	12	15	45
Sm	2.58	6.15	7.9	6.08	6.73	7.26	28.4	7.19
Sn	2.1	2.9	3.7	4.2	4.6	4.8	4.1	3.4
Sr	288	348	117	106	125	106	181	110
Ta	0.6	1.5	1.1	0.8	0.8	0.9	1.1	1.1
Tb	0.29	0.88	1.57	0.94	0.92	0.92	3.4	1.37
Th	5	4.7	5.2	17.1	18.6	18.6	73.2	6
U	0.68	1.87	1.63	2.45	3.71	3.71	12.1	1.61
V	36	118	501	66	63	63	43	378
Y	8.8	24.8	52	32	26.7	26.2	83.7	45.3
Yb	0.63	2.11	4.94	3.33	2.8	2.68	7	4.41
Zn	61.5	106	215	36.3	49.3	32	40.2	243
Zr	154	225	215	177	182	183	90	212

Sample #	200036-6020e	200036-6020f	200036-6021	200036-6022	200036-6023	200036-6024	200036-6025	200036-6026
Sample #	6020e	6020f	6021	6022	6023	6024	6025	6026
Drill hole	BHD1	BHD1	BHD1	BHD2	BHD2	BHD2	BHD2	BHD2
Suite	Donington	Donington		Donington	Donington	Donington	Donington	
Lith			dlt dyke					dlt dyke
Q	26.49	13.4	5.03	39.17	36.57	40.65	22.81	6.55
C	2.05	0.74	-	7.34	6.36	5.9	5.6	5.14
Z	0.03	0.05	0.04	0.04	0.04	0.04	0.02	0.04
Or	13.14	19.17	11.04	24.62	23.45	22.13	24.83	30.39
Ab	38.71	28.9	18.27	12.11	17.15	14.55	21.2	4.24
An	11.3	19.57	19.79	5.33	4.68	5.83	10.16	7.03
Ne	-	-	-	-	-	-	-	-
Di	-	-	12.25	-	-	-	-	-
Di(CaMg)	-	-	7.56	-	-	-	-	-
Hd	-	-	4.69	-	-	-	-	-
Hy	5.21	9.09	17.72	8.51	7.91	7.97	10.37	30.81
En	3.92	7.18	10.35	4.57	4.76	4.23	5.37	16.02
Fs	1.29	1.9	7.37	3.94	3.15	3.74	4.99	14.79
Ol	-	-	-	-	-	-	-	-
Fo	-	-	-	-	-	-	-	-
Fa	-	-	-	-	-	-	-	-
Mt	2.11	6.38	8.77	1.8	2.59	1.8	1.64	10.8
Cm	-	-	0.02	0.02	0.02	0.02	0.01	0.02
Hm	-	-	-	-	-	-	-	-
Il	0.74	2.07	6.17	0.97	1.12	1.05	0.87	4.38
Ap	0.24	0.71	0.95	0.18	0.18	0.15	2.63	0.66
Fr	0.12	0.16	0.21	0.11	0.13	0.12	-	0.26
Cc	-	-	-	-	-	-	-	-
Diff. Index	78.34	61.47	34.34	75.9	77.17	77.33	68.85	41.18
Colour Index	8.06	17.54	44.92	11.29	11.64	10.83	12.89	46.01
Pl	50.01	48.47	38.06	17.45	21.84	20.39	31.36	11.28
Norm Plag Comp	22.6	40.38	52	30.58	21.45	28.61	32.39	62.39
100An/(An+Ab^)	22.6	40.38	52	30.58	21.45	28.61	32.39	62.39
Ab^	38.71	28.9	18.27	12.11	17.15	14.55	21.2	4.24
Q"	27.96	15.99	9.8	41.43	38.71	42.77	25.56	14.71
Ol^	3.74	6.51	12.94	6.24	5.77	5.85	7.62	22.65
Ne^	20.98	15.66	9.9	6.56	9.3	7.89	11.49	2.3
Q^	45.69	29.22	18.17	46.98	46.56	49.44	35.27	16.65
mg number	63.02	57.03	47.89	51.09	53.12	49.82	51.79	46.32

Sample #	200036-6027	200036-6028	200036-6029a	200036-6029b	200036-6029c	200036-6029d	200036-6029e	200036-6030
Drill hole	ACD12	ACD12	ACD6	ACD6	ACD6	ACD6	ACD6	ACD6
Suite	GRV?	GRV?	Donington	Donington	Donington	Donington	Donington	
Lith	felsic dyke	felsic dyke						mafic dyke
SiO2	75.16	44.95	69	69.16	46.29	47.83	58.81	44.52
TiO2	0.19	0.33	0.81	0.6	1.73	1.64	1.29	1.03
Al2O3	11.48	8.97	13.6	14.3	19.27	19.56	16.83	15.67
Fe2O3tot	3.01	33.45	5.41	3.78	11.56	10.11	7.21	16.16
Fe2O3	1.52	30.13	1.47	1.16	2.69	2.09	1.72	2.16
FEO	1.34	2.99	3.55	2.36	7.98	7.22	4.94	12.6
MnO	0.06	0.07	0.05	0.04	0.15	0.11	0.09	0.2
MgO	0.4	0.47	2.09	1.53	5.36	5.14	2.67	7.79
CaO	0.06	0.2	3.19	2.46	7.76	8.1	5.45	7.22
Na2O	0.1	0.09	2.03	1.7	1.62	2.36	2.28	1.57
K2O	7.48	6.79	2.47	4.67	4.01	3.71	2.75	2.41
P2O5	0.03	0.06	0.01	0.02	0.11	0.13	0.3	0.12
SO3	0.07	0.77		–	–	–	–	0.19
LOI	0.15	0.33		–	–	–	–	1.4
Total	98.02	96.14	98.49	98.42	97.4	98.3	97.43	96.87
Ag	0.07	0.05	0.03	0.05	0.05	0.06	0.06	0.07
Ba	898	660	588	1851	678	920	745	568
Be	5.8	0.7	2	2.1	2.8	3.8	3.3	1.2
Bi	0	1	0.1	0.2	0.3	0.1	0.1	0.4
Cd	–	–	–	–	0.06	0.37	0.07	–
Ce	140	195	77.3	20.3	39.4	35.3	43.1	16.3
Cr	–	25	54	29	5	10	93	139
Cs	3.01	0.49	4.49	3.16	4.63	4.91	4.37	3.92
Cu	27	781	29	61	98	69	28	128
Dy	6.04	8.52	1.33	0.89	5.15	6.25	2.95	3.57
Er	4.28	5.27	0.61	0.56	2.83	3.3	1.67	2.31
Eu (ppb)	837	2704	1511	1393	1517	1513	1538	1068
F	1955	2181	1317	595	1540	2072	1445	972
Ga	19.1	22.8	19.1	16	24.3	26.3	21.9	16.6
Ge	1.6	1.8	1.5	1.4	1.9	2	1.5	1.8
Gd	6	8.85	2.53	0.92	5.92	6.85	3.59	3.3
Hf	6.4	3.4	8	8.8	2.1	1.5	10	1.4
Ho	1.27	1.77	0.24	0.17	1.04	1.21	0.58	0.76
La	72	102	41.3	12.4	16	14.7	21.9	6.99
Lu	0.73	0.63	0.16	0.17	0.36	0.39	0.3	0.27
Mo	3.6	27.7	1.9	1.5	1.7	1.5	1.6	2
Nb	32.5	3.9	14.5	11.1	11.4	13.1	15.9	4.9
Nd	41.6	66	27	6.22	21.4	21	18.3	9.86
Ni	7	40	28	19	20	14	31	133
Pb	15.5	5.7	15.9	22.8	11.8	13.6	12.9	16.4
Pr	12.9	19.1	7.61	1.84	4.93	4.63	4.67	2.09
Rb	356	230	152	172	243	241	176	168
Sb	0.7	0.5	0.2	0.1	0.4	0.6	0.3	0.7
Sc	3	7	16	8	38	44	12	37
Sm	7.43	10.4	3.69	0.92	5.36	6.06	3.81	2.74
Sn	3.8	5.2	1.7	1.4	3.6	2.6	1.8	3
Sr	36.9	33.3	230	309	385	344	363	149
Ta	3.3	0.2	1	1.1	0.9	0.9	1.4	0.3
Tb	1.06	1.58	0.27	0.12	0.93	1.16	0.54	0.61
Th	94.2	2.2	14.1	1.7	1.9	0.5	0.9	0.5
U	20.6	10.8	1.45	0.85	1.19	0.41	1.04	0.2
V	6	121	106	32	439	473	219	239
Y	40	53.3	7.2	5.1	29.7	34.3	17.3	22
Yb	5.16	4.87	0.71	0.7	2.59	2.74	1.69	2.32
Zn	56.2	32.7	59.8	52.6	127	117	74	164
Zr	187	127	263	285	77	43	339	53

Sample #	200036-6027	200036-6028	200036-6029a	200036-6029b	200036-6029c	200036-6029d	200036-6029e	200036-6030
Sample #								
Drill hole	ACD12	ACD12	ACD6	ACD6	ACD6	ACD6	ACD6	ACD6
Suite	GRV?	GRV?	Donington	Donington	Donington	Donington	Donington	
Lith	felsic dyke	felsic dyke						mafic dyke
Q	45.81	18.61	36.89	33.38	-	-	18.35	-
C	3.27	1.54	2.11	2.04	-	-	1.14	-
Z	0.04	0.03	0.05	0.06	0.02	0.01	0.07	0.01
Or	45.33	42.3	14.91	28.23	24.53	22.49	16.8	15.01
Ab	0.87	0.8	17.48	14.68	13.33	16.31	19.86	13.94
An	-	-	15.32	12.51	34.53	32.53	25.29	30.01
Ne	-	-	-	-	0.44	2.22	-	-
Di	-	-	-	-	3.03	5.39	-	5.24
Di(CaMg)	-	-	-	-	1.85	3.35	-	2.76
Hd	-	-	-	-	1.18	2.05	-	2.48
Hy	2.04	1.23	9.41	6.39	-	-	12.67	5.89
En	1.02	1.23	5.3	3.89	-	-	6.85	2.9
Fs	1.03	-	4.12	2.51	-	-	5.82	2.99
Ol	-	-	-	-	16.37	14.32	-	24.22
Fo	-	-	-	-	9.05	8.08	-	11.34
Fa	-	-	-	-	7.32	6.24	-	12.88
Mt	2.25	9.38	2.19	1.72	4.12	3.2	2.61	3.34
Cm	-	0.01	0.01	0.01	-	-	0.02	0.03
Hm	-	25.25	-	-	-	-	-	-
Il	0.37	0.66	1.57	1.16	3.39	3.18	2.52	2.05
Ap	0.1	0.17	0.02	0.05	0.27	0.32	0.74	0.3
Fr	0.58	0.5	0.27	0.12	0.3	0.4	0.24	0.18
Cc	<.55	<.31	-	-	-	-	-	-
Diff. Index	92	61.71	69.28	76.28	38.3	41.01	55.01	28.95
Colour Index	4.67	36.52	13.18	9.29	26.91	26.09	17.82	40.77
Pl	0.87	0.8	32.8	27.19	47.86	48.84	45.15	43.95
Norm Plag Comp	-	-	46.71	46.02	72.15	66.61	56.01	68.28
100An/(An+Ab^)	-	-	46.71	46.02	70.95	61.46	56.01	68.28
Ab^	0.87	0.8	17.48	14.68	14.14	20.4	19.86	13.94
Q"	46.35	18.98	39.41	35.11	-	-	21.72	1.55
Ol^	1.51	0.86	6.89	4.66	16.37	14.32	9.29	28.56
Ne^	0.47	0.43	9.47	7.96	7.66	11.06	10.76	7.55
Q^	46.75	19.34	47.41	41.83	6.1	7.47	30.82	7.93
mg number	34.72	21.88	51.2	53.6	54.48	55.92	49.06	52.42

Sample #	200036-6031	200036-6032a	200036-6032b	200036-6032c	200036-6032d	200036-6033	200036-6034a	200036-6034b	200036-6034c
Drill hole	IDD3	IDD3	IDD3	IDD3	IDD3	IDD3	WRD24	WRD24	WRD24
Suite		Donington	Donington	Donington	Donington		Donington	Donington	Donington
Lith	dlt dyke					c.g. grt dyke			
SiO2	48.76	65.65	70.51	68.83	63.3	72.04	64.37	64.72	65.71
TiO2	1.87	0.65	0.48	0.43	0.73	0.22	0.71	0.8	0.48
Al2O3	13.84	14.55	13.43	13.6	15.69	13.61	12.95	14.66	14.24
Fe2O3tot	14.62	5.79	3.54	4.77	6.48	1.88	10.44	8.16	6.96
Fe2O3	4.69	2.11	1.7	2.37	2.77	0.67	4.05	3.44	2.82
FEO	8.94	3.31	1.65	2.16	3.34	1.09	5.75	4.25	3.72
MnO	0.24	0.11	0.08	0.07	0.07	0.04	0.03	0.09	0.11
MgO	5.64	2.43	1.58	1.62	2.64	0.77	1.15	0.97	0.75
CaO	7.98	0.93	0.6	0.46	0.78	0.56	0.33	0.41	0.32
Na2O	1.9	1.17	1.42	1.18	1.42	2.71	0.12	0.16	0.29
K2O	1.76	6.03	6.03	6.7	5.96	6.43	5.14	6.41	8.09
P2O5	0.2	0.15	0.06	0.09	0.1	0.05	0.22	0.29	0.16
SO3	0.09	–	–	–	–	0.06	–	–	–
LOI	1	–	–	–	–	0.12	–	–	–
Total	96.91	97.31	97.8	97.78	97.07	98.36	95.39	96.57	96.99
Ag	0.04	0.06	0.06	0.04	0.06	0.06	0.05	0.06	0.06
Ba	392	1025	942	1192	969	860	714	745	1135
Be	1	2.2	1.6	1.1	2.8	0.2	2.1	2.8	1.6
Bi	0.1	0.3	0.2	0.1	0.1	0.2	0.4	0.9	0.1
Cd	0.13	–	–	0.22	–	–	–	–	–
Ce	45.6	28.6	105	73.6	109	69	243	299	172
Cr	126	21	31	37	29	21	11	11	6
Cs	2.9	4.98	3.35	3.42	3.46	0.66	1.79	3.24	1.98
Cu	225	51	51	42	20	29	1628	829	533
Dy	7.07	2.67	4.94	2.14	16.3	2.67	7.18	8.56	5.25
Er	4.37	1.6	2.53	1.04	13.7	1.27	4.11	4.63	2.66
Eu (ppb)	1814	768	1201	1009	1659	1013	2047	2824	2164
F	723	1335	789	1012	1298	339	2662	3359	3275
Ga	22.7	19.8	14	17	23	13.7	17.4	21.2	18.4
Ge	2.1	1.5	1.5	1.6	1.6	1.2	1.7	1.7	1.7
Gd	7.1	2.8	6.94	3.8	11.8	3.91	7.98	11.3	7.95
Hf	4.7	6.2	5.9	7.2	6.5	3.9	6.9	7.5	5.3
Ho	1.45	0.55	0.95	0.39	4.06	0.47	1.45	1.7	0.99
La	20.1	13.9	49.9	36.2	52	34.6	138	172	85.3
Lu	0.53	0.27	0.33	0.17	2.21	0.07	0.57	0.6	0.33
Mo	3.6	1.4	2.2	1.5	1.5	6	7.8	4.6	4
Nb	12.7	21	13.4	10.9	18.4	5.8	18.5	23.2	12.6
Nd	24.4	12	41.6	28.2	43.6	26.3	67	92	66.2
Ni	69	15	14	15	18	7	11	10	9
Pb	24.8	9	14.9	13.5	11.4	15.2	10.9	14.1	17.8
Pr	5.47	3.13	11.3	7.74	11.4	7.03	21.4	27.6	17.7
Rb	102	281	231	241	248	154	172	254	317
Sb	0.4	0.8	0.4	0.5	0.5	0.2	1.4	1.3	1
Sc	40	17	12	12	22	6	12	13	7
Sm	6.15	2.54	7.65	4.84	9.45	4.58	9.18	14.3	10.8
Sn	2.7	3.3	2.7	3.7	4.6	2.1	6.1	4.2	5.6
Sr	146	58.5	72.8	77.5	69	111	113	118	115
Ta	0.9	1.6	1.2	0.9	1.4	0.5	1.3	1.4	0.8
Tb	1.23	0.49	1.02	0.44	2.48	0.56	1.31	1.72	1.05
Th	4.9	8.2	24.6	14.3	22.5	20.3	16.9	35.3	20.8
U	1.33	1.39	2.95	1.47	4.16	2.24	5.62	7.39	5.06
V	375	69	51	58	75	31	53	61	34
Y	43.1	16.6	27.4	10.9	128	14.7	42.6	50.7	29.3
Yb	4.09	1.54	2.28	0.97	15.3	1.08	3.77	4.26	2.25
Zn	213	65.3	39.6	43.5	62.4	52.5	135	88	52.9
Zr	181	219	190	234	223	129	250	273	192

Sample #	200036-6031	200036-6032a	200036-6032b	200036-6032c	200036-6032d	200036-6033	200036-6034a	200036-6034b	200036-6034c
Sample #	6031	6032a	6032b	6032c	6032d	6033	6034a	6034b	6034c
Drill hole	IDD3	IDD3	IDD3	IDD3	IDD3	IDD3	WRD24	WRD24	WRD24
Suite		Donington	Donington	Donington	Donington		Donington	Donington	Donington
Lith	dlt dyke					felsic dyke			
Q	4.85	30.08	36.23	33.47	26.72	29.43	41.62	37.43	31.12
C	-	5.13	3.82	4.02	6.14	1.31	7.57	7.74	5.16
Z	0.04	0.04	0.04	0.05	0.04	0.03	0.05	0.05	0.04
Or	10.89	36.81	36.62	40.7	36.48	38.76	32.1	39.47	49.57
Ab	16.78	10.2	12.32	10.24	12.41	23.35	1.07	1.41	2.54
An	25.09	3.14	2.38	1.37	2.7	2.55	-	-	-
Ne	-	-	-	-	-	-	-	-	-
Di	11.96	-	-	-	-	-	-	-	-
Di(CaMg)	7.42	-	-	-	-	-	-	-	-
Hd	4.54	-	-	-	-	-	-	-	-
Hy	19.09	9.79	5.03	5.59	9.64	3.13	9.44	6.46	5.98
En	11.22	6.23	4.03	4.14	6.79	1.95	3.02	2.51	1.93
Fs	7.87	3.56	1	1.46	2.85	1.18	6.42	3.95	4.04
Ol	-	-	-	-	-	-	-	-	-
Fo	-	-	-	-	-	-	-	-	-
Fa	-	-	-	-	-	-	-	-	-
Mt	7.18	3.17	2.54	3.54	4.16	1	6.2	5.2	4.24
Cm	0.03	-	0.01	0.01	0.01	-	-	-	-
Hm	-	-	-	-	-	-	-	-	-
Il	3.71	1.27	0.93	0.84	1.43	0.43	1.42	1.58	0.94
Ap	0.5	0.38	0.15	0.24	0.26	0.13	0.59	0.76	0.44
Fr	0.11	0.26	0.16	0.21	0.26	0.07	0.56	0.69	0.75
Cc	-	-	-	-	-	-	<.55	<.74	<.59
Diff. Index	32.52	77.08	85.16	84.41	75.61	91.54	74.79	78.32	83.22
Colour Index	41.96	14.24	8.51	9.97	15.25	4.55	17.07	13.24	11.15
Pl	41.86	13.34	14.69	11.61	15.12	25.9	1.07	1.41	2.54
Norm Plag Comp	59.93	23.54	16.17	11.78	17.88	9.83	-	-	-
100An/(An+Ab^)	59.93	23.54	16.17	11.78	17.88	9.83	-	-	-
Ab^	16.78	10.2	12.32	10.24	12.41	23.35	1.07	1.41	2.54
Q"	10	32.75	37.66	35.04	29.4	30.28	43.99	39.09	32.62
Ol^	13.94	7.12	3.6	4.02	6.96	2.28	7.08	4.81	4.48
Ne^	9.09	5.53	6.68	5.55	6.73	12.66	0.58	0.76	1.38
Q^	17.68	37.42	43.3	39.73	35.08	40.98	44.48	39.73	33.78
mg number	52.92	56.68	63.05	57.2	58.48	55.73	26.28	28.91	26.43

Appendix 3

Standard Data

Table A3-1. SHRIMP analytical results for QGNG; mounts Z3677 and Z3678, analysis date 8/4/01, SHRIMP II.

Spot Name	204-corr Pb/U: UO/U^2	% err	206 /238 Age Ma	±	% comm 206	ppm U	ppm Th	232Th /238U	Ln UO/U	Ln Pb/U	204 overcts /sec (fr. 207)	4-corr 207 /206 age	±
901.1	.02220	0.4	1878	6	0.03	345	345	1.03	1.765	-0.282	+0.12	1848.3	5.2
902.1	.02171	0.5	1843	8	0.02	385	376	1.01	1.754	-0.329	+0.06	1850.1	5.0
903.1	.02121	0.5	1805	8	0.08	149	133	0.92	1.772	-0.299	+0.15	1842.5	9.9
904.1	.02163	0.4	1837	6	0.06	233	177	0.79	1.813	-0.200	-0.39	1865.9	6.9
905.1	.02160	0.4	1834	7	0.03	236	238	1.04	1.758	-0.319	-0.16	1857.7	6.3
906.1	.02154	0.3	1830	5	0.02	401	372	0.96	1.743	-0.347	+0.21	1846.8	5.4
907.1	.02136	0.4	1817	6	0.03	275	280	1.05	1.742	-0.355	-0.15	1856.8	8.5
908.1	.02192	0.6	1858	10	0.02	273	201	0.76	1.805	-0.202	-0.23	1858.9	5.5
909.1	.02188	0.8	1855	13	0.02	479	409	0.88	1.671	-0.481	+0.31	1844.6	5.2
910.1	.02185	0.4	1853	7	0.04	206	223	1.12	1.790	-0.244	-0.08	1854.8	6.2
911.1	.02202	0.6	1865	9	0.00	268	277	1.07	1.763	-0.290	-0.26	1860.0	5.2
912.1	.02204	0.4	1866	6	0.01	268	223	0.86	1.775	-0.260	+0.05	1849.9	5.5
913.1	.02180	0.5	1849	8	0.08	148	77	0.54	1.752	-0.315	+0.08	1846.9	7.8
914.1	.02170	0.4	1842	6	-0.01	283	273	1.00	1.769	-0.285	+0.19	1845.7	8.1
915.1	.02194	0.4	1859	6	0.05	234	234	1.03	1.776	-0.270	-0.14	1856.9	7.7
916.1	.02171	0.3	1843	5	0.04	427	399	0.97	1.768	-0.290	-0.30	1858.4	6.2
917.1	.02214	0.4	1874	7	0.08	204	172	0.87	1.737	-0.329	+0.25	1839.2	7.1
918.1	.02201	0.5	1865	9	0.06	115	67	0.61	1.765	-0.285	+0.06	1846.5	8.7
919.1	.02161	0.4	1835	6	-0.01	229	199	0.90	1.780	-0.266	+0.03	1850.3	5.7
920.1	.02189	0.4	1856	6	0.04	271	277	1.06	1.765	-0.288	+0.01	1851.3	6.0
921.1	.02183	0.4	1852	6	-0.02	282	210	0.77	1.743	-0.333	-0.24	1860.0	5.5
922.1	.02185	0.5	1853	8	0.06	139	81	0.60	1.770	-0.275	+0.08	1846.0	9.7
923.1	.02148	0.5	1825	8	0.08	141	111	0.81	1.767	-0.297	+0.01	1850.9	10.2
924.1	.02128	0.4	1811	6	0.04	355	341	0.99	1.805	-0.238	+0.17	1846.5	5.6
925.1	.02199	0.4	1863	6	0.01	372	198	0.55	1.785	-0.243	-0.05	1852.9	4.8
926.1	.02137	0.6	1818	9	0.03	112	64	0.59	1.708	-0.425	+0.20	1832.2	9.9
900.1	.02092	0.3	1784	5	0.03	643	403	0.65	1.765	-0.341	-0.11	1853.2	3.7
901.1	.02122	0.4	1806	6	0.04	240	243	1.05	1.781	-0.291	-0.03	1852.9	5.9
902.1	.02222	0.4	1880	6	0.01	600	378	0.65	1.833	-0.136	+0.10	1849.4	5.0
903.1	.02157	0.3	1832	5	0.01	475	327	0.71	1.743	-0.345	-0.02	1852.0	4.1
904.1	.02180	0.6	1849	9	0.02	105	59	0.58	1.752	-0.315	+0.00	1851.5	8.7
905.1	.02136	0.5	1816	9	0.08	114	83	0.76	1.803	-0.233	+0.18	1836.9	9.0
906.1	.02147	0.3	1824	5	0.01	382	248	0.67	1.767	-0.302	+0.30	1844.0	4.8
907.1	.02170	0.4	1842	6	0.03	386	367	0.98	1.794	-0.238	+0.39	1842.0	4.8
908.1	.02191	0.3	1857	6	0.02	336	185	0.57	1.783	-0.249	+0.13	1848.2	4.9
											average	**+0.03**	
											95%conf	**±0.06**	

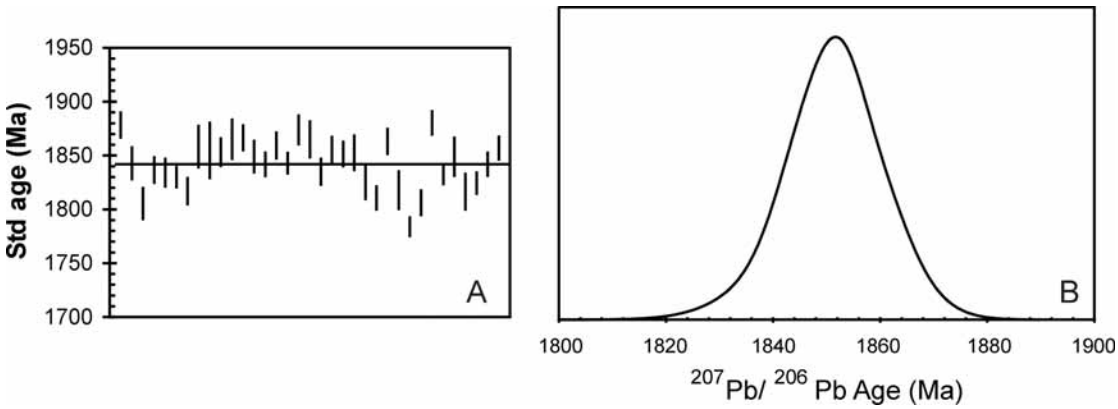

Figure A3-1. (A) Standard $^{206}Pb/^{238}U$ ages for QGNG; and (B) probability density diagram showing the weighted mean $^{207}Pb/^{206}Pb$ ages for QGNG standard analyses for mounts Z3677 and Z3678, analysis date 8/4/01, SHRIMP II.

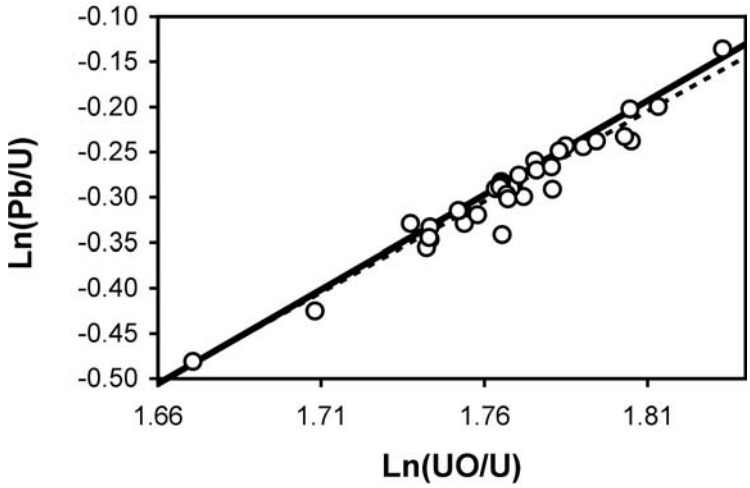

Figure A3-2. Pb/U calibration for mounts Z3677 and Z3678 analysis date 8/4/01, SHRIMP II. Thick line is robust fit: dashed line has slope = 2.

Table A3-2. SHRIMP analytical results for QGNG; mount Z3678, analysis date 4/6/01, SHRIMP II.

Spot Name	204-corr Pb/U: UO/U^2	% err	Age Ma	±	% comm 206	ppm U	ppm Th	232Th /238U	Ln UO/U	Ln Pb/U	204 overcts /sec (fr. 207)	4-corr 207 /206 age	±
904.2	.02127	0.8	1858	13	0.04	131	84	0.66	1.846	-0.167	+0.05	1846.3	9.4
908.2	.02066	0.4	1811	6	0.02	347	234	0.70	1.818	-0.238	+0.31	1841.8	5.3
909.1	.02118	0.4	1851	6	0.02	375	276	0.76	1.864	-0.125	-0.03	1852.6	5.3
910.1	.02107	0.4	1843	6	0.01	345	340	1.02	1.816	-0.219	+0.12	1847.2	5.7
911.1	.02115	0.5	1849	9	0.02	134	75	0.58	1.845	-0.155	+0.08	1845.2	9.2
912.1	.02110	0.5	1845	7	-0.01	192	152	0.82	1.857	-0.132	+0.01	1850.9	6.9
913.1	.02108	0.5	1844	7	0.02	177	138	0.81	1.835	-0.182	+0.01	1851.1	7.6
914.1	.02124	0.5	1855	7	0.00	212	183	0.89	1.768	-0.315	+0.02	1850.2	8.1
915.1	.02137	0.5	1865	7	0.02	195	162	0.86	1.870	-0.099	-0.24	1864.7	7.5
916.1	.02141	0.5	1869	8	0.06	168	106	0.65	1.886	-0.062	+0.03	1849.9	7.9
917.1	.02137	0.3	1865	6	0.05	408	246	0.62	1.890	-0.065	+0.17	1846.9	5.1
918.1	.02117	0.3	1851	5	0.01	423	280	0.68	1.857	-0.135	-0.08	1853.6	8.0
919.1	.02065	0.3	1810	5	0.00	373	269	0.75	1.820	-0.235	-0.25	1858.7	5.0
920.1	.02125	0.4	1857	7	0.03	255	142	0.57	1.842	-0.162	+0.28	1839.0	6.4
921.1	.02096	0.4	1834	6	0.01	362	280	0.80	1.853	-0.153	-0.15	1856.4	5.2
922.1	.02069	0.4	1814	7	-0.01	239	208	0.90	1.823	-0.225	-0.09	1856.5	6.7
922.2	.02027	0.9	1782	14	0.06	230	203	0.91	1.822	-0.247	+0.25	1838.2	7.6
923.1	.02153	0.4	1878	7	0.02	246	233	0.98	1.801	-0.234	+0.19	1841.2	6.8
924.1	.02102	0.6	1839	9	0.01	502	450	0.93	1.790	-0.280	+0.14	1848.2	4.6
925.1	.02107	0.4	1843	7	0.00	224	194	0.90	1.839	-0.176	-0.02	1852.6	6.6
926.1	.02074	0.7	1818	11	0.02	324	333	1.06	1.849	-0.169	-0.11	1855.3	5.3
926.2	.02093	0.4	1832	6	0.00	335	343	1.06	1.839	-0.186	+0.07	1849.2	5.4
927.1	.02103	0.4	1840	6	0.01	279	268	0.99	1.820	-0.219	+0.02	1850.7	5.8
909.2	.02107	0.4	1843	6	0.02	329	228	0.71	1.822	-0.213	+0.13	1847.1	5.5
										average	**+0.04**		
										95%conf	**±0.06**		

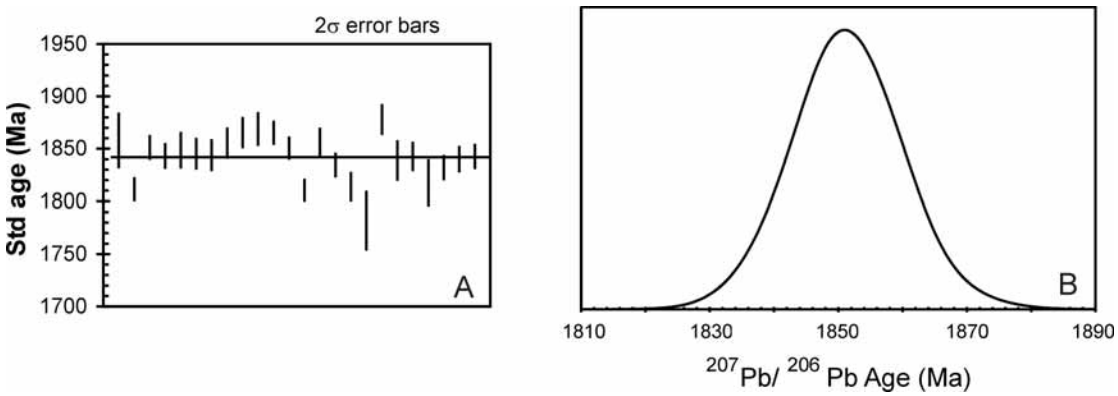

Figure A3-3. (A) Standard $^{206}Pb/^{238}U$ ages for QGNG; and (B) probability density diagram showing the weighted mean $^{207}Pb/^{206}Pb$ ages for QGNG standard analyses for mount Z3678, analysis date 4/6/01, SHRIMP II.

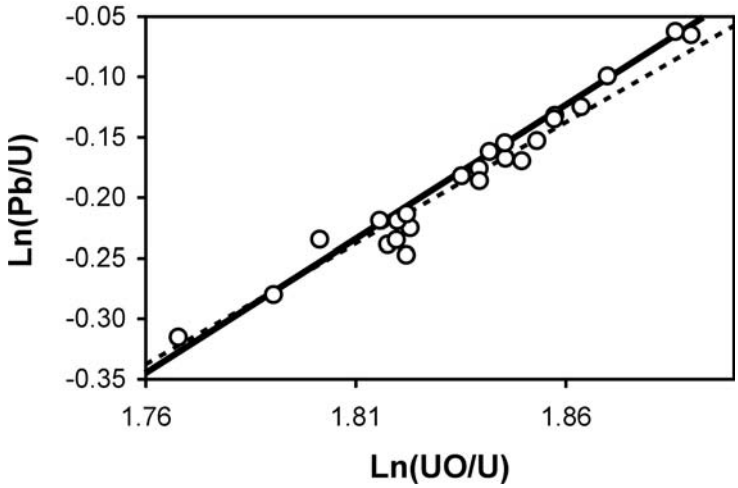

Figure A3-4. Pb/U calibration for mount Z3678, analysis date 4/6/01, SHRIMP II. Thick line is robust fit: dashed line has slope = 2.

Table A3-3. SHRIMP analytical results for QGNG; mount Z3931, analysis date 26/4/02, SHRIMP I.

Spot Name	204-corr Pb/U: UO/U^2	% err	Age Ma	±	% comm 206	ppm U	ppm Th	232Th /238U	Ln UO/U	Ln Pb/U	204 overcts /sec (fr. 207)	4-corr 207 /206 age	±
901.1	.01776	0.7	1803	10	0.07	314	253	0.83	1.838	-0.349	-0.03	1853.7	11.9
902.1	.01822	0.7	1844	11	0.12	396	280	0.73	1.789	-0.430	+0.42	1822.0	17.9
903.1	.01833	0.8	1854	13	0.07	232	184	0.82	1.892	-0.210	+0.10	1840.6	14.0
904.1	.01789	2.9	1815	46	0.08	358	273	0.79	1.992	-0.117	-2.28	2047.6	117.2
905.1	.01701	1.1	1737	17	0.09	269	287	1.10	2.005	-0.055	+0.15	1820.4	18.1
906.1	.01732	1.1	1765	17	-0.01	356	249	0.72	2.051	0.035	+0.16	1828.9	13.3
907.1	.01758	1.6	1788	24	0.04	193	218	1.17	2.085	0.130	-0.12	1893.2	22.4
908.1	.01709	1.9	1745	29	0.52	217	223	1.06	2.129	0.189	+0.06	1820.0	51.4
909.1	.01861	0.7	1879	12	0.18	253	148	0.60	1.893	-0.188	+0.10	1843.5	12.5
910.1	.01868	0.5	1885	9	0.00	448	423	0.97	1.927	-0.115	+0.20	1842.8	7.3
911.1	.01897	0.7	1910	12	0.10	216	141	0.68	1.915	-0.127	+0.01	1851.2	12.1
912.1	.01876	0.8	1891	14	-0.01	164	117	0.74	1.846	-0.280	-0.16	1871.4	12.1
913.1	.01800	0.7	1825	10	0.11	279	207	0.77	1.884	-0.231	+0.31	1828.7	14.3
914.1	.01902	0.9	1915	15	0.01	377	321	0.88	1.878	-0.197	+0.39	1833.8	6.8
915.1	.01875	0.5	1891	8	0.05	265	260	1.01	1.890	-0.190	+0.22	1837.9	7.9
916.1	.01878	0.6	1894	10	0.06	188	181	0.99	1.892	-0.186	+0.15	1838.0	10.2
917.1	.01847	0.4	1866	7	0.04	342	214	0.65	1.857	-0.268	-0.22	1862.3	7.6
918.1	.01889	0.7	1903	12	0.01	325	333	1.06	1.900	-0.168	+0.22	1841.4	6.4
919.1	.01800	0.7	1825	12	0.04	117	77	0.68	1.813	-0.381	+0.12	1834.1	12.8
920.1	.01923	4.4	1932	73	0.08	178	154	0.89	1.815	-0.216	+0.00	1851.4	9.3
921.1	.01708	2.9	1743	44	0.14	236	222	0.97	1.988	-0.141	+0.26	1830.4	9.7
922.1	.01785	0.7	1812	11	0.03	306	254	0.86	1.874	-0.271	+0.10	1845.5	7.7
923.1	.01838	1.6	1859	26	0.04	270	274	1.05	1.928	-0.138	+0.30	1828.7	14.1
924.1	.01815	0.5	1839	8	0.04	227	228	1.04	1.905	-0.196	-0.06	1855.3	9.7
925.1	.01822	0.5	1844	8	0.04	247	244	1.02	1.860	-0.281	+0.13	1844.0	7.9
926.1	.01844	0.8	1863	13	0.00	258	123	0.49	1.867	-0.253	-0.08	1855.9	7.9
927.1	.01863	1.1	1880	18	0.13	168	152	0.94	1.892	-0.190	+0.28	1827.1	10.6
928.1	.01779	0.6	1807	9	0.05	285	210	0.76	1.901	-0.219	+0.04	1848.3	10.1
929.1	.01758	0.5	1788	8	-0.03	251	228	0.94	1.885	-0.265	-0.13	1861.6	8.4
930.1	.01785	0.6	1812	10	0.05	214	165	0.80	1.912	-0.197	+0.04	1847.2	15.3
930.2	.01801	0.6	1826	9	0.11	203	151	0.77	1.913	-0.187	+0.17	1837.2	11.7
931.1	.01760	0.5	1790	7	0.00	257	270	1.09	1.906	-0.221	-0.06	1855.0	6.6
932.1	.01896	1.2	1909	19	0.08	212	138	0.67	1.927	-0.101	+0.15	1842.6	10.2
933.1	.01817	0.5	1840	8	0.08	198	220	1.15	1.892	-0.216	+0.23	1836.9	11.1
934.1	.01802	0.5	1827	8	0.02	193	199	1.07	1.884	-0.241	+0.15	1842.0	8.2
935.1	.01857	0.4	1875	6	-0.01	425	418	1.02	1.939	-0.109	+0.01	1851.2	4.8
936.1	.01825	0.4	1847	7	-0.01	243	180	0.77	1.864	-0.267	-0.19	1861.5	7.2
										average	**+0.10**		
										95%conf	**±0.06**		

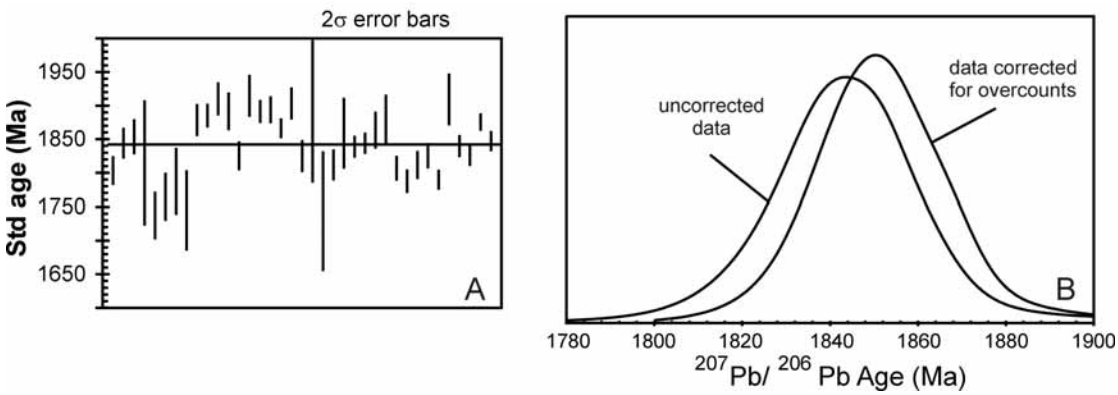

Figure A3-5. (A) Standard $^{206}Pb/^{238}U$ ages for QGNG; and (B) probability density diagram showing the uncorrected vs overcount-corrected weighted mean $^{207}Pb/^{206}Pb$ ages for QGNG standard analyses for mount Z3931, analysis date 26/4/02, SHRIMP I.

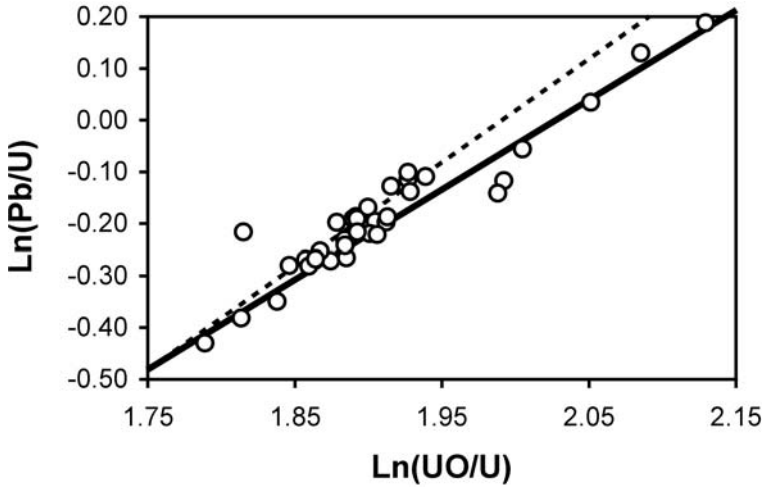

Figure A3-6. Pb/U calibration for mount Z3931, analysis date 26/4/02, SHRIMP I. Thick line is robust fit: dashed line has slope = 2.

Table A3-4. SHRIMP analytical results for QGNG; mount Z3966, analysis date 11/6/02, SHRIMP I.

Spot Name	204-corr Pb/U: UO/U^2	% err	206Pb/ 238U Age Ma	±	% comm 206	ppm U	ppm Th	232Th /238U	Ln UO/U	Ln Pb/U	204 overcts /sec (fr. 207)	4-corr 207 /206 age	±
901.1	.01927	0.7	1898	12	0.10	251	255	1.05	1.887	-0.167	+0.13	1839.8	12.4
902.1	.01938	3.7	1907	61	0.23	172	125	0.75	1.932	-0.053	+0.12	1832.8	20.1
903.1	.01883	1.9	1861	30	0.01	154	85	0.57	1.922	-0.113	-0.08	1863.2	14.7
904.1	.01731	0.7	1729	11	0.01	287	243	0.87	1.851	-0.343	+0.30	1821.4	11.6
905.1	.01876	0.9	1855	15	-0.06	168	149	0.92	1.807	-0.353	+0.24	1812.2	16.7
906.1	.01943	0.9	1912	15	-0.03	265	272	1.06	1.909	-0.121	-0.04	1855.5	16.9
907.1	.01894	0.8	1870	13	0.08	223	236	1.09	1.879	-0.200	+0.24	1824.8	14.9
908.1	.01829	0.8	1814	13	-0.03	216	157	0.75	1.894	-0.201	+0.02	1849.1	12.9
909.1	.01841	0.7	1825	12	-0.07	280	294	1.08	1.891	-0.202	-0.06	1857.5	11.7
910.1	.01873	0.8	1852	12	0.00	259	267	1.07	1.908	-0.154	+0.17	1835.1	10.8
911.1	.01782	0.9	1773	13	0.06	195	134	0.71	1.871	-0.276	+0.16	1830.9	15.9
912.1	.01853	0.7	1835	11	-0.04	207	162	0.81	1.887	-0.206	+0.05	1845.9	11.1
913.1	.01769	1.1	1762	17	0.10	104	67	0.67	1.820	-0.375	-0.08	1871.7	22.4
914.1	.01856	0.8	1837	12	0.14	159	131	0.85	1.900	-0.177	+0.14	1831.5	14.8
915.1	.01529	0.5	1549	7	0.34	558	186	0.34	2.048	-0.072	+2.10	1721.2	15.0
916.1	.02011	0.8	1970	13	0.27	168	53	0.32	1.761	-0.372	+0.41	1785.1	15.3
910.2	.01835	0.6	1819	10	0.03	247	257	1.08	1.849	-0.294	+0.44	1805.1	10.1
917.1	.01919	0.7	1891	12	0.21	183	192	1.09	1.905	-0.136	+0.21	1823.5	15.0
918.1	.01897	1.2	1872	19	0.01	155	134	0.89	1.887	-0.197	-0.05	1860.1	11.6
919.1	.01830	0.8	1815	12	0.05	179	125	0.72	1.814	-0.362	+0.16	1825.4	12.4
920.1	.01767	2.7	1760	41	0.06	129	69	0.55	1.890	-0.252	-0.03	1859.4	19.7
921.1	.01800	0.7	1789	11	-0.01	186	172	0.96	1.838	-0.340	-0.01	1852.5	10.6
922.1	.01890	0.6	1867	10	0.02	242	236	1.01	1.870	-0.223	+0.11	1841.3	9.8
923.1	.01886	0.6	1864	9	-0.05	256	282	1.14	1.865	-0.234	-0.12	1861.6	9.1
924.1	.01999	0.5	1960	9	0.03	288	214	0.77	1.823	-0.252	+0.29	1829.5	8.2
925.1	.01918	1.0	1890	17	-0.09	77	46	0.62	1.808	-0.330	+0.03	1843.7	20.5
926.1	.02003	34.1	1963	577	0.02	151	132	0.90	1.848	-0.265	-0.05	1858.6	12.5
927.1	.01830	0.4	1815	7	0.02	481	260	0.56	1.822	-0.350	-0.11	1857.5	6.8
928.1	.01842	0.8	1825	13	0.12	179	184	1.06	1.848	-0.303	+0.10	1835.5	13.4
929.1	.01826	0.5	1811	8	0.00	572	320	0.58	1.820	-0.357	-0.06	1854.0	5.8
930.1	.01870	0.5	1849	8	-0.02	325	294	0.93	1.803	-0.370	+0.16	1841.5	8.4
931.1	.01991	0.5	1953	8	0.00	608	402	0.68	1.843	-0.186	+0.07	1848.9	8.2
932.1	.01585	2.1	1600	29	0.13	144	115	0.82	1.913	-0.242	+0.11	1820.4	26.4
933.1	.01848	1.0	1830	17	-0.10	221	174	0.81	1.880	-0.233	-0.08	1862.9	20.3
934.1	.01886	1.2	1863	20	0.01	154	89	0.60	1.891	-0.179	-0.08	1865.7	18.2
935.1	.01874	1.4	1853	23	0.13	165	121	0.76	1.831	-0.320	+0.42	1774.9	18.5
936.1	.01894	0.7	1870	12	0.08	395	232	0.61	1.813	-0.334	+0.14	1841.0	11.4
937.1	.01824	0.6	1810	10	-0.03	536	394	0.76	1.857	-0.282	-0.25	1864.6	10.0
938.1	.01893	0.8	1869	12	-0.08	405	316	0.81	1.862	-0.234	+0.16	1840.3	12.1
939.1	.01896	1.5	1872	24	0.21	146	85	0.61	1.868	-0.227	+0.30	1792.2	24.1
940.1	.01726	0.8	1724	13	0.15	181	154	0.87	1.815	-0.421	+0.07	1836.0	16.1

Spot Name	204-corr Pb/U: UO/U^2	% err	206Pb/ 238UAge Ma	±	% comm 206	ppm U	ppm Th	232Th /238U	Ln UO/U	Ln Pb/U	204 overcts /sec (fr. 207)	4-corr 207 /206 age	±
902.2	.02014	0.8	1972	14	0.04	159	125	0.81	1.814	-0.275	+0.19	1819.7	13.9
941.1	.01809	1.0	1797	16	0.09	165	157	0.99	1.824	-0.354	-0.21	1883.7	23.3
942.1	.01904	1.1	1878	18	-0.24	144	117	0.84	1.868	-0.219	-0.20	1881.1	20.2
943.1	.01842	1.0	1825	15	0.09	279	303	1.12	1.869	-0.259	-0.15	1863.6	14.0
944.1	.01882	1.1	1859	17	0.08	157	100	0.66	1.834	-0.291	-0.04	1857.1	18.0
945.1	.01830	0.9	1815	14	0.14	234	179	0.79	1.881	-0.238	+0.27	1824.8	15.2
946.1	.01856	1.1	1837	18	0.15	178	139	0.80	1.857	-0.260	+0.37	1789.1	17.5
947.1	.01743	1.0	1739	16	0.05	332	313	0.97	1.890	-0.227	+0.18	1835.2	13.1
948.1	.01821	0.9	1807	14	0.00	308	348	1.17	1.896	-0.206	-0.06	1858.1	13.1
913.2	.01713	1.2	1713	19	0.51	90	54	0.62	1.838	-0.385	+0.18	1766.3	39.6
										average	**+0.08**		
										95%conf	**±0.05**		

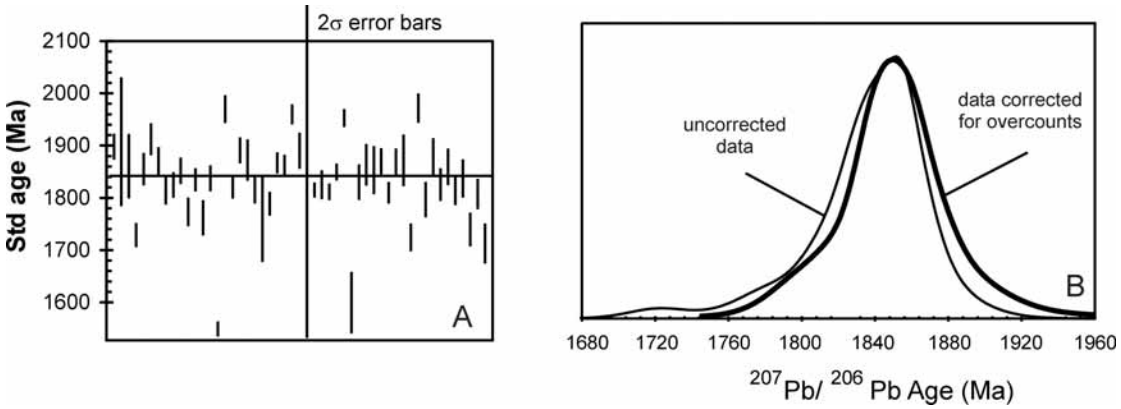

Figure A3-7. (A) Standard $^{206}Pb/^{238}U$ ages for QGNG; and (B) probability density diagram showing the uncorrected vs overcount-corrected weighted mean $^{207}Pb/^{206}Pb$ ages for QGNG standard analyses for mount Z3966, analysis date 11/6/02, SHRIMP I.

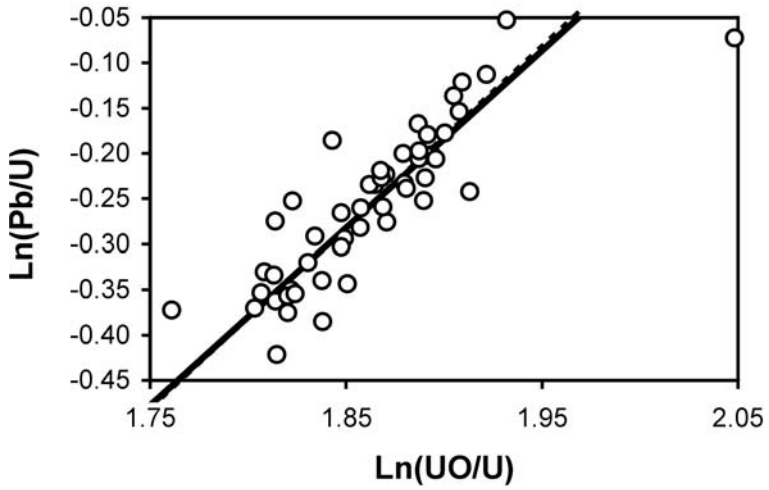

Figure A3-8. Pb/U calibration for mount Z3966, analysis date 11/6/02, SHRIMP I. Thick line is robust fit: dashed line has slope = 2.

Table A3-5. SHRIMP analytical results for QGNG; mount Z3962, analysis date 22/4/03, SHRIMP II.

Spot Name	204-corr Pb/U: UO/U^2	% err	206Pb/ 238U Age Ma	±	% comm 206	ppm U	ppm Th	232Th /238U	Ln UO/U	Ln Pb/U	204 overcts /sec (fr. 207)	4-corr 207 /206 age	±
909.1	.02223	0.4	1864	7	0.03	194	105	0.56	1.705	-0.385	+0.30	1839.5	5.6
910.1	.02289	0.4	1912	8	0.00	340	319	0.97	1.617	-0.538	+0.12	1847.2	4.4
911.1	.02234	0.3	1872	6	0.01	199	157	0.81	1.700	-0.397	-0.17	1856.0	5.4
912.1	.02228	0.6	1868	11	0.02	227	220	1.00	1.702	-0.395	+0.14	1845.7	6.3
913.1	.02224	0.3	1865	5	0.01	259	265	1.06	1.702	-0.398	+0.35	1840.4	5.2
914.1	.02197	0.3	1845	5	-0.01	271	216	0.82	1.697	-0.419	+0.47	1837.5	4.7
915.1	.02221	0.3	1863	6	0.00	241	172	0.74	1.598	-0.608	-0.24	1858.0	10.4
916.1	.02179	0.3	1832	6	-0.01	232	232	1.04	1.696	-0.429	-0.09	1852.9	5.1
917.1	.02193	0.2	1842	4	0.00	523	493	0.97	1.707	-0.403	+1.05	1835.1	3.4
918.1	.02221	0.3	1863	5	0.02	310	268	0.89	1.703	-0.396	-0.03	1850.8	4.9
919.1	.02251	0.4	1884	7	-0.02	379	372	1.01	1.698	-0.394	-0.15	1852.9	4.0
920.1	.02053	0.4	1739	8	0.04	118	69	0.61	1.701	-0.479	+0.07	1845.7	8.4
921.1	.02150	0.3	1810	5	0.01	243	250	1.06	1.694	-0.447	-0.10	1853.1	4.9
921.2	.02225	0.3	1866	5	0.00	292	310	1.10	1.685	-0.430	-0.07	1851.8	4.5
922.1	.02145	0.6	1807	10	0.07	123	73	0.61	1.695	-0.446	+0.40	1826.1	7.6
923.1	.02256	0.3	1888	6	-0.01	236	256	1.12	1.687	-0.415	-0.23	1857.0	5.7
924.1	.02138	0.5	1802	10	0.04	299	311	1.08	1.598	-0.647	+0.01	1849.6	5.3
925.1	.02255	0.3	1887	6	0.03	219	165	0.78	1.687	-0.413	-0.16	1855.1	5.2
925.2	.02257	0.3	1889	7	0.01	323	231	0.74	1.678	-0.431	+0.12	1847.3	4.3
926.1	.02221	0.3	1863	6	0.00	251	240	0.99	1.605	-0.603	-0.08	1852.7	5.1
927.1	.02388	0.3	1983	6	-0.01	246	257	1.08	1.658	-0.414	-0.18	1855.3	4.9
928.1	.02282	0.4	1907	7	0.01	556	524	0.97	1.679	-0.418	-0.07	1850.9	4.0
929.1	.02151	0.4	1811	7	0.00	342	351	1.06	1.527	-0.779	+0.10	1844.7	12.9
930.1	.02132	0.4	1797	7	0.05	271	204	0.78	1.717	-0.409	+0.18	1842.1	6.2
931.1	.02119	0.2	1788	3	0.00	1989	579	0.30	1.712	-0.419	-0.27	1851.7	2.7
932.1	.02151	0.3	1812	6	0.03	321	329	1.06	1.693	-0.445	-0.22	1858.4	5.6
934.1	.02251	1.1	1884	20	0.03	307	294	0.99	1.473	-0.838	+0.55	1817.9	7.0
935.1	.02164	0.3	1821	6	0.03	296	229	0.80	1.659	-0.506	-0.19	1857.7	9.6
936.1	.02132	0.4	1798	7	0.00	386	285	0.76	1.714	-0.403	+0.24	1843.3	5.4
937.1	.02224	0.4	1864	8	0.08	260	285	1.13	1.590	-0.624	-0.03	1851.5	7.1
										average	**+0.05**		
										95%conf	**±0.10**		

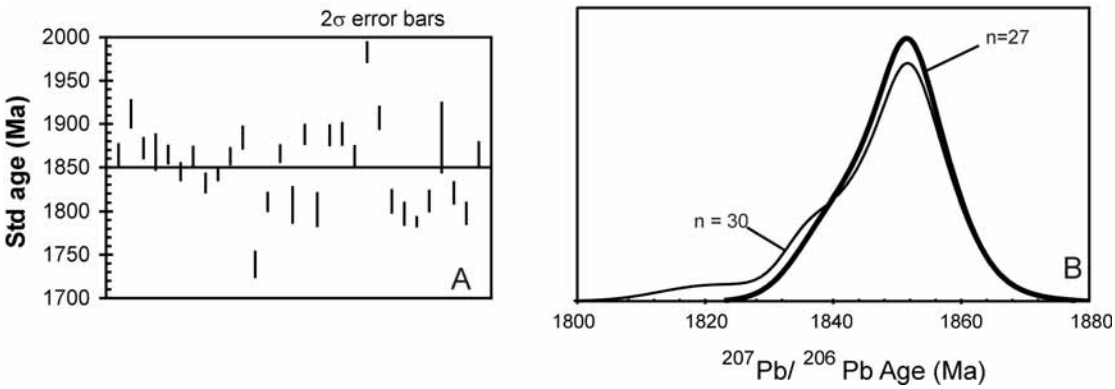

Figure A3-9. (A) Standard $^{206}Pb/^{238}U$ ages for QGNG; and (B) probability density diagram for QGNG standard analyses for mount Z3962, analysis date 22/4/03, SHRIMP II.

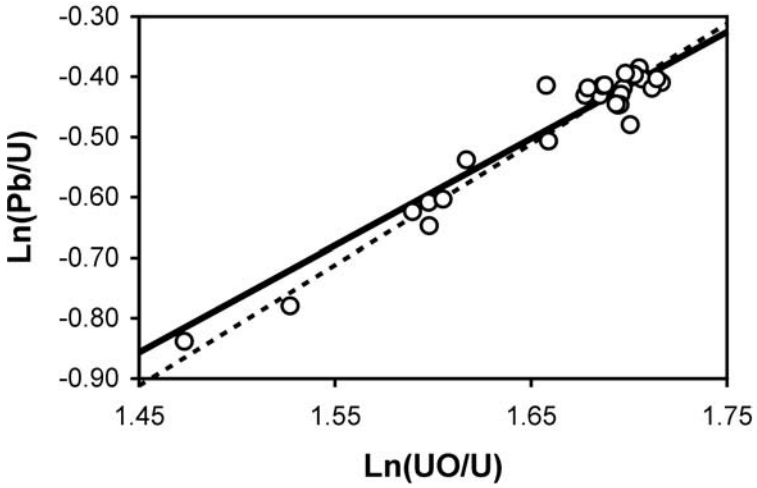

Figure A3-10. Pb/U calibration for mount Z3962, analysis date 22/4/03, SHRIMP II. Thick line is robust fit: dashed line has slope = 2.

Table A3-6. SHRIMP analytical results for QGNG; mount Z4125, analysis date 30/4/03, SHRIMP II.

Spot Name	204-corr Pb/U: UO/U^2	% err	Age Ma	±	% comm 206	ppm U	ppm Th	232Th /238U	Ln UO/U	Ln Pb/U	204 overcts /sec (fr. 207)	4-corr 207 /206 age	±
901.1	.02178	0.3	1785	5	0.01	317	325	1.06	1.675	-0.471	-0.08	1853.2	4.0
902.1	.02290	0.3	1864	4	0.06	151	107	0.73	1.661	-0.450	+0.37	1836.6	5.8
903.1	.02246	0.2	1833	3	0.00	334	209	0.65	1.656	-0.481	-0.11	1853.7	3.6
904.1	.02266	0.3	1847	5	0.02	95	49	0.53	1.676	-0.430	+0.07	1847.3	7.4
905.1	.02237	0.2	1827	4	0.04	181	192	1.10	1.662	-0.471	+0.36	1839.3	5.1
906.1	.02241	0.2	1830	3	0.01	275	283	1.06	1.668	-0.460	+0.00	1851.6	4.1
907.1	.02282	0.2	1859	3	0.00	256	250	1.01	1.657	-0.462	-0.04	1852.5	4.1
908.1	.02315	0.2	1882	3	0.02	318	328	1.07	1.655	-0.453	+0.34	1844.9	4.2
909.1	.02262	0.2	1844	4	0.00	198	105	0.55	1.682	-0.419	+0.00	1851.5	3.6
907.2	.02285	0.2	1861	3	0.00	286	286	1.03	1.695	-0.386	-0.05	1852.8	4.0
910.1	.02227	0.2	1820	4	0.02	177	160	0.94	1.673	-0.453	+0.04	1850.3	5.1
911.1	.02251	0.3	1837	5	0.02	329	314	0.98	1.662	-0.463	+0.25	1846.8	4.7
912.1	.02292	0.3	1865	5	0.00	187	101	0.56	1.662	-0.447	-0.15	1856.5	4.9
913.1	.02254	0.2	1839	3	0.01	344	326	0.98	1.664	-0.461	+0.14	1849.2	3.6
914.1	.02276	0.2	1855	3	0.01	234	118	0.52	1.675	-0.429	+0.58	1836.0	5.0
915.1	.02166	0.2	1776	3	0.04	263	246	0.97	1.727	-0.375	+0.63	1835.2	4.4
916.1	.02220	0.6	1815	9	-0.01	197	99	0.52	1.685	-0.432	+0.20	1844.7	5.3
917.1	.02214	0.2	1810	4	0.00	195	167	0.89	1.686	-0.433	-0.05	1853.2	6.0
918.1	.02257	0.3	1841	5	0.01	370	278	0.78	1.688	-0.412	+0.07	1850.4	3.5
919.1	.02258	0.2	1841	3	0.01	413	381	0.95	1.690	-0.405	+0.61	1842.0	5.0
920.1	.02313	0.2	1881	3	0.02	330	202	0.63	1.687	-0.393	-0.06	1852.9	4.2
921.1	.02259	0.2	1842	4	0.03	241	253	1.08	1.702	-0.383	-0.16	1856.5	5.4
922.1	.02308	0.2	1877	3	0.03	253	237	0.96	1.655	-0.454	-0.09	1854.2	5.6
923.1	.02240	0.2	1829	4	0.05	215	182	0.87	1.676	-0.443	+0.41	1838.5	5.0
924.1	.02269	0.2	1849	3	0.04	314	296	0.97	1.671	-0.439	+0.33	1844.5	3.9
925.1	.02312	0.3	1880	4	0.01	252	250	1.02	1.690	-0.392	+0.13	1848.0	4.9
										average	+0.14		
										95%conf	±0.10		

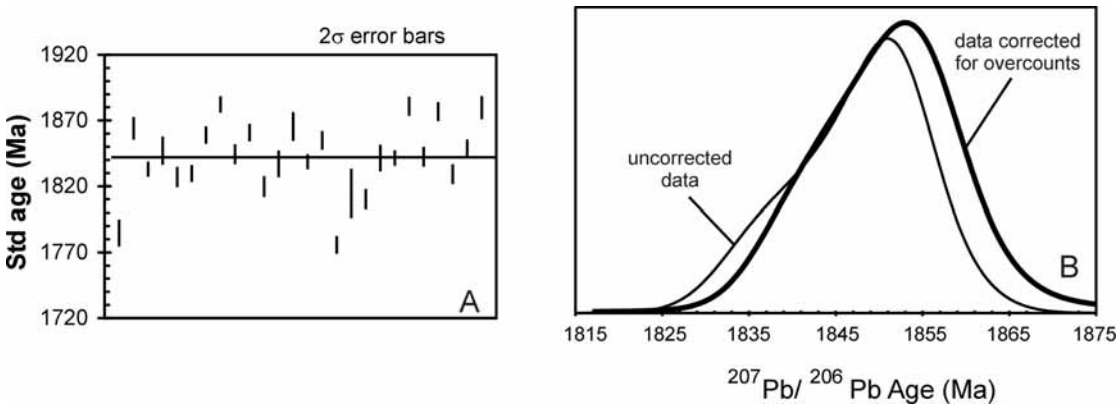

Figure A3-11. (A) Standard $^{206}Pb/^{238}U$ ages for QGNG; and (B) probability density diagram for QGNG standard analyses for mount Z4125,analysis date 30/4/03, SHRIMP II.

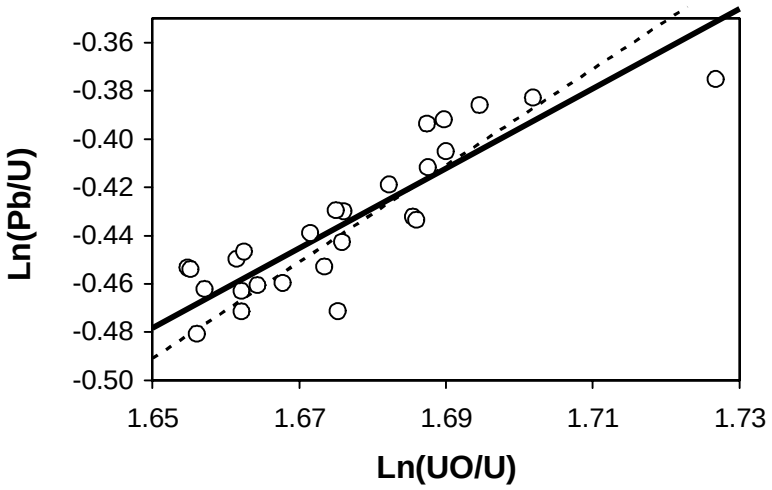

Figure A3-12. Pb/U calibration for mount Z4125,analysis date 30/4/03, SHRIMP II. Thick line is robust fit: dashed line has slope = 2.